UiT The Arctic University of Norway

Faculty for biosciences, fisheries and economy, UiT The Arctic University of Norway

Bioactive secondary metabolites from bacteria

Natural products from marine and terrestrial bacteria, dereplication, isolation and investigation of bacterial secondary metabolites.

Yannik Karl-Heinz Schneider

A dissertation for the degree of Philosophiae Doctor, July 2020.

Bioactive secondary metabolites from bacteria

Natural products from marine and terrestrial bacteria, dereplication, isolation and investigation of bacterial secondary metabolites.

A dissertation submitted in partial fulfilment of the requirements for the degree of

Philosophiae Doctor.

Yannik Karl-Heinz Schneider

Tromsø, July 2020

The work for this thesis was executed in the period from August 2017 to July 2020 at Marbio, The Norwegian College of fisheries science, belonging to the faculty of biosciences, fisheries and economy of UiT The Arctic University of Norway. The work was part of the Marie Skłodowska Curie Early Stage Training Network MarPipe, funded by the European Research Council.

Summary:

Natural products were the source for a big share of drugs that enabled modern pharmacotherapy. Examples for that are the over-the-counter drug aspirin or lifesaving antibiotics that are present in your daily life, which are in use now for many decades until today. Other natural product based drugs, like cyclosporine, enabled transplantation medicine as we know it and methylergometrine saved, and still saves, uncounted lives of young mothers.

From its historical roots, natural product chemistry became a scientific discipline where chemists and pharmacists isolated active molecules and started to modify them chemically, in order to get stronger effects, less side effects and molecules that were easier to obtain by synthesis. After the discovery of the first antibiotics, microorganisms, such as bacteria and fungi, became subject to screening programs that successfully led to the discovery of immunosuppressants, antibiotics and chemotherapeutics.

The last 30 years led to further insights in the properties that make natural products suitable drug candidates, which motivates to further investigate them in order to find better cancer medication and new antibiotics, effective against upcoming pathogens with antibiotic resistance. Bacteria are continuing to be a great source for new chemical entities and new drug candidates.

The present work deals with the isolation of natural products from bacteria. Starting with fifteen isolates from the Arctic Ocean, two isolates of the genus *Algibacter* were found to have antimicrobial bioactivity. Mass-spectrometric analysis of the extracts lead to the identification of one common metabolite that was isolated. Its structure was solved *via* NMR and found to be lipid 430.

From a co-culture of two bacteria, the siderophore serratiochelin A was isolated and its anti-cancer effect as well as its specific anti-microbial effect on *Staphylococcus aureus* were discovered. Investigation of the hydrolysed degradation product serraticohelin C revealed that the latter had no bioactivity raising the question if the bioactivity of serratiochelin A is caused by a specific effect instead of iron deprivation since both compounds are chelating Fe(III).

The investigation of a *Nostoc* sp. isolate led to the isolation of suomilide A and three new suomilides (B-D). Those highly modified glyco-peptides have been subject to previous synthetic approaches but their bioactivity was unknown. We were able to assign their potential biosynthetic cluster and to investigate their bioactivity. They showed no anti-bacterial or anti-biofilm effect and no toxicity towards human cell lines. The biological role and function of those complex cyanobacterial metabolites are still unknown.

Acknowledgements

The last three years were a very experience rich time, being challenging in a enjoyable way. I have to thank first and foremost my supervisors Prof. Dr. Jeanette Hammer Andersen, Dr. Kine Østnes Hansen and Prof. Dr. Espen Hansen for taking me as a PhD student and for supervising me. Despite your tight schedule, you had always an open ear for my questions and gave me a lot of freedom in my work. I received a lot of knowledge from you, which is not limited only to scientific matters; also your example on how to supervise and lead was a lesson for itself. I admire you for your great skills, knowledge and personality.

I was very fortunate to work together with many other people that substantially contributed to my work. My great thanks go to Dr. Johan Isaksson for taking the NMR spectra and for his great work in elucidating the structures of the compounds. Furthermore, I want to thank Dr. Anton Liaimer for the work he did on the cyanobacteria and for leaving KVJ20 over to me. “The Suomilides” were exactly the molecules I was looking for. I also want to thank my colleagues at Marbio, Kirsti Helland, Marte Albrigtsen, Dr. Sarah Ullsten Wahllund and Dr. Chun Li for their work with the bioassays, flow cytometry or molecular biology and a big thank you to all Marbank and Marbio people for many nice discussions and hours that were socially spent apart from work. My thanks go also to the other PhD students at Marbio, Ole Christian, Renate, Venke and my PhD-buddy Marte Jenssen.

Another part of my PhD program was that it was part of the MarPipe project, a Marie Skłodowska Curie Early Stage Training Network of the European Commision. It was a great pleasure to meet regularly with the eleven other PhD-students out of the same field and learn not only from my own supervisors, but also from the whole “cloud of supervisors and senior PIs”. A warm thank you to all who contributed and especially to Dr. Donatella de Pascale for coordinating MarPipe. The program gave me the opportunity for a two moth secondment at University College Cork within the group of Prof. Dr. Alan Dobson where I got practical education in genomic techniques. It was a great time together within the “MarPipe family”. Arianna, Anky, Florent, Maria, Kevin, Alejandro, Jane, Grant, Menia and Sloane, I will miss our project meetings, the time we spent together and your great personalities.

To settle fully into a new country was a new experience to me. However, it turned out to be one of the best decisions I made. The last three years where the so far best in my life and they would not be without the friends I made during that time, thanks to all of you.

Finally, I want to thank my family for their support and anchor. Particularly I want to thank my aunt, uncle, and my father, for contributing to become who I am.

Yannik Schneider Tromsø, July 2020

List of abbreviations

1D/2D	one/ two dimensional
AA	amino acid
ADME(T)	absorption, distribution, metabolism, elimination, (toxicity)
AEX	anion exchange chromatography
AMR	anti-microbial resistance
ASA	acetylsalicylic acid
B.C.	before Christ
CEX	cation exchange chromatography
CNS	central nervous system
CoA	Coenzyme A
DOS	diversity oriented synthesis
e.g.	*exempli gratia*
EI	electron impact ionization
ESI	electrospray ionization
et al.	*et alii*
etc.	*et cetera*
FDA	Food and Drug Administration
GPCR	G-protein coupled receptor
HPLC	high performance liquid chromatography
HR	high resolution
i.e.	*id est*
IPC	instrument personal computer
MIC	minimum inhibitory concentration
MP	mobile phase
MRSA	methicillin resistant *Staphylococcus aureus*
MS	mass spectrometry
NCI	National Cancer Institute
NMR	nuclear magnetic resonance (spectroscopy)
NP	normal phase
NRP	non-ribosomal peptide
NRPS	non-ribosomal peptide synthetase
OSMAC	one strain many compounds
p.a.	*per anum*
PCA	principal component analysis
PCR	polymerase chain reaction
PDB	Protein Data Base
PK	polyketide
PKS	polyketide synthetase
RiPPs	ribosomal synthesized posttranslational modified peptides
RP	reversed phase
SEC	size exclusion chromatography
SP	stationary phase
sp.	species
ToF	time of flight
US	United States
UV/Vis	ultra violet/ visible (spectrum of light)

List of publications

Paper I

Yannik K.-H. Schneider, Kine Ø. Hansen, Johan Isaksson, Sara Ullsten, Espen H. Hansen and Jeanette Hammer Andersen.
Anti-Bacterial Effect and Cytotoxicity Assessment of Lipid 430 Isolated from *Algibacter* sp.
Molecules, **2019**, *24*, 3991.

Paper II

Yannik Schneider[†], Marte Jenssen[†], Johan Isaksson, Kine Ø. Hansen, Jeanette Hammer Andersen and Espen H. Hansen.
Bioactivity of Serratiochelin A, a Siderophore Isolated from a Co-Culture of *Serratia* sp. and *Shewanella* sp.
Microorganisms, **2020**, *8*, 1042.

[†]Those authors contributed equally to the article

Paper III

Yannik K.-H. Schneider, Anton Liaimer, Johan Isaksson, Kine Ø. Hansen, Jeanette Hammer Andersen and Espen H. Hansen.
New suomilides isolated from *Nostoc* sp. KVJ20, bioactivity and biosynthesis
Manuscript

Table of Contents

Cover page i
Summary ii
Acknowledgements iii
List of abbreviations iv
List of publications v
Table of contents vi
List of tables vii
List of figures vii
1 Natural products as source for new drugs ... 1
1.1 Historical development ... 1
1.2 Microbial natural products ... 4
1.3 Definition of terms ... 5
1.4 Systematic screening of natural products ... 7
1.5 Natural products in drug discovery ... 8
1.6 The refocus on natural products in drug discovery ... 10
2 Chemistry of natural products ... 12
2.1 Chemical classification of natural products ... 12
2.2 Secondary metabolites of bacteria ... 12
2.2.1 Nonribosomal peptides ... 13
2.2.2 Polyketides ... 14
2.3 Chemical and pharmacological properties of natural products ... 14
2.4 Privileged structures in natural products, the repetitive structural patterns in bioactivity. ... 18
3 Taxonomic ranks of bacteria that are prolific producers of secondary metabolites ... 22
3.1 Actinobacteria ... 22
3.2 Myxobacteria ... 22
3.3 Cyanobacteria ... 23
3.4 Genome size and complex life cycles, indicators for the biosynthetic potential of bacteria. 23
4 Need for new drugs and drug leads ... 24
5 Process and techniques of natural product discovery ... 25
5.1 Cultivation and extraction of bacteria ... 25
5.2 High performance liquid chromatography ... 25
5.3 Mass spectrometry and dereplication ... 27
5.4 The bioprospecting workflow ... 30
5.5 Structure elucidation ... 31
5.6 Genomics as a new tool in natural product research ... 32

6 Aim of the work 33
7 Results and discussion of the work 34
7.1 Summary of papers 34
7.2 Discussion and conclusion 38
7.3 Further work and outlook 42
8 Works cited 43

List of Tables

Table 1: Classes of natural products and their building blocks. 12
Table 2: Differences between biosynthesis and synthesis. 18
Table 3: Number of antibacterial compounds from marine bacteria reported 2010-2015. 40

List of Figures

Figure 1: Structures of morphine, quinine, salicin, salicylic acid and acetylsalicylic acid. 1
Figure 2: *Claviceps purpurea*, ergot sclerotia on rye.† 2
Figure 3: Structures of lysergic acid, methylergometrine and ergometrine. 3
Figure 4: Arthur Stoll, portrait.† 3
Figure 5: Alfred Hofmann, portrait.† 3
Figure 6: Structures of penicillin G, streptomycin and actinomycin D. 5
Figure 7: *Taxus brevifolia* (Pacific yew three).† 7
Figure 8: Structures of cyclosporine A and taxol. 8
Figure 9: Origin of drugs between 1981 and 2014. 9
Figure 10: Structures of cytarabine, spongouridine, salinosporamide A, trabectedin and eribulin. 11
Figure 11: LIPINSKI's rules of five. 16
Figure 12: Targets and target families of small molecule drugs 19
Figure 13: X-ray structures and unique protein folds in PDB. 20
Figure 14: HPLC system for natural product isolation. 27
Figure 15: Schematic function of a mass spectrometer. 28
Figure 16: Electrospray ionization. 29
Figure 17: Bioprospecting workflow. 30
Figure 18: Fundamental strategies in natural product discovery. 33
Figure 19: Structure of lipid 430 34
Figure 20: Structures of serratiochelin A and C. 35
Figure 21: Structures of the suomilides and banyasides. 37

† See page 52 for picture sources and licenses.

1 Natural products as source for new drugs

1.1 Historical development

The genesis of natural product chemistry was probably the isolation of morphine (Figure 1, **1**) from *Papaver somniferum* by the German pharmacist FRIEDRICH W. A. SERTURNER in 1804. It was the first purification of an active principle from a biological material. It is also an example of innovation by breaking with old paradigms since his success was based on the idea that morphine could be an alkaline substance, which was in conflict with the (at that time) prevailing idea that all plant products were acidic. However, the recognition of the alkaline nature of morphine enabled SERTURNER to isolate the molecule [1]. Morphine served as valuable painkiller for more than hundred years and was certainly the first "blockbuster" drug.

However, the first medical use of natural products back in history was done through the application of herbs, mushrooms and other preparations in folk medicine and doctoring. Such use was probably based on trial and error or from coincidental observations. That way, prehistoric cultures gained knowledge *e.g.* about the effect of certain plants and how to use them to threat pathologic conditions [2]. The two oldest civilisations, Mesopotamia and Egypt, left us the first documented knowledge about pharmaceutical preparations. From about 2600 B.C., the first cuneiform documents describe the use of plants, *e.g.* cypress and myrrh, which are still in use in form of herbal preparations today. The Egyptian Ebers Papyrus dates back to 1500 B.C. and describes about 700, mostly plant based, drugs [3].

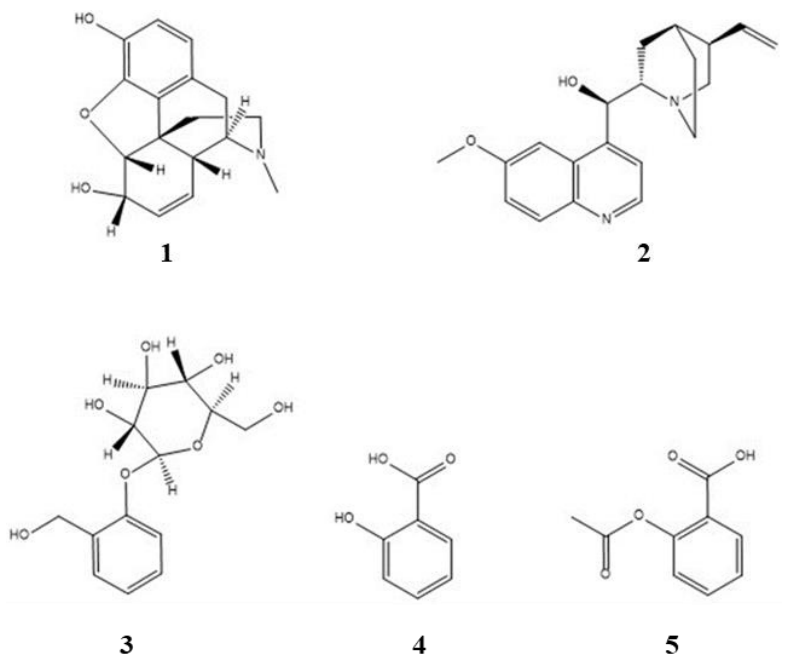

Figure 1: Morphine (**1**), quinine (**2**), salicin (**3**), salicylic acid (**4**) and acetylsalicylic acid (**5**).

The scientific development through the end of the renaissance was preparing the ground for a chemistry with scientific methodology that was capable of isolating the first active pharmaceutical ingredients. The isolation of morphine was followed by the isolation of the antimalarial drug quinine (Figure 1, **2**) from *Cinchona* species in 1820 by the French pharmacists CAVENTOU and PELLETIER [3]. For a long time in history, people have known the pain-reducing effect of the bark of the willow tree (*Salix* sp.), which is the source of salicin (**3**). Because of problematic unwanted side effects of salicin (gastritis), the chemists ARTHUR EICHENGRÜN and FELIX HOFFMANN, both working at Bayer & Co., were searching for a modification of salicylic acid that did not cause gastric irritation. In 1897, F. HOFFMAN successfully acetylated salicylic acid (**4**, a building block of salicin) yielding **a**cetyl**s**alicylic **a**cid (ASA, **5**) [4]. Beside its more common use to threat pain, inflammation and fever, ASA is also used to treat Kawasaki syndrome, coronary artery disease and many more indications [5]. It is an example, possibly the first, of the systematic chemical modification of a natural product in order to change its pharmacological properties, a process known as lead optimization [6].

Figure 2: *Claviceps purpurea*, ergot sclerotia on rye (dark structures on the rye ear that are bigger than the corns, similar for other grains) S. Nelson.

Another organism that was delivering the basis for a group of active substances was *Claviceps purpurea* (Ergot). The parasitic fungi infects the grains of rye, but also barley, oat and wheat and forms characteristic sclerotia (Figure 2) [7]. The fungi was causing severe intoxications when it came into the food chain, resulting in a condition known as Ergotism or St. Anthony's fire. In its most severe manifestation, Ergotism led to death or loss of limbs. The impact of the disease on the medieval society is reflected by its presence in medieval Cristian iconography. Ergot itself was possibly first mentioned around 600 B.C. on an Assyrian cuneiform tablet [8]. Already in 1582, ADAM LONICER described the use of three sclerotia to induce uterine contractions. In 1787, PAULIZKY described the administration of ergot as "*pulvis ad partum*" by midwifes and physicians [8]. The observation of the side effects in 1822, particularly stillbirths, banned the use of ergot as delivery accelerator. Ergot powder, which was previously termed "*pulvis ad partum*", was in spite of that renamed "*pulvis ad mortem*". Nevertheless, ergot powder was still used to treat postpartum hemorrhage after delivery for which it was found to be effective [7,9]. During the first half of the 20th century, scientists in Great Britain, namely DALE and BARGER, and in

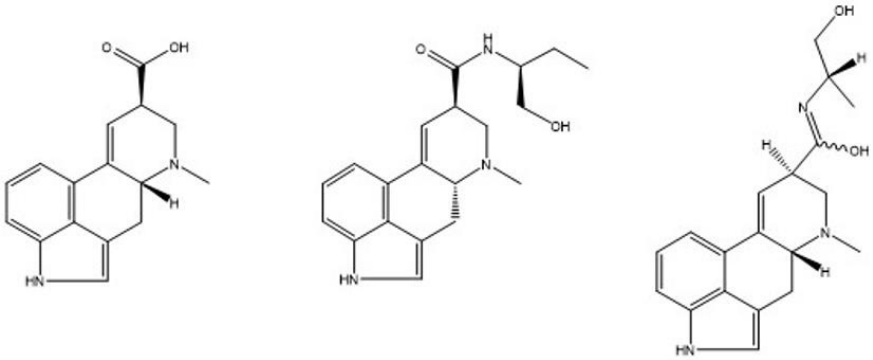

6 **7** **8**

Figure 3: Lysergic acid (**6**), the basic building block of ergot alkaloids, methylergometrine (**7**) and ergometrine (**8**).

Figure 4: Prof. Dr. Arthur Stoll (1887-1971), former head of the pharmaceutical department and "father" of natural product chemistry at Sandoz. Photography was kindly provided by the company archive of Novartis AG, Switzerland.

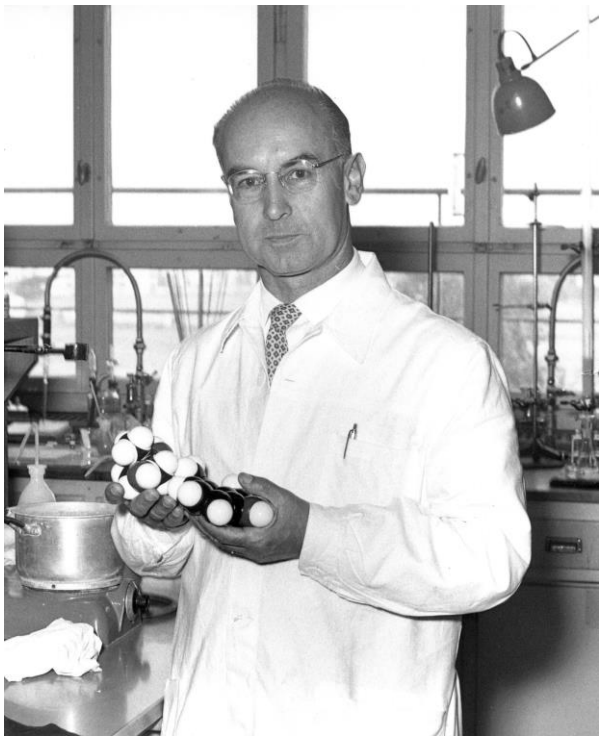

Figure 5: Dr. Alfred Hofmann (1906-2008), successor of Stoll at Sandoz, in his laboratory with a model of lysergic acid diethylamide. Photography was kindly provided by the company archive of Novartis AG, Switzerland.

Switzerland made ergot the subject of their investigation. In 1918, ARTHUR STOLL isolated ergometrine (Figure 3, **8**) at the Sandoz laboratories in Basel, Switzerland, which became a successful migraine medication and drug for preventing postpartum hemorrhage [10]. The further work of STOLL and ALBERT HOFMANN at Sandoz lead to the chemical elucidation of the different ergot alkaloids and synthesis of modifications that lead directly and indirectly to many drugs such as dihydergot,

methylergometrine (**7**) and bromocriptine [9,11]. Some people called ergot a "chemical mess" [10], but many would probably agree with HOFMANN describing ergot as "rich treasure house of valuable pharmaceuticals" [9].

1.2 Microbial natural products

The introduction gave some examples of molecules that were isolated from organisms and resulted in drugs with high therapeutic and life-saving values, and some of them are still in use today more than a century after their discovery. The molecules described in the previous examples were derived from sources that where known for a pharmaceutical effect for which they were used in folk medicine and doctoring. This approach using historical or traditional knowledge about a pharmaceutical effect of plants, mushrooms or other derived preparations is termed ethnopharmacy. The actual discovery for the previous examples was the isolation, structure elucidation and chemical modification of the active principle(s). This strategy, which was based on the knowledge of a certain activity of the source of the molecule, changed when microbes entered the field of natural product research. The development of screening-based natural product discovery was to a large degree triggered by the discovery of penicillin by ALEXANDER FLEMMING and the work of SELMAN WAKSMAN and colleagues.

In 1928 ALEXANDER FLEMMING reported his observation that a *Penicillium* mould was inhibiting the growth of *Staphylococcus aureus* and other bacteria [12]. This lead to the discovery of penicillin (Figure 6, **9**) as the active principle and spurred its investigation in animals and humans [13,14]. Penicillin finally found its way into clinics during the course of world war II [15]. In 1939 a group around WAKSMAN at Rutgers University started, based upon earlier observations, to screen soil actinomycetes and fungi for antimicrobial activity, which resulted in the discovery of streptomycin (**10**) [16]. Streptomycin, in contrast to penicillin, was active against *Mycobacterium tuberculosis*, providing a potential cure against one of the most problematic infectious diseases, tuberculosis [16]. Streptomycin was later the subject of the first randomized clinical study in history, proving its suitability for curing tuberculosis [16,17]. Through the work of WAKSMAN's group, actinomycetes were found to be prolific producers of bioactive molecules such as actinomycin (**11**), clavicin, fumigacin and others [16].

The discoveries of the antibacterial molecules produced by fungi and actinomycetes led to the so-called "golden age of antibiotics" between 1950 and 1970, in which all major classes of currently known antibiotics were discovered [18]. During this period, the interest in microbial natural product chemistry increased, and motivated by the previous success stories several companies entered the field and started to screen for natural products from microbes [19]. One of them, Elli Lilly, requested Christian missionaries to send soil samples for the isolation of microbes [19]. One soil sample from Borneo was

the source for the isolation of the actinobacteria *Streptomyces orientalis* which produced the antibacterial compound we know now as vancomycin [20]. Because of its toxicity, the preference in treatment was initially given to other antibiotics, but the arise of resistant strains, in particular MRSA, made vancomycin the preferred antibiotic for treating resistant infections [20]. It should be mentioned that the discovery of bioactive natural products from microbes was not limited to the drug class antibiotics. One of the first molecules discovered by WAKSMAN's group, actinomycin (Figure 6, **11**), was developed into a cancer chemotherapy agent [21] and the spinosyns are agricultural insecticides that were isolated from actinobacteria [22].

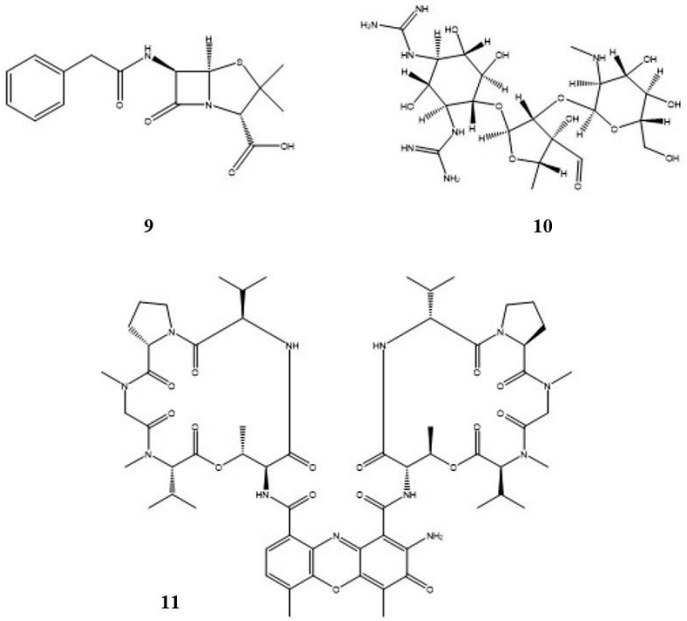

Figure 6: Penicillin G (**9**), streptomycin (**10**) and actinomycin D (**11**).

1.3 Definition of terms

Within the previous chapter, the term *natural product* was introduced without further explanation, which should be done now. A *natural product* is literally any molecule that is produced by any living organism [23]. This includes peptides, proteins, lipids, toxins *etc*. and most of those building blocks of life are present in all organisms alike, with some minor variations and modifications. On the other hand, some *natural products*, *e.g.* toxins, can be very specific to taxonomic groups or unique to a certain species. The subgroup of natural products that is of particular interest for natural product chemists is the latter, termed secondary metabolites.

Primary Metabolites:

Primary metabolites are a subgroup of natural products and can be seen as the aforementioned "basic building blocks of life" such as fatty acids, carbohydrates, amino acids *etc*. and they are an integral part of primary metabolism and are essential for sustaining the organism and its vital functions. They are, with some exceptions, present in all organisms alike [24].

Secondary Metabolites:

Secondary metabolites are another subgroup of natural products and not part of the cell's most vital chemical processes. They are molecules produced by the organism that are not essential to its vital functions, but give additional benefits *e.g.* in competition with other organisms or by acting as chemical defence mechanism [25]. The natural products mentioned in chapter 1.1 and 1.2 are examples of *secondary metabolites*.

Bioprospecting:

The search for natural products, commonly secondary metabolites, from living organisms is called *bioprospecting*. The term *bioprospecting* also includes the discovery and use of genes and construction principles that were copied from nature or inspired by organisms [26]. In summary, *bioprospecting* includes the discovery, development and commercialization of material as well as intellectual property either originating or derived from nature.

Dereplication:

The term *dereplication* describes one of the most critical working steps in the identification and isolation of a new natural product. When searching for new bioactive molecules by bioprospecting plants, bacteria and other organisms, one often start with testing an extract of an organism for bioactivity. An active extract or fraction can contain >100 molecules. To analyse the extract and to point out if its bioactivity is caused by a known molecule or not is called *dereplication*. The aim of *dereplication* is to identify the known molecules and to point out one or more molecules that are likely to be unknown and/or responsible for the extracts bioactivity*. *Dereplication* will result in terminating the work on an extract if its active principle is already known (*e.g.* production of a known β-lactam by a fungi or bacteria) [27,28]. *Dereplication* aims to avoid replicating the investigation of already known molecules.

*A new bioactivity of an already known molecule can be of interest as well.

1.4 Systematic screening of natural products

The discoveries of FLEMMING and WAXMANN were not only the start of screening programs for antibiotics. Scientists in different institutions and companies went out to search for natural products with different bioactivities and applications after recognizing the biosynthetic potential of living organisms, particularly that of actinobacteria and fungi. One of the pharmaceutical developments of the second half of the last century which changed immunosuppressive therapy was the discovery of cyclosporine (Figure 8, **12**). The associates of Sandoz were asked to bring soil and water samples from their business trips and private holidays, and from these samples microbes were isolated, fermented and screened [29]. In a screening for immunosuppression agents, the ferment of a fungi was found to have an immunosuppressive effect but no bone marrow toxicity. The active principle was found to be cyclosporine, a cyclic peptide produced by *Tricoderma polysporum* [30,31]. After overcoming issues with the bioavailability of the molecule and developing it into a drug, the product enabled organ transplantation by supressing the "graft versus host disease" and its immunosuppressive effect also aids Psoriasis patients by suppressing the autoimmune reaction directed to the patients skin [32,33].

Figure 7: Branch, fruits and leaves of *Taxus brevifolia* (Pacific yew three), not to be confused with *Taxus baccata* (common yew or European yew) J. Hollinger.

Another success story was the discovery of taxol (**13**). Initially it was discovered by the National Cancer Institute (NCI), US, during a large screening campaign, where thousands of plants were screened for their anti-cancer activity. The extract of the bark from *Taxus brefivolia* (see Figure 7) showed activity and its active principle, taxol, was identified in 1971. Due to the low abundance of the compound in the bark it was not possible to isolate sufficient amounts of taxol for further investigation. The isolation of substantial quantities would have threatened the population of *T. brefivolia*. Therefore, taxol remained without further attention until its unique mode of action was discovered in 1979. It was discovered that taxol is inhibiting the cell cycle trough stabilisation of the microtubule. Finally it was possible to circumvent the supply issue by using a semisynthetic approach using baccatin III or 10-acetylbaccatin III isolated from *Taxus baccata* as predecessors [34]. By date, taxol is approved for the treatment of several cancer types such as breast cancer, Kaposi's sarcoma and small cell lung cancer [35].

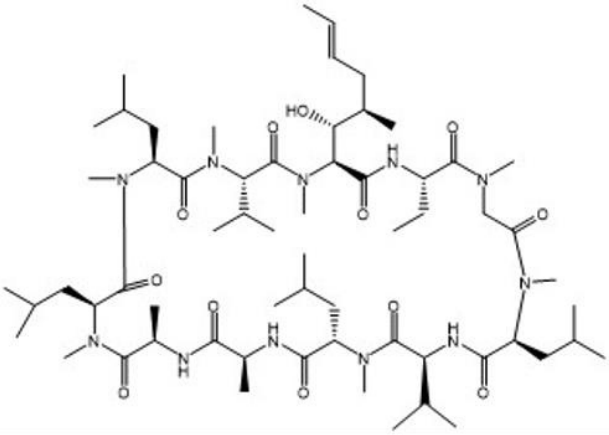

12

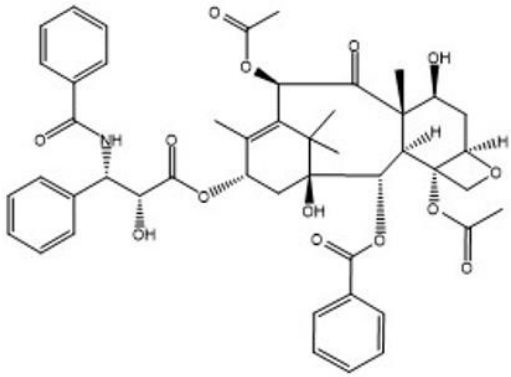

13

Figure 8: Cyclosporine A (**12**) and taxol (**13**).

1.5 Natural products in drug discovery

The examples given above were some individual discoveries with remarkable impact on pharmacotherapy. Nevertheless, the impact of natural products is also quantitatively recognizable. In 2016, NEWMAN & CRAGG published their review "Natural Products as sources of new Drugs from 1981 to 2014" [36]. A simplified summary for small molecules, excluding "non-chemical" drugs such as biologics and vaccines, is given in Figure 9. Overall, natural products, directly or indirectly as derivatives or similar, contributed to about ⅔ of the drugs in that period. For the antibiotics, natural products contributed directly or indirectly to 74% of the compounds discovered during that period. It clearly underscores the importance of natural products to our pharmaceutical armament. However, there is one group of organisms, which deserves special attention when it comes to being the source of bioactive natural products. This is microorganisms, more specific fungi and bacteria and among the latter to the biggest extent the actinobacteria. These microorganisms have contributed the lion's share of drugs and bioactive compounds that were discovered in screening campaigns for natural products [37,38].

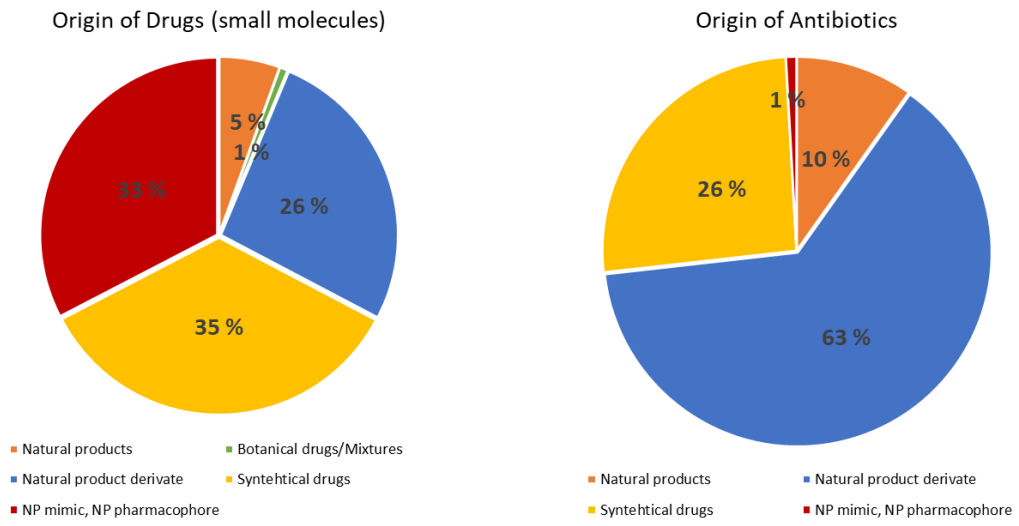

Figure 9: Origin of drugs between 1981 and 2014 according to NEWMAN & CRAGG [36].

During the 1980's, synthetic chemistry entered the field of drug discovery and many pharmaceutical companies left natural product drug discovery in favour of screening libraries of synthetic compounds. This was mainly because of technical difficulties associated with natural product libraries, but also because of high expectations in synthetic libraries generated by combinatorial chemistry [39]. There were technical difficulties associated with natural products, such as the rediscovery of known molecules and the supply of material, as well as the problem of "dereplication" (See chapter 4.3) [40]. The regime of 'blitz' screening (fast screening of a high number of compounds or samples) was less compatible with the long process of dereplication and isolation of natural products [40]. An important methodology that came into place in that time and played a role that cannot be neglected in that regard, is **h**igh **t**hroughput **s**creening (HTS). HTS enabled the fast screening of a high number of samples, thus, the development of HTS triggered a demand for vast compound libraries that were conveniently and relatively cheaply provided by combinatorial chemistry [41]. During the 1990s a relative decrease in natural product patents was observed, which is mainly attributed to the abandoning of natural product screening in the industry [41]. However, there are also opinions that the expectations that were associated with HTS of compound libraries generated *via* combinatorial chemistry were simply not realistic.

Another factor that contributed to the decline of interest and innovation in natural products in the 1990s was potential regulatory issues, caused for example by the Rio Convention on biological diversity in 1992 that raised legal concerns about sampling and intellectual property which may gave additional motivation for pharmaceutical companies to leave the field of natural product chemistry [41,42].

1.6 The refocus on natural products in drug discovery

In hindsight, the change towards using combinatorial libraries for HTS can be seen as one of those learning process triggering investigations that would not have taken place if that change was not done. Finally recognizing the disappointment or missed expectations associated with the synthetic libraries led to investigations looking into the properties of natural products and searching for the principles that made them suitable drug candidates. During the last two decades, the properties of natural products and underlying principles of their bioactivity were investigated, which will be topic of the next chapters. Moreover, there were technical improvements taking place in the field of analytical chemistry and structure elucidation. Antimicrobial resistance has additionally triggered the refocus on natural products for new antibiotics [43], a field in which natural products have shown their suitability.

In addition to technological improvements, a strategy evolved to look into previously under-investigated or ignored ecosystems and organisms. First, the biggest part of our soil microorganisms, which are easy to access with respect to sampling, is probably not yet cultivated and it is in part a question of effort to cultivate them [44]. Moreover, for those who are not accessible to conventional cultivation new techniques have evolved, such as *in-situ* cultivation [45]. For those microorganisms that are not cultivable at all, metagenomics techniques provide an opportunity for investigation [46].

A merely under-investigated environment is for example the deep sea, where technical issues of accessibility represented a considerable obstacle in the past. Advances in scuba diving or robot techniques made this space more accessible to the scientific community [47]. The first drugs that originated from the sea were cytarabine (**14**, approval 1969) derived from spongothymidine and vidarabine, derived from spongouridine (**15**, approval 1976). Both were originating from *Tectitethya crypta* and notably cytarabine is still in use today [48,49]. But there are other, more recent examples for drugs derived from marine natural products. Ziconotide against chronic and severe pain, derived from ω-conotoxin, a toxine of *Conus magnus* got approved in 2004 [48,50,51]. In addition, the alkaloid trabectedin (**17**) isolated from the tunicate *Ecteinascidia turbinata* got approval for treatment of soft tissue sarcoma and ovarian cancer [48]. Eribulin against metastatic breast cancer reached the market in 2010 (**18**). It is a simplified structural analogue of halichondrin B isolated from the sponge *Halichondria okadai* [52].

The drugs mentioned above were isolated from invertebrates. Interestingly, the actual producer organisms of the exotic metabolites found in invertebrates are often bacteria that are associated with the macroorganism. Especially sponges are hosts to a high number of bacteria in symbiotic relationships [53,54]. The bacterial symbionts of a sponge can make up 40% of the sponge biomass [54]. Synthesis of bioactive secondary metabolites by a bacterial symbiont is the case for trabectedin, where metagenomic

studies revealed that the actual producer is a bacterial endosymbiont *Candidatus Endoecteinascidia frumentensis* [55,56]. From prospecting marine bacteria, salinosporamide A (**16**) was isolated in 2003 from an isolate of the novel genus *Salinospora* and represents an example for structural motives exclusive for marine microorganisms [57]. Salinosporamide A is currently undergoing phase III clinical trials against glioblastoma [58].

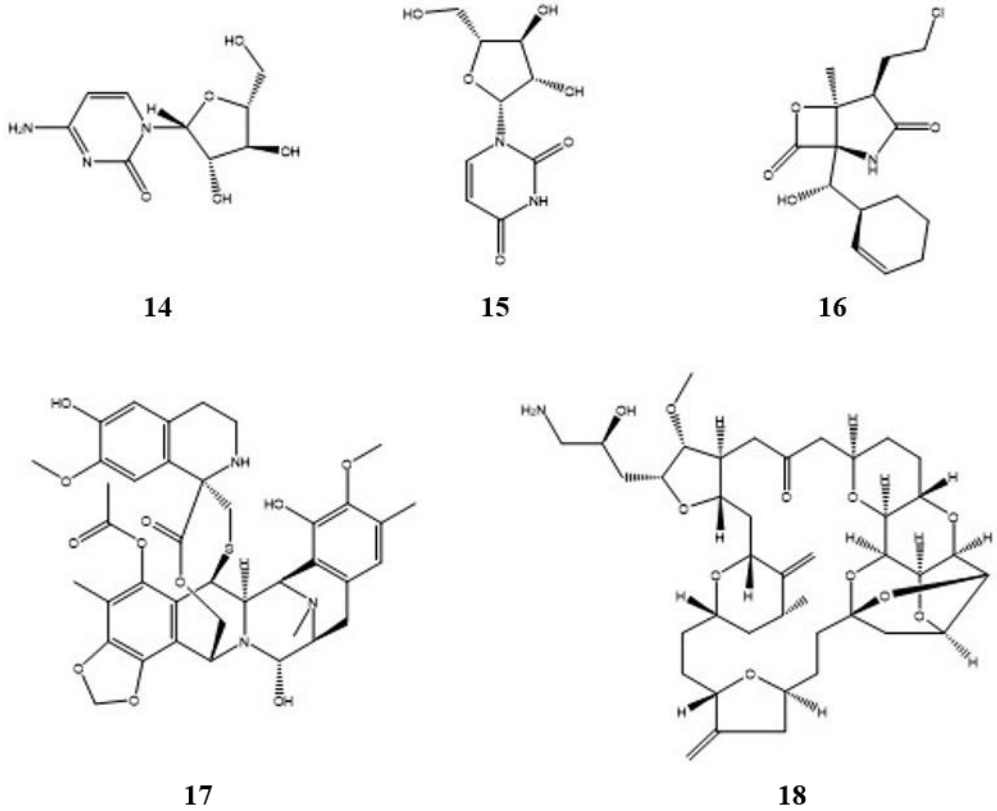

Figure 10: Drugs from the sea: cytarabine (**14**), spongouridine (**15**), salinosporamide A (**16**), trabectedin (**17**) and eribulin (**18**).

2 Chemistry of natural products

2.1 Chemical classification of natural products

Secondary metabolites can be divided into several classes according to the nature of their biosynthesis and the building blocks of which they are made. A possible classification (inspired by [59]) of secondary metabolites is given in Table 1. It is thereby important to note that the grouping of natural products is not rigid. There are hybrid natural products that are product of more than one pathway such as polyketide-nonribosomal-peptide hybrids and *e.g.* peptides that are esterified with a fatty acid or glycosylated [60].

Table 1: Classes of natural products and their building blocks, with inspiration of [59].

	Building blocs	**Examples**
Polyketides and Fatty acids	acetyl-CoA, malonyl-CoA	lipstatin, rapamycin
Terpenoids and Steroids	isoprene	camper, diosgenin, taxol
Phenylpropanoids	shikimic acid	cinnamic acid, corniferyl alcohol
Alkaloids	various	ergot alkaloids, trabectedin, caffeine
Specialized AAs and peptides	AA (D/L), other metabolites	cyclosporine, vancomycin
Specialized carbohydrates	carbohydrates	gentamicin, validamycin

2.2 Secondary metabolites of bacteria

Bacteria have been shown to be able to produce a wide range of secondary metabolites. The secondary metabolites produced by bacteria range from terpenoides to glycosides [61]. But among all the biosynthetic products of bacteria, there are two classes of secondary metabolites making up a big part

of the bacterial secondary metabolites. Those are **n**on**r**ibosomal **p**eptides (NRP) and **p**oly**k**etides (PK). NRPs and PKs are products of big multidomain enzyme complexes, so called NRP-**s**ynthases (NRPS) and PK-**s**ynthases (PKS) [62]. These are enzyme-complexes that assemble their respective products sequentially by connecting and modifying its building blocks [62].

2.2.1 Nonribosomal peptides

NRPS are big multidomain enzymes consisting of different modules, and each regular module consists of three domains and each of them is responsible for the incorporation of one building block/ **a**mino **a**cid (AA) into the final product. The AA that is incorporated is specific to the respective module. The three domains a module consists of are the **a**denylation (A) domain, the **p**eptidyl **c**arrier (PCP) domain (also thiolation (T) domain) and the **c**ondensation (C) domain. When adding a new AA to a chain the A-domain is activating it by adenylation under consumption of ATP. The aminoacryl-adenylate reacts with a thiol and is transferred to a serine in the PCP domain, where it is attached to the polymer by condensation trough the C-domain [63,64]. The first module of an NRPS is consequentially lacking a C-domain and the last module possesses a **t**hio**e**sterase (TE) domain to release the product, which is attached to the NRPS *via* a thioester bond throughout synthesis [63,64]. The function of a NRPS is thereby somewhat similar to the function of a ribosome, where the peptide is attached and sequentially prolonged. While ribosomal peptide synthesis can make use of the 22 proteinogenic AA, a NRPS can incorporate in addition almost 500 non proteinogenic AAs [65]. While a ribosome can synthesize theoretically max. 22^n possible peptides with the length of n (number of AA/ building blocks), a NRPS can synthesize ~ 500^n possible peptides of the same chain length (not considering **p**ost-**t**ranslational **m**odification, PTM, where the peptide is altered after peptide synthesis, *e.g.* by glycosylation) [63]. Consequentially, for a peptide with a length of n = 10 AA there are 2.66×10^{13} combinatorially possible ribosomal peptides, the same n = 10 building blocks chain length in NRPS yield ~ 9.77×10^{26} combinatorially possible NRPs (which is 3.68×10^{13} times as many theoretical combinations as in the "ribosomal case"!). Over more there are domains for internal heterocyclization of building blocks (such as serine, cysteine or threonine) [63] or for halogenation [66]. Tailoring enzymes can thereby modify the product during or after chain elongation *e.g.* trough glycosylation or methylation [67] finally, NRPs are often highly modified molecules chemically different from ribosomal peptides.

2.2.2 Polyketides

PKS work similar to NRPS by sequentially adding the building block acyl-CoA or malonyl-CoA to a product bound to the enzyme [62]. PKS are commonly grouped into three types. Type I PKS are consisting out of modules that synthesize a PK sequentially and noniteratively, each module is adding one building block to the product. Type II PKS are enzyme complexes where the modules carry out iterative reactions. Their products are often polycyclic polyketides. Type III PKS are iteratively synthesizing their product by condensation of the building blocks. Type III PKS do not employ a Acyl carrier protein (ACP) like Type I and II PKS and attach the acyl-CoA "directly" to the product [68]. The product of a PKS can be further modified *e.g. via* heterocyclisation or alkylation catalysed by tailoring enzymes [69,70]. PKS are also able to incorporate other building blocks as acyl- and malonyl-CoA such as benzylmalonyl-CoA and modified AAs [70,71].

2.3 Chemical and pharmacological properties of natural products

Around the year 2000, statistical and cheminformatical investigations started to look into the structural and chemical properties of natural products, drugs and synthetic compounds. This was motivated through the disappointing outcome of the screening campaigns using combinatorial libraries recognizing that they do not deliver the same yield of drug candidates or leads [39,72]. The property-distributions of natural products, drugs and synthetic molecules were studied by industrial groups as from Bayer [73], Roche [74] and SignalGene [75] as well as academic groups [76] which lines out the fields importance for commercial drug discovery. Despite starting from different datasets and employing different algorithms and definitions, they discovered the same or similar differences between natural products and synthetic molecules. Synthetic molecules have a higher number of heteroatoms, such as sulphur and halogens and in general, a higher number of nitrogen atoms compared to natural products [73,75]. On the other hand, natural products turned out to have a higher number of oxygen atoms and chiral centres [73,75]. Natural products have a higher molecular weight and more sp^3-hybridized bridgehead carbons and are in general more rigid [73,75]. HENKEL *et al.* [73] found that 40% of the set of natural products they investigated were structurally not represented within the synthetic compound-library. FEHER & SCHMIDT investigated the chemical space that is occupied by natural products, synthetic molecules and approved drugs. PCA of a random selection from the three compound classes revealed that natural products as well as drugs occupy a larger chemical space than synthetic compounds [75]. However, when doing comparisons between drugs, natural products and synthetic molecules and when drawing conclusions from that, one should keep in mind where the drugs are coming from. The drugs recruit

from the two aforementioned compound groups and they logically have interceptions in chemical space [75]. Nevertheless, both studies indicate that natural products occupy a wider chemical space than synthetic molecules. One of the structural attributes that is giving raise to favourable pharmacological properties of natural products is their higher rigidity compared to "synthetics". When binding to a protein target, a rigid ligand will exhibit a stronger bond trough lower entropic losses compared to a flexible ligand [77]. An explanation for the different chemical properties of both compound classes are the fundamental differences in biosynthesis and chemical synthesis, see Table 2. BÉRDY estimated in 2005 that from ~ 3×10^6 to 4×10^6 compounds that were synthesized by the pharmaceutical industry ~ 0.001% became approved drugs while ~ 0.2 to 0.3% of more than 5×10^4 natural products became approved drugs and roughly the same number served as lead molecules [37]. When interpreting those numbers, it should be kept in mind that isolation of natural products was often done guided by bioassays. The industrial and institutional screening campaigns started commonly with bioassay screening of extracts and cultures and employing bioassays during purification of the active principle to verify the bioactivity in respective fractions and preparations of pure compounds before expending their effort to structure elucidation. Therefore it should be expected, that the "space of isolated natural products" is in consequence of the above "biased towards bioactivity" when compared to randomly generated combinatorial compound libraries [37].

One example of the insufficient outcome of a common HTS campaign may be a screening study by Glaxo Smith Kline for new antibacterials [78]. They screened different targets in 67 HTS-campaigns in a target-based screening and executed three cell-based screening campaigns. Target based screening led to 15 hits and five leads while the cell-based screening resulted in three hits and no lead. Some of the leads were lacking novelty or being too specific in their antibacterial activity [78]. The outcome was doomed to be insufficient because multiple promising leads are needed due to the attrition rate in lead optimization and clinical development. According to Glaxo Smith Kline, the hit rate in antibacterial HTS was four to five-fold lower than for other therapeutic areas and targets. Antibiotics themselves differed from drugs for other indications such as CNS by having on average a higher hydrophilicity and a bigger size [78]. Occupying on average a different chemical space than drugs that target human cells could be a consequence of the prokaryotic target of antibiotics.

Regarding the chemical properties a molecule has to possess in order to be developed into a drug the ADME (**A**bsorption, **D**istribution, **M**etabolism and **E**xcretion; ADMET = the same + **T**oxicity) properties are crucial. In order for a drug to come into effect, absorption and the ability to pass cellular membranes is obviously important. LIPINSKI *et al.* published in 1997 their famous "Rules of five" "to estimate the solubility and permeability in discovery and development settings" [79], LIPINSKI's "Rules of five" are given in Figure 11.

According to LIPINSKI *et al.* poor absorption or permeation of a compound are more likely when:

i) There are more then 5 H-bond donors (sum of OH's and NH's)

ii) The molecular weight is over 500 u

iii) The LogP is over 5

iv) There are more than 10 H-bond acceptors (sum of N's and O's)

v) Compound classes that are substrates for biological transporters are exceptions to the rule.

Figure 11: LIPINSKI's rules of five to estimate the oral bioavailability of drug candidates.

Generally, when a compound is breaking more than one of the "Rules of five" it is considered to be a problematic candidate regarding permeability and solubility. However, for the natural product chemist LIPINSKI's fifth rule is the most important one. LIPINSKI and his co-authors at Pfizer recognized in their original study that natural products such as vitamins, cardiac glycosides and antibiotics frequently break more than one Lipinski-rule but still show excellent bioavailability because they are substrate to transporters, thus being able to overcome poor passive permeability.

The pharmacological properties of natural products were further investigated by GANESAN, who looked into the 24 unique natural products that led to an approved drug within the timespan between 1981 and 2006 according to strict criteria [38]. All the molecules, which were based on or could be traced down to metabolites (*e.g.* nucleoside analogues) or common human metabolites such as neurotransmitters, were excluded since they are more a result of drug design than natural product discovery. Also, derivatives of known structures or those based on a natural products discovered before 1970 were excluded leaving 24 candidates for further investigation. The purpose of this study was to investigate the properties of successful natural product drug candidates and leads as LIPINSKI did on "successful" (clinical phase II) compounds in medicinal chemistry programs. Five of the 24 compounds originated from plants and 19 from microorganisms. Four of the microbial compounds originated from fungi, 13 from actinobacteria and two from bacteria other than actinobacteria, which exemplifies the biosynthetic capacity of actinobacteria. When investigating the molecules upon their compliance with Lipinski's rules of five, the 24 molecules could be divided into two subgroups. One half (n = 12) of the molecules were compliant with Lipinski's rule and another half was having Lipinski descriptors that placed them out of the "Lipinski space". Interestingly, 50% of both groups became orally administrated drugs and 17 of the 24 compounds progressed "directly" into a drug without chemical modification. The drugs

that do not belong to the “Lipinski space” are however remarkably compliant regarding their logP value, indicating that this is the most important descriptor. The average molecular weight is 319 u for the compounds lying within “lipinsky space” and 917 u for those outside it, the average logP values were 0.0 and 2.2 respectively. The logP differs remarkably little while the average molecular weight is threefold bigger in the latter group. Natural products may employ polar functional groups and intramolecular H-bonds to maintain a low logP and favourable desolvation properties. Those intramolecular H-bonds represent a property of natural products that is difficult to design on purpose by medicinal chemistry. Regarding their stereochemistry, the two groups of natural products show on average 4 and 13 stereogenic centres, which is in approximate correlation with the increase in molecular weight. The complexity of natural products may discourage lead optimization as being reason for the fact that a relative high number of unaltered natural products end up as drugs. When discussing the different chemical properties of natural products and synthetic molecules the reason can be found in the difference of their synthesis, which are given in Table 2. Biosynthesis and synthesis rely on different principles causing different product properties. However, the favourable chemical properties of natural products and as GANESAN stated, to meet an unmet medical need are important factors for making up a successful drug [38].

Table 2: Differences between biosynthesis and synthesis according to GANESAN [38].

	Biosynthesis	**Synthesis**
Building blocs	Few	Many
Strategy	Branching of intermediate	Alteration of building block
Scaffold diversity	High	Low
Functional group tolerance	High	Low
Novel motifs	Common	Rare
C-H activation	Common, site-specific	Rare
Stereocontrol	Easy, enantioselective	Difficult, case-by-case basis

2.4 Privileged structures in natural products, the repetitive structural patterns in bioactivity

A genuine scientist would not be satisfied with the explanation that screening natural products "by coincidence" yields a higher hit rate. In addition would he ask for a root cause why natural products do have other favourable chemical properties that make them promising drug leads or drug substances. Obviously, natural products and synthetic compounds show different chemical properties and natural products are yielding a higher hit rate in screens, *vide supra*. But where lies the reason for that?

For some natural products, the medical or better technical application is based upon their natural function and the pharmacological effect they mediate is related to their toxic or "intentional" bioactivity. This accounts for example for the digitalis glycosides. They are toxins, which most probably protect the plant from predation and have evolved to be cardio toxic. But when they are correctly dosed in the form of Digoxin they are used to treat patients suffering from arterial fibrillation [80]. The question is why for example drugs like artemisinin from the plant *Artemisia annua* provide a malaria medication due to their anti-plasmodial effect [81]. Or why is rapamycin, produced by the bacterium *Streptomyces hygroscopicus* working as an immunosuppressive agent having at the same time anti-fungal activity [82,83]? Most of the microbial metabolites which have drug-like properties and which may be developed into drugs, have most likely not evolved to interact with targets in the human body [76].

Bioactive molecules in general and drugs in particular exhibit bioactivity by either unspecific reactions such as surfactants [84] or by specific interactions with drug targets. Drug targets are mostly proteins, such as receptors, ion channels and **G-p**rotein **c**oupled **r**eceptors (GPCRs). The site of interaction of a drug can thereby be a human protein or a protein belonging to a (human) pathogen [85]. In Figure 12. an overview over the targets of small molecular FDA approved drugs (not including biologics and vaccines) is given. The number of targets separated by target-organism (human or pathogen) and drug-target-class (protein or other biomolecule) is given in the pie chart to the left and the quantitative distribution of the protein families according to the number of drugs targeting them are given to the right. For small molecules proteins represent the main drug target with 98% of the small molecular drug targets being proteins either of human or pathogen origin and almost ¾ of the drug targets are human proteins [85]. It can therefore be concluded that for 98% of the drugs, proteins are the target class they have to interact with in order to have a physiologic effect.

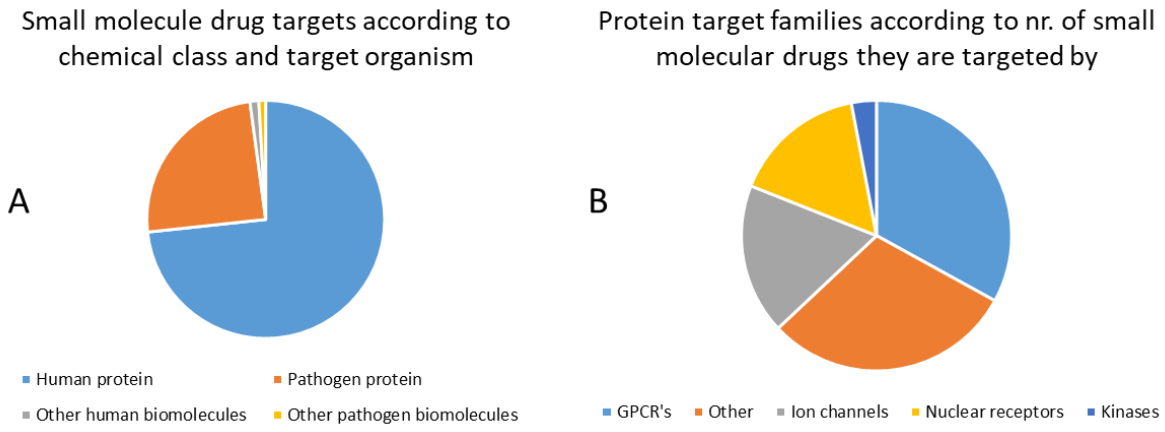

Figure 12: Targets of small molecule drugs (exclusive biologics and vaccines). A: Drugs according to their target class in humans and pathogens. 549 drugs targeting human proteins, 184 drugs targeting pathogen proteins, nine are targeting other human biomolecules and seven are targeting other biomolecules of pathogens. B: Small molecule drugs grouped according to their target families. 33% GPCR's, 30% others, 18% ion channels and 3% kinases [85].

The term privileged structures was introduced by EVANS *et al.* at Merck (US) who observed that derivatives of benzodiazepines do not only bind to the CNS benzodiazepine receptors but also CNS and peripheral cholecystokinin receptors with high affinity [86]. This was surprising since they have little similarity with the natural ligands of those receptors [86]. The recognition of the fact that some structures are predestined to interact with proteins, such as pyrimidine, oxopiperazine and benzopyran, lead to the successful application of privileged structures as building block for privileged-structure-based DOS (pDOS) screening libraries [87]. Proteins, which are mostly the target of drugs or bioactive molecules (see Figure 12), are consisting of domains. Protein domains are protein subunits of 100-150 AA and

fold independently into a structural subunit of the protein they are part of [88,89]. For eukaryotes the characteristic domain size (125 AA) is different from the domain size of prokaryotes (150 AA) [90]. The size of a domain underlies physical limitations and an optimal domain size was calculated to be 100 AA [89]. The physical limitations of protein domains are furthermore reflected by the high conservation of structural motives, protein structure is evolutionary three to ten times more conserved than amino acid sequence [91]. Existing physical constrains lead in consequence to a limited number of protein domains. The protein data bank (PDB, rcsb.org) [92] lists by end of 2019 n = 141587 X-ray structures of proteins or protein fragments or domains, n = 9665 of them were added to the PDB in 2019. The number of protein structures in the PDB is increasing and also the number of new structures added per year increases, see Figure 13 A. However, when looking at the unique folds discovered per year a different picture appears. Since the first submission the number of unique folds discovered per year was increasing from 1976 peaking in 1999 with 118 new folds annually and declining until 2010 with the last folds discovered in 2011 (two) and 2012 (one) (see Figure 13 B, identification of unique folding topologies according to CATH 4.0.0 [93]). In sum, the number of unique folds discovered to date is n = 1375. The number of identified folds remains stable while the number of protein structures increases ongoingly, indicating that the number of folds is limited. It is important to recognize that those unique fold topologies make up all the proteins in all organisms.

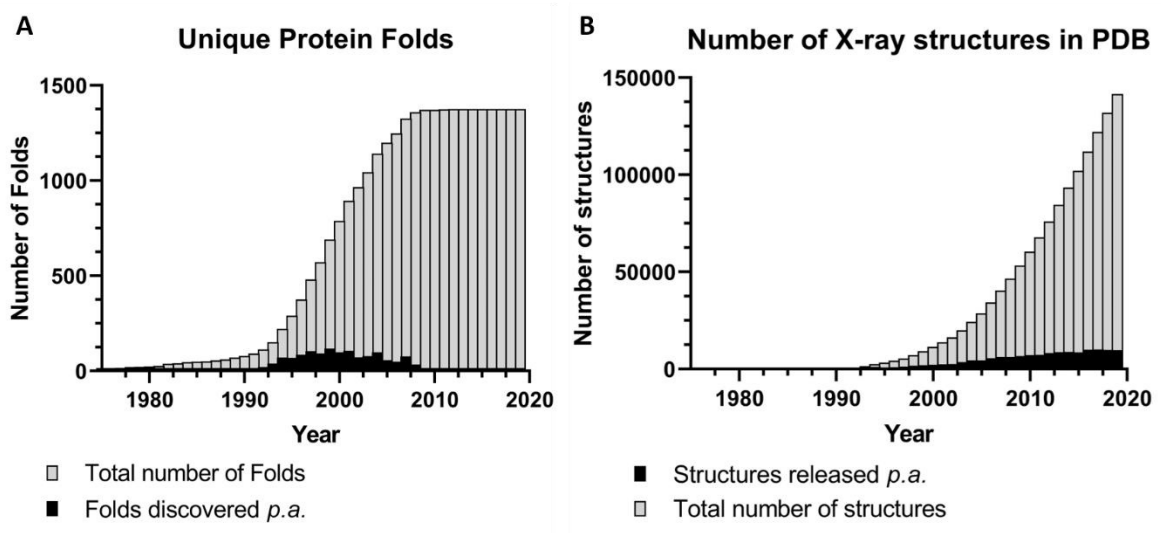

Figure 13: A: Unique protein folds in PDB. In black the number of new unique protein folds discovered by year and in grey the total number of unique folds in the PDB, stagnating at n = 1375 since 2012. B: Number of X-ray structure entries in the PDB. In grey the total number of X-ray structures and in black the number of structures added per year. By the end of 2019 there were n = 141587 structures deposited in the PDB of which 9665 were added throughout the year (rscb.org).

The limited space of proteins or better protein domains is giving a rational explanation for the fact that natural products make up formidable ligands and thereby potential drugs. Natural products are products of biosynthetic pathways employing enzymes, able to interact with natural products as well as their building blocks and some of the natural products are meant to interact with receptors, enzymes and other types of proteins as targets [94]. Given the limited number of folding motives, natural products are more likely to be privileged structures because they are capable of interactions with proteins due to their synthesis and/or their biological function [94,95]. The potential number of small molecules with a molecular weight <500 u on the other hand is as big as 10^{63} [96] not to speak of the further combinatorial explosion when going to higher molecular weights. Natural products seem therefore to be a very suitable way to narrow down the number of candidates to test, since they have proven to interact somehow with the several magnitudes smaller chemical space of protein domains. To summarize:

i. Drugs are merely targeting proteins
ii. Natural products are products of enzymatic biosynthesis* and often ligand to proteins
iii. There is a limited number of underlying folding motives making up all proteins

* The biosynthesis of a given natural product involves many reactions catalysed by a number of enzymes and in the case of NRPs or PKs the biosynthetic enzymes are big multi-domain enzymes. Therefore, the product has bound to a high number of protein domains making it more likely to be "privileged" for ligand-protein interaction.

I think the following quote summarises and lines out the consequences of the "limited number of protein domains" in a very literary way:

> *"You can ignore the fact that natural products have not evolved to interact with humans specifically. The point is natural products have evolved to interact with something and that something may not be so different from human proteins."*
>
> J. MEINWALD

3 Taxonomic ranks of bacteria that are prolific producers of secondary metabolites

When looking at the bacterial realm, the biosynthetic potential for secondary metabolites is not equally distributed, and some taxonomic ranks stand out among the others regarding their biosynthetic potential. Those genera are of particular interest for natural product research.

3.1 Actinobacteria

The actinobacteria, that were already mentioned, are the most prolific producers of bioactive metabolites in the bacterial kingdom. This is exemplified by the aforementioned study of GANESAN were 12 of the 24 unique natural products leading to drugs between 1981 and 2006 originated from actinobacteria [38]. Within the actinobacteria, the genus *Streptomyces* has been the most prolific producer of antibiotics and bioactive compounds and some estimations say that the majority of antibiotics from *Streptomyces* are to be discovered [37,97,98]. Actinobacteria are Gram-positive bacteria with high G + C content and are spread over terrestrial, aquatic and marine ecosystems [99]. They are spore forming filamentous bacteria with a high phenotypic diversity forming multicellular mycelia [99]. The genomes of *Actinomycetes* harbour a high number of biosynthetic gene clusters, in particular PKS and NRPS clusters [100]. Up to 5% of an actinobacterial genome can consist of biosynthetic gene clusters and the genome size for *Streptomycetes* ranges from 8-10 Mb. All *Streptomycetes* and some *Actinomycetes* possess linear genomes, breaking the rule that prokaryotes possess only circular chromosomes [100]. Besides the genus *Streptomyces* the so called “rare actinobactreia” (non-*Streptomyces* actinobacteria), including isolates from marine ecosystems, have moved into the focus during recent years in order to discover new bioactive metabolites [101,102].

3.2 Myxobacteria

One bacterial order that possesses many physiologic, genetic and macroscopic curiosities at the same time is the order myxobacteria. Myxobacteria show probably the most complex lifecycles and physical actions within the bacterial realm. Taxonomically they are Gram-positive δ-proteobacteria with the ability to form biofilms and to move towards nutrient sources. They possess the ability to glide over surfaces in order to “hunt” other bacteria and fungi, which they lyse by excretion of bacteriolytic enzymes [103,104]. Under unfavourable conditions, myxobacteria are capable of spore-formation in

macroscopic fruiting bodies [104]. This physiological complexity is reflected by the genome size of the members of that order ranging from 9 to 12.5 Mb [104,105]. Their genomes contain a high number of PKS-, NRPS-, and NRPS/PKS-hybrid-clusters and antibiotics of these classes have been isolated from myxobacteria [105,106]. While it was previously assumed that myxobacteria were terrestrial organisms, but halotolerant and obligate marine myxobacteria have now been reported [104]. Notably, the isolation and cultivation of myxobacteria is difficult and represents an high effort of laboratory work compared to most other bacterial phyla, making them a less investigated resource for natural product discovery [105].

3.3 Cyanobacteria

Cyanobacteria are photoautotrophic bacteria present in terrestrial and aquatic ecosystems using chlorophyll a as primary photosynthetic pigment [107,108]. On a cellular level, cyanobacteria show unicellular organization but they form filaments, mats and colonies as well [109]. Cyanobacteria show a high grade of cellular differentiation leading to highly specialized cell types and some are capable of true branching and complex reproduction *via* binary fission [110,111]. Beside their photosynthetic activity, many cyanobacteria have the capacity to fixate atmospheric nitrogen. This takes place in heterocysts which are highly specialized cells that are not capable of photosynthesis but fixing nitrogen [108]. More than 1100 secondary metabolites with different chemical structures were isolated from 39 cyanobacterial genera [112]. The most well-known effect of cyanobacterial secondary metabolites is intoxication of humans and animals *e.g.* from cyanobacterial water blooms [113,114]. The secondary metabolites of cyanobacteria are often products of NRPS and PKS type biosynthesis [115]. Another interesting family of cyanobacterial metabolites are peptides that are ribosomally synthesized and posttranslationally modified peptides (RiPPs) such as lantipeptides [116]. Over all, cyanobacteria are prolific producers of bioactive secondary metabolites of which some are unique to cyanobacteria [117].

3.4 Genome size and complex life cycles, indicators for the biosynthetic potential of bacteria.

The bacteria that are of particular interest as a source for bioactive secondary metabolites have apparently in common that their life cycles and cellular organization are complex. Another observation is the correlation between the biosynthetic potential and genome size of bacteria. In 2007 DONADIO *et al*. investigated 223 sequenced bacterial genomes upon the presence of thiotemplate systems (NRPS and PKS) [118]. They found that those are not present or rare in genomes under 3 Mb [118], this follows the

logic that those big biosynthetic machineries and clusters need to be harboured within the genome in addition to the primary metabolism. There are of course exceptions to this rule, however when reviewing the literature one can conclude that those exceptions are very rare. In addition to the genome size, the above-mentioned bacteria have in common that their life cycle, morphology and physiology is complex compared with the commonly not differentiated unicellular physiology of procarya. It has been stated for the cyanobacteria that they have developed beyond the microbial existence and need protection from macrograzers for which they developed an armament of toxins and deterrents for protection [119].

The same could possibly apply for the myxobacteria and actinobacteria. They form macroscopically visible multicellular structures, which represents a physiological effort. They are in addition rather slow growing bacteria. A slow growing but complex organism will at some point need protection from microbial overgrowth, predation, fouling *etc*. which would explain the production of bioactive secondary metabolites by the abovementioned bacterial phyla.

4 Need for new drugs and drug leads

There are several disease classes needing improved medication and sometimes the reasons for that are interconnected, since many fields of medicine such as surgery and cancer therapy depend indirectly on antibiotics. In case of the diseases that are related to age, it is important to keep in mind that "aging populations" or a demographic shift is considered a megatrend.

For the antibiotics we face the problem of antibiotic resistance where some pathogens developing resistance with increasing prevalence. A relatively small group of bacteria, namely *Enterococcus faecium*, *Staphylococcus aureus*, *Klebsiella pneumonia*e, *Acinetobacter baumanni*, *Pseudomonas aeruginosa* and *Enterobacter* sp. are causing the bulk of problematic infections in hospitals [120]. In 2016 a 70 years old woman in Nevada, US, died of an infection caused by a *Klebsialla pneumoniae* isolate resistant against 26 antibiotics [121]. The infection was probably acquired in India and its causing pathogen was resistant against all 26 antibiotics available in the US [122]. Currently there are estimations that 700'000 people dying *p.a.* of **a**nti**m**icrobial **r**esistance (AMR) and predictions that 10 million people will die of AMR in 2050 [123].

Another risk to our health and life and a burden to our health system is cancer. Currently it is estimated that about 8,2 million people are dying *p.a.* of cancer [123]. This current number is likely to increase since our population is aging and with an increasing age the incidence of cancer will increase too [124,125].

Over more, the issue of AMR indirectly affects patients that are not primarily suffering of infections. Cancer patients for example need antibiotics throughout their treatment because of surgeries and a compromised immune system due to chemotherapeutic agents. The field of surgery relies on antibiotics to treat opportunistically occurring infections that may occur during the procedure. Looking on those developments and in addition keeping the aging population in mind, the need for new chemotherapeutic and antibiotic agents is apparent. Natural products served as a source for antibiotics and chemotherapeutics and are likely to do so in the future [97,126].

5 Process and techniques of natural product discovery

5.1 Cultivation and extraction of bacteria

Searching for new bacterial metabolites starts commonly with cultivation and extraction of bacteria. As now commonly known, not all bacteria can be easily isolated and cultivated under laboratory conditions but it is also a question of practical cultivation effort and of sampling new or less investigated ecosystems to find and isolate hereto uncultivated bacteria [127-129]. It is possible to isolate specific bacterial genera that are known for their capacity of secondary metabolite synthesis (such as actinobacteria and myxobacteria) [129-132]. To isolate bacteria and get them into culture is just the first prerequisite to yield secondary metabolites; the second one is to trigger the production of secondary metabolites, which is not always a trivial task. One strategy can be the OSMAC (**o**ne **s**train **m**any **c**ultures) approach where culture conditions are varied [133] another one is co-cultivation of the bacteria of interest with other microorganisms [134,135]. To test for bioactivity and finally for isolation of compounds, the cultures are often extracted using liquid-liquid phase or liquid-solid phase extraction. The fermentation broth or extract of bacteria finally is the starting material for the subsequent biodiscovery-process.

5.2 High performance liquid chromatography

High Performance Liquid Chromatography (HPLC) is a technique for separating analytes according to their physicochemical properties. For separating the analytes, a mobile phase (liquid) and a stationary (solid) phase are used. In principle, HPLC is employing the same basic chemical principle as manual column chromatography or thin layer chromatography. One reason for the high chromatographic resolution in HPLC when separating the analytes is the small particle size of the stationary phase of

around 5 µm (down to 2.5 µm) which results in a high pressure (upper instrumentation and column pressure limit of commonly ~ 400 bar, maximal 600 bar) under which the mobile phase is pumped through the stationary phase. In the most common chromatographic experiments, the analytes are separated according the following molecular properties:

i. according to their polarity (**n**ormal **p**hase and **r**eversed **p**hase (NP/RP) chromatography)
ii. according to their molecular weight (**s**ize **e**xclusion **c**hromatography, SEC)
iii. according to their charge (**c**ation/ **a**nion **e**xchange **c**hromatography CEX, AEX)
iv. according to affinity (affinity chromatography)

In HPLC instruments, the principle of chromatographic separation is automated. A theoretical setup of an HPLC system is given in Figure 14, the function of the whole system is essentially to apply (load) the sample onto the column and to pump solvent, mostly as a gradient of two solvents, trough the column. The column is the compartment where the analytes get separated. The analytes eluting from the column (eluents) are commonly detected by a DAD or other kind of UV/Vis detector. Other detector-types may be employed as well, such as a refractometer or a mass spectrometer using electrospray ionization. For preparative HPLC the eluents are collected by a fraction collector either continuously or triggered by a signal (*e.g.* retention time, UV/Vis detector, MS (*m/z*) signal). The coupling of HPLC systems to a mass spectrometer is a very powerful technique not only for analytical setups but also for preparative applications. Because of its high resolution when working with complex mixtures of organic molecules, RP-HPLC is commonly used for analysis and for preparation of natural products. Resolution in the context of chromatography means the separation of analytes represented by their respective peaks in a chromatogram. A seperation is given when two analytes are separated, which means the two peaks are separated either by baseline or by given Rayleigh-criteria. The more similar the molecules are that can be separated (*e.g.* difference in one double bond or chiral separation), the higher the chromatographic resolution is. For RP-HPLC a matrix, commonly silica, is functionalized with nonpolar functional groups such as C8 ($R-(CH_2)_7-CH_3$), C18 ($R-(CH_2)_{17}-CH_3$), or fluorophenyl groups, just to mention a few. The stationary phase is thereon apolar while the **m**obile **p**hase (MP) is polar (water/more polar solvent) and changing its composition in a gradient, from example 100% of aquatic MP (A) to 100% of organic MP (B), *e.g.* acetonitrile. Importantly the two components have to be miscible. Throughout the gradient, the composition of MP changes and its elutive effect increases (for instance trough a lower polarity or a higher pi-electron share in the organic MP (B)), which elutes analytes gradually from the column. The analytes elute when their dissolvation is preferred over their interaction with the column material. To improve the separation of analytes according to their polarity, the mobile

phase (A+B) is commonly acidified (commonly formic acid or trifluoroacetic acid) for protonation of functional groups. The charge of functional groups can alter the polarity of an analyte, when protonated trough a low pH of the MP, this effect is suppressed. The peak shape is improved by constantly protonating the analytes and silanol groups on the stationary phase.

Ultra high performance liquid chromatography (UHPLC) is an improvement of HPLC where columns are used that are packed with a solid phase that possesses a particle size smaller than 2 µm [136]. This causes an increased pre-column pressure. Therefore, UHPLC systems have a higher pressure limit of up to 1200-1400 bar [136,137]. For the analyst the setup results in a better separation of the analytes (through narrower peaks) in a given time, UHPLC is therefore very suitable to analyse complex mixtures, such as extracts of bacterial cultures, plants and other organisms. Detectors, such as DAD or MS detectors have to have an appropriate data collection rate for UHPLC systems. This applies especially to MS detectors that need to have an appropriate scan rate [136,138].

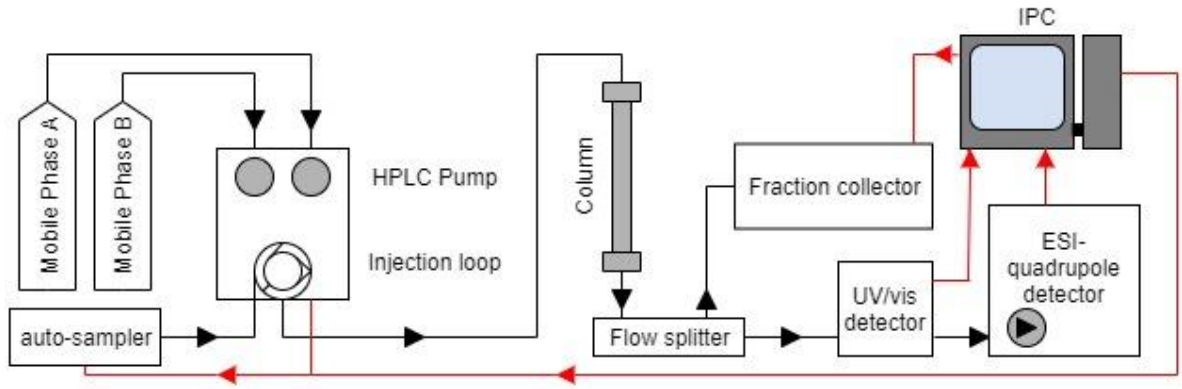

Figure 14: HPLC system for natural product isolation (simplified). The depicted system shows a HPLC system equipped with a gradient pump, auto sampler, fraction collector, **i**nstrument **PC** (IPC), UV/Vis and MS-detector. The isolation guided by mass spectrometry enables the operator to specifically isolate compounds that were identified by high resolution MS. The solvent-flow is depicted in black and the electronic control/"signal-flow" in red (simplified).

5.3 Mass spectrometry and dereplication

"A mass spectrometer is an instrument that generates a jet of gaseous ions out of a sample, separates them by mass and charge and generates a mass spectrum" [139]. In Figure 15, a schematic **m**ass **s**pectrometer (MS) is shown. In a MS the molecules in a sample are ionized and the ions are accelerated in an electrical field. Thereafter the ions are separated according to their mass to charge ratio using *e.g.* **T**ime **o**f **F**light (ToF) or quadrupole mass filters. Thereafter the separated ions are detected and

transformed into a signal. The signal output is given as an *m/z* value (mass per charge). It is the mass of an ion in u divided by its charge, which is commonly plus/minus one for small molecules, but even in a mass range <1000 u double charged (bivalent) ions occur frequently. Those bivalent ions can easily be identified by their isotope distribution, when the isotope signals (called isotope satellites) of an analyte are not distinct by full numbers (n × *m/z* unit) it indicates a bivalent (or higher) ion [139].

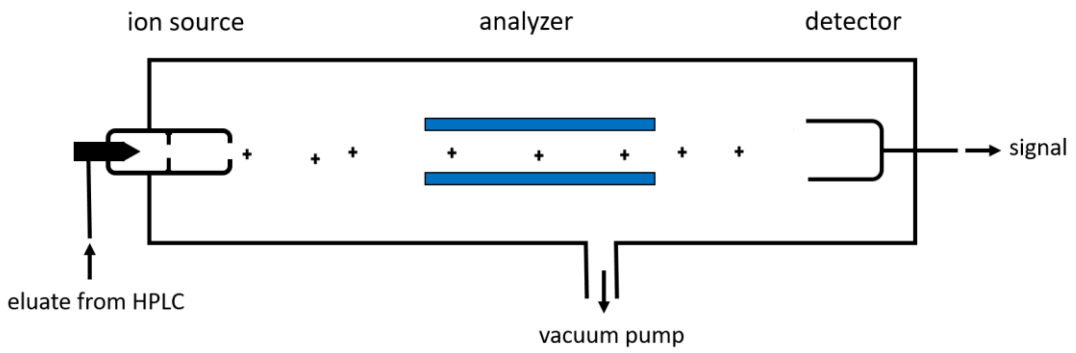

Figure 15: Schematic function of a mass spectrometer. To the right the ion source is generating ions that are accelerated in an electric field (in this example by ES-ionization, see Figure 16). The analyzer, *e.g.* quadrupole, is separating the ions according to their charge and mass and the detector (electron multiplier) detects the separated ions. Separation in the analyzer is done by distraction in electromagnetic field, ions with different molecular weights but the same charge will be distracted according to their *m/z* value. In order to enable the ion-beam to move through the instrument it has to be evacuated. Adopted from [140].

For natural product scientists the coupling of an HPLC to an electrospray mass spectrometer is a powerful technique because it enables the separation of a complex mixture and mass spectrometric analysis of the metabolites. The *m/z* value reveals the molecular weight of an analyte and with high resolution MS data calculation of its elemental composition is possible. The technique that enabled HPLC-MS coupling is electrospray ionization (ESI). Primarily electron impact ionization (EI) was the "state of the art", commonly coupled to gas chromatography for separation of complex mixtures. However, for EI, analytes need to be volatile (at elevated temperatures) and it is not directly compatible with HPLC due to the need for removal of the HPLC solvents. Electrospray ionization is however capable of ionizing the eluents in a mobile phase, its principle is shown in Figure 16 and its function is described below. ESI is capable of generating positive and negative ions, some analytes ionize (only) in positive ESI mode (proton accepting groups) and some (only) in negative ESI (proton donating groups) mode [141], because of the different functional groups that are often present in natural products commonly ionization on both modes but also increased ionization in one can be observed. In EI ionization the molecules in gas phase get ionized by impact of electrons (~70 eV), the odd electron ions generated in EI ionization often possess a high inner energy causing fragmentation of the ionized molecule into fragment ions [142,143]. ESI ionization does rarely cause fragmentation, which is on one

hand desirable to obtain the molecular weight of an analyte [141]. On the other hand, fragmentation can provide valuable information; common fragments can indicate chemical groups (*e.g.* glycosylation, sulphate) or identify related molecules. Fragments are also helpful in dereplicating molecules where there are many structures for a certain elemental composition. Searching databases using mass spectrometric (*i.e.* elemental composition and fragments) data is a common workflow in identification of analytes and dereplication of natural products [143]. Fragmentation using ESI-mass spectrometry can be achieved by using tandem mass spectrometers where a collision camber filled with (inert) collision gas (commonly N_2 or Ar) is placed between two mass analyzers [143]. **H**igh **r**esolution **m**ass **s**pectrometry (HR-MS) is capable of measuring *m/z* values to an accuracy of 10^{-4} *m/z* units, enabling the correct calculation of elemental formulas. Tandem HR-MS is therefore a valuable tool in analysing complex mixtures of natural products since it delivers the exact mass [144] and it is capable of distinguishing between molecules that are close in their molecular weight. The fragment data that is acquired in tandem MS experiments, enables not only the identification of molecules, it can give furthermore structural information that can aid structure elucidation [145].

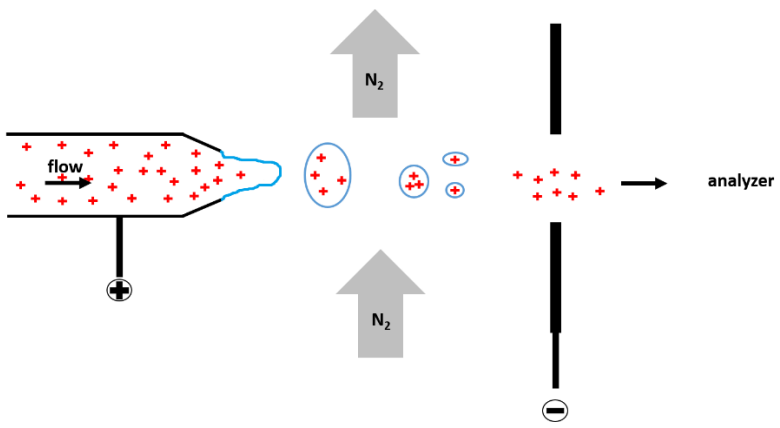

Figure 16: Electrospray ionization, adopted and changed from [139]. The purpose of ESI is to transform analytes in solvent into gaseous ions that can be analyzed. Therefore the liquid is pumped trough a positively charged capillary. At the end of the capillary drops form that disperse into smaller droplets, first, because of repulsion of the charges and second because a stream of drying gas is evaporating solvent from the droplets and at the end of the process a jet of gaseous ions can be directed to the analyzer. In addition, the ion source is heated up to increase the rate of solvent evaporation. The charges get accelerated by the charge difference of the aperture generating an electric field. In the figure, an ion source working in ESI+ mode is shown, generating positively charged ions. In ESI- the charges and voltage in Figure 16 would be simply inverse, generating negative ions.

When an extract of an organism is identified as active, it is important to identify the possibly active compounds within the mixture and prioritize them. Often the activity is caused by a compound that is already known and therefore not worth to be isolated. HPLC-MS analysis of an extract provides a solution for that problem, especially when coupled with database search for the identification of known molecules [27,146]. Additional data for decision making in analytics and dereplication can be provided

by a UV/Vis or DAD detector, which is commonly coupled to an HPLC [147,148]. It provides additional information and can either confirm or invalidate a potentially identified molecule according to published UV/Vis spectra or UV/Vis active functional groups. To compare the data of active and inactive fractions of an extract can also help to conclude on the possibly bioactive compounds. However, dereplication is a complex task that is implemented in the bioprospecting workflow, exemplified by the one described in chapter 4.4.

In order to be certain about a compounds identity, it can be necessary to isolate a candidate and take a first NMR spectrum, maybe insufficient for structure elucidation but enough to decide if the compound is most likely known. It can also be a viable strategy to isolate a small sub-mg quantity of a candidate compound just to confirm its bioactivity using the assay where the extract was active. This is a viable strategy especially when exclusively looking for bioactive compounds. To quote my supervisor ESPEN HANSEN, dereplication is about "reaching a certain degree of certainty".

5.4 The bioprospecting workflow

A bioprospecting workflow for bioassay-guided bioprospecting is exemplified in Figure 17. When detecting that a certain extract has bioactivity, the first thing to be checked if there is a known metabolite responsible for the bioactivity during dereplication [27,146].

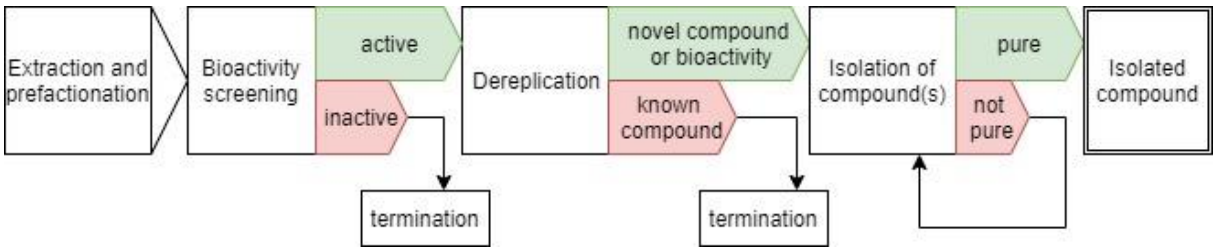

Figure 17: Bioprospecting workflow using bioassay guided purification [149].

The isolation of a natural product can be done guided by bioactivity (bioassay guided purification) or using chemical assays, *e.g.* mass spectrometry (looking for certain diagnostic fragments) or chemical assays to detect for instance siderophores [150,151]. One can decide upon a mass spectrum of a compound to isolate it because it shows interesting chemical composition such as halogenation or *e.g.* fragments that indicate similarity to other compounds of interest. Finally, it is a combination of initial extract bioactivity screening, screening of the isolated compound(s) for confirmation and mass

spectrometry for identification and priorization of candidates that seems most promising for discovering new bioactive metabolites *. Prefractionation of an extract before screening and dereplication can help to reduce the complexity of the extract and to ease the identification of its active principle(s) [152].

Different bioassays and chemical assays are used in bioprospecting, and they depend on what one is looking for (anti-cancer, anti-microbial or a specific target such as a receptor, kinase or an enzyme). But especially for the initial screening of extracts one should consider that phenotype based assays (assays based on whole cells/organisms, in HTS this applies rather for cell based assays) are more successful than target based assays in delivering new "first in class" drugs [153]. When using cell (or animal) based screens, the screen does not depend on a specific molecular mode of action, it will not discriminate between all the possible mode of actions within the cell or animal. In target based screens there is just the screened target that can be addressed by the potential ligand or effector [154,155]. However, for developing follow up drugs (not first in class/ no new mode of action) for known targets, target-based screens have been proven to be a suitable strategy [154].

* The strict separation into bioassay guided and chemistry guided purification is in my opinion more an idealized model with little practical meaning. The workflow in Figure 14 is for example employing mass spectrometry for derelpication, which is a genuine physical-chemical technique.

5.5 Structure elucidation

Structure elucidation of natural products is mainly done by **n**uclear **m**agnetic **r**esonance (NMR) spectroscopy. 1D and 2D NMR experiments are the main techniques for structure elucidation of small molecules in natural product chemistry. NMR relies on the nuclear spin of NMR active nuclei (^{1}H, ^{13}C) and their resonance to radiofrequency when their energy states are excited by a strong applied magnetic field. The NMR spectrum enables the operator to conclude the electric environment and neighbouring nuclei. There are plenty of experiments (pulse sequences) that can reveal the relative location and connection of nuclei over one or more bonds or through space. A great advantage of NMR is the fact that the method is not using up the sample, similar to taking up a UV/Vis spectrum in a photometer, the sample can be regained. Improvements in NMR techniques and equipment enabled the structure elucidation down to a sample size of 1 mg [156], optimal are 5-10 mg, generally depending on the size and proton content of the compound.

To solve the structure of a molecule by NMR alone would be a difficult task without having additional information provided by high resolution MS which is in particular the exact mass to calculate the elemental composition of a compound. In addition to that, chemical techniques like hydrolysis and pre-column derivatization can be used to reveal the building blocks of a natural product (*e.g.* an NRP) and

the stereochemistry of the respective building block if a standard is available [157]. A technique that is less frequently employed in natural product chemistry is X-ray crystallography. X-ray crystallography relies ideally on a crystal of the respective molecule and commonly needs higher compound quantities for structure elucidation than NMR, which can be critical in natural product discovery. In turn, it provides the possibility to reveal the stereochemistry or even the identification of a molecules absolute structure [144].

5.6 Genomics as a new tool in natural product research

During the last two decades, genome mining as a new tool was added to the toolset of natural product scientists, particularly for bacterial bioprospecting. Tools like antiSMASH [158] enable fast and convenient analysis of sequenced genomes for biosynthetic clusters [158]. Genomics do of course not replace the isolation and final testing of a natural product. But identified biosynthetic clusters are an indicator for where to allocate resources since they show if there is a genetic capacity to produce the secondary metabolites one is looking for. The sequencing of the first whole genomes of *Streptomyces* and others revealed that even in well-studied strains there are clusters for which the product is not discovered yet [159]. An intrinsic advantage of genome mining is that it does not rely on the actual production of the secondary metabolite, which maybe is not the case under (the selected) laboratory conditions for cultivation of a bacterial strain [160]. Notably, the decrease in sequencing costs for whole bacterial genomes is crucial for making genome mining widely applicable and paved the path for the development in genome mining including the increasing number of sequenced microbial genomes and biosynthetic gene clusters available [161]. Another strategy that does not rely on whole-genome-sequencing is PCR- based screening (and sequencing of the PCR-product) for PKS and NRPS genes using primers for highly conserved motives of those enzymes [159]. Once the biosynthetic potential of a bacterium is known, it is possible to vary culture conditions or even attempt heterologous expression of an identified biosynthetic gene cluster in order to yield secondary metabolites [162].

Thereon the present techniques for discovering secondary metabolites can be divided into two subsections: The bottom-up and top-down approaches [160]. Top-down approaches start with an organism or biomass as subject of investigation and represent the classical bioassay and/or chemistry guided isolation, while bottom-up approaches start with genetic information. A schematic illustration is given in Figure 18.

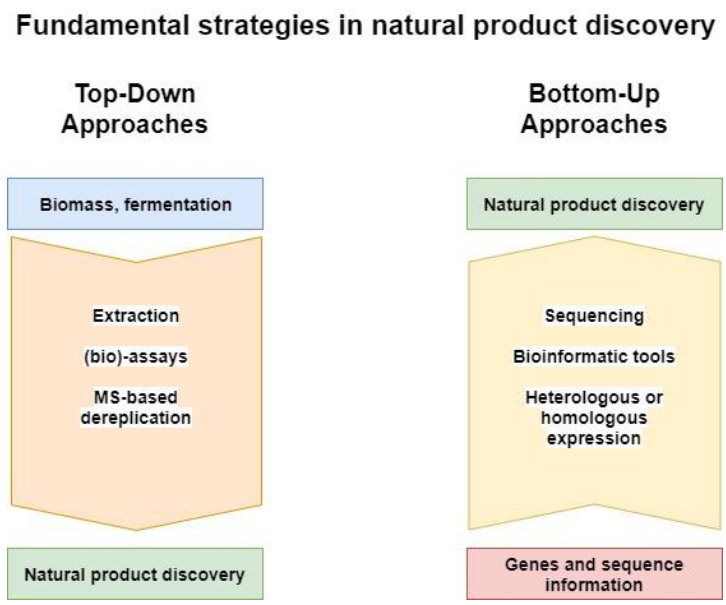

Figure 18: Fundamental strategies in natural product discovery. The toolset of natural product discovery divided in Bottom-Up approaches starting with genetic information and Top-Down approaches which include the common tools of bioprospecting such as chemical dereplication and bioassay guided isolation. With inspiration of [160].

The distinction between two fundamental strategies as illustrated in Figure 18 should however not lead to percept them separately, as two independent silos. It is merely to illustrate the two different underlying principles. The task of a scientist is to select the most appropriate methods of the two strategies that are complementing each other to solve a given problem.

6 Aim of the work

The aims of this work were:

i. Discover new, ideally bioactive bacterial secondary metabolites.

ii. Discover unknown bioactivities of known metabolites.

iii. Investigate the mode of action and natural function of discovered metabolites, if possible.

iv. Investigate the biosynthesis of the metabolites using genomic methods, if possible.

7 Results and discussion of the work

7.1 Summary of papers

Paper I

Anti-Bacterial Effect and Cytotoxicity Assessment of Lipid 430 Isolated from *Algibacter* sp.

Yannik K.-H. Schneider, Kine Ø. Hansen, Johan Isaksson, Sara Ullsten, Espen H. Hansen and Jeanette Hammer Andersen.

Molecules, **2019**, *24*, 3991.

Two the extracts of two bacterial isolates, both belonging to the genus *Algibacter* sp., where showing anti-microbial effect in an initial screening. Cultivation, extraction, fractionation and retesting confirmed the hit of the initial screening. The fact that there was no bioactivity reported from *Algibacter* sp. gave additional motivation to investigate the extracts of the strains. Dereplication of the active fraction resulted in the identification of a molecule with *m/z* 431.3112 ($[M + H]^+$). The candidate, with the elemental composition of $C_{22}H_{42}N_2O_6$, was isolated and structure elucidation *via* NMR proved it to be lipid 430 (see Fig. 19), a short lipopeptide that is known for being a toll like receptor two agonist and virulence factor originally isolated from *Porphyromonas gingivalis*. The study revealed an anti-microbial effect against *Streptococcus agalactiae* with an IC_{50} concentration of around 30 µM. The lipid had an anti-proliferative effect on a melanoma cell line, which was relatively weak (50% inhibition of cell growth at ~ 175 µM). Given its amphiphilic structure, the hypothesis was that the effect was caused by lysing the cells which we investigated using propidium iodide-staining and flow cytometry, a way to measure the membrane integrity of human cells. The results indicate that the compound is not acting as detergent, not directly affecting the membrane integrity of the melanoma cells.

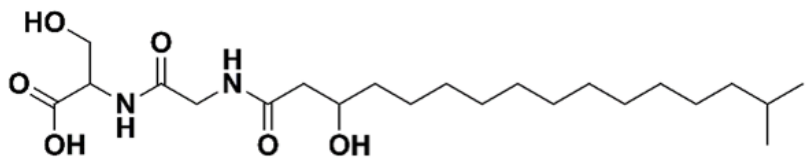

Figure 19: Structure of lipid 430

Paper II

Bioactivity of Serratiochelin A, Produced by *Serratia* sp. in a co-culture with *Shewanella* sp.

Yannik Schneider[†], Marte Jenssen[†], Johan Isaksson, Kine Ø. Hansen, Jeanette Hammer Andersen and Espen H. Hansen.

Microorganisms, **2020**, *8*, 1042.

[†] Those authors contributed equally to the article

Serratiochelin A is a siderophore exclusive to the genus *Serratia* sp. During investigation of UHPLC-MS data of bacterial extracts, one isolate appeared to produce a compound with *m/z* = 430.1594. The compound was produced in DVR1 medium but not in same medium supplemented with 160 µM Fe in form of $FeSO_4$. Serratiochelin A was isolated from the culture. The degradation of serratiochelin A to serratiochelin C (hydrolysis of its oxazoline ring, see Figure 20) made it necessary to adapt the purification protocol that enabled separation without acidified mobile phase. The structures of serratiochelines A-C, their ability to chelate iron and the liability for hydrolysis of serratiochelin A was already published. However, there was no further investigation of bioactivity done on serratiochelines, maybe partly owed to its chemical properties. While serratiochelin C did not show any bioactivity, serratiochelin A had an anti-bacterial effect on *Staphylococcus aureus* but not on the other tested bacteria *Escherichia coli*, *Enterococcus faecialis*, *Streptococcus agalactiae* and MRSA. Serratiochelin A had also an anti-proliferative effect on lung fibroblast cells and melanoma cells, while serratiochelin C had none. The two molecules have different bioactivities, despite their high structural similarity. The mode of action is uncertain since serratiochelin A affects specifically *S. aureus* but none of the other tested bacteria. It also affects proliferation of the tested human cell-lines where it affects the lung fibroblasts little more than the melanoma cells.

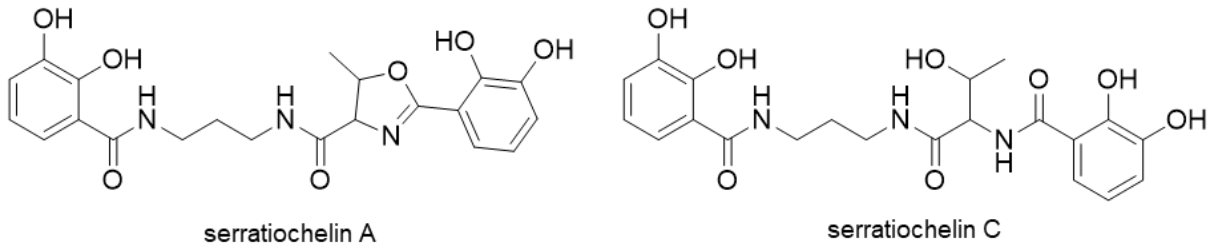

Figure 20: Structures of serratiochelin A (left) and C (right).

Paper III

New suomilides isolated from *Nostoc* sp. KVJ20, bioactivity and biosynthesis

Yannik K.-H. Schneider, Anton Liaimer, Johan Isaksson, Kine Ø. Hansen, Jeanette Hammer Andersen and Espen H. Hansen.

The *Nostoc* sp. isolate KVJ20 was isolated from a liverwort originating from Kvaløya, Tromsø, Norway. UHPLC-MS dereplication of a methanol extract of the cyanobacterial biomass revealed four banyaside/suomilide-like compounds present in the extract with elemental compositions of $C_{39}H_{62}N_8O_{19}S$ (M_{mi} 978.39 u), $C_{41}H_{66}N_8O_{19}S$ (M_{mi} 1006.42 u), $C_{43}H_{68}N_8O_{20}S$ (M_{mi} 1048.43 u), and $C_{45}H_{72}N_8O_{20}S$ (M_{mi} 1076.46 u). The molecules were isolated *via* preparative HPLC and two of their structures were elucidated by 1D and 2D NMR experiments. The structures are given in Figure 21. The structure of S-1006 was proposed upon HR-MS data and we speculate that S-1048 is the previously isolated suomilide A. The molecules turned out to possess the same aglycon as suomilide and differed in the modification of their glycon. The structures showed a highly modified peptide azabicyclononane aglycon, sulfated and glycosylated. The glucose glycons were esterified with short fatty acids and aminoformic acid in different patterns. The modifications of the glycon characterize the respective suomilide. The molecules were tested for biological activities, and since they represent complex chemical entities produced by the same organism, they are expected to have biological function(s). At concentrations up to 100 µM the suomildes had no effect on the biofilm formation of *Staphylococcus epidermidis* or on the growth of the bacteria *Escherichia coli*, *Enterococcus faecalis*, *Staphylococcus aureus*, *Streptococcus agalactiae* or MRSA. Furthermore the compounds did not have any effect on human melanoma cells and a human lung fibroblast cell-line. However, a weak effect on myeloma cells was detected at 100 µM for two of the suomilides. It was in combination with 1% DMSO as solvent, which had already an effect on the cell line as shown by a control. Since the structurally similar banyasides where reported to inhibit enzymatic activity of trypsin a trypsin-inhibition assay was executed with negative outcome. The assumed biological function of the suomilides being complex secondary metabolites remains therefore unknown.

The published genome of KVJ20 enabled us to propose and investigate the biosynthetic gene cluster for for suomilides, which are possessing the characteristic azabicyclononane core. Interestingly the proposed cluster contains merely genes similar to those found in the biosynthetic clusters of aeruginosin (BGC0000297) and saxitoxin (BGC0000887).

Appart from the trypsin inhibition of banyasides there was no bioactivity of suomilides or banyasides reported. The testing of suomilides suggests that their function is neither cytotoxic nor anti-bacterial, biofilm-inhibition or inhibition of trypsin. Interestingly, the suomilides with their distinctive azabicyclononane core structure are product of a biosynthetic cluster that comprises parts of aeruginosin and saxitoxin gene clusters but it synthesizes a chemical structure with significantly differing structural attributes.

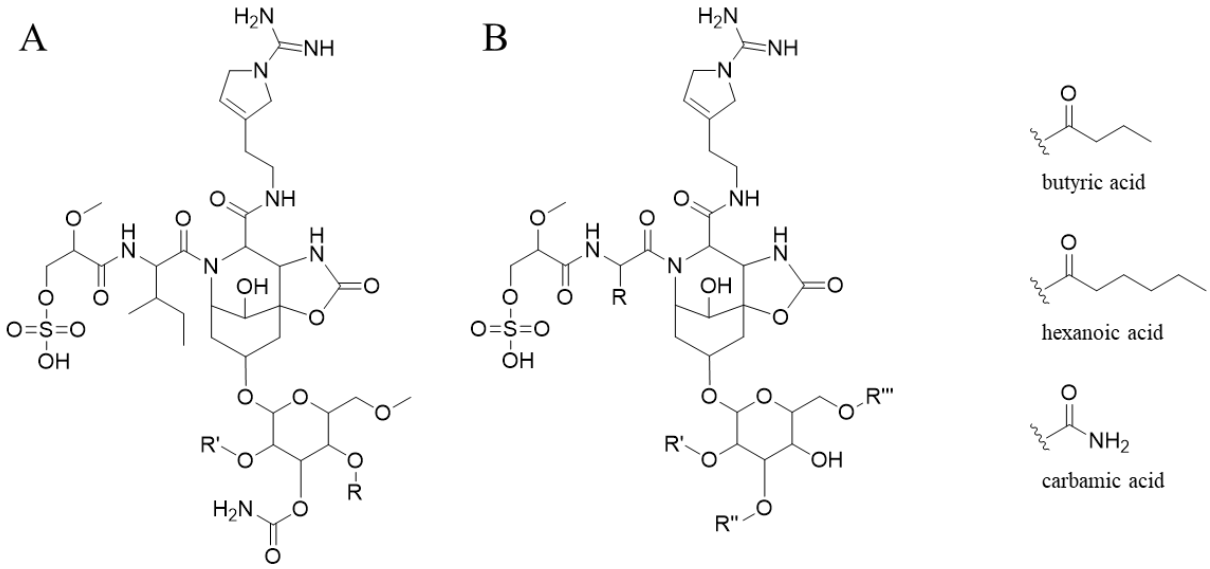

1: R= hexanoic acid, R'= butyric acid
2: R= -H, R'= butyric acid
3: R= hexanoic acid, R'= -H
4: R= isoleucine, R'= hexanoic acid , R''= -H, R'''= hexanoic acid
5: R= leucine, R'= hexanoic acid, R''= carbamic acid, R'''= -H
6: R= leucine, R'= -H, R''= -H. R'''= hexanoic acid

Figure 21: A: Structures of the compounds isolated within this study. Suomilide B (**1**), C (**2**) and S-1006 (**3**) (proposed structure upon HR-MS data). B: Structures of the known compounds suomilide A (**4**) and the banyasides A & B (**5** & **6**). Banyasides posess a leucine were suomildes posess isoleucine. The banyasides and suomildes are characterized by the modification of their glycon *via* esterification with carbamic acid, hexanoic acid and/or butyric acid respectively.

7.2 Discussion and conclusion

All three papers have the common subject of isolation of bioactive or new molecules from bacteria. The basis for the project was a selection of Arctic marine bacteria that were randomly isolated from sediment, sea water and macro-organisms. The first two papers have marine bacteria as subject while Paper III is about molecules isolated from a terrestrial *Nostoc* sp. isolate. The project, as initially planned, started with fifteen bacteria that were isolated from different Arctic marine sources with the aim of discovering new bacterial secondary metabolites in those strains. The bacteria were cultivated (using four different culture media), extracted and pre-fractionated into six fractions in an earlier work. Those fractions were tested in anti-cancer and anti-microbial assays and some yielded bioactivity at concentrations of 25-50 µg crude extract fraction per mL, and were selected for further investigation.

From of this set of extracts of 15 bacterial strains, it was possible to identify lipid 430 as active principle in two extracts of two different *Algibacter* sp. strains. This was, to the best of my knowledge, the first report of a bioactive secondary metabolite isolated from the genus *Algibacter*. The fact that there was no reported bioactivity from *Algibacter* sp. was additional motivation to investigate the two hits of the two strains. It was therefore interesting that there were two hits from two different *Algibacter* strains. Bioassay testing of the pure compound revealed that lipid 430 had a weak anti-bacterial effect and a very weak anti-proliferative effect on melanoma cells not sufficient for any further investigation.

During the investigation of the Arctic marine isolates, we found that one of the isolates produced the siderophore serratiochelin A. We discovered the production by a co-culture, but not by an axenic culture of *Serratia* sp. The degradation of serratiochelin A to C in presence of acid was a major problem for obtaining a pure sample of serratiochelin A. However, it was possible to get a sufficiently pure sample of serratiochelin A by using FLASH liquid-chromatography, to use for bioactivity-testing. Serratiochelin A had an effect on human lung fibroblast and human melanoma cells. Among the tested bacteria serratiochelin A had an anti-bacterial effect on *S. aureus*. We also tested serratiochelin C, the degradation product of serratiochelin A, which had no bioactivity.

The investigation of the marine bacteria did not result in the identification of new molecules. However, it resulted in the identification of unknown bioactivities of known molecules. The previous investigation of serratiochelin did not go beyond chemical characterization, maybe also due to its chemical instability and lipid 430 was not assayed against bacterial cells and cancer cells before.

My initial knowledge about bacteria and their biosynthetic potential was limited. I have come from the chemical side being most interested in the task of identifying and isolating the active principles in order to elucidate their structures. The work with the 15 active fractions was then ending up in terminating one after the other because it was in some cases not possible to assign candidates for isolation and it

seemed to be unspecific activity caused by bacterial metabolites, according to our analysis most likely lipids. In many cases, especially for *Pseudomonas*-strains, it was possible to dereplicate and identify rhamnolipids being most likely the cause of bioactivity [163,164]. Those lipids have already been isolated by a colleague in the same experimental and analytical setup [165], therefore their identity was unambiguous.

By acquiring more knowledge in the field of microbiology, in particular microbial bioprospecting, the observation described above made more and more sense to me. The bacteria I had selected were from genera that are not known for being prolific source of secondary metabolites. There were only a few actinobacteria available in the selection, regardless of looking for bacteria that have produced active or inactive extracts. When searching for bacterial secondary metabolites, the process starts with the isolation of the right bacteria. The most promising bacterial producers, actinobacteria as well as myxobacteria, would require specialized isolation procedures. Of course, there is the argument to employ a higher number of different cultivation conditions for the 15 selected strains in order to test a broader spectrum of conditions under which the bacteria could produce other metabolites which is called the OSMAC approach [133]. But the number of conditions to be tested would increase the effort exponentially, conditions like carbon and nitrogen source, trace elements, salinity, pH or temperature can be varied [166,167]. The effort is then not only limited to the cultivation itself but also to the labour and material spent on extractions and the subsequent bioassays and chemical analysis that increases with the number of cultivation conditions. Such a resource intensive process should therefore be spent on strain collections that have high biosynthetic potential or a high potential for novelty because they possess unknown gene-clusters or biosynthetic genes.

It is of course possible to find bioactivity in other bacterial genera than those three mentioned in chapter 3. In a review by SCHINKE *et al*. for instance, the anti-bacterial compounds isolated from marine bacteria between 2010 and 2015 were summarised [168], and the results are shown in Table 3 below. In addition to the actinobacteria, bacilli and γ-proteobacteria were also producers of anti-microbial secondary metabolites. The cut-off in this study was set at MIC ≤ 20 µg/mL of the respective compound in the respective assay [168]. It is important to note that the bacilli produced mostly short linear lipopeptides, macrolactins and gageomacrolactins as well as one antibacterial protein. The structural variety of anti-bacterial small molecules within the bacilli is, based on that data, rather low. *Bacillus* and also *Pseudomonas* are both well studied and known for producing lipopeptides [84]. But lipopeptides often have rather unspecific bioactivity, mostly affecting the integrity of cell-membranes [84,169].

Table 3: Number of antibacterial compounds from marine bacteria reported 2010-2015 [168].

Producer:	**Active compounds**	**New compounds**	**New compounds active against Gram negative bacteria.**	**Known compounds with novel activity.**
Actinobacteria	36	27	7	9
Bacilli	12	12	12	-
γ-proteobacteria	4	3	3	1
total	52	42	22	10

For me there are two revealing insights when it comes to the production of secondary metabolites by bacteria. First, the study of DONADINO *et al.* linking the genome size of bacteria to their biosynthetic potential. Second, the rather complex life cycles and morphologies of actinobacteria, myxobacteria and cyanobacteria (chapter 3) seem to indicate biosynthetic potential of bacteria. This thought evolved particularly throughout a discussion with my colleague and fungi expert TEPPO RÄMÄ, since fungi are also source for secondary metabolites (*e.g.* cyclosporine, penicillin) and show morphological similarities with the mentioned bacteria. I just know two examples of the observation that thiotemplate systems (NRPS and PKS) are not or seldom present in genomes having a size below 3 Mb. One of them is an isolate belonging to the *Micrococcaceae* having a 2.7 Mb genome [170] and the other one is an obligate symbiont with a genome of about 2.3 Mb [171]. It seems that genome size is a very robust indicator for biosynthetic potential or more precise: A small genome size is a very robust indicator for no biosynthetic potential (considering NRPS and PKS).

During the project, a strain of cyanobacteria provided by ANTON LIAIMER was included in our investigations. The draft genome of the bacteria *Nostoc* sp. KVJ20 [172] was already published which enabled the investigation of its biosynthetic clusters [173]. UHPLC-MS investigation of the cyanobacterial extract was then identifying four, most likely suomilide-like, molecules that were isolated. Structure elucidation confirmed that one of the molecules is suomilde and the other three are new variants. The suomilides were tested in anti-proliferative, anti-bacterial and anti-biofilm bioassays at concentrations up to 100 µM without considerable bioactivity. Inhibition of trypsin-activity was also tested since the structurally closely related banyasides were reported to inhibit trypsin, which is not the case for the suomilides. Upon correspondence with CORINNA SCHINDLER, who synthesized the core of the aglycon and nominal banyaside B [174,175], it was problematic to dissolve the compounds which prevented further bio-testing. A potential explanation for the observed protease inhibiting activity of the banyasides could also be trace amounts of other protease inhibitors within the preparation [176]. The

proposed biosynthetic cluster for the suomilides consists merely of genes that are involved in aeruginosin and saxitoxin synthesis [177-179].

Another two molecules, probably yet unknown alkylresorcinols [180], were also identified in an ethyl acetate extract of KVJ20 and are awaiting to be isolated. The discovery of new molecules in KVJ20 was on one hand the confirmation for the suitability of our MS-based dereplication strategy. The identification of unknown molecules *via* elementary composition and fragments was straightforward and beside that, it increased my certainty that there were no unknown secondary metabolites to be found in the other bacterial extracts that were investigated in the beginning of the project *. On the other hand, and not surprising to me, KVJ20 is a further example for the biosynthetic potential of bacteria with large genomes, complex lifecycles and morphology. Its genome of 9.2 Mb belongs to the larger bacterial genomes and its filamentous morphology is also in compliance with the hypothesis outlined in chapter 3.

Based on the above, the practical experience throughout my work and the background given in chapter 3.1 I came to the conclusion that bioprospecting for new molecules with anti-bacterial, anti-cancer, and other bio-activity's should be focussed on actinobacteria, myxobacteria and cyanobacteria if one is looking for a "high hit rate of novel bioactive molecules". To sample specifically the (deep) Arctic Sea seems to be a very promising approach. Up to 2005, less than 3% of the known marine natural products originate from the polar seas/cold waters [181], and less than 2% of the natural products described up to 2007 originate from deep sea samples [182]. The strategy to sample the deep Arctic Sea seems to be still a rational approach taking into account that the oceans cover 70% of Earth's surface and 95% of the oceans are deeper than 1000 m. This indicates that the deep sea was previously neglected in bioprospecting efforts or less available due to technical limitations. However, sampling the deep Arctic Sea needs to be combined with an approach to isolate specifically the bacterial genera that are known to be prolific producers of secondary metabolites, which will certainly increase the output of our bacterial bioprospecting. The random sampling of marine bacteria is definitely not recommendable from the viewpoint of efficient bioprospecting. In addition, marine macroorganisms and invertebrates can be a source for bioprospecting, not only for new molecules but also for isolation of bacteria [53,183]. The experimental findings in this project, as well as in the literature [168,184] support that the marine microbes do not evade the rules we observed for terrestrial ones when it comes to select genera for bioprospecting.

* An analogy that is frequently used to describe the task of dereplication is "to find the needle in the haystack" [27]. One can imagine that this task will become very frustrating if nobody told you that there is no needle within the haystack(s).

7.3 Further work and outlook

The work on lipid 430 is finished because of insufficient bioactivity. The anti-proliferative activity of serratiochelin A is an interesting observation since the structurally quite similar serratiochelin C did not have bioactivity at all. The question remains if serratiochelin A is simply a better chelator having higher affinity to iron and is causing iron deprivation. Another mode of action is also a possibility. The fact that serratiochelin A has such a specific effect on *Staphylococcus aureus* questions the hypothesis of anti-bacterial effect by iron chelation. Further knowledge about the bioactivity, mode of action and structure-activity relationship can be investigated since we are able to produce and isolate both molecules in sufficient quantities (> 30 mg). Oxazoline and oxazole are privileged structures and are present in many molecules with anti-proliferative effect, and the hydrolysis of the heterocycle is the only difference between the bioactive serratiochelin A, having the bioactivity and inactive serratiochelin C [185,186]. The effect of serratiochelin A on other *S. aureus* isolates will be investigated in further studies, as well as the testing against other cancer cell lines than those tested.

The suomilides are chemically complex molecules having a set of functional groups that range from guanidine to sulphate and possess glycosylation. In our bioassay testing, we were not able to find a bioactivity that could indicate a function of the molecules. The biological function of the suomilides is therefore not revealed yet and they seem not to be protease inhibitors as originally reported for the structurally closely related banyasides. It remains a question if the observation of no bioactivity could also be caused by bad bioavailability of the suomilides or if their biological role is very different from what we have tested.

The findings regarding the poor yield of novelty from our previously collected bacteria will be implemented within the next research cruise in August 2020 in form of the specific isolation of actinobacteria. The specific isolation of this genus is a strategy that is properly supported by published data and a robust theory is explaining its biosynthetic potential.

8 Works cited

1. Krishnamurti, C.; Rao, S.S.C. The isolation of morphine by Serturner. *Indian Journal of Anaesthesia* **2016**, *60*, 861-862.
2. Dias, D.A.; Urban, S.; Roessner, U. A historical overview of natural products in drug discovery. *Metabolites* **2012**, *2*, 303-336.
3. Cragg, G.M.; Newman, D.J. Biodiversity: A continuing source of novel drug leads. *Pure and Applied Chemistry* **2005**, *77*, 7-24.
4. Desborough, M.J.R.; Keeling, D.M. The aspirin story – from willow to wonder drug. *British Journal of Haematology* **2017**, *177*, 674-683.
5. www.drugs.com, entry about aspirin, retrieved: 20.04.**2020**.
6. Konrad, H.B.; Hans-Joachim, B.; Klaus, M.; Alexander, I.A. A guide to drug discovery: Hit and lead generation: beyond high-throughput screening. *Nature Reviews Drug Discovery* **2003**, *2*, 369.
7. Lee, M.R. The history of ergot of rye (*Claviceps purpurea*) I: from antiquity to 1900. *J. R. Coll Physicians Edinb.* **2009**, *39*, 179-184.
8. van Dongen, P.W.J.; de Groot, A.N.J.A. History of ergot alkaloids from ergotism to ergometrine. *European Journal of Obstetrics & Gynecology* **1995**, *60*, 109-116.
9. Hofmann, A. Historical View on Ergot Alkaloids. *Pharmacology* **1978**, *16*, 1-11.
10. Lee, M.R. The history of ergot of rye (*Claviceps purpurea*) II: 1900-1940. *J. R. Coll Physicians Edinb.* **2009**, *39*, 365-369.
11. Lee, M.R. The history of ergot of rye (*Claviceps purpurea*) III: 1940-80. *J. R. Coll Physicians Edinb.* **2010**, *40*, 77-80.
12. Fleming, A. On the antibacterial action of cultures of a penicillium, with special reference to their use in the isolation of *B. influenzae*. *The British Journal of Experimental Pathology* **1929**, *10*, 226-236.
13. Abraham, E.P.; Chain, E.; Fletcher, C.M.; Gardner, A.D.; Heatley, N.G.; Jennings, M.A.; Florey, H.W. Further observations on penicillin. *The Lancet* **1941**, *238*, 177-189.
14. Florey, M.E.; Adelaide, M.B.; Florey, H.W. General and local administration of penicillin. *The Lancet* **1943**, *241*, 387-397.
15. Grossman, C.M. The first use of penicillin in the United States. *Annals of internal medicine* **2009**, *150*, 737.
16. Sakula, A. Selman Waksman (1888-1973), discoverer of streptomycin: a centenary review. *British journal of diseases of the chest* **1988**, *82*, 23-31.
17. Hill, A.B. Memories of the British streptomycin trial in tuberculosis: The first randomized clinical trial. *Controlled Clinical Trials* **1990**, *11*, 77-79.
18. Aminov, R. A brief history of the antibiotic era: lessons learned and challenges for the future. *Front. Microbiol.* **2010**, *1*.
19. Gould, K. Antibiotics: from prehistory to the present day. *Journal of Antimicrobial Chemotherapy* **2016**, *71*, 572-575.
20. Levine, D.P. Vancomycin: A History. *Clinical Infectious Diseases* **2006**, *42*, 5-12.
21. Actinomycin. *Nature* **1960**, *186*, 771-72.
22. Tietze, L.F.; Schützmeister, N.; Grube, A.; Scheffer, T.; Baag, M.M.; Granitzka, M.; Stalke, D. Synthesis of Spinosyn Analogues for Modern Crop Protection. *European Journal of Organic Chemistry* **2012**, 5748-5756.

23. All natural. *Nature Chemical Biology* **2007**, *3*, 351-351.

24. Dewick, P.M. *Secondary Metabolism: The Building Blocks and Construction Mechanisms*. John Wiley & Sons, UK, **2001**.

25. Maplestone, R.A.; Stone, M.J.; Williams, D.H. The evolutionary role of secondary metabolites — a review. *Gene* **1992**, *115*, 151-157.

26. Beattie, A.J.; Hay, M.; Magnusson, B.; de Nys, R.; Smeathers, J.; Vincent, J.F.V. Ecology and bioprospecting. *Austral. Ecol.* **2011**, *36*, 341-356.

27. Cordell, G.; Shin, Y. Finding the needle in the haystack. The dereplication of natural product extracts. *Pure and Applied Chemistry.* **1999**, *71*, 1089-1094.

28. Hubert, J.; Nuzillard, J.-M.; Renault, J.-H. Dereplication strategies in natural product research: How many tools and methodologies behind the same concept? *Fundamentals and Perspectives of Natural Products Research* **2017**, *16*, 55-95.

29. Gafner, P.; Dettwiler, W. *Von Basel in die Welt: Die Entwicklung von Geigy, CIBA und Sandoz zu Novartis*. NZZ Libro, Zürrich, Switzerland **2012**.

30. Rüegger, A.; Kuhn, M.; Lichti, H.; Loosli, H.-R.; Huguenin, R.; Quiquerez, C.; von Wartburg, A. Cyclosporin A, ein immunsuppressiv wirksamer Peptidmetabolit aus Trichoderma polysporum. *Helvetica Chimica Acta* **1976**, *59*, 1075-1092.

31. Dreyfuss, M.; Härri, E.; Hofmann, H.; Kobel, H.; Pache, W.; Tscherter, H. Cyclosporin A and C. *European journal of applied microbiology and biotechnology* **1976**, *3*, 125-133.

32. Heusler, K.; Pletscher, A. The controversial early history of cyclosporin. *Swiss medical weekly* **2001**, *131*, 299-302.

33. Tofte, S. Cyclosporine. *Journal of the Dermatology Nurses' Association* **2011**, *3*, 161-162.

34. Bocca, C. Taxol: A short history of a promising anticancer drug. *Minerva Biotecnologica* **1998**, *10*, 81-83.

35. www.drugs.com, entry about taxol, retrieved: 20.04.**2020**.

36. Newman, D.; Cragg, G. Natural Products as Sources of New Drugs from 1981 to 2014. *J. Nat. Prod.* **2016**, *79*, 629-661.

37. János, B. Bioactive Microbial Metabolites. *The Journal of Antibiotics* **2005**, *58*, 1-26.

38. Ganesan, A. The impact of natural products upon modern drug discovery. *Current Opinion in Chemical Biology* **2008**, *12*, 306-317.

39. Ortholand, J.-Y.; Ganesan, A. Natural products and combinatorial chemistry: back to the future. *Current Opinion in Chemical Biology* **2004**, *8*, 271-280.

40. Lam, K.S. New aspects of natural products in drug discovery. *Trends in Microbiology* **2007**, *15*, 279-289.

41. Koehn, F.; Carter, G. The evolving role of natural products in drug discovery. *Nature Reviews. Drug Discovery* **2005**, *4*, 206-220.

42. Kirsop, B.E. The Convention on Biological Diversity: Some implications for microbiology and microbial culture collections. *Journal of Industrial Microbiology and Biotechnology* **1996**, *17*, 505-511.

43. Eom, S.-H.; Kim, Y.-M.; Kim, S.-K.; Eom, S.-H. Marine bacteria: potential sources for compounds to overcome antibiotic resistance. *Applied Microbiology and Biotechnology* **2013**, *97*, 4763-4773.

44. Joint, I.; Mühling, M.; Querellou, J. Culturing marine bacteria – an essential prerequisite for biodiscovery. *Microbial Biotechnology* **2010**, *3*, 564-575.

45. Ling, L.L.; Schneider, T.; Peoples, A.J.; Spoering, A.L.; Engels, I.; Conlon, B.P.; Mueller, A.; Schäberle, T.F.; Hughes, D.E.; Epstein, S., *et al*. A new antibiotic kills pathogens without detectable resistance. *Nature* **2015**, *517*, 455.

46. Alan, L.H.; Ruangelie, E.-E.; Ronald, J.Q. The re-emergence of natural products for drug discovery in the genomics era. *Nature Reviews Drug Discovery* **2015**, *14*, 111-129.

47. Jha, R.; Zi-Rong, X.; Jha, R. Biomedical Compounds from Marine Organisms, *Marine Drugs* **2004**, *2*, 123-146.

48. Mayer, A.M.S.; Glaser, K.B.; Cuevas, C.; Jacobs, R.S.; Kem, W.; Little, R.D.; McIntosh, J.M.; Newman, D.J.; Potts, B.C.; Shuster, D.E. The odyssey of marine pharmaceuticals: a current pipeline perspective. *Trends in Pharmacological Sciences* **2010**, *31*, 255-265.

49. Newman, D.J.; Cragg, G.M.; Battershill, C.N. Therapeutic agents from the sea: biodiversity, chemo-evolutionary insight and advances to the end of Darwin's 200th year. *Diving and hyperbaric medicine* **2009**, *39*, 216-225.

50. Rauck, R.L.; Wallace, M.S.; Burton, A.W.; Kapural, L.; North, J.M. Intrathecal Ziconotide for Neuropathic Pain: A Review. *Pain Practice* **2009**, *9*, 327-337.

51. Staats, P.S.; Yearwood, T.; Charapata, S.G.; Presley, R.W.; Wallace, M.S.; Byas-Smith, M.; Fisher, R.; Bryce, D.A.; Mangieri, E.A.; Luther, R.R., *et al*. Intrathecal Ziconotide in the Treatment of Refractory Pain in Patients With Cancer or AIDS: A Randomized Controlled Trial. *JAMA* **2004**, *291*, 63-70.

52. Perry, C. Eribulin. *Drugs* **2011**, *71*, 1321-1331.

53. Hentschel, U.; Usher, K.M.; Taylor, M.W. Marine sponges as microbial fermenters. *FEMS Microbiology Ecology* **2006**, *55*, 167-177.

54. Ute, H.; Jörn, P.; Sandie, M.D.; Michael, W.T. Genomic insights into the marine sponge microbiome. *Nature Reviews Microbiology* **2012**, *10*, 641-154.

55. Schofield, M.M.; Jain, S.; Porat, D.; Dick, G.J.; Sherman, D.H. Identification and analysis of the bacterial endosymbiont specialized for production of the chemotherapeutic natural product ET-743. *Environmental microbiology* **2015**, *17*, 3964-3975.

56. Rath, C.M.; Janto, B.; Earl, J.; Ahmed, A.; Hu, F.Z.; Hiller, L.; Dahlgren, M.; Kreft, R.; Yu, F.; Wolff, J.J., *et al*. Meta-omic characterization of the marine invertebrate microbial consortium that produces the chemotherapeutic natural product ET-743. *ACS chemical biology* **2011**, *6*, 1244-1256.

57. Feling, R.H.; Buchanan, G.O.; Mincer, T.J.; Kauffman, C.A.; Jensen, P.R.; Fenical, W. Salinosporamide A: A Highly Cytotoxic Proteasome Inhibitor from a Novel Microbial Source, a Marine Bacterium of the New Genus Salinospora. *Angewandte Chemie International Edition* **2003**, *42*, 355-357.

58. www.clinicaltrials.gov, entry for clinical trials of salinosporamide A, retrieved: 30.03.**2020.**

59. Hanson, J.R. The classes of natural product and their isolation. In *Natural Products: The Secondary Metabolites*, The Royal Society of Chemistry **2003**, *17*, 1-34.

60. Felnagle, E.A.; Jackson, E.E.; Chan, Y.A.; Podevels, A.M.; Berti, A.D.; McMahon, M.D.; Thomas, M.G. Nonribosomal peptide synthetases involved in the production of medically relevant natural products. *Mol. Pharm.* **2008**, *5*, 191-211.

61. Elshahawi, S.I.; Shaaban, K.A.; Kharel, M.K.; Thorson, J.S. A comprehensive review of glycosylated bacterial natural products. *Chem. Soc. Rev.* **2015**, *44*, 7591-7697.

62. Weissman, K. The structural biology of biosynthetic megaenzymes. In *Nat. Chem. Biol.*, **2015**, *11*, 660-670.

63. Challis, G.L.; Naismith, J.H. Structural aspects of non-ribosomal peptide biosynthesis. *Curr. Opin. Struct. Biol.* **2004**, *14*, 748-756.

64. Miller, B.R.; Gulick, A.M. Structural Biology of Nonribosomal Peptide Synthetases. *Methods Mol. Biol.* **2016**, *1401*, 3-29.

65. Walsh, C.T.; O'Brien, R.V.; Khosla, C. Nonproteinogenic amino acid building blocks for nonribosomal peptide and hybrid polyketide scaffolds. *Angew. Chem. Int. Ed. Engl.* **2013**, *52*, 7098-7124.

66. Kittilä, T.; Kittel, C.; Tailhades, J.; Butz, D.; Schoppet, M.; Büttner, A.; Goode, R.J.A.; Schittenhelm, R.B.; van Pee, K.-H.; Süssmuth, R.D., et al. Halogenation of glycopeptide antibiotics occurs at the amino acid level during non-ribosomal peptide synthesis. *Chemical Science* **2017**, *8*, 5992-6004.

67. Walsh, C.T.; Chen, H.; Keating, T.A.; Hubbard, B.K.; Losey, H.C.; Luo, L.; Marshall, C.G.; Miller, D.A.; Patel, H.M. Tailoring enzymes that modify nonribosomal peptides during and after chain elongation on NRPS assembly lines. *Current Opinion in Chemical Biology* **2001**, *5*, 525-534.

68. Shen, B. Polyketide biosynthesis beyond the type I, II and III polyketide synthase paradigms. *Current Opinion in Chemical Biology* **2003**, *7*, 285-295.

69. Sundaram, S.; Hertweck, C. On-line enzymatic tailoring of polyketides and peptides in thiotemplate systems. *Current Opinion in Chemical Biology* **2016**, *31*, 82-94.

70. Ridley, C.P.; Lee, H.Y.; Khosla, C. Evolution of polyketide synthases in bacteria. *Proceedings of the National Academy of Sciences* **2008**, *105*, 4595-4600.

71. Ray, L.; Moore, B.S. Recent advances in the biosynthesis of unusual polyketide synthase substrates. *Natural product reports* **2016**, *33*, 150-161.

72. Harvey, A. Strategies for discovering drugs from previously unexplored natural products. *Drug Discovery Today* **2000**, *5*, 294-300.

73. Henkel, T.; Brunne, R.M.; Müller, H.; Reichel, F. Statistical Investigation into the Structural Complementarity of Natural Products and Synthetic Compounds. *Angewandte Chemie International Edition* **1999**, *38*, 643-647.

74. Lee, M.-L.; Schneider, G. Scaffold Architecture and Pharmacophoric Properties of Natural Products and Trade Drugs: Application in the Design of Natural Product-Based Combinatorial Libraries. *Journal of Combinatorial Chemistry* **2001**, *3*, 284-289.

75. Feher, M.; Schmidt, J.M. Property distributions: Differences between drugs, natural products, and molecules from combinatorial chemistry. *Journal of Chemical Information and Computer Sciences* **2003**, *43*, 218-227.

76. Kristina, G.; Gisbert, S. Properties and Architecture of Drugs and Natural Products Revisited. *Current Chemical Biology* **2007**, *1*, 115-127.

77. Klebe, G.; Böhm, H.-J. Energetic and Entropic Factors Determining Binding Affinity in Protein-Ligand Complexes. *Journal of Receptors and Signal Transduction* **1997**, *17*, 459-473

78. Payne, D.J.; Gwynn, M.N.; Holmes, D.J.; Pompliano, D.L. Drugs for bad bugs: confronting the challenges of antibacterial discovery. *Nature Reviews Drug Discovery* **2006**, *6*, 29-40.

79. Lipinski, C.A.; Lombardo, F.; Dominy, B.W.; Feeney, P.J. Experimental and computational approaches to estimate solubility and permeability in drug discovery and development settings. *Advanced Drug Delivery Reviews* **1997**, *23*, 3-25.

80. Wahl, M. *Digitalis* glycosides in *Encyclopedia of Toxicology*, p 45-47, 2nd ed., Elsevier **2005**.

81. Krishna, S.; Bustamante, L.; Haynes, R.; Staines, H. Artemisinins: their growing importance in medicine. *Trends in pharmacological sciences* **2008**, *29*, 520-527.

82. Pritchard, D.I. Sourcing a chemical succession for cyclosporin from parasites and human pathogens. *Drug Discovery Today* **2005**, *10*, 688-691.

83. Vezina, C.; Kudelski, A.; Sehgal, S.N. Rapamycin (AY-22,989), a new antifungal antibiotic. I. Taxonomy of the producing streptomycete and isolation of the active principle. *J. Antibiot.* **1975**, *28*, 721-726.

84. Raaijmakers, J.M.; De Bruijn, I.; Nybroe, O.; Ongena, M. Natural functions of lipopeptides from Bacillus and Pseudomonas: more than surfactants and antibiotics. *FEMS Microbiology Reviews* **2010**, *34*, 1037-1062.

85. Santos, R.; Ursu, O.; Gaulton, A.; Bento, A.P.; Donadi, R.S.; Bologa, C.G.; Karlsson, A.; Al-Lazikani, B.; Hersey, A.; Oprea, T.I., *et al*. A comprehensive map of molecular drug targets. *Nature Reviews Drug Discovery* **2017**, *16*, 19-34.

86. Evans, B.E.; Rittle, K.E.; Bock, M.G.; Dipardo, R.M.; Freidinger, R.M.; Whitter, W.L.; Lundell, G.F.; Veber, D.F.; Anderson, P.S.; Chang, R.S. Methods for drug discovery: development of potent, selective, orally effective cholecystokinin antagonists. *Journal of medicinal chemistry* **1988**, *31*, 2235-2246.

87. Kim, J.; Kim, H.; Park, S.B. Privileged Structures: Efficient Chemical "Navigators" toward Unexplored Biologically Relevant Chemical Spaces. *Journal of the American Chemical Society* **2014**, *136*, 14629-14638.

88. Tsai, C.J.; Nussinov, R. Hydrophobic folding units derived from dissimilar monomer structures and their interactions. *Protein Sci.* **1997**, *6*, 24-42.

89. Xu, D.; Nussinov, R. Favorable domain size in proteins. *Folding and Design* **1998**, *3*, 11-17.

90. Berman, A.L.; Kolker, E.; Trifonov, E.N. Underlying order in protein sequence organization. *Proceedings of the National Academy of Sciences of the United States of America* **1994**, *91*, 4044-4047.

91. Illergård, K.; Ardell, D.H.; Elofsson, A. Structure is three to ten times more conserved than sequence—A study of structural response in protein cores. *Proteins: Structure, Function, and Bioinformatics* **2009**, *77*, 499-508.

92. Bernstein, F.C.; Koetzle, T.F.; Williams, G.J.; Meyer, E.F., Jr.; Brice, M.D.; Rodgers, J.R.; Kennard, O.; Shimanouchi, T.; Tasumi, M. The Protein Data Bank: a computer-based archival file for macromolecular structures. *J. Mol. Biol.* **1977**, *112*, 535-542.

93. Dawson, N.L.; Lewis, T.E.; Das, S.; Lees, J.G.; Lee, D.; Ashford, P.; Orengo, C.A.; Sillitoe, I. CATH: an expanded resource to predict protein function through structure and sequence. *Nucleic Acids Research* **2016**, *45*, 289-295.

94. Breinbauer, R.; Vetter, I.R.; Waldmann, H. From protein domains to drug candidates - Natural products as guiding principles in the design and synthesis of compound libraries. **2002**, *41*, 2878-2890.

95. Rouhi, A.M. Rediscovering Natural Products. *Chemical & Engineering News Archive* **2003**, *81*, 77-91.

96. Bohacek, R.S.; McMartin, C.; Guida, W.C. The art and practice of structure-based drug design: A molecular modeling perspective. *Medicinal Research Reviews* **1996**, *16*, 3-50.

97. Watve, M.; Tickoo, R.; Jog, M.; Bhole, B. How many antibiotics are produced by the genus Streptomyces ? *Archives of Microbiology* **2001**, *176*, 386-390.

98. de Lima Procópio, R.E.; Da Silva, I.R.; Martins, M.K.; de Azevedo, J.L.; de Araújo, J.M. Antibiotics produced by Streptomyces. *Brazilian Journal of Infectious Diseases* **2012**, *16*, 466-471.

99. Barka, E.A.; Vatsa, P.; Sanchez, L.; Gaveau-Vaillant, N.; Jacquard, C.; Klenk, H.P.; Clement, C.; Ouhdouch, Y.; Wezel, G.P.V. Taxonomy, Physiology, and Natural Products of Actinobacteria. *Microbiology and Molecular Biology Reviews* **2016**, *80*, 1-43.

100. Nett, M.; Ikeda, H.; Moore, B.S. Genomic basis for natural product biosynthetic diversity in the actinomycetes. *Natural Product Reports* **2009**, *26*, 1362-1384.

101. Bundale, S.; Singh, J.; Begde, D.; Nashikkar, N.; Upadhyay, A. Rare actinobacteria: a potential source of bioactive polyketides and peptides. *World J. Microbiol. Biotechnol.* **2019**, *35*, 92.

102. Dhakal, D.; Pokhrel, A.R.; Shrestha, B.; Sohng, J.K. Marine Rare Actinobacteria: Isolation, Characterization, and Strategies for Harnessing Bioactive Compounds. *Frontiers in Microbiology* **2017**, *8*, 1106.

103. Davila-Cespedes, A.; Hufendiek, P.; Crusemann, M.; Schaberle, T.; Konig, G. Marine-derived myxobacteria of the suborder Nannocystineae: An underexplored source of structurally intriguing and biologically active metabolites. *Beilstein J. Org. Chem.*, **2016**; *12*, 969-984.

104. Gemperlein, K.; Zaburannyi, N.; Garcia, R.; La Clair, J.; Müller, R. Metabolic and Biosynthetic Diversity in Marine Myxobacteria. *Marine Drugs* **2018**, *16*, 314.

105. Schäberle, T.F.; Goralski, E.; Neu, E.; Erol, O.; Hölzl, G.; Dörmann, P.; Bierbaum, G.; König, G.M. Marine myxobacteria as a source of antibiotics--comparison of physiology, polyketide-type genes and antibiotic production of three new isolates of Enhygromyxa salina. *Marine drugs* **2010**, *8*, 2466.

106. Schäberle, T.F.; Lohr, F.; Schmitz, A.; König, G.M. Antibiotics from myxobacteria. *Natural product reports* **2014**, *31*, 953.

107. Woese, C.R. Bacterial evolution. *Microbiol. Rev.* **1987**, *51*, 221-271.

108. Boone, D.R.; Castenholz, R.W.; Garrity, G.M.; Bergey, D.H. *Bergey's manual of systematic bacteriology : The archaea and the deeply branching and phototrophic bacteria*, 2nd ed., Springer, New York, US **2001**.

109. Dworkin, M.; Falkow, S.; Rosenberg, E.; Schleifer, K.-H.; Stackebrandt, E. *The Cyanobacteria—Isolation, Purification and Identification,* Springer, New York, US, **2006**.

110. Gugger, M.F.; Hoffmann, L. Polyphyly of true branching cyanobacteria (Stigonematales). *International Journal of Systematic and Evolutionary Microbiology* **2004**, *54*, 349-357.

111. Schirrmeister, B.E.; Antonelli, A.; Bagheri, H.C. The origin of multicellularity in cyanobacteria. *BMC Evolutionary Biology* **2011**, *11*, 45.

112. Dittmann, E.; Gugger, M.; Sivonen, K.; Fewer, D.P. Natural Product Biosynthetic Diversity and Comparative Genomics of the Cyanobacteria. *Trends in Microbiology* **2015**, *23*, 642-652.

113. de Figueiredo, D.R.; Reboleira, A.S.S.P.; Antunes, S.C.; Abrantes, N.; Azeiteiro, U.; Gonçalves, F.; Pereira, M.J. The effect of environmental parameters and cyanobacterial blooms on phytoplankton dynamics of a Portuguese temperate Lake. *Hydrobiologia* **2006**, *568*, 145-157.

114. Namikoshi, M.; Rinehart, K. Bioactive compounds produced by cyanobacteria. *Journal of Industrial Microbiology* **1996**, *17*, 373-384.

115. Kehr, J.; Picchi, D.G.; Dittmann, E. Natural product biosyntheses in cyanobacteria: A treasure trove of unique enzymes. *Beilstein J. Org. Chem.* **2011**, *7*, 1622-1635.

116. Arnison, P.G.; Bibb, M.J.; Bierbaum, G.; Bowers, A.A.; Bugni, T.S.; Bulaj, G.; Camarero, J.A.; Campopiano, D.J.; Challis, G.L.; Clardy, J., et al. Ribosomally synthesized and post-translationally modified peptide natural products: overview and recommendations for a universal nomenclature. *Natural product reports* **2013**, *30*, 108-160.

117. Nunnery, J.K.; Mevers, E.; Gerwick, W.H. Biologically active secondary metabolites from marine cyanobacteria. *Current Opinion in Biotechnology* **2010**, *21*, 787-793.

118. Donadio, S.; Monciardini, P.; Sosio, M. Polyketide synthases and nonribosomal peptide synthetases: the emerging view from bacterial genomics. *Natural Product Reports* **2007**, *24*, 1073-1109.

119. Paul, D.G.N.; J., V. Production of secondary metabolites by filamentous tropical marine cyanobacteria: Ecological functions of the compounds. *Journal of Phycology* **1999**, *35*, 1412-1421.

120. Rice, L.B. Federal funding for the study of antimicrobial resistance in nosocomial pathogens: No ESKAPE.(Editorial). *Journal of Infectious Diseases* **2008**, *197*, 1079-1081.

121. Chen, L.; Todd, R.; Kiehlbauch, J.; Walters, M.; Kallen, A. Pan-Resistant New Delhi Metallo-Beta-Lactamase-Producing Klebsiella pneumoniae - Washoe County, Nevada, 2016. *Morbidity and Mortality Weekly Report* **2017**, *66*, 33.

122. McCarthy, M. Woman dies after infection with bacteria resistant to all antibiotics available in US. *British Medical Journal* **2017**, *356*, 254.

123. The Review on Antimicrobial Resistance. Tackling Drug-Resistant Infections Globally: Final Report and Recommendations. **2016**.

124. Smetana, K., Jr.; Lacina, L.; Szabo, P.; Dvorankova, B.; Broz, P.; Sedo, A. Ageing as an Important Risk Factor for Cancer. *Anticancer Res.* **2016**, *36*, 5009-5017.

125. Yancik, R. Population Aging and Cancer: A Cross-National Concern. *The Cancer Journal* **2005**, *11*, 437-441.

126. Demain, A.L.; Vaishnav, P. Natural products for cancer chemotherapy. *Microb. Biotechnol.* **2011**, *4*, 687-699.

127. Watve, M.; Shejval, V.; Sonawane, C.; Rahalkar, M.; Phadnis, N.; Champhenkar, A.; Damle, K.; Karandikar, S.; Kshirsagar, V.; Jog, M., et al. The 'K' selected oligophilic bacteria: A key to uncultured diversity? *Current Science* **2000**, *78*, 1535-1542.

128. Davis, K.E.R.; Joseph, S.J.; Janssen, P.H. Effects of Growth Medium, Inoculum Size, and Incubation Time on Culturability and Isolation of Soil Bacteria. *Applied and Environmental Microbiology* **2005**, *71*, 826-834.

129. Yi Jiang, Q.L., Xiu Chen and Chenglin Jiang. Isolation and Cultivation Methods of Actinobacteria, Actinobacteria - Basics and Biotechnological Applications. *IntechOpen* **2016**.

130. Iizuka, T.; Jojima, Y.; Fudou, R.; Yamanaka, S. Isolation of myxobacteria from the marine environment. *FEMS Microbiology Letters* **1998**, *169*, 317-322.

131. Magarvey, N.A.; Keller, J.M.; Bernan, V.; Dworkin, M.; Sherman, D.H. Isolation and Characterization of Novel Marine-Derived Actinomycete Taxa Rich in Bioactive Metabolites. *Applied and Environmental Microbiology* **2004**, *70*, 7520-7529.

132. Zhang, L.; Wang, H.; Fang, X.; Stackebrandt, E.; Ding, Y. Improved methods of isolation and purification of myxobacteria and development of fruiting body formation of two strains. *Journal of Microbiological Methods* **2003**, *54*, 21-27.

133. Bode, H.B.; Bethe, B.; Höfs, R.; Zeeck, A. Big Effects from Small Changes: Possible Ways to Explore Nature's Chemical Diversity. *Chembiochem : a European journal of chemical biology* **2002**, *3*, 619-627.

134. Bader, J.; Mast-Gerlach, E.; Popović, M.K.; Bajpai, R.; Stahl, U. Relevance of microbial coculture fermentations in biotechnology. *Journal of Applied Microbiology* **2010**, *109*, 371-387.

135. Seyedsayamdost, M.R.; Traxler, M.F.; Clardy, J.; Kolter, R. Old meets new: using interspecies interactions to detect secondary metabolite production in actinomycetes. *Methods Enzymol.* **2012**, *517*, 89-109.

136. Walter, T.H.; Andrews, R.W. Recent innovations in UHPLC columns and instrumentation. *Trends in Analytical Chemistry* **2014**, *63*, 14-20.

137. Fekete, S.; Schappler, J.; Veuthey, J.-L.; Guillarme, D. Current and future trends in UHPLC. *Trends in Analytical Chemistry* **2014**, *63*, 2-13.

138. De Vos, J.; Broeckhoven, K.; Eeltink, S. Advances in Ultrahigh-Pressure Liquid Chromatography Technology and System Design. *Analytical Chemistry* **2016**, *88*, 262-278.

139. Budzikiewicz, H.; Schäfer, M. *Massenspektrometrie Eine Einführung*, 5th ed. Willey-Vch, Weinheim, Germany **2005**.

140. Siuzdak, G. *The expanding role of mass spectrometry in biotechnology*, MCC Press, San Diego, CA, US **2003**.

141. Steckel, A.; Schlosser, G. An Organic Chemist's Guide to Electrospray Mass Spectrometric Structure Elucidation. *Molecules* **2019**, *24*, 611.

142. Fenn, J.B.; Mann, M.; Meng, C.K.; Wong, S.F.; Whitehouse, C.M. Electrospray Ionization for Mass Spectrometry of Large Biomolecules. *Science* **1989**, *246*, 64-71.

143. Bouslimani, A.; Sanchez, L.M.; Garg, N.; Dorrestein, P.C. Mass spectrometry of natural products: current, emerging and future technologies. *Nat. Prod. Rep.* **2014**, *31*, 718-729.

144. Přichystal, J.; Schug, K.A.; Lemr, K.; Novák, J.i.; Havlíček, V.r. Structural Analysis of Natural Products. *Analytical Chemistry* **2016**, *88*, 10338-10346.

145. Johnson, A.R.; Carlson, E.E. Collision-Induced Dissociation Mass Spectrometry: A Powerful Tool for Natural Product Structure Elucidation. *Analytical Chemistry* **2015**, *87*, 10668-10678.

146. Sashidhara, K.; Rosaiah, J. Various dereplication strategies using LC-MS for rapid natural product lead identification and drug discovery. *Nat. Prod. Commun.* **2007**, *2*, 193-202.

147. Klitgaard, A.; Iversen, A.; Andersen, M.R.; Larsen, T.O.; Frisvad, J.C.; Nielsen, K.F. Aggressive dereplication using UHPLC-DAD-QTOF: screening extracts for up to 3000 fungal secondary metabolites. *Anal. Bioanal. Chem.* **2014**, *406*, 1933-1943.

148. Nielsen, K.F.; Månsson, M.; Rank, C.; Frisvad, J.C.; Larsen, T.O. Dereplication of Microbial Natural Products by LC-DAD-TOFMS. *Journal of Natural Products* **2011**, *74*, 2338-2348.

149. Svenson, J. MabCent: Arctic marine bioprospecting in Norway. *Phytochem Rev.* **2013**, *12*, 567-578.

150. Camp, D.; Davis, R.A.; Evans-Illidge, E.A.; Quinn, R.J. Guiding principles for natural product drug discovery. *Future Med. Chem.* **2012**, *4*, 1067-1084.

151. Schwyn, B.; Neilands, J.B. Universal chemical assay for the detection and determination of siderophores. *Analytical Biochemistry* **1987**, *160*, 47-56.

152. Butler, M.S. The role of natural product chemistry in drug discovery. *J. Nat. Prod.* **2004**, *67*, 2141-2153.

153. Eder, J.; Sedrani, R.; Wiesmann, C. The discovery of first-in-class drugs: origins and evolution. *Nature Reviews Drug Discovery* **2014**, *13*, 577-587.

154. David, C.S.; Jason, A. How were new medicines discovered? *Nature Reviews Drug Discovery* **2011**, *10*, 507-519.

155. Swinney, D.C. Phenotypic vs. Target-Based Drug Discovery for First-in-Class Medicines. *Clinical Pharmacology & Therapeutics* **2013**, *93*, 299-301.

156. Breton, R.C.; Reynolds, W.F. Using NMR to identify and characterize natural products. *Nat. Prod. Rep.* **2013**, *30*, 501-524.

157. Fujii, K.; Ikai, Y.; Oka, H.; Suzuki, M.; Harada, K.-I. A nonempirical method using LC/MS for determination of the absolute configuration of constituent amino acids in a peptide: combination of Marfey's method with mass spectrometry and its practical application. (liquid chromatography/mass spectrometry). *Analytical Chemistry* **1997**, *69*, 3346-3352.

158. Medema, M.H.; Blin, K.; Cimermancic, P.; de Jager, V.; Zakrzewski, P.; Fischbach, M.A.; Weber, T.; Takano, E.; Breitling, R. antiSMASH: rapid identification, annotation and analysis of secondary metabolite biosynthesis gene clusters in bacterial and fungal genome sequences. *Nucleic Acids Research* **2011**, *39*, 339-346.

159. Ziemert, N.; Alanjary, M.; Weber, T. The evolution of genome mining in microbes – a review. *Natural Product Reports* **2016**, *33*, 988-1005.

160. Luo, Y.; Cobb, R.E.; Zhao, H. Recent advances in natural product discovery. *Current Opinion in Biotechnology* **2014**, *30*, 230-237.

161. Baltz, R.H. Natural product drug discovery in the genomic era: realities, conjectures, misconceptions, and opportunities. *Journal of Industrial Microbiology & Biotechnology* **2019**, *46*, 281-299.

162. Zhang, G.; Li, J.; Zhu, T.; Gu, Q.; Li, D. Advanced tools in marine natural drug discovery. In *Curr. Opin. Biotechnol.*, **2016**, *42*, 13-23.

163. Abdel-Mawgoud, A.; Lépine, F.; Déziel, E. Rhamnolipids: diversity of structures, microbial origins and roles. *Applied Microbiology and Biotechnology* **2010**, *86*, 1323-1336.

164. Chrzanowski, Ł.; Ławniczak, Ł.; Czaczyk, K. Why do microorganisms produce rhamnolipids? *World Journal of Microbiology and Biotechnology* **2012**, *28*, 401-419.

165. Kristoffersen, V.; Rämä, T.; Isaksson, J.; Andersen, J.H.; Gerwick, W.H.; Hansen, E. Characterization of Rhamnolipids Produced by an Arctic Marine Bacterium from the Pseudomonas fluorescence Group. *Marine Drugs* **2018**, *16*, 163.

166. Giubergia, S.; Phippen, C.; Gotfredsen, C.H.; Nielsen, K.F.; Gram, L. Influence of Niche-Specific Nutrients on Secondary Metabolism in *Vibrionaceae*. *Applied and Environmental Microbiology* **2016**, *82*, 4035-4044.

167. Romano, S.; Jackson, S.A.; Patry, S.; Dobson, A.D.W. Extending the "one strain many compounds" (OSMAC) principle to marine microorganisms. *Marine Drugs* **2018**, *16*, 244.

168. Schinke, C.; Martins, T.; Queiroz, S.C.N.; Melo, I.S.; Reyes, F.G.R. Antibacterial Compounds from Marine Bacteria, 2010-2015. *Journal of Natural Products* **2017**, *80*, 1215-1228.

169. Hamley, I.W. Lipopeptides: from self-assembly to bioactivity. *Chem. Commun.* **2015**, *51*, 8574-8583.

170. Palomo, S.; González, I.; de La Cruz, M.; Martín, J.; Tormo, J.R.; Anderson, M.; Hill, R.T.; Vicente, F.; Reyes, F.; Genilloud, O. Sponge-derived Kocuria and Micrococcus spp. as sources of the new thiazolyl peptide antibiotic kocurin. *Marine Drugs* **2013**, *11*, 1071.

171. Zan, J.; Li, Z.; Tianero, M.D.; Davis, J.; Hill, R.T.; Donia, M.S.; Zan, J. A microbial factory for defensive kahalalides in a tripartite marine symbiosis. *Science* **2019**, *364*, 1056.

172. Liaimer, A.; Jensen, J.B.; Dittmann, E. A Genetic and Chemical Perspective on Symbiotic Recruitment of Cyanobacteria of the Genus Nostoc into the Host Plant *Blasia pusilla* L. *Frontiers in Microbiology* **2016**, *7*, 1693.

173. Halsør, M.-J.H.; Liaimer, A.; Pandur, S.; Ræder, I.L.U.; Smalås, A.O.; Altermark, B. Draft Genome Sequence of the Symbiotically Competent Cyanobacterium Nostoc sp. Strain KVJ20. *Microbiol. Resour. Announc.* **2019**, *8*, e01190-01119.

174. Schindler, C.S.; Stephenson, C.R.J.; Carreira, E.M. Enantioselective Synthesis of the Core of Banyaside, Suomilide, and Spumigin HKVV. *Angewandte Chemie International Edition* **2008**, *47*, 8852-8855.

175. Schindler, C.S.; Bertschi, L.; Carreira, E.M. Total Synthesis of Nominal Banyaside B: Structural Revision of the Glycosylation Site. *Angewandte Chemie International Edition* **2010**, *49*, 9229-9232.

176. Sieber, S.; Grendelmeier, S.M.; Harris, L.A.; Mitchell, D.A.; Gademann, K. Microviridin 1777: A Toxic Chymotrypsin Inhibitor Discovered by a Metabologenomic Approach. *Journal of Natural Products* **2020**, *83*, 438-446.

177. Mihali, T.K.; Kellmann, R.; Neilan, B.A. Characterisation of the paralytic shellfish toxin biosynthesis gene clusters in Anabaena circinalis AWQC131C and Aphanizomenon sp. NH-5. *BMC Biochem.* **2009**, *10*, 8.

178. Ishida, K.; Christiansen, G.; Yoshida, W.Y.; Kurmayer, R.; Welker, M.; Valls, N.; Bonjoch, J.; Hertweck, C.; Börner, T.; Hemscheidt, T., *et al*. Biosynthesis and structure of aeruginoside 126A and 126B, cyanobacterial peptide glycosides bearing a 2-carboxy-6-hydroxyoctahydroindole moiety. *Chem. Biol.* **2007**, *14*, 565-576.

179. Murakami, M.; Ishida, K.; Okino, T.; Okita, Y.; Matsuda, H.; Yamaguchi, K. Aeruginosins 98-A and B, trypsin inhibitors from the blue-green alga Microcystis aeruginosa (NIES-98). *Tetrahedron Letters* **1995**, *36*, 2785-2788.

180. Martins, T.P.; Rouger, C.; Glasser, N.R.; Freitas, S.; De Fraissinette, N.B.; Balskus, E.P.; Tasdemir, D.; Leo, P.N. Chemistry, bioactivity and biosynthesis of cyanobacterial alkylresorcinols. *Nat. Prod. Rep.* **2019**, *36*, 1437-1461.

181. Lebar, M.D.; Heimbegner, J.L.; Baker, B.J. Cold-water marine natural products. *Natural Product Reports* **2007**, *24*, 774-797.

182. Skropeta, D. Deep-sea natural products. *Natural Product Reports* **2008**, *25*, 1131-1166.

183. Hansen, K.Ø.; Andersen, J.H.; Bayer, A.; Pandey, S.K.; Lorentzen, M.; Jørgensen, K.B.; Sydnes, M.O.; Guttormsen, Y.; Baumann, M.; Koch, U., *et al*. Kinase Chemodiversity from the Arctic: The Breitfussins. *Journal of Medicinal Chemistry* **2019**, *62*, 10167-10181.

184. Pilkington, L.I. A Chemometric Analysis of Deep-Sea Natural Products. *Molecules* **2019**, *24*, 3942.

185. Chiacchio, M.A.; Lanza, G.; Chiacchio, U.; Giofrè, S.V.; Romeo, R.; Iannazzo, D.; Legnani, L. Oxazole-Based Compounds As Anticancer Agents. *Curr. Med. Chem.* **2019**, *26*, 7337-7371.

186. Zhang, H.-Z.; Zhao, Z.-L.; Zhou, C.-H. Recent advance in oxazole-based medicinal chemistry. *European Journal of Medicinal Chemistry* **2018**, *144*, 444-492.

Picture sources:

Figure 2 Scot Nelson, 2014, CC license: www.creativecommons.org/publicdomain/zero/1.0/ (07.07.2020)

Figure 4 & 5 Provided by the company archive of Novartis Pharma AG Switzerland for use within this thesis.

Figure 7 Jason Hollinger, 2005, CC license: www.creativecommons.org/licenses/by/2.0/deed.en (07.07.2020)

Paper I

molecules

MDPI

Article

Anti-Bacterial Effect and Cytotoxicity Assessment of Lipid 430 Isolated from *Algibacter* sp.

Yannik K.-H. Schneider [1,*], Kine Ø. Hansen [1], Johan Isaksson [2], Sara Ullsten [1], Espen H. Hansen [1] and Jeanette Hammer Andersen [1]

1 Marbio, Faculty for Fisheries, Biosciences and Economy, UiT—The Arctic University of Norway, Breivika, N-9037 Tromsø, Norway; kine.o.hanssen@uit.no (K.Ø.H.); sara.m.ullsten-wahlund@uit.no (S.U.); espen.hansen@uit.no (E.H.H.); jeanette.h.andersen@uit.no (J.H.A.)

2 Department of Chemistry, Faculty of Natural Sciences, UiT—The Arctic University of Norway, Breivika, N-9037 Tromsø, Norway; johan.isaksson@uit.no

* Correspondence: yannik.k.schneider@uit.no; Tel.: +47-77649267

Academic Editor: George Kokotos

Received: 2 October 2019; Accepted: 4 November 2019; Published: 5 November 2019

Abstract: Two bacterial isolates from the Barents Sea, both belonging to the genus *Algibacter*, were found to yield extracts with anti-bacterial bioactivity. Mass spectrometry guided dereplication and purification of the active extracts lead to the isolation of the same active principle in both extracts. The structure of the bioactive compound was identified via mass spectrometry and nuclear resonance spectroscopy and it turned out to be the known lipopeptide Lipid 430. We discovered and determined its previously unknown anti-bacterial activity against *Streptococcus agalactiae* and revealed a cytotoxic effect against the A2058 human melanoma cell line at significantly lower concentrations compared to its anti-bacterial concentration. Flow cytometry and microscopy investigations of the cytotoxicity against the melanoma cell line indicated that Lipid 430 did not cause immediate cell lysis. The experiments with melanoma cells suggest that the compound functions trough more complex pathways than acting as a simple detergent.

Keywords: flavolipin; marine bacteria; natural products; lipopeptides; *algibacter*

1. Introduction

The genus Bacteriocides represents the second most abundant bacterial phylum within the marine heterotrophic picoplankton [1]. Bacteriocides, to which *Flavobacteria* belong, have the enzymes required to degrade proteins and carbohydrates [2], and play an important role in the degradation of organic matter within the marine environment. Remarkably, the observation of the abundance of marine *Flavobacteria* and the hypothesis that their presence is linked to their ability to degrade algal polymers dates back to 1946 [3]. Within the *Flavobacteriaceae* family, the genus *Algibacter* was erected in 2004. It represents a taxon of rod-shaped, facultative anaerobic, Gram negative bacteria, unable to form endospores [4]. Its first representative, *Algibacter lectus,* was isolated from green algae and described in 2004 by Nedashkovskaya et al. [4]. Further representatives have been isolated from seawater [5,6], invertebrates [7] and from algae or in close proximity to them [4,8–10]. *Algibacter alginolytica* was isolated from a brown seaweed (*Laminaria japonica*). Sequencing and genomic analysis revealed that it has the highest proportion of carbohydrate-active enzymes (~7.5%) among the Flavobacteria. The bacterium was shown to hydrolyze Tween 20, Tween 40, Tween 60, Tween 80, galantine, alginate and starch, which indicates the ecological significance of *Algibacter* in breaking down algal biopolymers [10]. As part of this work, a lipopeptide known as Lipid 430 (**1**, Figure 1) was isolated. A novel serine dipeptide lipid, Lipid 654 (**2**, Flavolipin, Figure 1), was first isolated from *Flavobacterium menigosepticum* in 1988 [11,12]. *F. menigosepticum* is an opportunistic

pathogen able to cause neonatal meningitis and nosocomial infections in immunocompromised individuals [13]. Stereo-controlled synthesis of **2** and bioactivity testing revealed that its observed macrophage activating effect [14] is triggered stereospecifically by the L-serine dipeptide lipid *N*-[*N*-[(3*R*)-15-methyl-3-(13-methyltetradecanoyloxy)hexadecanoyl]glycyl]-L-serine, showing the same bioactivity as natural **2** [12]. An early investigation suggested that **2** was a Toll-like receptor 4 ligand [15], but recent investigations have shown that it acts as ligand on human and murine Toll-like receptor 2 (TLR-2) [16]. Compound **1** (Figure 1) is also shown to trigger TLR-2 [16]. The structures of both lipids (Figure 1) have been verified by total synthesis [17]. In the previously mentioned study, **1** and **2** were isolated from *Porphyromonas gingivalis*. The pathogen is reported to be a virulence factor in destructive periodontal disease, and lipids, such as dihydroceramides, have been shown to be involved in TLR-2 mediated inflammation and inhibition of osteoblast differentiation [18,19]. Compounds **1** and **2** also inhibit osteoblast differentiation and function. Notably, the effect of **2** is mediated trough TLR-2 while the effect of **1** on osteoblasts is only partly mediated via TLR-2, indicating another target for **1** in osteoblasts beside TLR-2 [20]. Due to that, serine-dipeptide lipids, together with sphingolipids, are suggested to be virulence factors of *P. ginvialis* [21]. Interestingly, all those lipids likely to be virulence factors share the attribute of an isobranched aliphatic fatty acid as a common feature, but they have a large degree of variation in the head groups [21]. It has been shown that **1** and **2** are produced by commensal oral and intestinal bacteria of the Bacteroidetes phylum, and they can be detected in human tissue samples [22]. Notably, **2** is stereospecifically deacetylated by phospholipase 2, yielding a free fatty acid and **1** [17,23].

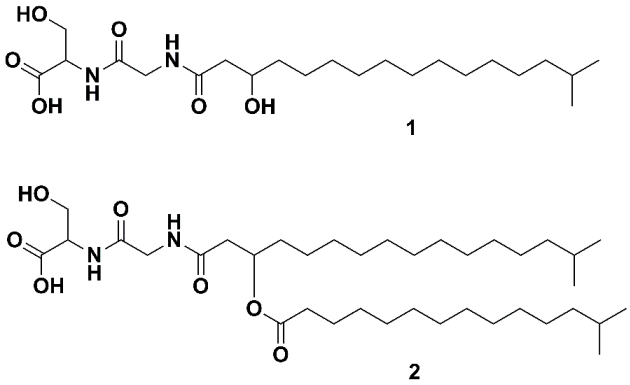

Figure 1. The two serine dipeptide lipids Lipid 430 (**1**) and Lipid 654 (**2**), according to [16].

In the present study, we investigated two marine *Algibacter* sp. isolates for anti-microbial and anti-cancer activities. Dereplication of the bioactive extracts revealed that both contained the same unidentified compound and the purification of the compound led to the isolation and identification of the lipopeptide **1** from both *Algibacter* strains. The previously unknown anti-bacterial effect against *S. agalactiae* was investigated and its cytotoxicity against lung fibroblasts and two cancer cell lines was assessed.

2. Results

2.1. High Troughput Screening and Identification of the Strains

Through an in house high-throughput screening campaign where marine microorganisms were cultivated, extracted, fractionated and screened for potential anti-cancer and anti-microbial activities, two strains showed anti-microbial activity. Sequencing of the 16S rRNA and nucleotide blast against 16S ribosomal RNA sequences revealed that the strains M09B557 and M09B045 belong to the genus *Algibacter* (Sequences in Appendix A). Strain M09B557 was isolated from the bryozoan *Alcyonidium gelatinosum* and strain M09B045 was isolated from a soft coral commonly called "sea strawberry" (*Gersemia rubiformis*), both sampled in the Barents Sea.

2.2. Bioactivity Screening and Dereplication

The strains were recultivated in three 300 mL cultures each to produce sufficient material for confirming the bioactivity detected in the previous high throughput screening campaign. The raw extracts were fractionated into six fractions using reversed phase flash liquid chromatography and subsequently tested in cell-based anti-microbial and anti-cancer assays. At concentrations of 200 and 100 µg/mL, respectively, an anti-bacterial effect of fraction five from both extracts against *Streptococcus agalactiae* was detected (see Figure 2), while no cytotoxic effect was observed against A2058 melanoma cells at a concentration of 200 µg/mL. The six flash fractions from each extract were analyzed using UHPLC-HR-MS, and the active fractions five were compared with the "flanking" inactive fractions four and six in an attempt to identify the component(s) responsible for the observed bioactivity. By comparing the MS data of the active fraction with the flanking fractions it is possible to identify compounds that are only present in the active fraction or there in the highest abundance. In addition, extracts of the growth media were prepared according to the same protocol as used for bacterial cultures. The media references were fractionated and analyzed via UHPLC-HR-MS to be compared to the extracts in order to exclude media-components present within the bacterial extracts. Compounds that were unique to the active fraction or present in higher amounts than in the inactive fractions, were further investigated by calculation of elemental compositions, and along with the MS-fragments, they were used for database searches. Using this approach, we were able to identify a candidate with a positive ion mass of *m*/*z* 431.3103 and retention time of 8.28 min present in fraction five from the extracts of both M09B557 and M09B045.

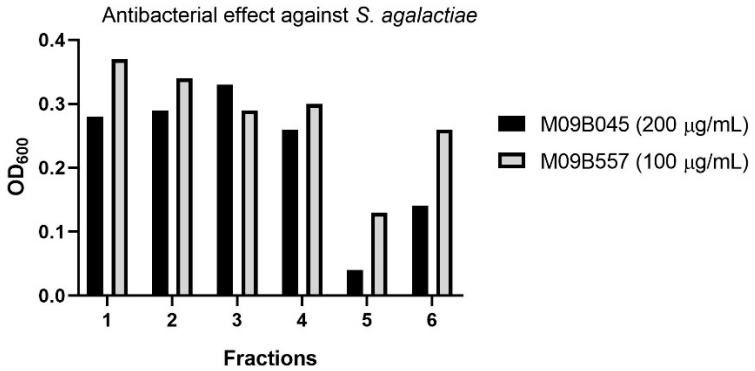

Figure 2. Anti-bacterial effect of the fractions generated by flash liquid chromatography from extracts of the cultures of the two *Algibacter* strains M09B045 and M09B557. Note that the tested assay concentrations are different for the two strains but the purpose of the test was to identify candidates for isolation rather than quantitative comparison of bioactivity.

2.3. Isolation of Lipid 430

For isolation of **1**, 16 × 450 mL of M09B557 and 12 × 450 mL of M09B045 were cultivated, extracted and fractionated. The resulting flash fraction five from each extract was pooled, dried and dissolved in DMSO (40 mg/mL) and then diluted 1:4 (*v*/*v*) in methanol. For the first HPLC-purification step, a column with C-18 functionalized stationary phase was employed. Different gradients were used to purify the target compound with fraction collection triggered by retention time. The collected fractions were reduced to dryness by vacuum centrifugation and redissolved in methanol. For the second HPLC-purification step a fluorophenyl column in combination with mass guided fraction triggering was chosen. The final yields of the isolated compound were 1.7 mg from M09B045 and 2.3 mg from M09B557. The purities of the preparations were tested using UHPLC-HR-MS and the two samples were pooled. The chromatograms (BPI and extracted ion chromatogram as well as A_{254nm}) of the purity test are given in the Supplementary Information (Figure S1).

2.4. Structure Elucidation via NMR and MS/MS Analysis

Through 1D (^{1}H, ^{13}C, Table 1) and 2D (HMBC, HSQC, H2BC, COSY, Figure 3 and Figures S2–S6 in the Supplementary Information) data recorded for **1**, the compound was confirmed to be Lipid 430. Due to significant overlap of the central CH_2 groups (13-CH_2 to 19-CH_2), in agreement with what has previously been observed for **1** as well as the ester-linked iso C15:0 variant of **1** [16], these methylene groups could not be unambiguously assigned by NMR, though the integral sum of the unresolved region was consistent with the expected number of contributing protons. Based on HR-MS/MS the elemental composition was calculated to be $C_{22}H_{42}N_2O_6$ (*m/z* 431.3112 $[M + H]^+$ in ESI+, calcd 431.3121 and 429.2970 $[M - H]^-$ in ESI−, calcd 429.2965). Taking the MS results and the NMR spectra together, the proposed structure is the only conformation that fits both datasets.

Table 1. ^{1}H and ^{13}C assignments for "Lipid 430 (**1**)" (see Figure 3) (^{1}H 600 MHz, ^{13}C 150 MHz, CD_3OH).

Lipid 430 (1)		
Position	**δ_C, Type**	**δ_H (*J* in Hz)**
1	173.8, C	
2	56.5, CH	4.47, dt (8.2, 4.2)
3a	63.2, CH_2	3.89, dd (9.3, 5.2)) [c]
3b		3.82, dd (11.3, 3.9)
4		7.99, d (7.8)
5	171.5, C	
6a	43.6, CH_2	3.98, dd (16.7, 5.9) [b]
6b		3.89, dd (9.3, 5.2) [c]
7		8.31, t (5.9)
8	175.0, C	
9a	44.8, CH_2	2.40, dd (13.9, 4.1)
9b		2.33, dd (14.0, 8.8)
10	70.0, CH	3.98, dd (16.7, 5.9) [b]
11	38.3, CH_2	1.50–1.47, m
12	26.5, CH_2	1.47–1.42, m
13	30.9–30.6 [a], CH_2	1.29, p (6.1, 5.4) [e]
14	30.9–30.6 [a], CH_2	1.29, p (6.1, 5.4) [e]
15	30.9–30.6 [a], CH_2	1.29, p (6.1, 5.4) [e]
16	30.9–30.6 [a], CH_2	1.29, p (6.1, 5.4) [e]
17	30.9–30.6 [a], CH_2	1.29, p (6.1, 5.4) [e]
18	30.9–30.6 [a], CH_2	1.29, p (6.1, 5.4) [e]
19	30.9–30.6 [a], CH_2	1.29, p (6.1, 5.4) [e]
20	28.4, CH_2	1.29, p (6.1, 5.4) [e]
21	40.1, CH_2	1.16, q (7.1, 6.7)
22	29.0, CH	1.56–1.50, m
23	22.9, CH_3	0.87, d (6.6) [d]
24	22.9, CH_3	0.87, d (6.6) [d]

[a–e] Signals are overlapping.

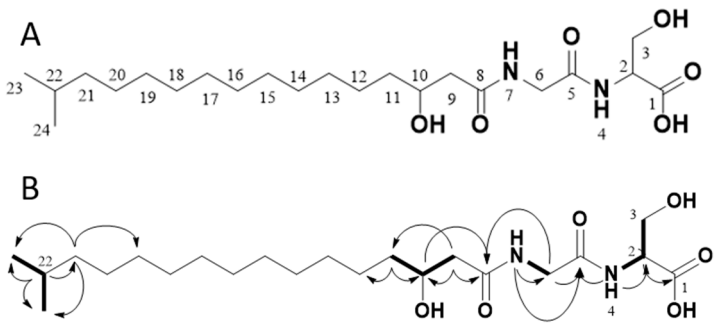

Figure 3. The structure of the isolated compound Lipid 430 (**1**) (**A**) and 2D-NMR correlations measured from our isolated sample (**B**). In B, selected COSY correlations are indicated in bold bonds and selected HMBC correlations are shown as arrows. The structure proposed upon the NMR data complies with Lipid 430 (**1**).

2.5. Anti-microbial effect of Lipid 430

Compound **1** was tested for anti-bacterial activity against *S. aureus*, *E. coli*, *E. faecialis*, *P. aeruginosa*, *S. agalactiae* and Methicillin resistant *S. aureus* (MRSA) at concentrations of 50, 25, 10, 5, 2.5 and 1 μg/mL, equal to molar concentrations of 116, 58, 23, 12, 6 and 2 μM, respectively. The tests were conducted twice, using two technical replicates in two independent experiments for *S. agalactiae*. A significant effect on *S. agalactiae* and MRSA was observed, see Figure 4. The calculated IC_{50} of **1** against *S. agalactiae* was 30 μM or 13 μg/mL respectively. At a concentration of 58 μM the growth of *S. agalactiae* was completely inhibited. For MRSA the IC_{50} was not determined as the highest tested concentration of (**1**) (116 μM or 50 μg/mL) reduced growth by 38%. To test if the observed effect on *S. agalactiae* was bactericidal or bacteriostatic, the 100 μL incubation volume of the growth assay for 58 μM **1** was streaked out further on brown agar and incubated at 37 °C. No colony or sign of bacterial growth was visible after 4 days of incubation (two technical replicates). There were no colonies formed after incubation with the compound, which indicated that **1** exerted bactericidal effect against *S. agalactiae* at a concentration of 58 μM.

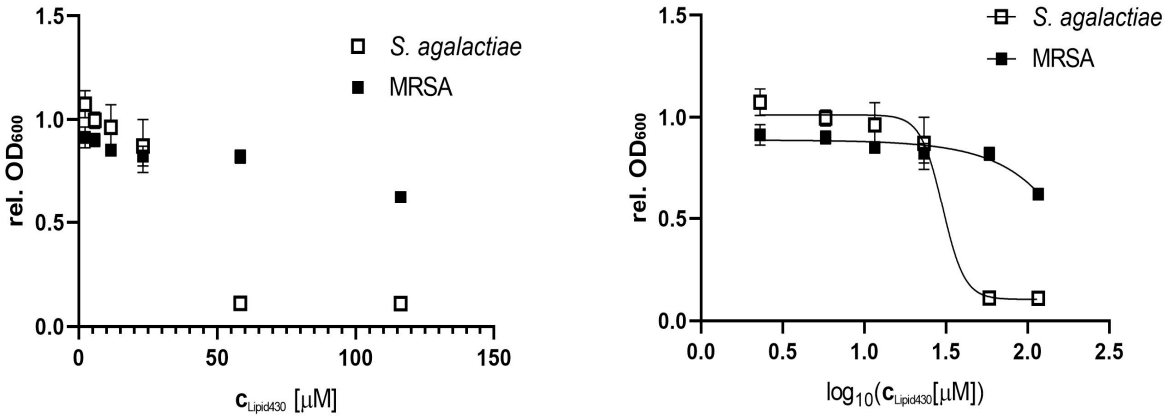

Figure 4. Anti-microbial effect of Lipid 430 (**1**) on *S. agalactiae* (two technical replicates in two experiments) and MRSA (two technical replicates). IC_{50} for *S. agalactiae* was 30.16 μM using a sigmoidal fit (Span ± 0.91 μM; Degrees of Freedom 20; R squared 0.97; Adjusted R squared 0.97, Sum of squares 0.13). IC_{50} of MRSA is >116 μM and was not determined.

2.6. Cytotoxic Effect of *1*

2.6.1. Cytotoxicity Assay

The effect of **1** was tested against three human cell lines, the melanoma cell line A2058, the colon carcinoma cell line HT29 and the lung fibroblast cell line MRC5. The compound was tested at concentrations of 100, 75, 50, 25, 10 and 5 μg/mL equal to molar concentrations of 233, 175, 116, 58, 23 and 12 μM, respectively. There was no significant effect observed against the lung fibroblast or colon carcinoma cells at the tested concentrations. The results for all tested cell lines and positive controls are shown in the Supplementary Information (Figure S7). For the melanoma cell line, a dose dependent cytotoxic effect was observed, see Figure 5. The IC_{50} of **1** against the melanoma cell line was calculated to be 175 μM (75 μg/mL). The test was executed in two independent experiments with three technical replicates each.

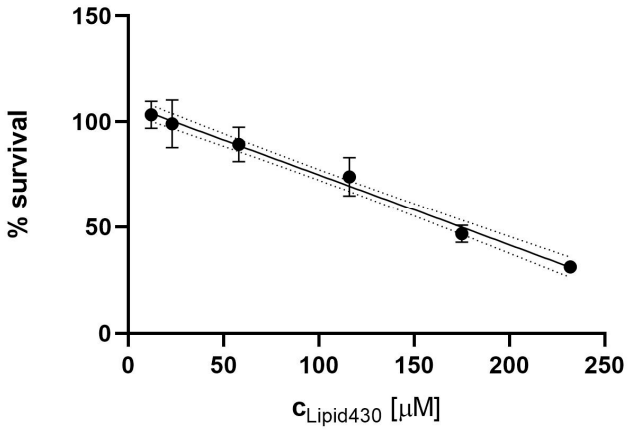

Figure 5. Cytotoxic effect of Lipid 430 (**1**) against the A2058 melanoma cell line. A linear correlation with % Survival = −0.00332c+1.08 {c ∈ ℝ | c ≥ 12 μM ˆ c ≤ 233 μM} was found (R square 0.93, Sy.x 0.07442). The 95% Confidence intervals are shown in dot lines. The calculated IC_{50} for **1** in the linear model is 175 μM.

2.6.2. Propidium Iodide Staining and Flow Cytometry

To investigate whether the cytotoxic effect of **1** was mediated by affecting the integrity of the cell membrane, propidium iodide (PI) staining in combination with flow cytometry was employed. PI is indicating integrity of the cell membrane by passing through damaged membranes and intercalating into the DNA. As a positive control, TritonX™ was tested at concentrations of 0.005, 0.01 and 0.05%. (*v*/*v*). Compound **1** was tested at concentrations of 20, 50 and 100 μM. The results are shown in Figure 6. The PI positive cells indicate the population of cells with affected cell membranes increasing with the concentration of the detergent TritonX. For **1**, no tendency was observable (see Figure 6A). The exemplary dot plot graphs of the Control and of 100 μM **1** support this assumption (see Figure 6B,C). Due to the limited amount of compound, the experiment was carried out only once, this should be considered critically when interpreting the gained data. The dot plot graphs for all conditions are given in the Supplementary Information S8.

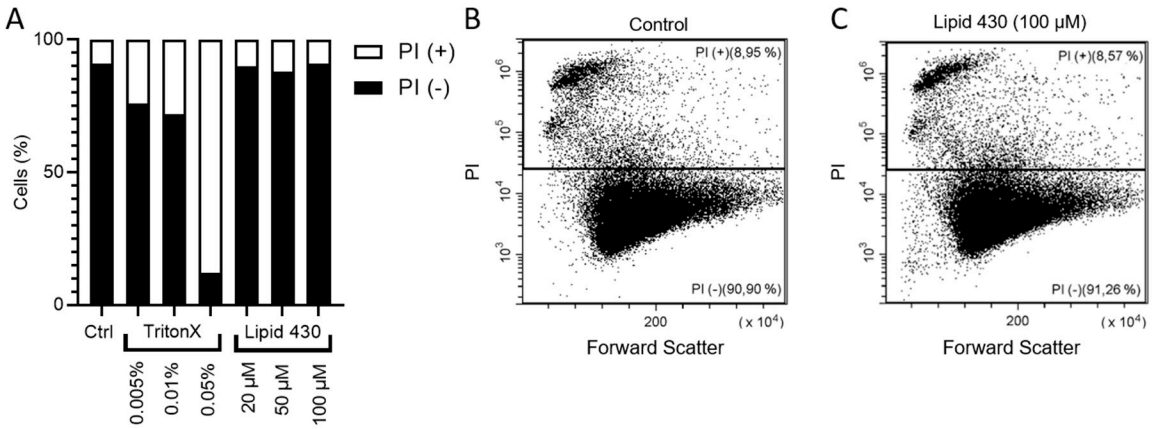

Figure 6. Results of the flow cytometry experiments with melanoma cell line A2058. In (**A**) the relative ratio between PI positive (+) and PI negative (−) is shown. The exact results are the following: stained control (Ctrl.), 8.46% PI+; 0.01% TritonX, 27.61% PI+; 0.05% TritonX, 87.38% PI+; 20 μM **1**, 9.45% PI+; 50 μM Lipid 430, 11.26% PI+; 100 μM Lipid 430, 8.72% PI+. (**B**) depicts the flow cytometry results as dot plot graph of the stained control and in (**C**) a dot plot graph of the cells threated with 100 μM **1** is given. Forward scatter is displayed on the X-axis and propidium iodide absorption on the Y-axis. The relative ratio of events is given in %.

2.6.3. Microscopic Investigation of the Melanoma Cell Line A2058

For the microscopic examination, the cells were exposed for 4 h to concentrations of 100- and 500 μg/mL of **1**, equal to molar concentrations of 233 μM and 1165 μM, respectively. In both cases, no morphological difference between the treatment and the control could be observed at 100× magnification. Microscopic pictures of the investigation are shown in the Supplementary Information (Figure S9).

2.7. Lipid Isolation, Detection of Lipid 654

Compound **1** is known to be a de-acetylation product of **2** catalyzed by phospholipases. Likewise, **1** could be the biosynthetic predecessor of **2** trough esterification of **1**. Therefore, the raw extracts of both bacteria were analyzed using UHPLC-HR-MS in order to look for **2**, but no mass signal was found that could be related to **2**. To ensure that the absence of **1** was not a result of the extraction protocol using HP-20 beads, chloroform extraction was executed with cultures of both strains. The chloroform extracts were analyzed using UHPLC-HR-MS, but no signals potentially related to **2** were detected.

3. Discussion

The active principle of the two extracts from two *Algibacter* isolates was identified and investigated upon its bioactivity towards bacteria and mammalian cell lines. The observed anti-bacterial effect of **1** against *Streptococcus agalactiae* was higher compared to the pathogen MRSA which possessed a significantly higher tolerance against **1**. Notably, *S. agalactiae* was the most sensitive among the tested bacterial strains. When screening the bacterial extracts, we frequently observed that fractions containing for instance phosphocolines or rhamnolipids were active against *S. agalactiae* while no or only weak activities were observed against the other bacteria (data not shown) [24]. The sensitivity of the melanoma cell line against **1** was significantly (at least seven times) lower compared to the anti-bacterial effect against *S. agalactiae*. Furthermore, no effects were observed on colon carcinoma cells and lung fibroblasts. This corresponds well with the observation that the initial screening of the flash fractions of the crude extracts did not show activity in the anti-cancer assays while it did in the anti-microbial assays.

The fact that **1** showed activity against the bacterial strain and cancer cell line that in our experience are most sensitive to surfactants gives rise to the suspicion that the compound is affecting the integrity of the cell membranes in an unspecific way. Given the known bioactivity of **1**, being a ligand to TLR-2 on one hand and the structure of the molecule on the other one, it was questionable if the cytotoxic effect was mediated by lysing the cells. The aliphatic, iso-branced fatty acid with a polar head consisting of two amino acids could suggest that it acts as surfactant. Therefore, PI staining followed by flow cytometry analysis was done to check if the lipid affected the membrane integrity of melanoma cells. This turned out to not be the case for any of the tested concentrations. PI staining is a technique capable of staining cells with reduced membrane integrity that can be detected by flow cytometry [25,26] with high linearity [27]. We used TritonX™ as detergent to test the suitability of the method. However, we did not observe a cellular effect after one hour of incubation with propidium iodide when analyzed with flow cytometry or after 4 h when inspecting the cells in the microscope, at least not at the tested concentrations. The effect we detected in the cytotoxicity assay was observed after 72 h of incubation with **1**, conclusively the effect is taking place during a longer incubation time maybe affecting cell division or cell cycle.

It is known that lipopeptides have a broad spectrum of activity including anti-fungal, anti-bacterial, anti-cancer and anti-inflammatory effects [28–30]. The lipopeptide antibiotic daptomycin is used to treat infections by Gram positive bacteria and was introduced into the marked in 2001 [31]. Surfactin, a lipopeptide with high surfactant power [32], exhibits also various bioactivities such as anti-inflammatory, anti-cancer and thrombolytic bioactivities [30]. The anti-bacterial and cytotoxic mode of action of both compounds relies on affecting the integrity of the cell membrane of target

cells [30,33]. However, those two marketed lipopeptides differ significantly from **1**. Daptomycin is a 13 amino acid cyclic lipopeptide (10 amino acids forming a ring structure) linked to decanoic acid [34] while Surfactin consists of a seven aminoacid cycle, linked to a 13−15 carbon chain [35]. Note that there are also linear lipopeptides as for example gageostatins, isolated from a marine *Bacillus*, showing similar bioactivities [36]. However, the mentioned cyclic lipopeptides differ greatly from the linear two-amino acid **1** in structure and molecular mass. Even the Gageostratins with an Mw > 1000 u appear to be rather distant relatives. It seems more appropriate to consult the results of Makovitzki et al. [37] who investigated synthetic lipo-tetrapeptides linked to C-12, C-14 and C-16 fatty acids. They observed varying anti-fungal, anti-bacterial and hemolytic activities depending on the respective peptide sequence and length of the fatty acid chain. Their effect in vivo corresponded with the respective lipopeptide's ability to disrupt the membrane of the respective organisms, indicating a membranolytic mode of action. Taking that together, **1** rather seemed to be a candidate for membranolytic bioactivity. Its anti-bacterial effect varies between the species and already between the two Gram positive bacteria MRSA and *S. agalactiae*. Taking all together, we conclude that **1** is not lysing the cells or affecting their integrity immediately. Taking the general bioactivity of lipopeptides into account, mostly affecting the cell membrane, possibly the lipid is interfering with the membrane during cell division, representing a more fragile state of cell integrity. It would be valuable to investigate its effect on melanoma cells more in detail, which was not possible in the present study due to a limited quantity of **1**.

After isolating **1**, the extracts of the bacterial fermentations were investigated upon the presence of the related Lipid 654 (**2**). The UPLC-MS/MS profiles of the solid phase extracts have not shown any signal that indicated the presence of **2**. However, it was reported that **2** is soluble in chloroform. To exclude that the lack of **2** was caused by unsuitability of solid phase extraction for that compound, we used chloroform liquid–liquid phase extraction and UHPLC-HR-MS to investigate its presence with negative outcome.

The natural role of *Algibacter*, being decomposers degrading algal biomass, may suggests that **1** is produced as a surfactant for mobilizing nutrients, in a similar way as the rhamnolipids do [38,39]. An additional role, or side effect, as an antibacterial agent cannot be excluded. There is no indication that the water insoluble Compound **2** is produced by the two *Algibacter* strains under the selected conditions; this could support the hypothesis that **1** is produced as a surfactant to mobilize hydrophobic nutrients. It furthermore supports the hypothesis that **1** is the biosynthetic precursor of **2** [17].

4. Materials and Methods

4.1. Bacterial Isolates

Two *Algibacter* sp. strains were isolated from organisms collected in the Barents Sea. Strain M09B557 was isolated from *Alcyonidium gelatinosum* sampled at 28.05.2009 at 70°6,60000′ N and 28°56,206190′ E. Strain M09B045 was isolated from *Gersemia rubiformis* sampled at the 14.05.2019 at 78°7,80000′ N and 13°34,962001′ E. The bacteria were isolated from the surface of the animals after washing them under filtrated seawater. Using a inoculation loop the surface of the organisms was sampled and potentially adhering bacteria were streaked out on FMAP agar, prepared of: 15 g Difco marine broth (Becton, Dickinson and Company, Franklin Lakes, NJ, USA), 15 g agar (Sigma, St. Louis, Mo, USA), 5 g peptone (Sigma), 700 mL ddH_2O and 300 mL filtrated seawater. For storage of the isolates, liquid FMAP media was inoculated with the respective strain, grown until turbidity of the media was visible and cryo-conserved at −80 °C after adding 30% (*v*/*v*) glycerol (Sigma).

4.2. PCR and Identification of the Strains

The cryo-conserved isolates were plated out on FMAP agar in petri dishes and cultivated at 10 °C. After 7 d, colonies were picked and dissolved with 100 µL ddH_2O in an Eppendorf tube. The sample was subsequently boiled for 5 min to break up the cells. For PCR, 1 µL of the bacterial lysate was used for a PCR reaction of 25 µL with 1 µM of forward and reverse primer (forward primer: 27F,

AGAGTTTGATCMTGGCTCAG; reverse primer: 1492rR, CGGTTACCTTGTTACGACTT) and 12,5 µL ThermoPrimeTM 2 × ReddyMix PCR master mix (ThermoFisher Scientific, Waltham, MA, USA). The reactions were amplified using an Mastercycler epgradient S (Eppendorf, Hamburg, Germany) with the following program: 95 °C initial denaturation for 5 min followed by 30 cycles of 94 °C for 30 s, 55 °C for 30 s and 72 °C for 1 min. Final extension was at 72 °C for 10 min. Afterwards the PCR reaction was analyzed for purity on a 1.0% agarose gel and the results were documented using a Syngene Bioimaging system. For purification of the 16S rRNA gene PCR amplificate the QIAquick PCR purification kit was used according to manufacturer's instructions (QIAGEN, Hilden, Germany). The PCR product purified from the gel was sequenced at the University Hospital of North Norway (Tromsø, Norway) employing the two primers mentioned above. For sequence homology comparison the online Basic Local Alignment Search Tool (BLAST) was used (www.ncbi.nlm.nih.gov/BLAST). The strains were identified according to their phylogenetic interference.

4.3. Fermentation and Extraction of Algibacter Cultures

M09B557 was cultivated in 1 L Warburg flasks containing 450 mL modified DSGC medium for 7 d at 130 rpm and 10 °C. M10B738 was cultivated for 12 d under the same conditions in 1 L Warburg flasks containing 450 mL DVR1 medium. Modified DSGC medium was prepared of 1 L filtrated seawater, 4.0 g D-glucose (Sigma) and 3.0 g Peptone (from casein, enzymatic digest, Sigma). DVR1 medium was prepared from 0.5 L filtrated seawater, 0.5 L ddH_2O, 6.7 g malt extract (Sigma), 11.1 g Peptone (from casein, enzymatic digest, Sigma) and 6.7 g yeast extract (Sigma). All media were autoclaved at 120 °C for 30 min. The filtrated seawater was prepared by filtrating seawater through a Millidisk® 40 Cartridge with Durapore® 0.22 µm filter membrane (Millipore, Burlington, MA, USA).

For extraction of metabolites, solid phase extraction using Diaion®HP-20 resin (13607, Supelco Analytica, Bellefonte, PA, USA) was executed. The resin had been activated by incubation in methanol for a minimum of 30 min and washed with ddH_2O for 15 min. 40 g of resin were added to 1 L of culture three days before the culture was harvested. The resin was separated from the fermentation broth by vacuum filtration using a cheesecloth mesh (1057, Dansk Hjemmeproduktion, Ejstrupholm, Danmark) to restrain the resin. Thereafter the resin was washed with 100 mL of ddH_2O to remove remaining fermentation broth. The molecules bound to the resin were eluted with 150 mL methanol (HiPerSolv, VWR, Radnor, Penns., USA) per 40 g resin (shaking at 130 rpm for 30 min) and vaccuumfiltration using Whatman No. 3 filterpaper (Whatman plc, Buckinghamshire, UK). The elution from the resin was done twice and the methanolic extract was dried under reduced pressure at 40 °C and stored at −20 °C upon further processing.

4.4. Fractionation

Crude extracts were fractionated using flash liquid chromatography. The extracts were loaded onto resin (Diaion® HP-20ss, Supelco) by dissolving them in 90% methanol aq. (*v*/*v*) and adding resin in a ratio of 1:1.5 (resin/dry extract, *w*/*w*). Subsequently, the solution was dried under reduced pressure at 40 °C. Flash columns (Biotage® SNAP Ultra, Biotage, Uppsala, Sweden) were prepared by activating the resin by incubation in methanol for 20 min, washing with ddH_2O and loading it into the column ensuring the resin being always covered with water. 6.5 g HP-20ss resin was loaded on one column. The fractionation was performed using a Biotage SP4™ system and a water: methanol gradient from 5–100% methanol over 36 min (6 min 5% B, 6 min 25% B, 6 min 50% B, 6 min 75% B, 12 min 100% B) followed by a methanol: acetone step-gradient (4 min methanol, 12 min acetone). The flow rate was set to 12 mL/min. 27 eluent fractions to 24 mL each were collected in glass tubes and pooled to six flash fractions in total (1–3 were pooled to fraction 1; 4–6 to fraction 2; 7–9 to fraction 3; 10–12 to fraction 4; 13–15 to fraction 5; 16–27 to fraction 6). An appropriate amount of extract-resin mixture was loaded onto the column after equilibration to 5% methanol aq. (*v*/*v*). The flash fractions were dried under reduced pressure at 40 °C.

4.5. UHPLC-HR-MS and Dereplication

UHPLC-HR-MS data for dereplication was recorded using an Acquity I-class UPLC (Waters, Milford, MA, USA) coupled to a PDA detector and a Vion IMS QToF (Waters). The chromatographic separation was performed using an Acquity C-18 UPLC column (1.7 µm, 2.1 mm × 100 mm) (Waters). Mobile phases consisted out of acetonitrile (HiPerSolv, VWR) for mobile phase A and ddH_2O produced by the in-house Milli-Q system as mobile phase B, both containing 1% formic acid (*v*/*v*) (33015, Sigma). The gradient was run from 10% to 90% B in 12 min at a flow rate of 0.45 mL/min. Samples were run in ESI+ and ESI- ionization mode. The data was processed and analyzed using UNIFI 1.8.2 (Waters).

4.6. Isolation of Lipid 430

Purification of compound **1** was done using a semi preparative HPLC system (Waters) made up by a 600 HPLC pump, a 3100 mass spectrometer, a 2996 photo diode array detector and a 2767 sample manager. A 515 HPLC pump and a flow splitter were used to infuse the analytes into the MS. The mobile phases were degassed by an in-line degasser. For controlling the system, the software MassLynx™ 4.1 (Waters) was used. The columns used for isolation were X-Terra RP-18 preparative column (10 µm, 10 mm × 250 mm) and XSelect CSH preparative Fluoro-Phenyl column (5 µm, 10 mm × 250mm), both columns were purchased from Waters. The mobile phases for the gradients were A [ddH_2O with 0.1% (*v*/*v*) formic acid] and B [acetonitrile with 0.1% (*v*/*v*) formic acid], flow rate was set to 6 mL/min. Acetonitrile (Prepsolv®, Merk KGaA, Darmsatdt, Germany) and formic acid (33015, Sigma) were purchased in appropriate quality, ddH_2O was produced with the in-house Milli-Q® system. For the MS-detection of the eluting compounds one percent of the flow was split from the fractions in line, blended with 80% Methanol in ddH_2O (*v*/*v*) acidified with 0.2% Formic acid (Sigma) and directed to the ESI-quadrupole-MS.

4.7. NMR Spectroscopy

All NMR spectra were recorded on a Bruker Avance III HD spectrometer equipped with an inverse detected TCI probe with cryogenic enhancement on ^{1}H, ^{2}H and ^{13}C. The operating frequencies were 599.90 MHz for ^{1}H and 150.86 MHz for ^{13}C. The samples were prepared in methanol-d_3 and recorded at 298 K.

All experiments were recorded using standard pulse sequences for Proton, Presat, Carbon, DQFCOSY, HSQC, HMBC, H2BC, NOESY and ROESY (gradient selected and adiabatic versions, with matched sweeps where applicable) in Topspin 3.5pl7 and processed in Mnova 12.0.0. Spectra were referenced on the residual solvent peak of methanol-d_3 ($\delta H = 3.31$ and $\delta C = 49.00$).

4.8. Lipid Extraction

Total lipids were extracted by shaking 25 mL of bacterial culture with 25 mL chloroform (EMSURE®, Merck) in screw cap centrifuge tubes (21008-242, VWR) for 3 h at 40 rpm using a tube-rotator (SB3, Stuart, Stone, UK). Afterwards the organic phase was separated and centrifuged for 10 min at 4600 rpm (Multifuge 3, rotor 75006445, S-R, Heraeus, Hanau, Germany) to remove debris and particles. Thereafter the organic phase was vacuum filtrated trough Whatman No. 3 filter paper (Whatman) and concentrated to 5 mL under nitrogen.

4.9. Anti-Microbial Assays

4.9.1. Growth Inhibition Assay

To determine and quantify anti-microbial activity, a bacteria growth inhibition assay in liquid media was executed. The samples were tested against *S. aureus* (ATCC 25923), *E. coli* (ATCC 259233), *E. faecialis* (ATCC 29122), *P. aeruginosa* (ATCC 27853), *S. agalactiae* (ATCC 12386) and Methicillin resistant *S. aureus* (MRSA) (ATCC 33591). *S. aureus*, MRSA, *E. coli* and *P. aeruginosa* were grown in Muller Hinton

broth (275730, Becton, Dickinson and Company). *E. facalis* and *S. agalactiae* were cultured in brain hearth infusion broth (53286, Sigma). Fresh bacteria colonies were transferred in the respective medium and incubated at 37 °C over night. The bacterial cultures were diluted to a culture density representing the log phase and 50 μL/well were pipetted into a 96-well microtiter plate (734-2097, Nunclon™, Thermo Scientific, Waltham, MA, USA). The final cell density was 1500–15,000 CFU/well. Flash fractionated extracts were diluted in 1% (*v*/*v*) dimethyl sulfoxide (DMSO, D4540, Sigma). Pure compound was diluted in 2% (*v*/*v*) DMSO in ddH_2O, the final assay concentration was 50% of the prepared sample, since 50 μL of sample in DMSO/water were added to 50 μL bacterial culture. After adding the samples to the plates, they were incubated over night at 37 °C and the growth was determined by measuring the optical density at λ = 600 nm (OD_{600}) with a 1420 Multilabel Counter VICTOR^3™ (Perkin Elmer, Waltham, MA, USA). A water sample was used as reference control, growth medium without bacteria was used as a negative control and a dilution series of gentamycin (A2712, Merck) from 32 to 0.01 μg/mL was used as positive control and visually inspected for bacterial growth. The positive control was used as system suitability test and the results of the antimicrobial assay were only considered valid when positive control was passed. The final concentration of DMSO in the assays was ≤ 2% (*v*/*v*) known to have no effect in the tested bacteria. The data was processed using GraphPad Prism 8.

4.9.2. Bactericidal Assay

For investigation of bactericidal effect, the 100 μL reactions of the *S. agalactiae* anti-microbial assay were streaked on brown agar plates (University hospital of northern Norway, Tromsø, Norway) and incubated for four days at 37 °C, the plates were visually investigated after 1 day and 4 days of incubation.

4.10. Cell Proliferation Assay

The inhibitory effect of fractions and compounds was tested using an MTS in vitro cell proliferation assay against two cancer cell lines and one normal cell line. The cancer cell lines were human melanoma A2058 (ATCC, CLR-1147™) and human colon carcinoma HT29 (ATCC HTB-22™), as cell line for the general cytotoxicity assessment, non-malignant MRC5 lung fibroblast cells (ATCC CCL-171™) were employed. The cells were cultured and assayed in Roswell Park Memorial Institute medium (RPMI-16040, FG1383, Merck) containing 10% (*v*/*v*) Fetal Bovine serum (FBS, 50115, Biochrom, Cambridge, UK). The cell-concentration was 4000 cells/well for the lung fibroblast cells and 2000 cells/well for the cancer cells. After seeding, the cells were incubated 24 h at 37 °C and 5% CO_2. The medium was then replaced with fresh RPMI-1640 medium supplemented with 10% (*v*/*v*) FBS and gentamycin (10 μg/mL, A2712, Merck). After adding 10 μL of sample diluted in 2% (*v*/*v*) DMSO in ddH_2O the cells were incubated for 72 h at 37 °C and 5% CO_2. For assaying the viability of the cells 10 μL of CellTiter 96®AQ_{ueous} One Solution Reagent (G3581, Promega, Madison, WI, USA) containing tetrazolium [3-(4,5-dimethylthiazol-2-yl)-5-(3-carboxymethoxyphenyl)-2-(4-sulfophenyl)-2H-tetrazolium, inner salt] and phenazine ethosulfate was added to each well and incubated for one hour. The tests were executed with three technical replicates. The plates were read using a DTX 880 plate reader by measuring the absorbance at λ = 485 nm. The cell viability was calculated using the media control. As a negative control RPMI-1640 with 10% (*v*/*v*) FBS and 0.5% Triton™ X-100 (Sigma-Aldrich) was used as a positive control. The data was processed and visualized using GraphPad Prism 8

4.11. Mode of Action Studies

4.11.1. Flow Cytometry

For the investigation of the mode of action of **1** on the A2058 cells, cells were seed in six well plates (Nunclon™, Thermo Fisher) with a density of one million cells in three mL of Eagle's medium (Dulbecco's modified Eagles medium, D6171, Sigma) with 10% (*v*/*v*) FBS. Cells were incubated over

night at 37 °C and 5% CO_2 and medium was exchanged to two mL Eagle's medium, the respective amount of compound or Triton™ X-100 (Sigma-Aldrich) as positive control, propidium iodide (Sigma) to a final concentration of 5 μg/mL and the wells were filled up to 3 mL with phosphate buffered saline (PBS, Dulbecco's PBS, D8537, Sigma). One unstained control without propidium iodide and one negative control without compound were prepared. The reactions were incubated for 1 h at 37 °C and 5% CO_2, media was removed, the cells were spilled with PBS buffer and trypsinated using 400 μL of trypsine solution (Trypsin-EDTA 10 ×, Biowest, Nuaillé, France) and redissolved in 1 mL of PBS with propidium iodide (5 μg/mL). The cell suspensions were transferred into sample tubes and analyzed using a Cytoflex flow cytometer (Beckman Coulter, Brea, Cal., US) and CytExpert.

4.11.2. Microscopic Investigation of Melanoma Cells

For the microscopic investigation of melanoma cells, the A2058 cells were seed out in Eagle's medium at a concentration of 2000 cells/well in 100 μL medium per well. The cells were incubated over night at 37 °C and 5% CO_2. The media in the wells was replaced with 50 μL Eagle's medium, compound **1** was added and the wells were filled up with PBS to a total volume of 100 μL. The reactions were incubated at 37 °C and 5% CO_2 for 4 h, 50 μL of media were removed and replaced with 50 μL of 0.4% Trypan blue solution (Sigma) and incubated at room temperature for three minutes. Then the media with Trypan blue was removed, leaving the bottom of the wells covered with a thin liquid layer and examined microscopically at a magnification of 10 × 10 (Leica DMIC, Leica, Germany). Pictures were taken using a microscope camera (Marlin F-046B IRF, Allied vision, Germany).

5. Conclusions

It was shown that two strains of the genus *Algibacter* were capable of producing Lipid 430 (**1**). The bioactivity of **1** seems to be comparable to other lipopeptides such as synthetic lipo-tetrapeptides. It showed cytotoxicity against melanoma cells with a IC_{50} concentration of 175 μM after 72 h of incubation, the exact mode of action remains to be investigated but our experimental results indicate that **1** did not lyse the cells immediately. The IC_{50} concentration against *S. agalactiae* was determined to be 30 μM, at a concentration of 58 μM it was shown to be bactericidal against *S. agalactiae*. To the best of our knowledge, this is the first report of bioactive compounds isolated from the genus *Algibacter*.

Supplementary Materials: The following are available online, Figure S1: purity analysis of prepared compound **1**, Figure S2: ^{1}H NMR spectrum of **1**, Figure S3: ^{13}C NMR spectrum of **1**, Figure S4: HSQC + HMBC spectrum of **1**, Figure S5: COSY spectrum of **1**, Figure S6: H2BC spectrum of **1**, Figure S7: results of the cytotoxicity assays, Figure S8: results of the flow cytometry experiments, Figure S9: pictures of the microscopic investigation of melanoma cells.

Author Contributions: Y.K.-H.S. fermented and extracted the cultures, dereplicated and isolated the compound; J.I., K.Ø.H. and Y.K.-H.S. elucidated the structure; S.U. and Y.K.-H.S. planned and executed the investigation of the cytotoxicity; J.H.A., E.H.H. and Y.K.-H.S. designed the study; Y.K.-H.S., K.Ø.H., E.H.H. and J.H.A. prepared the manuscript.

Funding: This project received funding from the Marie Skłodowska-Curie Action MarPipe, grant agreement GA 721421 H2020-MSCA-ITN-2016, of the European Union and from UiT – The Arctic University of Norway.

Acknowledgments: The authors want to acknowledge our colleagues from The Norwegian Marine Biobank (Marbank) for isolation and identification of the bacterial strains. Marte Albrigtsen and Kirsti Helland are gratefully acknowledged for execution of the bioassays and their help in solving many experimental issues.

Conflicts of Interest: The authors declare no conflict of interest.

Appendix A

16S rRNA sequencing results

Strain ID	Genus	16s rRNA sequence
M09B557	*Algibacter* sp.	TTGGGTTTAAGGGTCCGTAGGTGGATAATTAAGTCAGAGGTGAAAGTT TGCAGCTCAACTGTAAAATTGCCTTTGATACTGGTTATCTTGAATCATT ATGAAGTGGTTAGAATATGTAGTGTAGCGGTGAAATGCATAGATATT ACATAGAATACCAATTGCGAAGGCAGATCACTAATAATGTATTGACA CTGATGGACGAAAGCGTGGGGAGCGAACAGGATTAGATACCCTGGTA GTCCACGCCGTAAACGATGGATACTAGCTGTTCGGAACTTGTTTCTGA GTGGCTAAGCGAAAGTGATAAGTATCCCACCTGGGGAGTACGTTCGC AAGAATGAAACTCAAAGGAATTGACGGGGGCCCGCACAAGCGGTGG AGCATGTGGTTTAATTCGATGATACGCGAGGAACCTTACCAGGGCTTA AATGTAGATTGACAGGACTAGAGATAGTTTTTTCTTCGGACAATTTAC AAGGTGCTGCATGGTTGTCGTCAGCTCGTGCCGTGAGGTGTCAGGTTA AGTCCTATAACGAGCGCAACCCCTGTTGTTAGTTGCCAGCGAGTCAAG TCGGGAACTCTAACAAGACTGCCAGTGCAAACTGTGAGGAAGGTGGG GATGACGTCAAATCATCACGGCCCTTACGTCCTGGGCTACACACGTGC TACAATGGTAGGGACAGAGAGCAGCCACTGGGCGACCAGGAGCGAA TCTATAAACCCTATCACAGTTCGGATCGGAGTCTGCAACTCGACTCCG TGAAGCTGGAATCGCTAGTAATCGCATATCAGCCATGATGCGGNGAA TACGTTCCCGGGNNNT
M09B045	*Algibacter* sp.	TGANNGTTTGCAGCTCANNNNNNAAATTGCCTTTGATACNNGTTATC TTGAATCATTATGANNNNNNTAGANTNNGNANNNNNGCGGTGAAA TGCATAGATATTACATAGAATACCAATTGCGAAGGCAGATCACTAAT AATGTATTGACACTGATGGACGAAAGCGTGGGGAGCGAACAGGATTA GATACCCTGGTAGTCCACGCCGTAAACGATGGATACTAGCTGTTCGG AACTTGTTTCTGAGTGGCTAAGCGAAAGTGATAAGTATCCCACCTGGG GAGTACGTTCGCAAGAATGAAACTCAAAGGAATTGACGGGGGCCCG CACAAGCGGTGGAGCATGTGGTTTAATTCGATGATACGCGAGGAACC TTACCAGGGCTTAAATGTAGATTGACAGGACTAGAGATAGTTTTTTCT TCGGACAATTTACAAGGTGCTGCATGGTTGTCGTCAGCTCGTGCCGTG AGGTGTCAGGTTAAGTCCTATAACGAGCGCAACCCCTGTTGTTAGTTG CCAGCGAGTCATGTCGGGAACTCTAACAAGACTGCCAGTGCAAACTG TGAGGAAGGGGGGGGGATGACGTCAAATCATCACGGCCCTTACGTCC TGGGCTACACACGTGCTACAATGGTAGGGACAGAGAGCAGCCACTGG GCGACCAGGAGCGAATCTATAAACCCTATCACAGTTCGGATCGGAGT CTGCAACTCGACTCCGTGAAGCTGGAATCGCTAGTAATCGCATATCAG CCATGATGCGGTGAATACGTTCCCGGGCCTTGTACACACCGCCCGTCA AGCCATGGAAGCTGGGANTGNCTGAAGTCCGTCACCGTAAGGGAGC GGGC

References

1. Kirchman, D.L. The ecology of Cytophaga-Flavobacteria in aquatic environments. *FEMS Microb. Ecol.* **2002**, *39*, 91–100. [CrossRef]
2. Fernández-Gómez, B.; Richter, M.; Schüler, M.; Pinhassi, J.; Acinas, S.G.; González, J.M.; Pedrós-Alió, C. Ecology of marine Bacteroidetes: A comparative genomics approach. *ISME J.* **2013**, *7*, 1026–1037. [CrossRef]
3. Gómez-Pereira, P.R.; Fuchs, B.M.; Alonso, C.; Oliver, M.J.; Beusekom, J.E.E.; Amann, R. Distinct flavobacterial communities in contrasting water masses of the north Atlantic Ocean. *ISME J.* **2010**, *4*, 472–487. [CrossRef]
4. Nedashkovskaya, O.I.; Kim, S.B.; Han, S.K.; Rhee, M.S.; Lysenko, A.M.; Rohde, M.; Zhukova, N.V.; Frolova, G.M.; Mikhailkov, V.V.; Bae, K.S. *Algibacter lectus* gen. nov., sp. nov., a novel member of the family *Flavobacteriaceae* isolated from green algae. *Int. J. System. Evol. Microbiol.* **2004**, *54*, 1257–1261. [CrossRef]

5. Park, S.C.; Hwang, Y.M.; Choe, H.N.; Baik, K.S.; Kim, H.; Seong, C.N. *Algibacter aquimarinus* sp. nov., isolated from a marine environment, and reclassification of *Pontirhabdus pectinivorans* as *Algibacter pectinivorans* comb. nov. *Int. J. System. Evol. Microbiol.* **2013**, *63*, 2038–2042. [CrossRef]
6. Park, S.C.; Hwang, Y.M.; Lee, J.H.; Baik, K.S.; Seong, C.N. *Algibacter agarivorans* sp. nov. and *Algibacter agarilyticus* sp. nov., isolated from seawater, reclassification of *Marinivirga aestuarii* as *Algibacter aestuarii* comb. nov. and emended description of the genus *Algibacter*. *Int. J. System. Evol. Microbiol.* **2013**, *63*, 3494–3500. [CrossRef]
7. Nedashkovskaya, O.I.; Vancanneyt, M.; Kim, S.B.; Hoste, B.; Bae, K.S. *Algibacter mikhailovii* sp. nov., a novel marine bacterium of the family *Flavobacteriaceae*, and emended description of the genus *Algibacter*. *Int. J. System. Evol. Microbiol.* **2007**, *57*, 2147–2150. [CrossRef]
8. Park, S.; Jung, Y.T.; Yoon, J.H. *Algibacter miyuki* sp. nov., a member of the family *Flavobacteriaceae* isolated from leachate of a brown algae reservoir. *Antonie Van Leeuwenhoek* **2013**, *104*, 253–260. [CrossRef]
9. Yoon, J.H.; Park, S. *Algibacter wandonensis* sp nov., isolated from sediment around a brown algae (*Undaria pinnatifida*) reservoir. *Int. J. System. Evol. Microbiol.* **2013**, *63*, 4771–4776. [CrossRef]
10. Sun, C.; Fu, G.; Zhang, C.; Hu, J.; Xu, L.; Wang, R.; Su, Y.; Han, S.; Yu, X.; Cheng, H.; et al. Isolation and complete genome sequence of *Algibacter alginolytica* sp. nov., a novel seaweed-degrading *Bacteroidetes* bacterium with diverse putative polysaccharide utilization loci. *Appl. Environ. Microbiol.* **2016**, *82*, 2975–2987. [CrossRef]
11. Kawai, Y.; Yano, I.; Kaneda, K. Various kinds of lipoamino acids including a novel serine-containing lipid in an opportunistic pathogen *Flavobacterium*. *Eur. J. Biochem.* **1988**, *171*, 73–80. [CrossRef]
12. Shiozaki, M.; Deguchi, N.; Mochizuki, T.; Wakabayashi, T.; Ishikawa, T.; Haruyama, H.; Kawai, Y.; Nishijima, M. Revised structure and synthesis of Flavolipin. *Tetrahedron* **1998**, *54*, 11861–11876. [CrossRef]
13. Ratner, H. Flavobacterium meningosepticum. *Inf. Contr.* **1984**, *5*, 237–239. [CrossRef]
14. Kawai, Y.; Akagawa, K. Macrophage activation by an ornithine-containing lipid or a serine-containing lipid. *Inf. Immun.* **1989**, *57*, 2086–2091.
15. Gomi, K.; Kawasaki, K.; Kawai, Y.; Shiozaki, M.; Nishijima, M. Toll-like receptor 4-MD-2 complex mediates the signal transduction induced by Flavolipin, an amino acid-containing lipid unique to *Flavobacterium meningosepticum*. *J. Immun.* **2002**, *168*, 2939–2943. [CrossRef]
16. Clark, B.R.; Cervantes, J.L.; Maciejewski, M.W.; Farrokhi, V.; Nemati, R.; Yao, X.; Anstadt, E.; Fujiwara, M.; Wright, K.T.; Riddle, C.; et al. Serine lipids of *Porphyromonas gingivalis* are human and mouse toll-like receptor 2 ligands. *Inf. Immun.* **2013**, *81*, 3479–3489. [CrossRef]
17. Dietz, C.; Hart, T.K.; Nemati, R.; Yao, X.; Nichols, F.C.; Smith, M.B. Structural verification via convergent total synthesis of dipeptide–lipids isolated from *Porphyromonas gingivalis*. *Tetrahedron* **2016**, *72*, 7557–7569. [CrossRef]
18. Wang, Y.H.; Jiang, J.; Zhu, Q.; AlAnezi, A.Z.; Clark, R.B.; Jiang, X.; Rowe, D.W.; Nichols, F.C. *Porphyromonas gingivalis* lipids inhibit osteoblastic differentiation and function. *Infect. Immun.* **2010**, *78*, 3726–3735. [CrossRef]
19. Nichols, F.C.; Housley, W.J.; O'Conor, C.A.; Manning, T.; Wu, S.; Clark, R.B. Unique lipids from a common human bacterium represent a new class of toll-like receptor 2 ligands capable of enhancing autoimmunity. *Ame. J. Pathol.* **2009**, *175*, 2430–2438. [CrossRef]
20. Wang, Y.H.; Nemati, R.; Anstadt, E.; Liu, Y.; Son, Y.; Zhu, Q.; Yao, X.; Clark, R.B.; Rowe, D.W.; Nichols, F.C. Serine dipeptide lipids of *Porphyromonas gingivalis* inhibit osteoblast differentiation: Relationship to Toll-like receptor 2. *Bone* **2015**, *81*, 654–661. [CrossRef]
21. Olsen, I.; Nichols, F.C. Are Sphingolipids and serine dipeptide lipids underestimated virulence factors of *Porphyromonas gingivalis*? *Infect. Immun.* **2018**, *86*, e00035-18. [CrossRef]
22. Nemati, R.; Dietz, C.; Anstadt, E.J.; Cervantes, J.; Liu, Y.; Dewhirst, F.E.; Clark, R.B.; Finegold, S.; Gallagher, J.J.; Smith, M.B.; et al. Deposition and hydrolysis of serine dipeptide lipids of *Bacteroidetes* bacteria in human arteries: Relationship to atherosclerosis. *J. Lipid Res.* **2017**, *58*, 1999–2007. [CrossRef]
23. Nemati, R.; Dietz, C.; Anstadt, E.; Clark, R.; Smith, M.; Nichols, F.; Yao, X. Simultaneous determination of absolute configuration and quantity of lipopeptides using chiral liquid chromatography/mass spectrometry and diastereomeric internal standards. *Anal. Chem.* **2017**, *89*, 3583–3589. [CrossRef]

24. Kristoffersen, V.; Rämä, T.; Isaksson, J.; Andersen, J.H.; Gerwick, W.H.; Hansen, E. Characterization of Rhamnolipids produced by an arctic marine bacterium from the *Pseudomonas fluorescence* group. *Mar. Drugs* **2018**, *16*, 163. [CrossRef]
25. Sasaki, D.T.; Dumas, S.E.; Engleman, E.G. Discrimination of viable and non-viable cells using propidium iodide in two color immunofluorescence. *Cytometry* **1987**, *8*, 413–420. [CrossRef]
26. Pietkiewicz, S.; Schmidt, J.H.; Lavrik, I.N. Quantification of apoptosis and necroptosis at the single cell level by a combination of imaging flow cytometry with classical annexin V/propidium iodide staining. *J. Immun. Methods* **2015**, *423*, 99–103. [CrossRef]
27. Mascotti, K.; McCullough, J.; Burger, S.R. HPC viability measurement: Trypan blue versus acridine orange and propidium iodide. *Transfusion* **2000**, *40*, 693–696. [CrossRef]
28. Hamley, I.W. Lipopeptides: From self-assembly to bioactivity. *Chem. Commun.* **2015**, *51*, 8574–8583. [CrossRef]
29. Raaijmakers, J.M.; De Bruijn, I.; Nybroe, O.; Ongena, M. Natural functions of lipopeptides from *Bacillus* and *Pseudomonas*: More than surfactants and antibiotics. *FEMS Microbiol. Rev.* **2010**, *34*, 1037–1062. [CrossRef]
30. Seydlová, G.; Svobodová, J. Review of surfactin chemical properties and the potential biomedical applications. *Cent. Eur. J. Med.* **2008**, *3*, 123–133. [CrossRef]
31. Baltz, R.H. Daptomycin: Mechanisms of action and resistance, and biosynthetic engineering. *Curr. Opin. Chem. Biol.* **2009**, *13*, 144–151. [CrossRef] [PubMed]
32. Mor, A.; Gurwitz, D. Peptide-based antibiotics: A potential answer to raging antimicrobial resistance. *Drug Dev. Res.* **2000**, *50*, 440–447. [CrossRef]
33. Humphries, R.M.; Pollett, S.; Sakoulas, G. A current perspective on Daptomycin for the clinical microbiologist. *Clin. Microbiol. Rev.* **2013**, *26*, 759–780. [CrossRef] [PubMed]
34. Debono, M.; Abbott, B.J.; Molloy, R.M.; Fukuda, D.S.; Hunt, A.H.; Daupert, V.M.; Counter, F.T.; Ott, J.L.; Carrell, C.B.; Howard, L.C.; et al. Enzymatic and chemical modifications of lipopeptide antibiotic A21978C: The synthesis and evaluation of Daptomycin (LY146032). *J. Antibiot.* **1988**, *41*, 1093–1105. [CrossRef] [PubMed]
35. Peypoux, F.; Bonmatin, J.M.; Wallach, J. Recent trends in the biochemistry of surfactin. *Appl. Microbiol. Biotech.* **1999**, *51*, 553–563. [CrossRef] [PubMed]
36. Tareq, F.S.; Lee, M.A.; Lee, H.-S.; Lee, J.-S.; Lee, Y.-J.; Shin, H.J. Gageostatins A-C, antimicrobial linear lipopeptides from a marine *Bacillus Subtilis*. *Mar. Drugs* **2014**, *12*, 871–885. [CrossRef] [PubMed]
37. Makovitzki, A.; Avrahami, D.; Shai, Y. Ultrashort antibacterial and antifungal lipopeptides. *Proc. Natl. Acad. Sci. USA* **2006**, *103*, 15997–16002. [CrossRef]
38. Chrzanowski, Ł.; Ławniczak, Ł.; Czaczyk, K. Why do microorganisms produce rhamnolipids? *World J. Microbiol. Biotechnol.* **2012**, *28*, 401–419. [CrossRef]
39. Abdel-Mawgoud, A.; Lépine, F.; Déziel, E. Rhamnolipids: Diversity of structures, microbial origins and roles. *Appl. Microbiol. Biotechnol.* **2010**, *86*, 1323–1336. [CrossRef]

Sample Availability: Samples of the compound **1** are available from the authors.

© 2019 by the authors. Licensee MDPI, Basel, Switzerland. This article is an open access article distributed under the terms and conditions of the Creative Commons Attribution (CC BY) license (http://creativecommons.org/licenses/by/4.0/).

Supplementary Information

Purity of the prepared Lipid 430 (1) by UHPLC-DAD-MS/MS

Figure S1 ESI− BPI chromatogram (A), Extracted Ion chromatogram of **1** (B) and $A_{254\ nm}$ chromatogram (C)

NMR Spectroscopic Data for Lipid 430 (1)

Figure S2 ^{1}H NMR (600 MHz, CD_3OD) spectrum of **1**

Figure S3 ^{13}C NMR (151 MHz, CD_3OD) spectrum of **1**

Figure S4 HSQC + HMBC (600 MHz, CD_3OD) spectrum of **1**

Figure S5 COSY (600 MHz, CD_3OD) spectrum of **1**

Figure S6 H2BC (600 MHz, CD_3OD) spectrum of **1**

Results of the cytotoxicity assay

Figure S7 Results of the cytotoxicity assays for all tested cell lines

Results of the mode of action studies for all concentrations of Lipid 430 (1) and controls

Figure S8 Results of the flow cytometry experiments with propidium iodide staining

Figure S9 Pictures of the microscopic investigation

Figure S1. ESI− BPI chromatogram (A), Extracted Ion chromatogram of Lipid 430 (B) and $A_{254\ nm}$ (C)

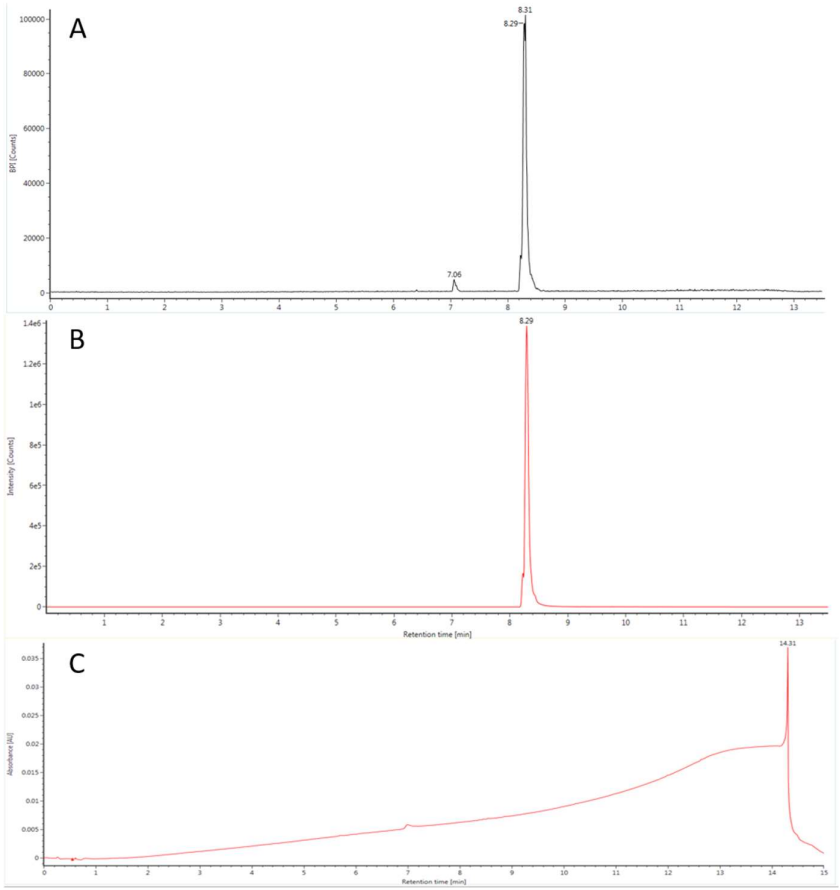

Chromatograms of the UHPLC analysis of the isolated Lipid 430 (**1**). In A the base peak intensity chromatogram of the ESI-MS/MS signal is depicted. In B the extracted ion chromatogram of the most abundant isotopic peak (m/z 429.2972, $[M-H]^-$) and in C the absorption at 254 nm. The signal at RT = 7.06 min is also visible when injecting the blank solution.

Figure S2. ^{1}H NMR (600 MHz, CD_3OD) spectrum of **1**

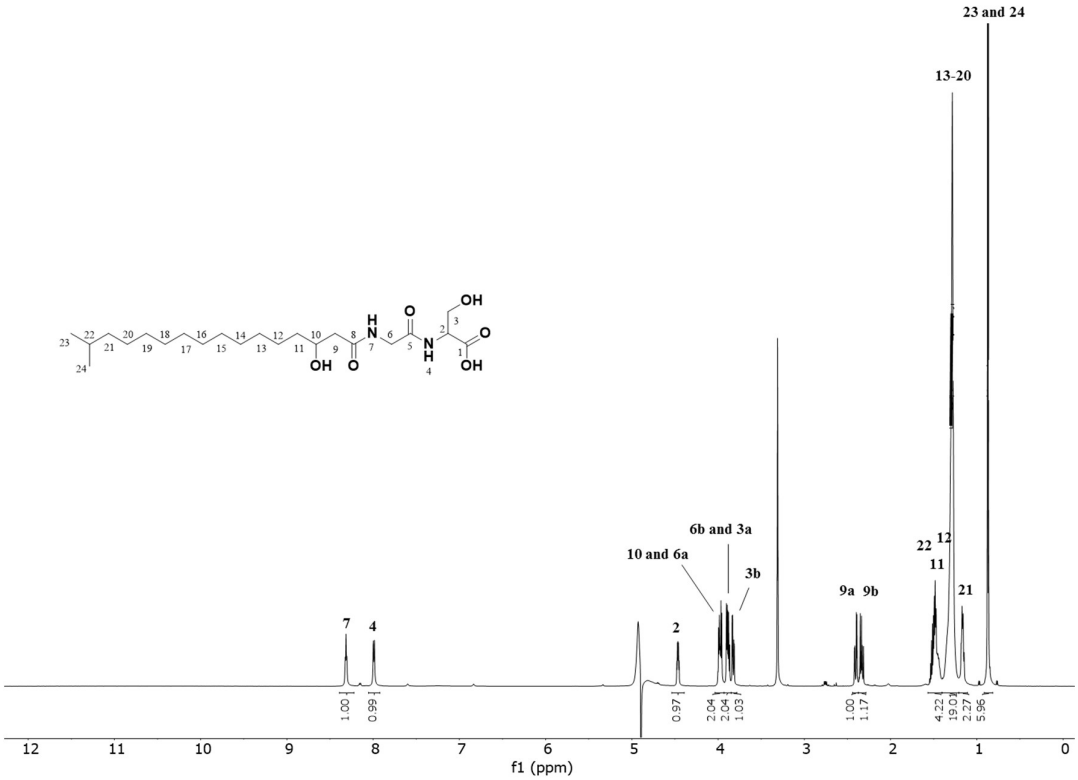

Figure S3. ^{13}C NMR (151 MHz, CD_3OD) spectrum of **1**

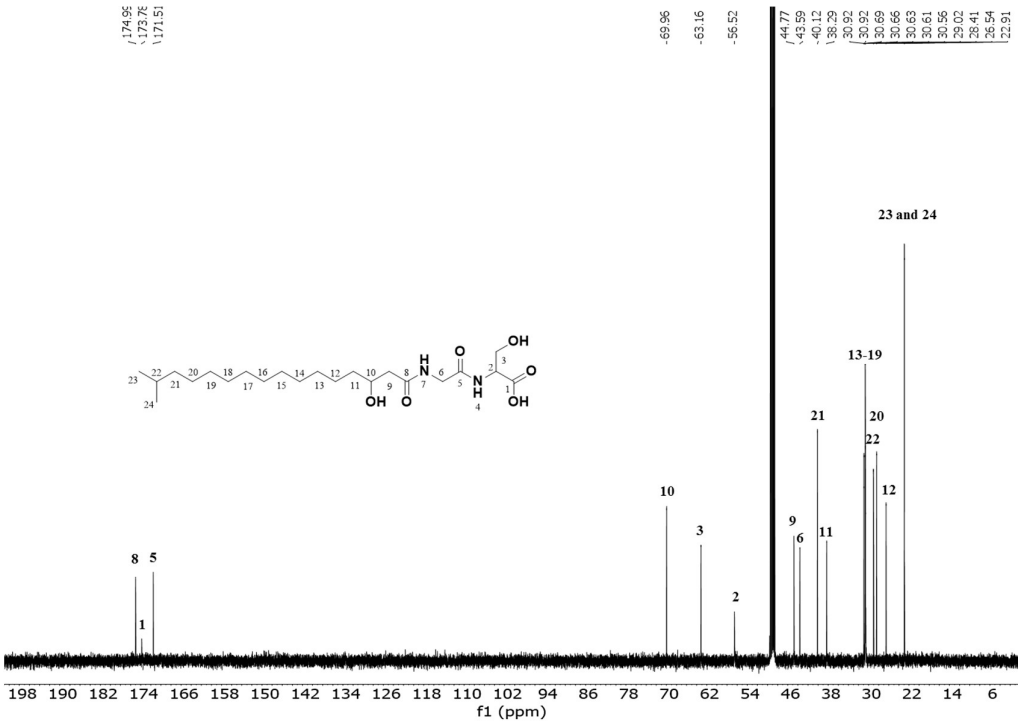

Figure S4. HSQC + HMBC (600 MHz, CD_3OD) spectrum of **1**

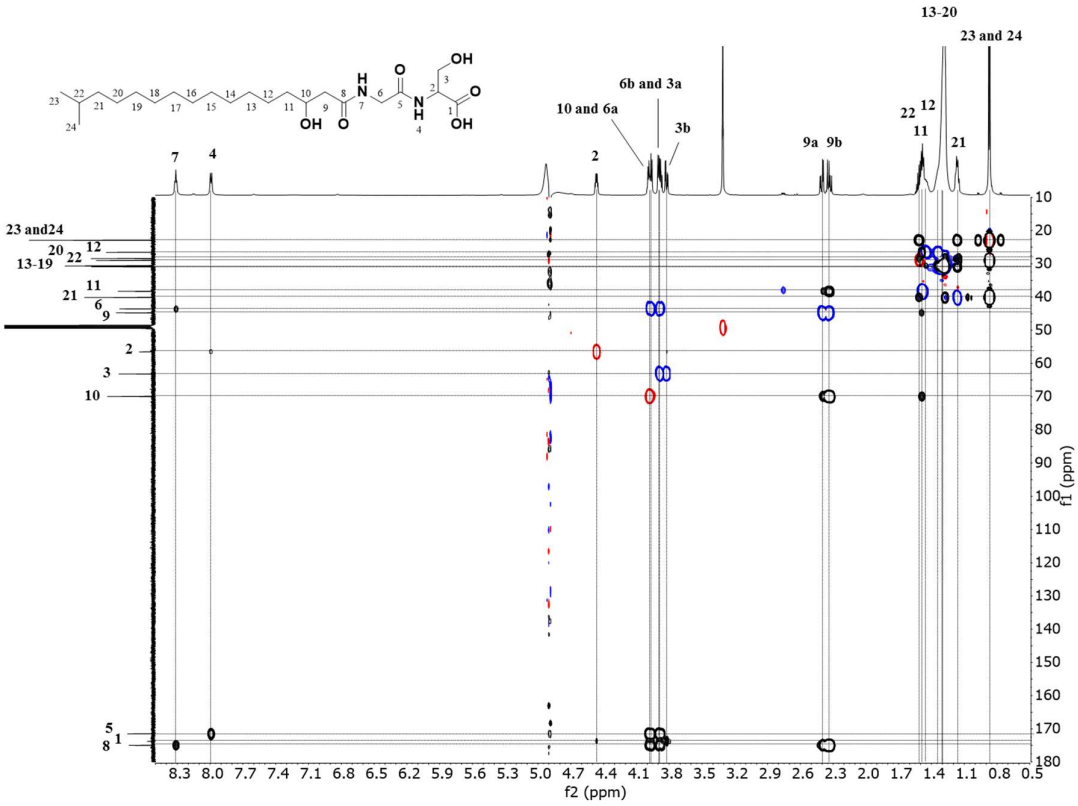

Figure S5. COSY (600 MHz, CD_3OD) spectrum of **1**

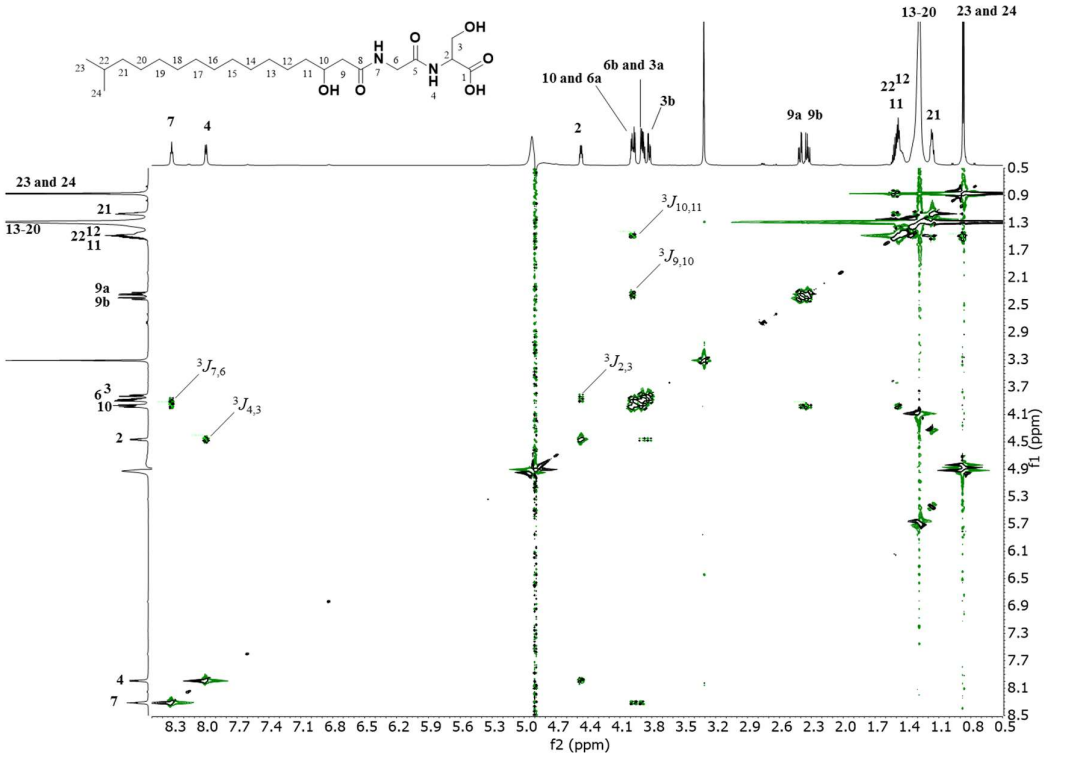

Figure S6. H2BC (600 MHz, CD_3OD) spectrum of **1**

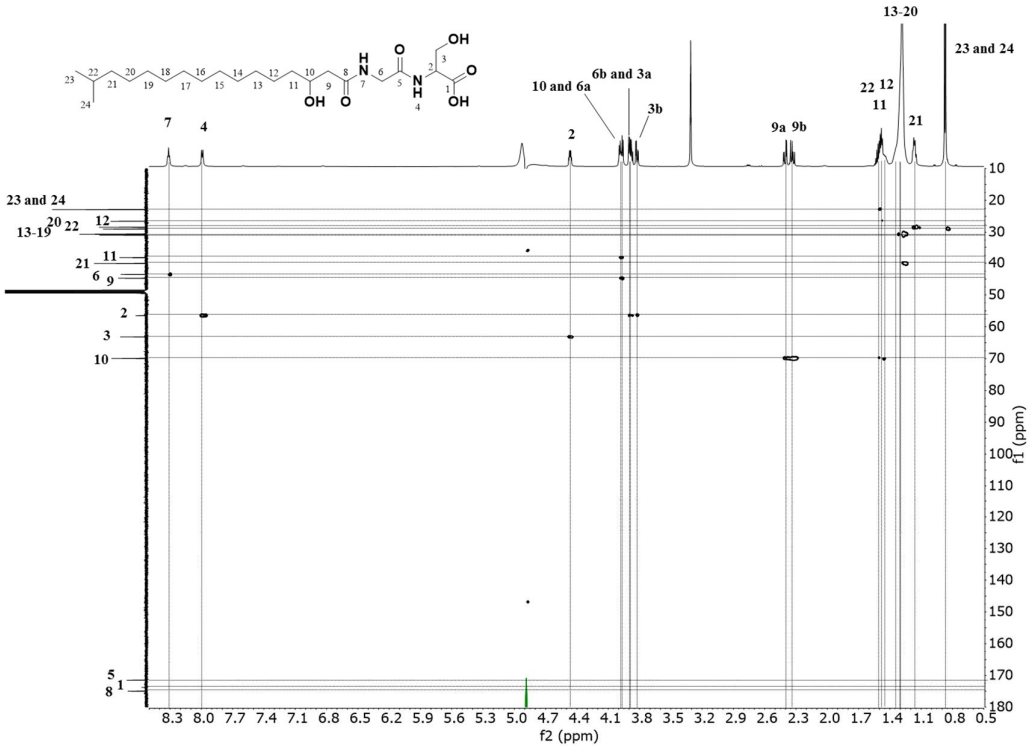

Figure S7. Results of the cytotoxicity assays for all tested cell lines

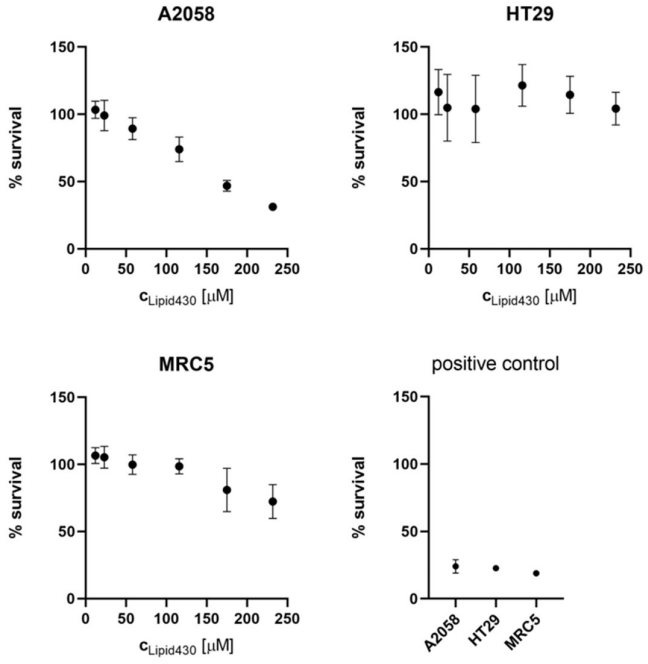

Cytotoxicity assay results for the melanoma (A2058), colon carcinoma (HT29) and lung fibroblast (MRC5) cells. The assay result is given as % survival on the y-axis and the concentrations of Lipid 430 on the x-axis. The exact tested concentrations were of 233, 175, 116, 58, 23 and 12 µM or 100, 75, 50, 25, 10 and 5 µg/mL respectively. 0.5% Triton™ X-100 was used as positive control.

Figure S8. Results of the flow cytometry experiments with propidium iodide staining

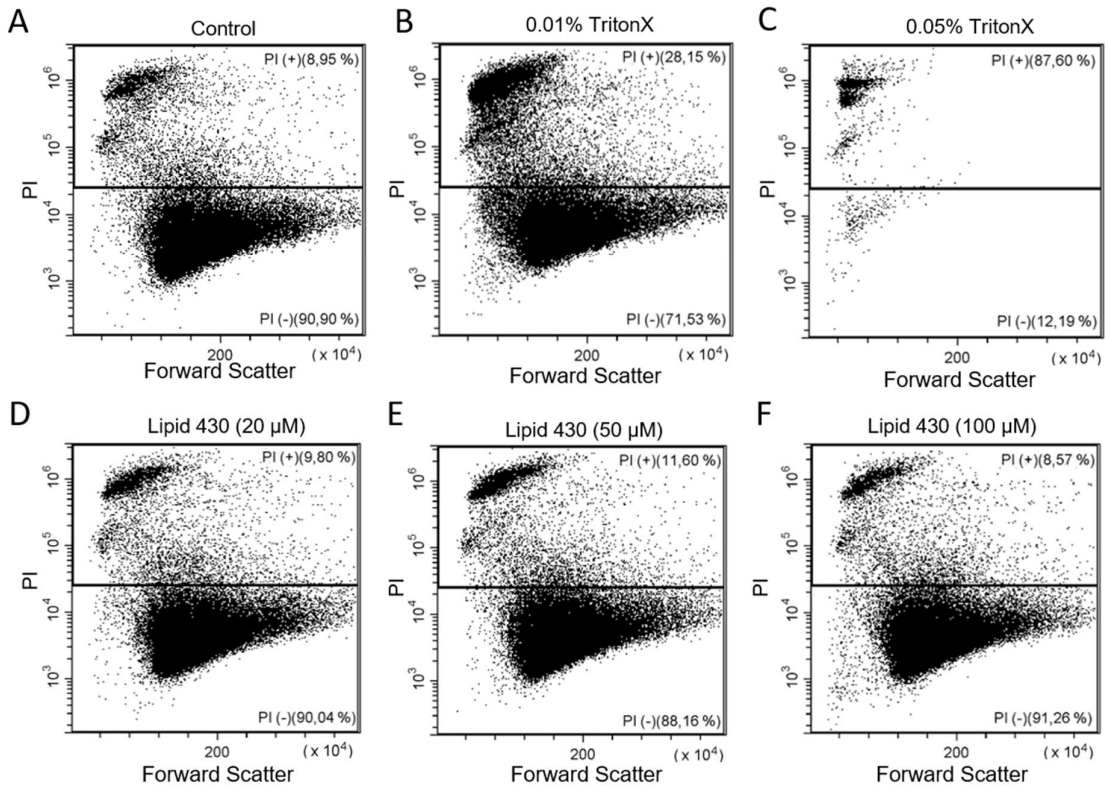

DotPlot graphs of the flow cytometry experiments with melanoma cell line A2058. In the upper sections the propidiumiodide positive (PI+) events (cell integrity destroyed/ affected) and in the lower the propidiumiodide negative events (PI -, physiologic cells). Forward scatter is displayed on the x-axis and propidiumiodide absorption on the y-axis. The relative ratio of events is given in %. A: stained control, 8.95% PI+; B: 0.01% TritonX, 28.15% PI+; C: 0.05% TritonX, 87.60% PI+; D: 20 µM Lipid 430, 9.80% PI+; E: 50 µM Lipid 430, 11.60% PI+; F: 100 µM Lipid 430, 8.57% PI+.

Figure S9. Results of the microscopic investigation

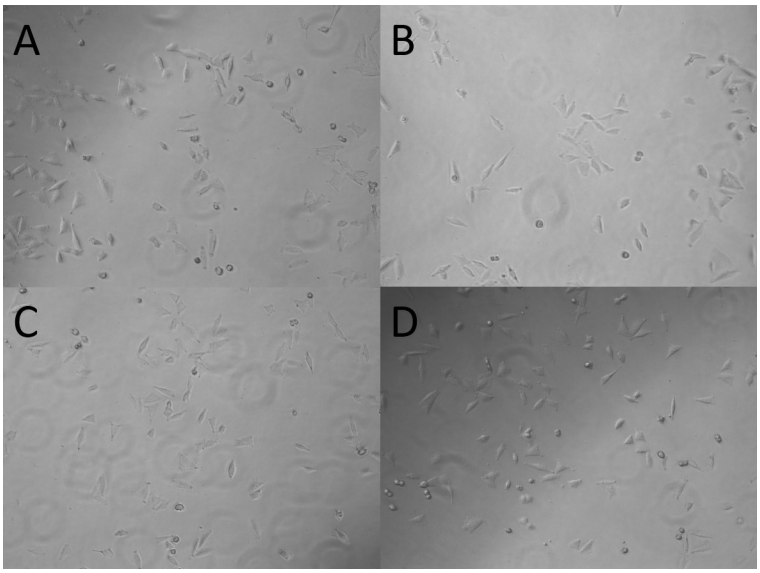

Microscopic investigation of Melanoma cells (A2058) after 1h of incubation with test solution. Inspection was done at 100× magnification. A: PBS-control; B: 1% (v/v) DMSO; C: Lipid 430, 100 µg/mL; D: Lipid 430, 500 µg/mL.

Paper II

microorganisms

MDPI

Article

Bioactivity of Serratiochelin A, a Siderophore Isolated from a Co-Culture of *Serratia* sp. and *Shewanella* sp.

Yannik Schneider [1,*,†], Marte Jenssen [1,*,†], Johan Isaksson [2], Kine Østnes Hansen [1], Jeanette Hammer Andersen [1] and Espen H. Hansen [1]

1 Marbio, Faculty for Fisheries, Biosciences and Economy, UiT—The Arctic University of Norway, Breivika, N-9037 Tromsø, Norway; kine.o.hanssen@uit.no (K.Ø.H.); jeanette.h.andersen@uit.no (J.H.A.); espen.hansen@uit.no (E.H.H.)

2 Department of Chemistry, Faculty of Natural Sciences, UiT—The Arctic University of Norway, Breivika, N-9037 Tromsø, Norway; johan.isaksson@uit.no

* Correspondence: yannik.k.schneider@uit.no (Y.S.); marte.jenssen@uit.no (M.J.); Tel.: +47-7764-9267 (Y.S.); +47-7764-9275 (M.J.)

† These authors contributed equally to the work.

Received: 15 June 2020; Accepted: 10 July 2020; Published: 14 July 2020

Abstract: Siderophores are compounds with high affinity for ferric iron. Bacteria produce these compounds to acquire iron in iron-limiting conditions. Iron is one of the most abundant metals on earth, and its presence is necessary for many vital life processes. Bacteria from the genus *Serratia* contribute to the iron respiration in their environments, and previously several siderophores have been isolated from this genus. As part of our ongoing search for medicinally relevant compounds produced by marine microbes, a co-culture of a *Shewanella* sp. isolate and a *Serratia* sp. isolate, grown in iron-limited conditions, was investigated, and the rare siderophore serratiochelin A (**1**) was isolated with high yields. Compound **1** has previously been isolated exclusively from *Serratia* sp., and to our knowledge, there is no bioactivity data available for this siderophore to date. During the isolation process, we observed the degradation product serratiochelin C (**2**) after exposure to formic acid. Both **1** and **2** were verified by 1-D and 2-D NMR and high-resolution MS/MS. Here, we present the isolation of **1** from an iron-depleted co-culture of *Shewanella* sp. and *Serratia* sp., its proposed mechanism of degradation into **2**, and the chemical and biological characterization of both compounds. The effects of **1** and **2** on eukaryotic and prokaryotic cells were evaluated, as well as their effect on biofilm formation by *Staphylococcus epidermidis*. While **2** did not show bioactivity in the given assays, **1** inhibited the growth of the eukaryotic cells and *Staphylococcus aureus*.

Keywords: Serratiochelin A; Serratiochelin C; *Serratia* sp.; siderophore; iron; anticancer; natural products; microbial biotechnology; degradation; antibacterial; *S. aureus*

1. Introduction

Iron is the fourth most abundant metal in the Earth's crust and is an absolute requirement for life [1]. Iron is an essential nutrient vital for several biological processes, such as respiration, gene regulation, and DNA biosynthesis [1,2]. Despite its abundance, iron is a growth-limiting factor for organisms in many environments [1]. To tackle this, microorganisms produce a vast range of iron-chelating compounds, called siderophores. Siderophores are compounds of low molecular weight (<1000 Da) that have high affinity and selectivity for ferric iron (iron(III)) [1], with the function of mediating iron uptake by microbial cells [3]. Siderophore production is commonly regulated by the iron concentration in the surroundings [4]. The siderophores are accumulated by membrane-bound iron receptors and brought inside the cell by active transport. Subsequently, the iron is normally reduced from iron(III) to

iron(II). Since the affinity towards iron(II) is much lower than to iron(III), the iron is released from the iron-siderophore complex and can be utilized by the microorganism [4]. One of the major functional groups of siderophores is catecholate. Many siderophores of the catecholate type contain building blocks consisting of dihydroxybenzoic acid coupled to an amino acid [3]. The first catecholate-type siderophore, a glycine conjugate of 2,3-dihydroxybenzoic acid, was identified in 1958. The compound was produced by *Bacillus subtilis* under iron-poor conditions [5].

The genus *Serratia* is part of the family *Enterobacteriaceae*, whose type species is *Serratia marcescens* [6,7]. Species of the genus *Serratia* have been detected in diverse habitats, such as soil, humans, invertebrates, and water. For *Serratia plymuthica*, water appears to be the principal habitat [6]. Bacteria from this genus are also problematic in health care, as *Serratia marcescens* is an opportunistic pathogen causing infections in immunocompromised patients. One of the pathogenicity factors of the bacterium is its production of potent siderophores. Several different siderophores are produced by bacteria of this genus [8], one example being the serratiochelins produced by *Serratia* sp. V4 [9,10].

The serratiochelins are catecholate siderophores produced by *Serratia* sp. [9,10]. In a paper from 2012 by Seyedsayamdost and co-authors, a new siderophore biosynthetic pathway was proposed for the production of the serratiochelins [10]. The new pathway consisted of genes originating and recombined from two known siderophore biosynthetic clusters: The clusters for enterobactin (*Escherichia coli*) and vibriobactin (*Vibrio cholera*). The study mentions three different serratiochelins, serratiochelin A (**1**), B, and C (**2**); the structures of **1** and **2** can be seen in Figure 1. In the study from 2012, only two of the three compounds, **1** and serratiochelin B, were found in the untreated culture extracts, while **2** is a hydrolysis product of **1**, which was produced in the presence of formic acid. Sayedsayamdost et al. indicated that **1** and serratiochelin B were the native compounds produced by the bacterium [10].

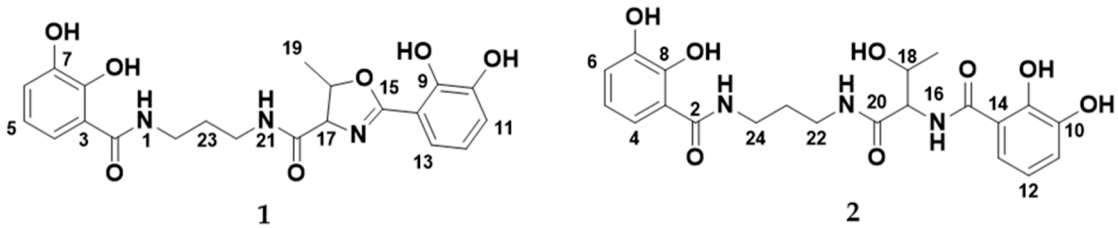

Figure 1. The structures of serratiochelin A (**1**) and C (**2**).

Siderophores are of pharmaceutical interest. They can be used in their native form to treat iron overload diseases, like sickle cell disease. Desferal® (Deferoxamine) is a siderophore-based drug used to treat iron poisoning and thalassemia major, a disease that leads to iron overload, which can lead to severe organ damage [11,12]. Siderophores can furthermore be used to facilitate active uptake of antibiotics by bacteria, and by the production of siderophore-antibiotic drug conjugates (SADCs). For some antibiotics, this strategy can reduce the minimal inhibitory concentration (MIC) by 100-fold, compared to an unbound antibiotic that enters the bacterial cell by passive diffusion [13]. The sideromycins are one example of SADCs. Albomycin, which belongs to this group, enters via the ferrichrome transporter, and has broad-spectrum antibiotic activity and is active against different Gram-negative bacteria [4,14]. The main problem with the use of SADCs is that most pathogenic bacteria have different routes for iron uptake, which could lead to higher frequency in resistance [4].

Due to the important role of *Shewanella* sp. and *Serratia* sp. in the environmental iron cycle, we were intrigued by observing a compound in high yields in an iron-limited co-culture of the two bacteria, which was not found in cultures supplemented with iron nor in axenic cultures of the bacteria. Here, we report the isolation of **1** from a co-culture of *Shewanella* sp. and *Serratia* sp. The degradation of **1** into **2** in the presence of acid was confirmed. To our knowledge, there is no published data regarding the bioactivity of these compounds. In this study, **1** and **2** were tested against a panel of bacterial and human cells, and for their ability to inhibit biofilm formation of the biofilm-producing bacterium *S. epidermidis*.

2. Materials and Methods

2.1. Bacterial Isolates

Compound **1** was isolated from bacterial cultures started from a non-axenic glycerol stock. The bacterial glycerol stock originally contained a *Leifsonia* sp. isolate. The stock was found to be contaminated with both *Shewanella* sp. and *Serratia* sp. after several steps of cultivation and production of new glycerol stock solutions. The non-axenic glycerol stock was inoculated onto three different agar plates, in order to gather information of the different isolates present. Originally, the *Leifsonia* sp. isolate was provided as an axenic culture by The Norwegian Marine Biobank (Marbank, Tromsø, Norway) (Reference number: M10B719). The bacterium was isolated from the intestine/stomach of an Atlantic hagfish (*Myxine glutinosa*) collected by benthic trawl in Hadselfjorden (Norwegian Sea, 16th of April, 2010). The bacterium was grown in liquid FMAP medium (15 g Difco Marine Broth (Becton Dickinson and Company, Franklin Lakes, NJ, USA), 5 g peptone from casein, enzymatic digest (Sigma, St. Louis, MS, USA), 700 mL ddH_2O, and 300 mL filtrated sea water) until sufficient turbidity, and cryo-conserved at −80 °C with 30% glycerol (Sigma). Filtration of sea water was done through a Millidisk® 40 Cartridge with a Durapore® 0.22-µm filter membrane (Millipore, Burlington, MA, USA).

2.2. PCR and Identification of the Strains

The glycerol stock was plated onto three different types of agar: FMAP agar (FMAP medium with 15 g/L agar), DVR1 agar (6.7 g malt extract (Sigma), 11.1 g peptone from casein, enzymatic digest (Sigma), 6.7 g yeast extract (Sigma), 0.5 L filtered sea water, 0.5 L ddH_2O), and potato glucose agar (Sigma). The plates with bacteria were incubated at 10 °C until sufficient growth, and transferred to 4 °C for temporary storage. This plating experiment resulted in the discovery of three different bacterial isolates, based on bacterial morphology and sequencing of the 16S rRNA gene. Clear colonies were picked from the plates, and inoculated into 100 µL of autoclaved ddH_2O. The samples were stored at −20 °C until PCR amplification. The characterization of the bacterial strains was done with sequencing of the 16S rRNA gene through colony PCR and Sanger sequencing. The primer set used for amplification of the gene was the 27F primer (forward primer; 5′-AGAGTTTGATCMTGGCTCAG) and the 1429R primer (reverse primer; 5′-TACCTTGTTACGACTT), both from Sigma. Prior to the amplification PCR, the bacterial samples were vortexed and diluted 1:100 and 1:1000 in UltraPure Water (BioChrom GmbH, Berlin, Germany). For PCR, 1 µL of the diluted bacterial sample was combined in a 25-µL PCR reaction, together with 12.5 µL DreamTaq Green PCR Master Mix (2×) (Thermo Scientific, Vilnius, Lithuania), 10.5 µL ultrapure water, and 0.5 µL of the forward and reverse primers (10 µM) mentioned above. The amplification was done using a Mastercycler ep gradient S (Eppendorf AG, Hamburg, Germany) with the following program: 95 °C initial denaturation for 3 min, followed by 35 cycles of 95 °C for 30 s, 47 °C for 30 s, and 72 °C for 1 min. Final extension was 72 °C for 10 min. The success and purity of the PCR reaction was analyzed on a 1.0% agarose gel (Ultrapure™ Agarose, Invitrogen, Paisley, UK) with Gel-Red® Nucleic Acid Gel Stain (Biotium, Fremont, CA, USA), and the results were documented using a Syngene Bioimaging system (Syngene, Cambridge, UK). Successfully amplified samples were purified by the A'SAP PCR clean up kit (ArcticZymes, Tromsø, Norway). The purified PCR product was used for sequencing PCR, using 1 µL PCR product, 2 µL BigDye™ 3.1 (Applied Biosystems, Foster City, CA, USA), 2 µL 5× sequencing buffer (Applied Biosystems, Foster City, CA, USA), 4 µL of UltraPure water, and 1 µL of primer (1 µM of 27F primer or 1429R primer). The program for the sequencing PCR was as follows: 96 °C initial denaturation for 1 min, followed by 30 cycles of 96 °C for 10 s, 47 °C for 5 s, and 60 °C for 2 min. The PCR product was sequenced at the University Hospital of North Norway (Tromsø, Norway).

The forward and reverse sequences obtained were assembled using the Geneious Prime® 2020.0.5 software (https://www.geneious.com). The sequences were assembled by using the built-in Geneious assembler. Prior to assembly, the sequences were trimmed using a 0.05 error probability limit. Sequence homology comparison was conducted using the built-in Basic Local Alignment Search

Tool (BLAST) [15] in Geneious, excluding environmental samples, metagenomes, and uncultured microorganisms, for phylogenetic identification of the strains.

To identify which strain was responsible for the production of **1**, the three bacterial strains were isolated on separate agar plates and inoculated in small cultures of DVR1 medium (for media contents, see below). The bacteria were pelleted by centrifugation, and the supernatant was diluted 1:1 in methanol and ran on the UHPLC-HR-MS for identification of the compound.

2.3. Fermentation and Extraction of Bacterial Cultures

For extraction of compounds, the bacteria were cultivated in 1000-mL flasks containing 300 mL DVR1 medium (6.7 g malt extract (Sigma), 11.1 g peptone from casein, enzymatic digest (Sigma), 6.7 g yeast extract (Sigma), 0.5 L filtered sea water, and 0.5 L ddH_2O) cultures for 16 days, at 10 °C and 130 rpm. A total of 12 flasks were inoculated, giving 3.6 L of culture. The medium was autoclaved for 30 min at 120 °C prior to inoculation. Cultures were started by loop inoculation from the non-axenic glycerol stock solution.

Extraction of metabolites from the liquid media was done with Diaion® HP-20 resin (Supelco, Bellefonte, PA, USA). The resin was activated by incubation in methanol for 30 min, followed by washing with ddH_2O for 15 min, and added to the cultures (40 g/L). The cultures were incubated with resin for 3 days prior to compound extraction. For extraction, the resin beads were separated from the liquid by vacuum filtration through a cheesecloth mesh (Dansk Hjemmeproduktion, Ejstrupholm, Denmark), the resin was washed with ddH_2O, and finally extracted two times with methanol. The extract was vacuum filtered through a Whatman No. 3 filter paper (Whatman plc, Maidstone, UK), and dried under reduced pressure at 40 °C.

2.4. Fractionation by FLASH Chromatography

Due to the degradation of **1** in the presence of acid, the culture extract was fractionated for bioactivity testing and structure verification, using FLASH chromatography (Biotage SP4™ system, Uppsala, SE), removing the use of acid in the purification process. The extract (3667.9 mg) was re-dissolved in 90% methanol, before adding Diaion® HP20-SS resin (Supelco) in a ratio of 1:1.5 (resin:dry extract, *w/w*) and drying under reduced pressure at 40 °C. Due to the high amount of the extract, it was fractionated in two rounds. FLASH columns were prepared with 6.5 g activated Diaion® HP-20SS resin per column. The dried extract was applied to the column, and ran with a water: methanol gradient from 5–100% methanol over 36 min at a flow rate of 12 mL/min. This resulted in 15 fractions per run. The fractions eluting at 100% methanol were analyzed on the UHPLC-HR-MS, and the purest fraction (fraction no 13, >95% pure based on UV/Vis) was used and dried under reduced pressure at 40 °C. The fraction yielded 50.9 mg and was used for the bioactivity testing.

2.5. UHPLC-HR-MS and Dereplication

UHPLC-HR-MS data for dereplication and to analyze the various experiments was recorded using an Acquity I-class UPLC (Waters, Milford, MA, USA) coupled to a PDA detector and a Vion IMS QToF (Waters). The chromatographic separation was performed using an Acquity C-18 UPLC column (1.7 µm, 2.1 mm × 100 mm) (Waters). Mobile phases consisted of acetonitrile (HiPerSolv, VWR, Radnor, PA, USA) for mobile phase B and ddH_2O produced by the in-house Milli-Q® system (Millipore, Burlington, MA, USA) as mobile phase A, both containing 1% formic acid (*v/v*) (33015, Sigma). The gradient was run from 10% to 90% B in 12 min at a flow rate of 0.45 mL/min. Samples were run in ESI+ and ESI- ionization mode. The data was processed and analyzed using UNIFI 1.9.4 (Waters). Exact masses and isotopic distributions were calculated using ChemCalc (https://www.chemcalc.org).

2.6. Purification by Preparative HPLC

Initially, the purification of **1** and **2** was done by preparative HPLC-MS using a 600 HPLC pump, a 3100 mass spectrometer, a 2996 photo diode array detector, and a 2767 sample manager (Waters).

For infusion of the eluents into the ESI-quadrupole-MS, a 515 HPLC pump (Waters) and a flow splitter were used and 80% methanol in ddH_2O (*v/v*) acidified with 0.2% formic acid (Sigma) as make-up solution at a flow rate of 0.7 mL/min. The columns used for isolation were a Sunfire RP-18 preparative column (10 µm, 10 mm × 250 mm) and XSelect CSH preparative fluoro-phenyl column (5 µm, 10 mm × 250mm), both columns were purchased from Waters. The mobile phases for the gradients were A (ddH_2O with 0.1% (*v/v*) formic acid) and B (acetonitrile with 0.1% (*v/v*) formic acid), flow rate was set to 6 mL/min. Acetonitrile (Prepsolv®, Merck, Darmstad, Germany) and formic acid (33015, Sigma) were purchased in appropriate quality, ddH_2O was produced with the in-house Milli-Q® system. The collected fractions were reduced to dryness at 40 °C in vacuo and freeze drying using an 8L laboratory freeze dryer (Labconco, Fort Scott, KS, USA).

2.7. NMR analysis

NMR spectra were acquired in DMSO-d_6 on a Bruker Avance III HD spectrometer (Bruker, Billerica, MA, USA) operating at 600 MHz for protons, equipped with an inverse TCI cryo probe enhanced for ^{1}H, ^{13}C, and ^{2}H. All NMR spectra were acquired at 298 K, in 3-mm solvent-matched Shigemi tubes using standard pulse programs for proton, carbon, HSQC, HMBC, COSY, and ROESY with gradient selection and adiabatic versions where applicable. ^{1}H/^{13}C chemical shifts were referenced to the residual solvent peak (DMSO-d_6: δH = 2.50, δC = 39.51).

2.8. Cultivation Study

Due to the hypothesis that the compound had iron-chelating properties for the bacteria, a cultivation study with and without the addition of iron to the medium was conducted. To investigate if the production was temperature specific, the bacteria were also grown at two different temperatures. The bacteria were grown in DVR1 medium and DVR2 medium (DVR1 with added 5.5 mL $FeSO_4$ 7 H_2O (8 g/L stock, ≙ 28.8 mM Fe)), at room temperature and at 10 °C with 130 rpm shaking. Samples were taken from the cultures, under sterile conditions, after 7, 14, and 21 days, for chemical analysis by UHPLC-HR-MS. From the cultures, 5 mL of sample were taken and centrifuged to pellet the bacteria, 1 mL of the supernatant was transferred to a new tube and centrifuged again, before sterile filtration using an Acrodisc syringe filter 0.2 µm, supor membrane (Pall Corp., East Hills, NY, USA) The filtered sample was mixed 1:1 with methanol prior to injecting on the UHPLC-HR-MS for investigation.

2.9. Marfey's Amino Acid Analysis

A small quantity of **1** was dissolved in 1 mL of 6N HCL and incubated for 6 h at 110 °C using 1.5-mL reaction tubes and a thermoblock. After cooling down to room temperature, the reaction was reduced to dryness by vacuum centrifugation at 40 °C. The dry sample after hydrolysis was re-dissolved in 100 µL of H_2O. The derivatization was carried out by mixing the re-dissolved hydrolystate with 180 µL FDAA in acetone (Marfey's reagent, Sigma), N_α-(2,4-Dinitro-5-fluorophenyl)-L-alaninamide), and 20 µL 1N $NaHCO_3$. The reaction was incubated at 40 °C using a thermoblock. After incubation, the reaction was acidified with 30 µL of 1N HCl and diluted with 2.5 mL of methanol. Then, 0.1 mg of L-threonine and D-threonine dissolved in 100 µL water were used to prepare standards of the amino acids using the same derivatization procedure as described for the sample hydrolysate. The standards and sample diluted in methanol were analyzed using UHPLC-MS/MS as described above.

2.10. Iron Chelation Experiment

For testing the capability of **1** and **2** to chelate iron, a chelation assay was performed. The molecule was dissolved in water (0.2 mg/mL) and 75 µL of the molecule were mixed with 25 µL of 10 mg/mL $FeCl_3 \times 6\ H_2O$. The preparation was done in HPLC vials, the reaction was thoroughly mixed by vortexing, centrifuged, and subsequently analyzed by UHPLC-MS/MS.

2.11. Hydrolyzation with Formic Acid

For testing the liability for hydrolyzation, a 1-mg sample of **1** was dissolved in 1 mL 10% (*v/v*) DMSO *aq.* and incubated for 24 h at room temperature with formic acid concentrations of 0% (control), 0.1%, 1.0%, 5.0%, and 10% (*v/v*). The reaction product was analyzed by UHPLC-MS/MS.

2.12. Production of Serratiochelin C

For testing the bioactivity of **2** in comparison to **1**, a sample of non-degraded **1** was hydrolyzed by adding 10% (*v/v*) formic acid and incubation over 24 h at room temperature. The formic acid was removed by vacuum centrifugation at 40 °C and subsequent freeze drying using a laboratory freeze dryer (Labconco).

2.13. Bioactivity Testing

2.13.1. Growth Inhibition Assay

To determine antimicrobial activity, a bacterial growth inhibition assay was executed. Compounds **1** and **2** were tested against *Staphylococcus aureus* (ATCC 25923), *Escherichia coli* (ATCC 259233), *Enterococcus faecialis* (ATCC 29122), *Pseudomonas aeruginosa* (ATCC 27853), *Streptococcus agalactiae* (ATCC 12386), and Methicillin-resistant *Staphylococcus aureus* (MRSA) (ATCC 33591), all strains from LGC Standards (Teddington, London, UK). *S. aureus*, MRSA, *E. coli*, and *P. aeruginosa* were grown in Muller Hinton broth (275730, Becton). *E. faecalis* and *S. agalactiae* were cultured in brain hearth infusion broth (53286, Sigma). Fresh bacterial colonies were transferred to the respective medium and incubated at 37 °C overnight. The bacterial cultures were diluted to a culture density representing the log phase and 50 µL/well were pipetted into a 96-well microtiter plate (734-2097, Nunclon™, Thermo Scientific, Waltham, MA, USA). The final cell density was 1500–15,000 colony forming units/well. The compound was diluted in 2% (*v/v*) DMSO (Dimethyl sulfoxide) in ddH_2O, and the final assay concentration was 50% of the prepared sample, since 50 µL of sample in DMSO/water were added to 50 µL of bacterial culture. After adding the samples to the plates, they were incubated over night at 37 °C and the growth was determined by measuring the optical density at λ = 600 nm (OD_{600}) with a 1420 Multilabel Counter VICTOR3™ (Perkin Elmer, Waltham, MA, USA). A water sample was used as the reference control, growth medium without bacteria as a negative control, and a dilution series of gentamycin (32 to 0.01 µg/mL, A2712, Merck) as the positive control and visually inspected for bacterial growth. The positive control was used as a system suitability test and the results of the antimicrobial assay were only considered valid when the positive control was passed. The final concentration of DMSO in the assays was ≤2% (*v/v*), known to have no effect in the tested bacteria. The data was processed using GraphPad Prism 8 (GraphPad, San Diego, CA, USA).

2.13.2. Cell Proliferation Assay

The inhibitory effect **1** and **2** was tested using an MTS in vitro cell proliferation assay against two cell lines: The human melanoma cell line A2058 (ATCC, CLR-1147™), and for general cytotoxicity assessment, the non-malignant MRC5 lung fibroblast cells (ATCC CCL-171™) were employed. The cells were cultured and assayed in Roswell Park Memorial Institute medium (RPMI-16040, FG1383, Merck) containing 10% (*v/v*) fetal bovine serum (FBS, 50115, Biochrom, Holliston, MA, USA). The cell concentration was 4000 cells/well for the lung fibroblast cells and 2000 cells/well for the cancer cells. After seeding, the cells were incubated for 24 h at 37 °C and 5% CO_2. The medium was then replaced with fresh RPMI-1640 medium supplemented with 10% (*v/v*) FBS and gentamycin (10 µg/mL, A2712, Merck). After adding 10 µL of sample diluted in 2% (*v/v*) DMSO in ddH_2O, the cells were incubated for 72 h at 37 °C and 5% CO_2. For assaying the viability of the cells, 10 µL of CellTiter 96® AQueous One Solution Reagent (G3581, Promega, Madison, WI, USA) containing tetrazolium [3-(4,5-dimethylthiazol-2-yl)-5-(3-carboxymethoxyphenyl)-2-(4-sulfophenyl)-2*H*-tetrazolium, inner salt] and phenazine ethosulfate was added to each well and incubated for one hour. The tests were executed

with three technical replicates. The plates were read using a DTX 880 plate reader (Beckman Coulter, CA, USA) by measuring the absorbance at λ = 485 nm. The cell viability was calculated using the media control. As a negative control, RPMI-1640 with 10% (*v/v*) FBS and 10% (*v/v*) DMSO (Sigma) was used as a positive control. The data was processed and visualized using GraphPad Prism 8.

2.13.3. Biofilm Inhibition Assay

For testing the inhibition of biofilm formation, the biofilm-producing *Staphylococcus epidermidis* (ATCC 35984) was grown in Tryptic Soy Broth (TSB, 105459, Merck, Kenilworth, NJ, USA) overnight at 37 °C. The overnight culture was diluted in fresh medium with 1% glucose (D9434, Sigma) before being transferred to a 96-well microtiter plate; 50 μL/well were incubated overnight with 50 μL of the test compound dissolved in 2% (*v/v*) DMSO aq. added in duplicates. The bacterial culture was removed from the plate and the plate was washed with tap water. The biofilm was fixed at 65 °C for 1 h before 70 μL of 0.1% crystal violet (115940, Millipore) were added to the wells for 10 min of incubation. Excess crystal violet solution was then removed and the plate dried for 1 h at 65 °C. Seventy microliters of 70% ethanol were then added to each well and the plate incubated on a shaker for 5–10 min. Biofilm formation inhibition were assessed by the presence of violet color and was measured at 600-nm absorbance using a 1420 Multilabel Counter VICTOR3™. Fifty microliters of a non-biofilm-forming *Staphylococcus haemolyticus* (clinical isolate 8-7A, University Hospital of North Norway Tromsø, Norway) mixed in 50 μL of autoclaved Milli-Q water was used as a control; 50 μL of *S. epidermidis* mixed in 50 μL of autoclaved Milli-Q water was used as the control for biofilm formation; and 50 μL of TSB with 50 μL of autoclaved Milli-Q water was used as a medium blank control.

3. Results

Compound **1** was isolated from a co-culture of *Serratia* sp. and *Shewanella* sp. when cultivated in an iron-limited medium. The bacteria were also cultivated in iron-supplemented media, where **1** was not detected. Compound **1** was only produced in co-cultures started directly from the glycerol stock by loop inoculation, and not found in any axenic cultures. The cultures were extracted, and the extracts were fractionated using FLASH chromatography to isolate serratiochelin A (**1**), a siderophore previously isolated exclusively from a *Serratia* sp., also when grown under iron-limited conditions [10]. During preparative HPLC-MS isolation, it was observed that the compound was degraded, and the degradation product was found to be serratiochelin C (**2**), which corresponds to previous observations [10]. A study of the iron binding of the compounds and a degradation study with formic acid was conducted. The structures of the compounds were verified by 1-D and 2-D NMR and MS experiments, and Marfey's analysis was used to find the configuration of the threonine moiety of the molecule. Compound **1** and **2** were tested for their antibacterial activities, their abilities to inhibit the formation of biofilm, and their toxicity towards human cells. This is the first study on the bioactivity of **1** since its original discovery in 1994 [9].

3.1. Identification of Co-Culture and Serratiochelin A Production Strain

When streaking out the glycerol stock onto three different agar plates, three morphologically different bacterial colonies were observed (Figure S14). The 16S rRNA gene of these bacteria was amplified and sequenced by Sanger sequencing, showing that the stock solution contained *Leifsonia* sp. (original isolate in stock), *Shewanella* sp., and *Serratia* sp. The 16S rRNA sequences for the three isolates can be found in the Supplementary Material (Texts S15–S17). *Shewanella* sp. and *Serratia* sp. are assumed to be of marine origin, as strains of the same genera have been cultivated at the same time as the *Leifsonia* sp. isolate, and the 16S rRNA sequences are similar to two strains of the Marbank strain collection (*Shewanella* sp. M10B851 and *Serratia* sp. M10B861, Marbank ID). In order to investigate if all bacteria were able to co-exist in the liquid culture started from the glycerol stock, a 450-mL culture of DVR1 was inoculated with the glycerol stock (identically as was done with the culture from which **1** was isolated) and the culture was streaked out on agar after 3 and 10 days of cultivation.

After three days of cultivation, the colony forming units (CFUs) of both *Shewanella* sp. and *Serratia* sp. were observed on the plates (Figure S14), proven by morphological identification and sequencing of the 16S rRNA gene. After 10 days of culturing, no CFUs of *Shewanella* sp. were observed from the culture, and the experiment detected exclusively CFUs of *Serratia* sp. No *Leifsonia* colonies were observed from the liquid cultures, not after 3 nor 10 days of cultivation. This indicates that the *Serratia* sp. isolate outgrow the other two isolates in the cultivation done in this study. After re-streaking the three bacterial isolates present in the glycerol stock to obtain pure cultures, the different isolates were cultivated separately in 50-mL cultures in DVR1 to identify the actual producer of **1**. Compound **1** was only produced in co-cultures started directly from the glycerol stock, and not by any of the cultures started from axenic colonies from agar plates.

3.2. Dereplication and Isolation

Serratiochelin A (**1**) was obtained as a brown powder. The bacterial extracts and fractions were analyzed using UHPLC-IMS-MS and **1** was detected at *m/z* 430.1594 ($[M+H]^+$) in ESI+ eluting at 4.45 min. The calculated elemental composition was $C_{21}H_{23}N_3O_7$ (Calc. *m/z* 430.1614 $[M+H]^+$), corresponding to 12 degrees of unsaturation. The elemental composition gave several hits for natural products in available databases, including serratiochelin A (**1**). As **1** had been previously isolated from *Serratia* sp., we saw it as a clear possibility that we had a positive identification of the compound. However, to confirm this, isolation and structure elucidation was necessary. After the first round of isolation using preparative HPLC, we detected two species of the product, one at RT= 4.45 min (**1**) and another at RT = 2.07 min (**2**), both having the same *m/z* and elemental composition in ESI+. We later confirmed that the *m/z* of **2** in ESI+ was not the *m/z* of the molecular ion due to neutral water loss in the ion source. The masses of **1** and **2** are thus not equivalent, which was later confirmed by ESI-ionization, which confirmed the mass of **2** to be equal to that of **1**+H_2O.

It was not possible to obtain **1** as a pure compound after the purification, as it was always accompanied by **2**, indicating a possible degradation of **1**. Compound **2,** on the other hand, was obtained as a pure compound after using preparative HPLC for isolation. To distinguish between the two molecules, the collision cross section (CCS) and drift time of the compounds were compared, and the samples were also investigated in ESI- (see Table 2 for the respective values, the high- and low-energy MS spectra, as well as UV/Vis spectra for **1** and **2** that are given in Figures S11 and S12). For isolating **1,** FLASH chromatography was used, since there was no **2** detected using this protocol, where no acid was employed. The collected fractions were assayed individually using UHPLC-MS and the first fraction eluting at 100% methanol was found to be sufficiently pure for structure elucidation via NMR and further bioactivity testing (results of the purity assay are given in Figure 2), yielding 50.9 mg **1** from 3667.9 mg of extract. Compound **1** was not readily dissolved in water and methanol but it dissolved in DMSO. Solutions of **1** were prepared in 100% DMSO and further diluted in water. The same was done with **2,** which also dissolved in methanol.

Serratiochelin C (**2**) was obtained as a brown powder, after acid-catalyzed degradation of **1**. From the ESI-, it was possible to elucidate the elemental composition of **2**. Compound **2** was detected, with *m/z* 446.1568 ($[M-H]^-$) in ESI- eluting at 2.07 min. The calculated elemental composition was $C_{21}H_{25}N_3O_8$ (Calc. *m/z* 446.1563 $[M-H]^-$), corresponding to 11 degrees of unsaturation.

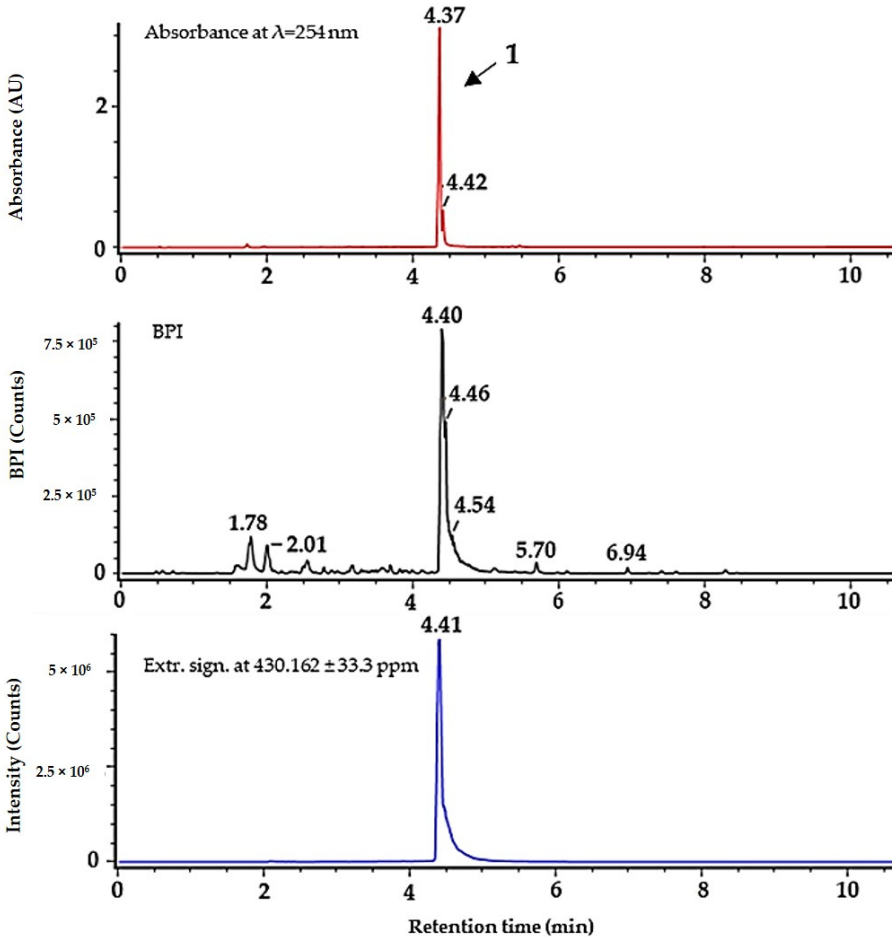

Figure 2. Purity of serratiochelin A (**1**) after isolation using FLASH chromatography, analyzed by UHPLC-MS. Top (in red) absorbance at 254 nm, middle (black) BPI chromatogram, bottom (blue) extracted signal for *m/z* = 430.162 (±33.3 ppm). ΔRT for UV/Vis detector is ~−0.05 min.

3.3. Structure Elucidation

Close inspection of 1-D (^{1}H and ^{13}C, Table 1) and 2-D (HSQC, HMBC, COSEY, and ROESY) NMR data of **1** confirmed that we isolated the previously reported compound serratiochelin A (**1**). All NMR spectra can be seen in the Supplementary Material (Figures S1–S5). Key COSY and HMBC correlations used to assign the structure of **1** can be seen in Figure 3.

In preparations treated with formic acid, we detected a third molecule eluting at 2.60 min. According to its signal, fragments, and retention time, we concluded it was serratiochelin B [10]. Serratiochelin B was not isolated or verified by NMR. Serratiochelin B and **2** were not present within the crude extract or within fractions obtained by FLASH chromatography but were detected after treatment with acid. The conformation of threonine was found to be L by Marfey's method, which is in compliance what has been published previously [10]. Results are given within the Supplementary Material (Figure S13).

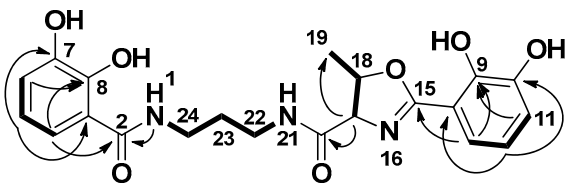

Figure 3. Key COSY (bold) and HMBC (arrow) correlations for serratiochelin A (**1**).

Table 1. ^{1}H- and ^{13}C-NMR data for serratiochelin A (**1**) and C (**2**) in DMSO-d_6.

NMR Data	Serratiochelin A (1)		Serratiochelin C (2)	
Position	δ_C, Type	δ_H (*J* in Hz)	δ_C, Type	δ_H (*J* in Hz)
1		8.30, t (5.9)		8.01, t (5.9)
2	169.6, C		169.73, C	
3	114.9, C		114.92, C	
4	117.1, CH	7.25, dd (8.1, 1.5)	117.04, CH	7.25, dd (8.2, 1.5)
5	117.8, CH	6.67, t (7.9)	117.84, CH	6.66, t (8.0)
6	118.7, CH	6.9, dd (7.8, 1.4)	118.65, CH	6.89, dd (7.8, 1.5)
7	146.3, C		146.27, C	
8	149.8, C		149.81, C	
9	148.3, C		146.12, C	
10	145.7, C		148.27, C	
11	119.4, CH	6.96, dd (7.8, 1.6)	118.18, CH	6.92, dd (7.7, 1.5)
12	118.7, CH	6.73, t (7.9)	117.77, CH	6.69, t (7.9)
13	117.9, CH	7.07, dd (7.9, 1.6)	118.92, CH	7.37, dd (8.1, 1.6)
14	110.3, C		116.77, C	
15	165.7, C		168.01, C	
16				8.66, s
17	73.7, CH	4.45, d (87.3)	59.18, CH	4.34, dd (8.0, 4.4)
18	78.8, CH	4.86, p (6.4)	66.38, CH	4.10, qd (6.1, 4.7)
19	20.7, CH_3	1.45, d (6.3)	20.30, CH_3	1.09, d (6.4)
20	169.8, C		169.99, CH	
21		8.81, s		8.78, t (5.3)
22	36.7, CH_2	3.30, m	36.58, CH_2	3.29, q (6.7)
23	28.9, CH_2	1.72, p (7.0)	28.96, CH_2	1.67, p (7.0)
24	36.6, CH_2	3.18, m	36.41, CH_2	3.20–3.08, m

The structure of serratiochelin C (**2**) was confirmed in a similar manner to that of **1**. All NMR spectra can be seen in the Supplementary Material (Figures S6–S10).

3.4. Detection of Iron Chelation

Compounds **1** and **2** were mixed with aqueous $FeCl_3$ solution to investigate if the compounds were able to chelate iron. Both **1** and **2** chelated iron, and the mass spectrometric data given in Table 2 indicate chelation of iron by the loss of three protons through coordination, as published previously [10]. The calculated exact mass for chelation of **1** was *m/z* 483.0729 ([M+Fe-2H]$^+$) and for **2** and serratiochelin B *m/z* 501.0835 ([M+Fe-2H]$^+$). In ESI-, the calculated *m/z* ratios were *m/z* 481.0572 ([M+Fe-4H]$^+$) for **1** and *m/z* 499.0678 ([M+Fe-4H]$^+$) for **2**.

Table 2. IMS and MS data for the apo- and ferrylspecies of serratiochelin A (**1**), serratiochelin B, and serratiochelin C (**2**).

Compounds	Form	Ionization	RT * [min]	*m/z*	CCS ** [A^2]	Drift Time [ms]
Serratiochelin C (earliest eluting)	apo	ESI+	2.07	430.1610 ***	202.88	7.00
	apo	ESI-	2.05	446.1568 ***	198.35	6.94
	ferri	ESI+	2.09	501.0844	208.06	6.75
	ferri	ESI-	2.11	499.0680	203.54	7.12
Serratiochelin B (middle eluting)	apo	ESI+	2.64	448.1714	210.99	6.84
	apo	ESI-	2.60	446.1573	199.52	6.98
	ferri	ESI+	2.61	501.0822	211.91	6.89
	ferri	ESI-	2.62	499.0673	201.16	7.04
Serratiochelin A (late eluting)	apo	ESI+	4.45	430.1611	202.85	6.99
	apo	ESI-	4.37	428.1466	201.47	7.05
	ferri	ESI+	4.46	483.0723	206.88	6.70
	ferri	ESI-	4.39	481.5058	208.50	7.30

* Retention time, ** Collision cross section, *** Loss of water of apo-serratiochelin C (**2**) in ESI+, not in ESI-, and not for the ferri-siderophores.

3.5. Degradation Study with Formic Acid

The study confirmed that the degradation was triggered by formic acid. In order to obtain a pure sample of **1**, we used FLASH fraction no. 13, which predominantly contained **1** since during the extraction process and the FLASH chromatography, no formic acid or acidic solution is used that could induce degradation. This sample was used for the degradation study. Formic acid at concentrations of 0.1%, 1.0%, 5.0%, and 10% (*v/v*) were tested and compared to the control (no acid), as can be seen in Figure 4. It was found that the degradation correlates with the concentration of formic acid. The degradation takes place not only in the presence of formic acid. When incubated with 1% (*v/v*) hydrochloric acid or acetic acid, we observed degradation to approximately the same extent (data not shown). The acid-catalyzed degradation mechanism turning **1** into **2** via intermediates **1a**–**e** can be seen in Figure 5.

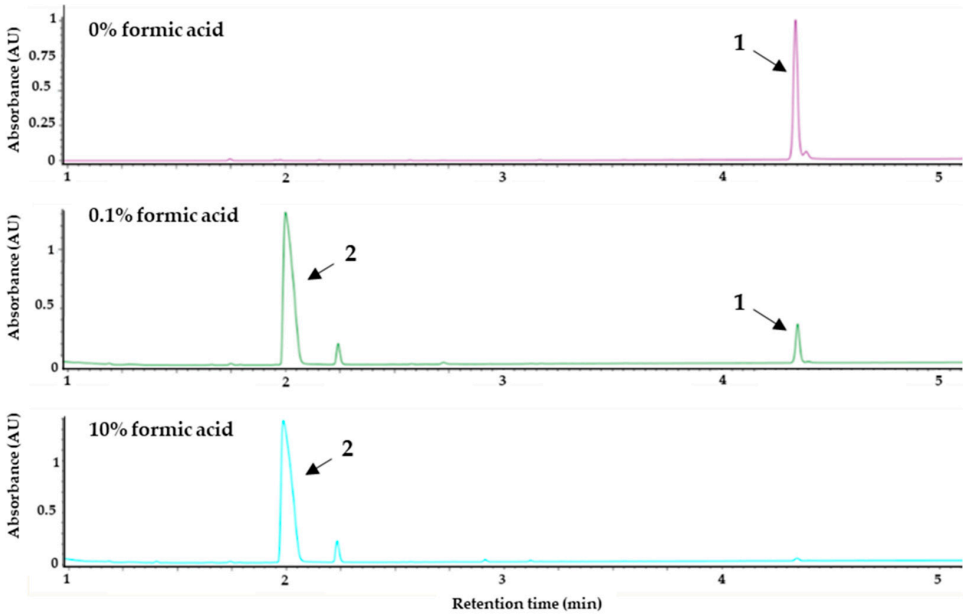

Figure 4. UV-max plot chromatogram. Degradation study showing the effect of formic acid on serratiochelin A (**1**). The purified sample of **1** was treated with different concentrations of formic acid (% (*v/v*)) for 24 h at room temperature and subsequently analyzed via UHPLC-PDA-MS. The chromatograms of the control (0% formic acid), 0.1% formic acid, and 10% formic acid are given above. The degradation of **1** (RT = 4.45 min) into serratiochelin C (**2**) (RT = 2.07 min) corresponds to the amount of formic acid used.

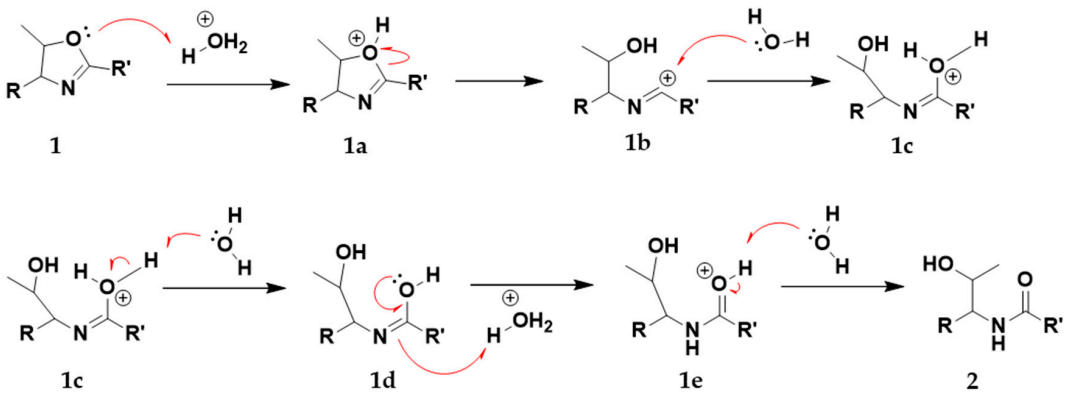

Figure 5. The proposed acid-catalyzed degradation reaction of the central methylated oxazoline ring of **1**, turning **1** into **2** via intermediates **1a** to **1e**.

3.6. Cultivation Study

The cultivation study revealed that **1** was only produced in the iron-deficient co-cultures, as can be seen in Figure 6. Cultures grown in media supplemented with 160 μM $FeSO_4$ did not produce **1** after 7, 14, and 21 days when grown at room temperature nor when grown at 10 °C (Figure 6). Within the iron-deficient cultures, **1** was detected after 7, 14, and 21 days cultivation at 10 °C as well as when cultivated at room temperature. Additionally, when extracting two cultures grown for 14 days at 10 °C using solid-phase extraction, there was no **1** present within the iron-supplemented media while it was a major component in the extract of the iron-deficient culture. Serratiochelin B and **2** were not detected in the cultures, nor in crude extracts after solid-phase extraction.

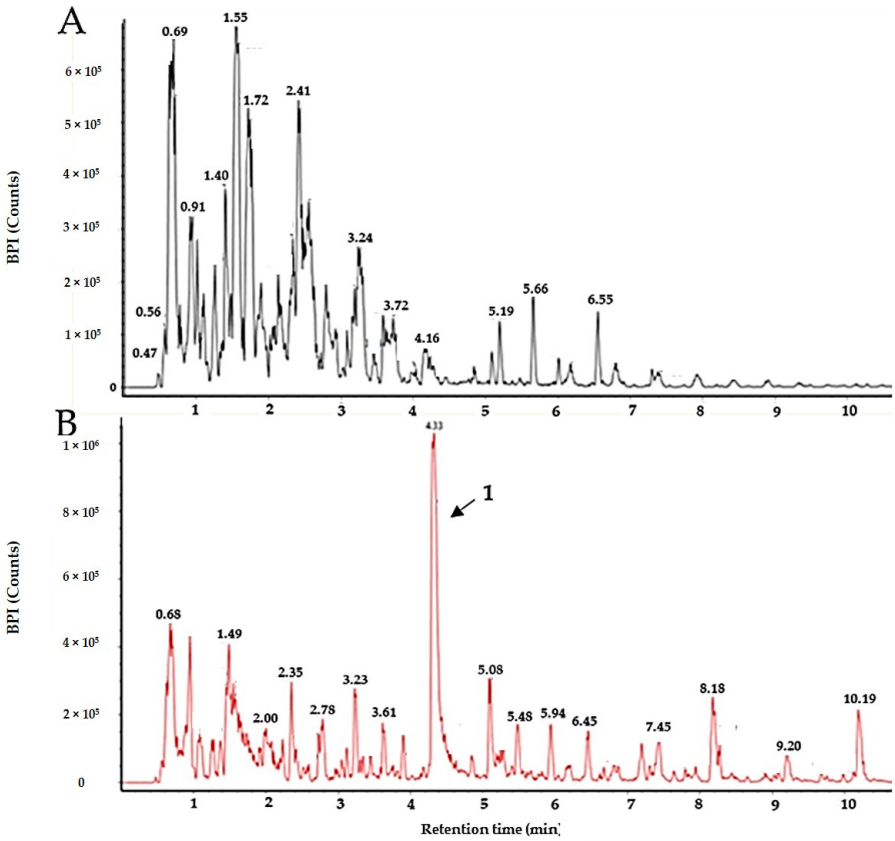

Figure 6. BPI chromatograms of the extracts of two co-cultures. (**A**) The extract of a 14-day culture (10 °C) supplemented with 160 μM Fe(III). (**B**) The extract of a 14-day culture (10 °C) grown in iron-deficient media. The peak of serratiochelin A (**1**) is indicated by the black arrow.

3.7. Bioassays

The growth-inhibiting properties of **1** and **2** were tested against several Gram-positive and Gram-negative strains. The antimicrobial assay detected an effect of **1** on *S. aureus*. Interestingly, there was no effect of **2** on *S. aureus* detected in the assay. There was no antimicrobial effect of **1** and **2** against *S. agalactiae*, *P. aeruginosa*, *E. coli*, *E. faecalis*, and MRSA observed. The results against all the test strains can be seen in Figure 7. The antimicrobial assay with *S. aureus* was repeated to verify the effect of **1**. Among the tested concentrations, 25 μM was the lowest concentration of **1**, which completely inhibited the growth of *S. aureus*, as displayed in Figure 8. Compound **1** and **2** were also tested for their ability to inhibit biofilm formation by *S.epidermidis* in concentrations up to 200 μM. Compound **1** showed some weak effects (assay result of ~ 40%, meaning 60% inhibition, normal cut-off used for further investigation is minimum 70% inhibition) at 200 μM. Compound **2** showed no visible effect up to 200 μM.

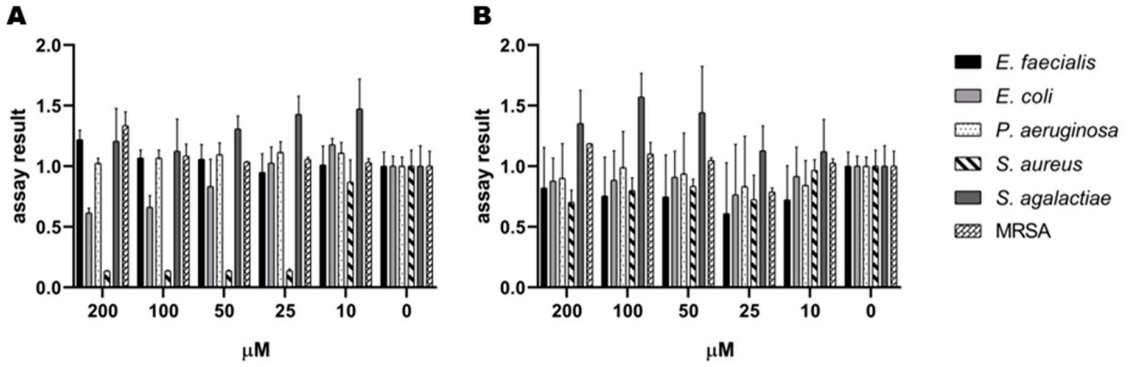

Figure 7. Initial screen of antibacterial activity of (**A**) serratiochelin A (**1**) and (**B**) serratiochelin C (**2**) on *E. faecialis*, *E. coli*, *P. aeruginosa*, *S. agalactiae*, and MRSA, normalized assay results. The experiment was executed twice with two technical replicates each.

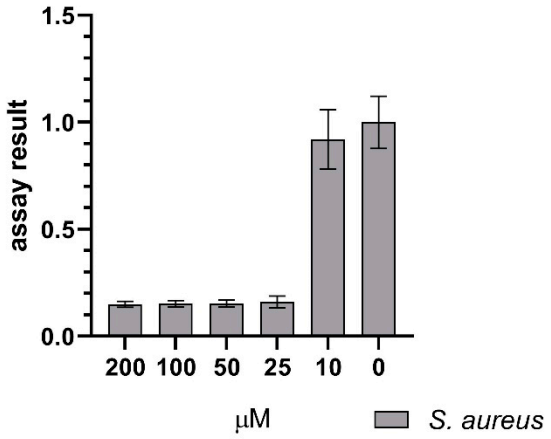

Figure 8. Effect of serratiochelin A (**1**) on *S. aureus* showing inhibition of growth down to 25 µM, normalized assay results. The assay was executed in four experiments with 3 × 2 and 1 × 3 technical replicates.

The effects of the compounds on eukaryotic cells was evaluated using the human melanoma cell line A2058 and the non-malign lung fibroblast cell line MRC5, see Figure 9. The effect of **2** on both cell lines is insufficient, while **1** reduces the cell proliferation of both MRC5 and A2058 cells. The effect of **1** is stronger against MRC5 cells than against A2058.

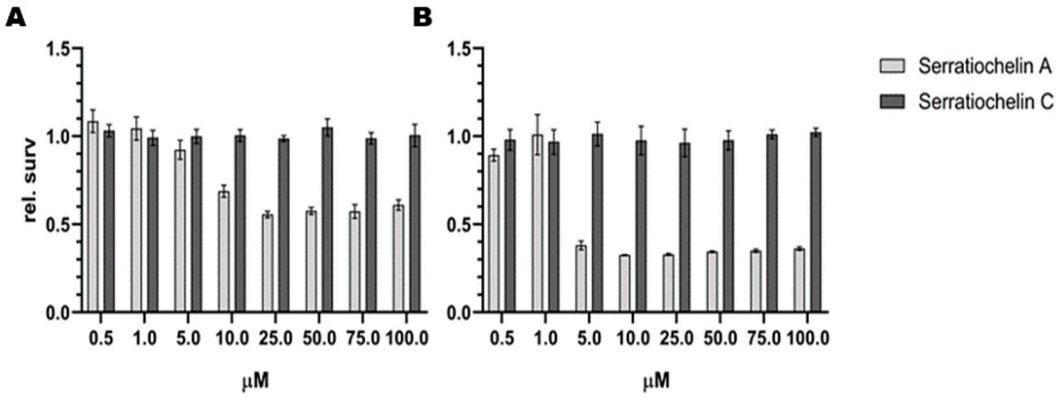

Figure 9. Antiproliferative effect of serratiochelin A (**1**) and C (**2**) on (**A**) A2058 (melanoma) and (**B**) MRC-5 (non-malignant lung fibroblasts) cell lines. The experiments were repeated twice with three technical replicates.

4. Discussion

In this study, a siderophore was isolated from a co-culture of a *Shewanella* sp. and *Serratia* sp. bacteria, both of which come from bacterial genera that are important for environmental iron metabolism. Bacteria from the genus *Shewanella* are known for their important role in iron metabolism, especially in aquatic environments. Previously, several siderophores have been isolated from bacteria of the genus *Serratia*, among these serratiochelin A (**1**).

Shewanella is a genus of Gram-negative rod-shaped γ-proteobacteria, within the order Alteromonadales, found mostly in aquatic habitats [16]. Bacteria from this genus have been isolated from several aquatic sources, both marine and freshwater [17–20]. The genus was established in 1985 [21], after a reconstruction of the *Vibrionaceae* family. *Shewanella* is part of the monogeneric family Shewanellaceae [16], which consists only of this one genera. The genus has high respiratory diversity, with the capability to respire approximately 20 different compounds, including toxic compounds and insoluble metals, one example being reducing Fe(III) chelate and Fe(III) oxide to produce soluble Fe(II) [22]. Bacteria from this genus are often involved in the iron metabolism in their environment, and several iron chelators (siderophores) have been isolated from this genus. Putrebactin is a cyclic dihydroxamate siderophore, produced and isolated from *S. putrefaciens* [23].

To investigate if the three bacterial isolates present in the glycerol stock co-exist in the liquid DVR1 cultures, the culture was streaked out on several agar plates after 3 and 10 days of incubation. The *Shewanella* colonies appeared first, followed by *Serratia* forming colonies on top of the *Shewanella* sp. colonies (Figure S14). After 10 days, there were only colony forming units of *Serratia* sp. present from the liquid co-culture, and the *Shewanella* could not be detected when streaked out on agar. Serratiochelins have previously only been isolated from the *Serratia* genus, and are considered to be rare siderophores [10]. As *Serratia* completely dominates the *Serratia-Shewanella* co-culture after 10 days, and based on data reported regarding previous isolation of **1** [**9**,**10**], it seems to be reasonable to hypothesize that *Serratia* is the true producer of **1** in this co-culture and that it is outcompeting *Shewanella* because of its specific iron acquisition. As **1** was not observed in axenic cultures of *Shewanella* or *Serratia*, we assume that the co-culturing is inducing the production of the compound, possibly due to the competition for iron in the culture.

Compound **1** was isolated from the co-culture after modifying the purification protocol. The degradation of **1** to **2** was triggered by formic acid used in the mobile phase during chromatographic isolation of the compounds. We confirmed that the degradation correlates with the concentration of formic acid as previously published [10]. In addition, the same acidic hydrolyzation of an oxazoline ring was also observed for the compound agrobactin after exposure to hydrochloric acid [24]. We also confirmed the chelation of iron in a hexadecanoate coordination indicated by the loss of three protons, observed in HR-MS experiments [10]. Compound **1** was only produced when no additional iron was added to the co-culture. In the presence of iron, **1** was not detected in the bacterial culture media. We did not detect serratiochelin B and **2** in the culture media, extract, or FLASH fractions (where no acid was used). Previously, it was reported that **1** and serratiochelin B are the initial biosynthetic products of *Serratia* [10]. For our isolate, the results strongly indicate that **1** is the only biosynthetic product, while serratiochelin B and **2** are degradation products of **1**. To obtain **1**, its liability for acid degradation is a significant disadvantage. The FLASH liquid chromatography represents a rather inefficient method for isolation since we were taking only the fraction with the highest purity. Thus, a considerable amount of compound eluted before and after together with other impurities, which diminished the yield of pure **1** significantly, and the purification protocol was not optimized regarding yields but for obtaining **1** without its degradation product. We assume that within the producer isolates' natural environment, **1** is, however, most likely not degrading into **2** due to the rather alkaline pH of seawater [25].

The acid-free isolation enabled us to isolate **1** for bioactivity testing. Since there is no bioactivity data present for **1** and **2**, and the purpose of our investigation was to find new bioactive molecules, it was prioritized for isolation. The testing of both compounds revealed some interesting insights into their bioactivity. Compound **2** displayed no activity in the tested assays and at the tested concentrations,

while **1** had antibacterial activity against *S. aureus* and toxic effects on both eukaryotic cell lines tested. Its antibacterial effect was specific towards *S. aureus*, while not having an effect on the other bacteria, including MRSA. Its cytotoxic effect was evaluated against the melanoma cell line (A2058), as we frequently observed that it is the most sensitive cancer cell line in our screening of extracts and compounds. The non-malignant lung fibroblasts (MRC5) was included as a general control of toxicity. The observed effect was stronger on lung fibroblasts than melanoma cells. Of interest to us was the observed difference in activity between **1** and **2** despite the fact that the two structures are closely related. It is questionable if the antiproliferative effect of **1** is caused by iron deprivation as observed for other siderophores [26] or by another effect. The same applies for the observed antibacterial effect on *S.aureus*, while the lack of effect on the other bacteria might indicate a specific target. Both molecules are capable of chelating iron, so either **1** has a higher affinity to iron than **2**, or it has another mode of action. The species-specific antibacterial effect indicates the latter. Gokarn and co-authors investigated the effect of iron chelation by exochelin-MS, mycobactin S, and deferoxiamine B on mammalian cancer cell lines and an antiproliferative effect was observed at concentrations between 0.1 to 1.0 mg/mL. Only HEPG2 cells have shown 23% cell survival at 20 μg/mL for mycobactin S. They observed a different sensitivity among the tested cell lines and siderophores [26]. Compound **1** had an effect at concentrations of <43 μg/mL (40% cell survival was detected at 2.15 μg/mL of **1** against MRC5). Therefore, testing of **1** against more cell lines and testing of **2** at higher concentrations would be an approach for further studies on the antiproliferative effects of **1** and **2**. Some siderophores are known to have additional functions, such as a virulence factor and modulation of the host of a pathogen [27]. Assuming another mode of action than iron chelation, the most relevant structural difference would be the 5-methyl-2-oxazoline heterocycle in **1**, which is hydrolyzed in **2**. Oxazole and oxazoline moieties are structural motives present in molecules with an antibacterial and antiproliferative effect [28,29]. They are ligands to a number of different protein targets and can be regarded as "privileged structures" [29,30]. Further bioactivity elucidation of the two serratiochelins and the mode of action studies of **1** will be the subject of further investigation.

5. Conclusions

We proved the production of **1** in high yields by a co-culture of *Serratia* sp. and *Shewanella* sp., while the compound was not observed in axenic cultures. We confirmed the iron chelation, as well as the degradation of **1** to **2**. We did not observe the production of any compound that could be related to serratiochelin B in the bacterial cultures nor in the extract, but we observed its generation in traces during acid-induced degradation, which gives rise to the assumption that serratiochelin B and **2** are both hydrolyzation products of **1** in this study.

While **1** showed antiproliferative activity on human cancer cells but also on non-malignant lung fibroblasts, and a specific antimicrobial effect on *S. aureus*, **2** did not show any bioactivity in the assays conducted in this study. Since **1** and **2** differ in the presence of a structural motif that can be seen as a privileged structure, we hypothesize that the hydrolyzation of the 5-methyl-2-oxazoline explains the difference in bioactivity. The liability for hydrolyzation, however, represents a strong disadvantage for developing this candidate further as a drug lead.

Supplementary Materials: The following are available online at http://www.mdpi.com/2076-2607/8/7/1042/s1, Figure S1: ^{1}H NMR (600 MHz, DMSO-d_6) spectrum of **1**; Figure S2: ^{13}C (151 MHz, DMSO-d_6) spectrum of **1**; Figure S3: HSQC + HMBC (600 MHz, DMSO-d_6) spectrum of serratiochelin A; Figure S4: COSY (600 MHz, DMSO-d_6) spectrum of **1**; Figure S5: ROESY (600 MHz, DMSO-d_6) spectrum of **1**; Figure S6: ^{1}H NMR (600 MHz, DMSO-d_6) spectrum of **2**; Figure S7: ^{13}C (151 MHz, DMSO-d_6) spectrum of **2**; Figure S8: HSQC + HMBC (600 MHz, DMSO-d_6) spectrum of **2**; S9: HSQC + HMBC (600 MHz, DMSO-d_6) spectrum of **2** (**2**), zoomed in crowded area; Figure S10: COSY (600 MHz, DMSO-d_6) spectrum of **2**; Figure S11: Mass spectra of **1** and **2**; Figure S12: UV/Vis spectra of **1**and **2**; Figure S13: Chromatograms of Marfey's analysis of **1**; Figure S14: Isolation of the bacteria and co-culture of *Serratia* sp. and *Shewanella* sp., Text S15: Consensus sequence of *Shewanella* sp.; Text S16: Consensus sequence of *Serratia* sp.; Text S17: Consensus sequence of *Leifsonia* sp.

Author Contributions: Conceptualization, J.H.A., Y.S. and M.J.; investigation, M.J. and Y.S.; structure elucidation J.I.; writing—original draft preparation, M.J., K.Ø.H. and Y.S.; writing—review and editing, J.I., J.H.A. and E.H.H. All authors have read and agreed to the published version of the manuscript.

Funding: This project received funding from the following projects: The Marie Skłodowska-Curie Action MarPipe of the European Union and from UiT-The Arctic University of Norway (grant agreement GA 721421 H2020-MSCA-ITN-2016), The DigiBiotics project of the Research Counsil of Norway (project iD 269425) and the AntiBioSpec project of UiT the Arctic University of Norway (Cristin iD 20161326). The publication charges for this article have been funded by a grant from the publication fund of UiT-The Arctic University of Norway.

Acknowledgments: Yannik Schneider has been supported by the MarPipe Project, and Marte Jenssen by the DigiBiotics project and the AntiBioSpec project. Kirsti Helland and Marte Albrigtsen are gratefully acknowledged for executing the bioactivity assays and Chun Li for his help with identifying the strains. We want to acknowledge our colleagues of The Norwegian Marine Biobank (Marbank) for sampling and isolation of the bacterial strains.

Conflicts of Interest: The authors declare no conflict of interest.

References

1. Andrews, S.C.; Robinson, A.K.; Rodríguez-Quiñones, F. Bacterial iron homeostasis. *FEMS Microbiol. Rev.* **2003**, *27*, 215–237. [CrossRef]
2. Sandy, M.; Butler, A. Microbial iron acquisition: marine and terrestrial siderophores. *Chem. Rev.* **2009**, *109*, 4580–4595. [CrossRef]
3. Winkelmann, G. Microbial siderophore-mediated transport. *Biochem. Soc. Trans.* **2002**, *30*, 691–696. [CrossRef]
4. Hider, R.C.; Kong, X. Chemistry and biology of siderophores. *Nat. Prod. Rep.* **2010**, *27*, 637–657. [CrossRef] [PubMed]
5. Ito, T.; Neilands, J.B. Products of "low-iron fermentation" with bacillus subtilis: Isolation, characterization and synthesis of 2, 3-dihydroxybenzoylglycine. *J. Am. Chem. Soc.* **1958**, *80*, 4645–4647. [CrossRef]
6. Dworkin, M.; Falkow, S.; Rosenberg, E.; Schleifer, K.-H.; Stackebrandt, E. *The Genus Serratia*; Springer: New York, NY, USA, 2006; pp. 219–244. [CrossRef]
7. Martinec, T.; Kocur, M. The taxonomic status of Serratia marcescens Bizio. *Int. J. Syst. Evol. Microbiol.* **1961**, *11*, 7–12. [CrossRef]
8. Khilyas, I.; Shirshikova, T.; Matrosova, L.; Sorokina, A.; Sharipova, M.; Bogomolnaya, L. Production of siderophores by Serratia marcescens and the role of MacAB efflux pump in siderophores secretion. *BioNanoScience* **2016**, *6*, 480–482. [CrossRef]
9. Ehlert, G.; Taraz, K.; Budzikiewicz, H. Serratiochelin, a new catecholate siderophore from Serratia marcescens. *Z. Nat.* **1994**, *49*, 11–17. [CrossRef]
10. Seyedsayamdost, M.R.; Cleto, S.; Carr, G.; Vlamakis, H.; João Vieira, M.; Kolter, R.; Clardy, J. Mixing and matching siderophore clusters: Structure and biosynthesis of serratiochelins from *Serratia* sp. V4. *J. Am. Chem. Soc.* **2012**, *134*, 13550–13553. [CrossRef]
11. Modell, B.; Letsky, E.A.; Flynn, D.M.; Peto, R.; Weatherall, D.J. Survival and desferrioxamine in thalassaemia major. *Br. Med. J.* **1982**, *284*, 1081–1084. [CrossRef] [PubMed]
12. Saha, M.; Sarkar, S.; Sarkar, B.; Sharma, B.; Bhattacharjee, S.; Tribedi, P. Microbial siderophores and their potential applications: A review. *Environ. Sci. Pollut. Res.* **2015**, *23*, 3984–3999. [CrossRef] [PubMed]
13. Braun, V.; Pramanik, A.; Gwinner, T.; Koberle, M.; Bohn, E. Sideromycins: Tools and antibiotics. *Biometals* **2009**, *22*, 3–13. [CrossRef]
14. Pramanik, A.; Stroeher, U.H.; Krejci, J.; Standish, A.J.; Bohn, E.; Paton, J.C.; Autenrieth, I.B.; Braun, V. Albomycin is an effective antibiotic, as exemplified with Yersinia enterocolitica and Streptococcus pneumoniae. *Int. J. Med. Microbiol.* **2007**, *297*, 459–469. [CrossRef]
15. Altschul, S.F.; Gish, W.; Miller, W.; Myers, E.W.; Lipman, D.J. Basic local alignment search tool. *J. Mol. Biol.* **1990**, *215*, 403–410. [CrossRef]
16. Ivanova, E.P.; Flavier, S.; Christen, R. Phylogenetic relationships among marine Alteromonas-like proteobacteria: Emended description of the family Alteromonadaceae and proposal of Pseudoalteromonadaceae fam. nov., Colwelliaceae fam. nov., Shewanellaceae fam. nov., Moritellaceae fam. nov., Ferrimonadaceae fam. nov., Idiomarinaceae fam. nov. and Psychromonadaceae fam. nov. *Int. J. Syst. Evol. Microbiol.* **2004**, *54*, 1773–1788. [CrossRef]

17. Lee, O.O.; Lau, S.C.; Tsoi, M.M.; Li, X.; Plakhotnikova, I.; Dobretsov, S.; Wu, M.C.; Wong, P.K.; Weinbauer, M.; Qian, P.Y. *Shewanella irciniae* sp. nov., a novel member of the family Shewanellaceae, isolated from the marine sponge Ircinia dendroides in the Bay of Villefranche, Mediterranean Sea. *Int. J. Syst. Evol. Microbiol.* **2006**, *56*, 2871–2877. [CrossRef] [PubMed]
18. Ivanova, E.P.; Nedashkovskaya, O.I.; Sawabe, T.; Zhukova, N.V.; Frolova, G.M.; Nicolau, D.V.; Mikhailov, V.V.; Bowman, J.P. *Shewanella affinis* sp. nov., isolated from marine invertebrates. *Int. J. Syst. Evol. Microbiol.* **2004**, *54*, 1089–1093. [CrossRef]
19. Kizhakkekalam, K.V.; Chakraborty, K.; Joy, M. Antibacterial and antioxidant aryl-enclosed macrocyclic polyketide from intertidal macroalgae associated heterotrophic bacterium Shewanella algae. *Med. Chem. Res.* **2019**, *29*, 145–155. [CrossRef]
20. Bowman, J.P.; McCammon, S.A.; Nichols, D.S.; Skerratt, J.H.; Rea, S.M.; Nichols, P.D.; McMeekin, T.A. *Shewanella gelidimarina* sp. nov. and *Shewanella frigidimarina* sp. nov., novel Antarctic species with the ability to produce eicosapentaenoic acid (20:5 omega 3) and grow anaerobically by dissimilatory Fe(III) reduction. *Int. J. Syst. Evol. Microbiol.* **1997**, *47*, 1040–1047. [CrossRef]
21. MacDonell, M.T.; Colwell, R.R. Phylogeny of the Vibrionaceae, and recommendation for two new genera, Listonella and Shewanella. *Syst. Appl. Microbiol.* **1985**, *6*, 171–182. [CrossRef]
22. Hau, H.H.; Gralnick, J.A. Ecology and biotechnology of the genus Shewanella. *Annu. Rev. Microbiol.* **2007**, *61*, 237–258. [CrossRef] [PubMed]
23. Ledyard, K.M.; Butler, A. Structure of putrebactin, a new dihydroxamate siderophore produced by Shewanella putrefaciens. *J. Biol. Inorg. Chem.* **1997**, *2*, 93–97. [CrossRef]
24. Ong, S.A.; Peterson, T.; Neilands, J.B.; Ong, S.A. Agrobactin, a siderophore from Agrobacterium Tumefaciens. *J. Biol. Chem.* **1979**, *254*, 1860–1865. [PubMed]
25. Halevy, I.; Bachan, A. The geologic history of seawater pH. *Science* **2017**, *355*, 1069–1071. [CrossRef]
26. Gokarn, K.; Sarangdhar, V.; Pal, R.B. Effect of microbial siderophores on mammalian non-malignant and malignant cell lines. *BMC Complement. Altern. Med.* **2017**, *17*, 145. [CrossRef]
27. Behnsen, J.; Raffatellu, M. Siderophores: More than stealing iron. *MBio* **2016**, *7*, e01906–e01916. [CrossRef]
28. Chiacchio, M.A.; Lanza, G.; Chiacchio, U.; Giofrè, S.V.; Romeo, R.; Iannazzo, D.; Legnani, L. Oxazole-based compounds as anticancer agents. *Curr. Med. Chem.* **2019**, *26*, 7337–7371. [CrossRef]
29. Zhang, H.-Z.; Zhao, Z.-L.; Zhou, C.-H. Recent advance in oxazole-based medicinal chemistry. *Eur. J. Med. Chem.* **2018**, *144*, 444–492. [CrossRef]
30. Kim, J.; Kim, H.; Park, S.B. Privileged structures: Efficient chemical "navigators" toward unexplored biologically relevant chemical spaces. *J. Am. Chem. Soc.* **2014**, *136*, 14629–14638. [CrossRef]

© 2020 by the authors. Licensee MDPI, Basel, Switzerland. This article is an open access article distributed under the terms and conditions of the Creative Commons Attribution (CC BY) license (http://creativecommons.org/licenses/by/4.0/).

Bioactivity of Serratiochelin A, a Siderophore Isolated from a Co-Culture of *Serratia* sp. and *Shewanella* sp.

Yannik Schneider [1†*], Marte Jenssen [1†*], Johan Isaksson [2], Kine Ø. Hansen [1], Jeanette Hammer Andersen [1] and Espen H. Hansen [1]

[1] Marbio, Faculty for Fisheries, Biosciences and Economy, UiT—The Arctic University of Norway, Breivika, N-9037 Tromsø, Norway; kine.o.hanssen@uit.no (K.Ø.H.); espen.hansen@uit.no (E.H.H.); jeanette.h.andersen@uit.no (J.H.A.)

[2] Department of Chemistry, Faculty of Natural Sciences, UiT—The Arctic University of Norway, Breivika, N-9037 Tromsø, Norway; johan.isaksson@uit.no (J.I.)

* Correspondence: yannik.k.schneider@uit.no; Tel.: +47-77649267; marte.jenssen@uit.no; Tel.: +47-77649275

† Authors contributed equally to the work

Supplemental Information Table of Contents

NMR Spectroscopic results

Serratiochelin A (1)

Figure S1 ^{1}H NMR (600 MHz, DMSO-d_6) spectrum of serratiochelin A (**1**)

Figure S2 ^{13}C (151 MHz, DMSO-d_6) spectrum of serratiochelin A (**1**)

Figure S3 HSQC + HMBC (600 MHz, DMSO-d_6) spectrum of serratiochelin A (**1**)

Figure S4 COSY (600 MHz, DMSO-d_6) spectrum of serratiochelin A (**1**)

Figure S5 ROESY (600 MHz, DMSO-d_6) spectrum of serratiochelin A (**1**)

Serratiochelin C (2)

Figure S6 ^{1}H NMR (600 MHz, DMSO-d_6) spectrum of serratiochelin C (**2**)

Figure S7 ^{13}C (151 MHz, DMSO-d_6) spectrum of serratiochelin C (**2**)

Figure S8 HSQC + HMBC (600 MHz, DMSO-d_6) spectrum of serratiochelin C (**2**)

Figure S9 HSQC + HMBC (600 MHz, DMSO-d_6) spectrum of serratiochelin C (**2**), zoomed in crowded area

Figure S10 COSY (600 MHz, DMSO-d_6) spectrum of serratiochelin C (**2**)

Results chemistry and mass spectrometry

Figure S11 Mass spectra of serratiochelin A (**1**) and serratiochelin C (**2**)

Figure S12 UV/Vis spectra of serratiochelin A (**1**) and serratiochelin C (**2**)

Figure S13 Chromatograms of Marfey's analysis of serratiochelin A (**1**)

Pictures of culture plates

Figure S14 Isolation of the bacteria and co-culture of *Serratia* sp. and *Shewanella* sp.

Consensus sequences of the bacterial isolates

Text S15: Consensus sequence of *Shewanella* sp.

Text S16: Consensus sequence of *Serratia* sp.

Text S17: Consensus sequence of *Leifsonia* sp

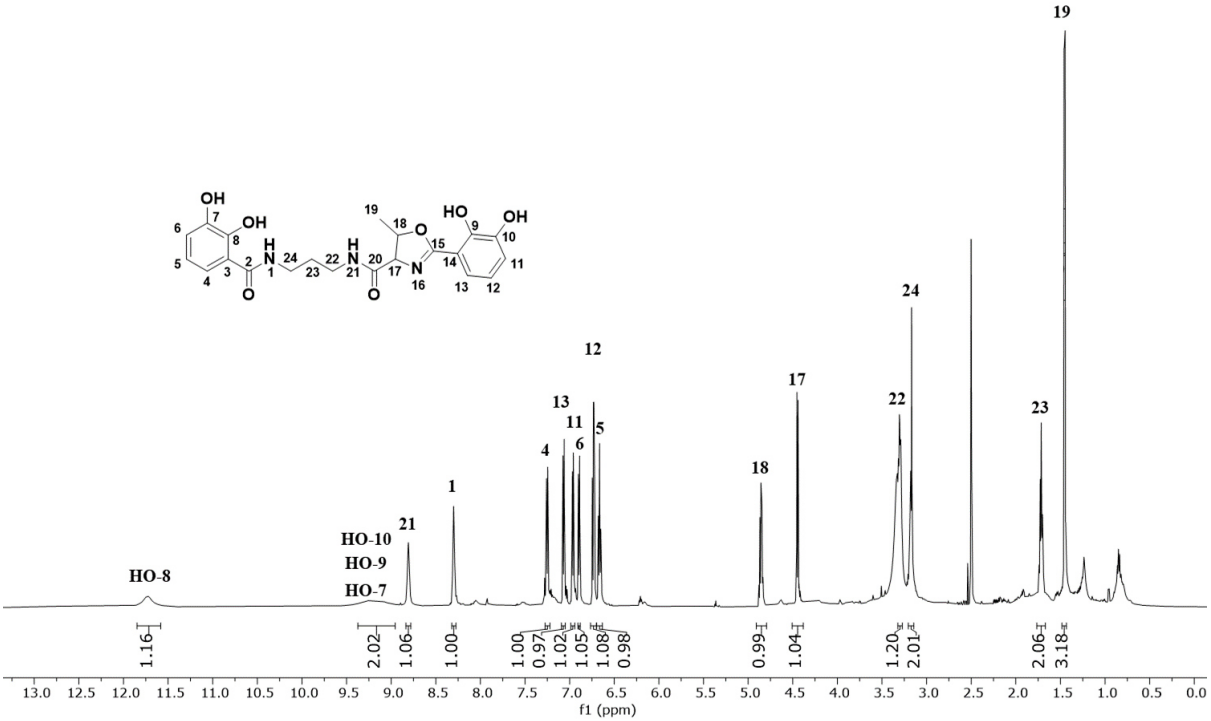

S1. ^{1}H NMR (600 MHz, DMSO-d_6) spectrum of serratiochelin A (**1**)

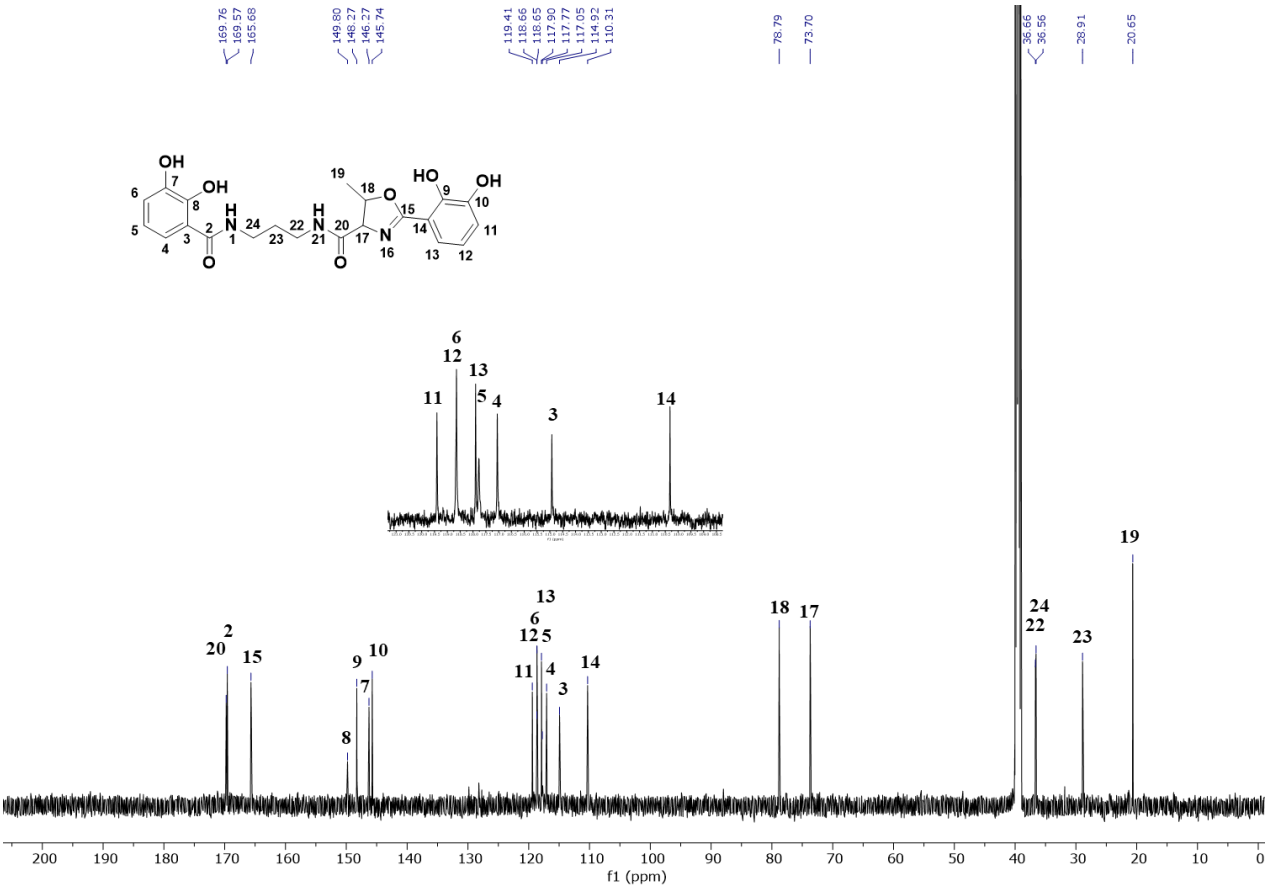

S2. ^{13}C (151 MHz, DMSO-d_6) spectrum of serratiochelin A (**1**)

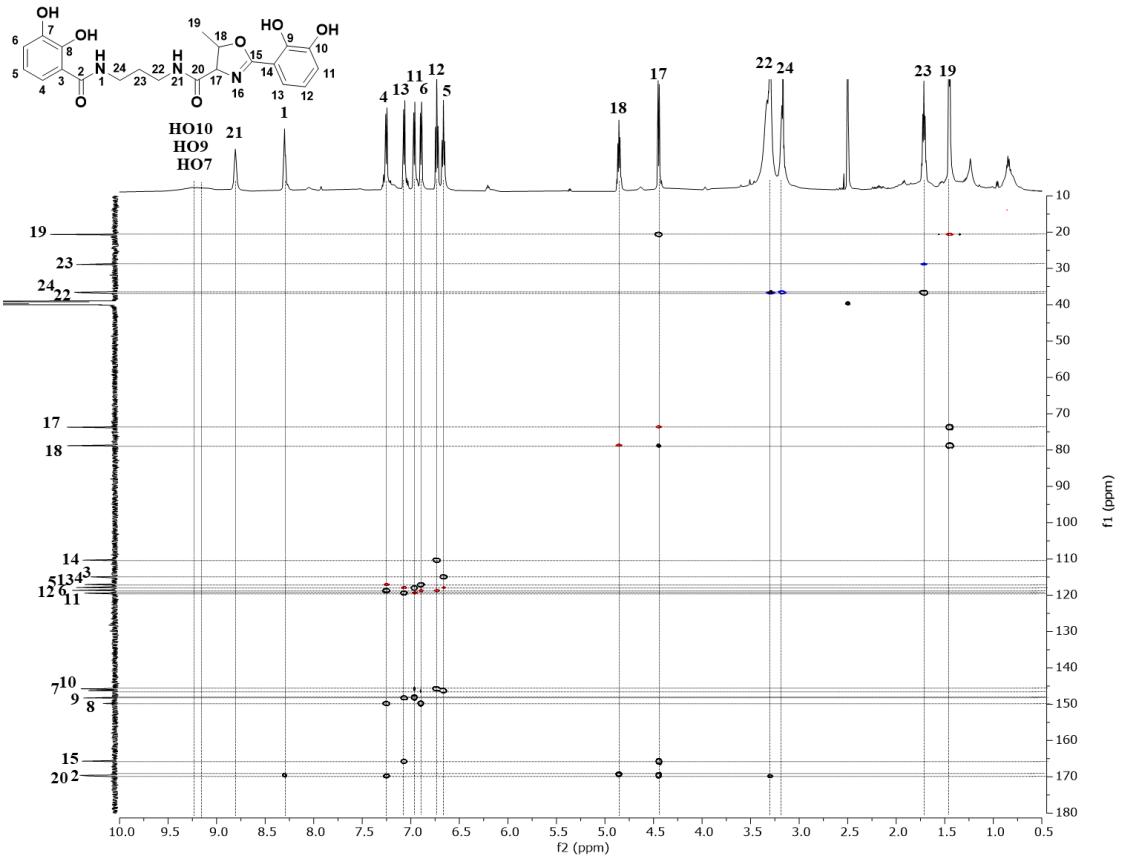

S3. HSQC + HMBC (600 MHz, DMSO-d_6) spectrum of serratiochelin A (**1**)

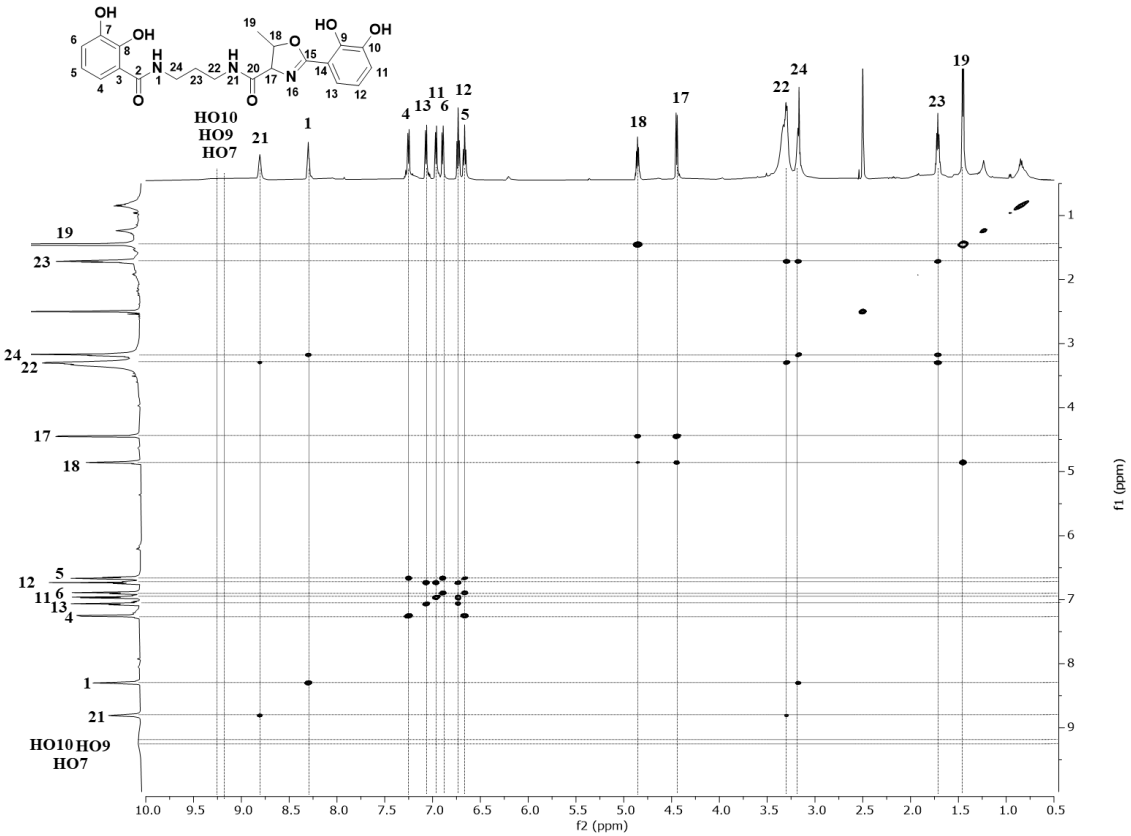

S4. COSY (600 MHz, DMSO-d_6) spectrum of serratiochelin A (**1**)

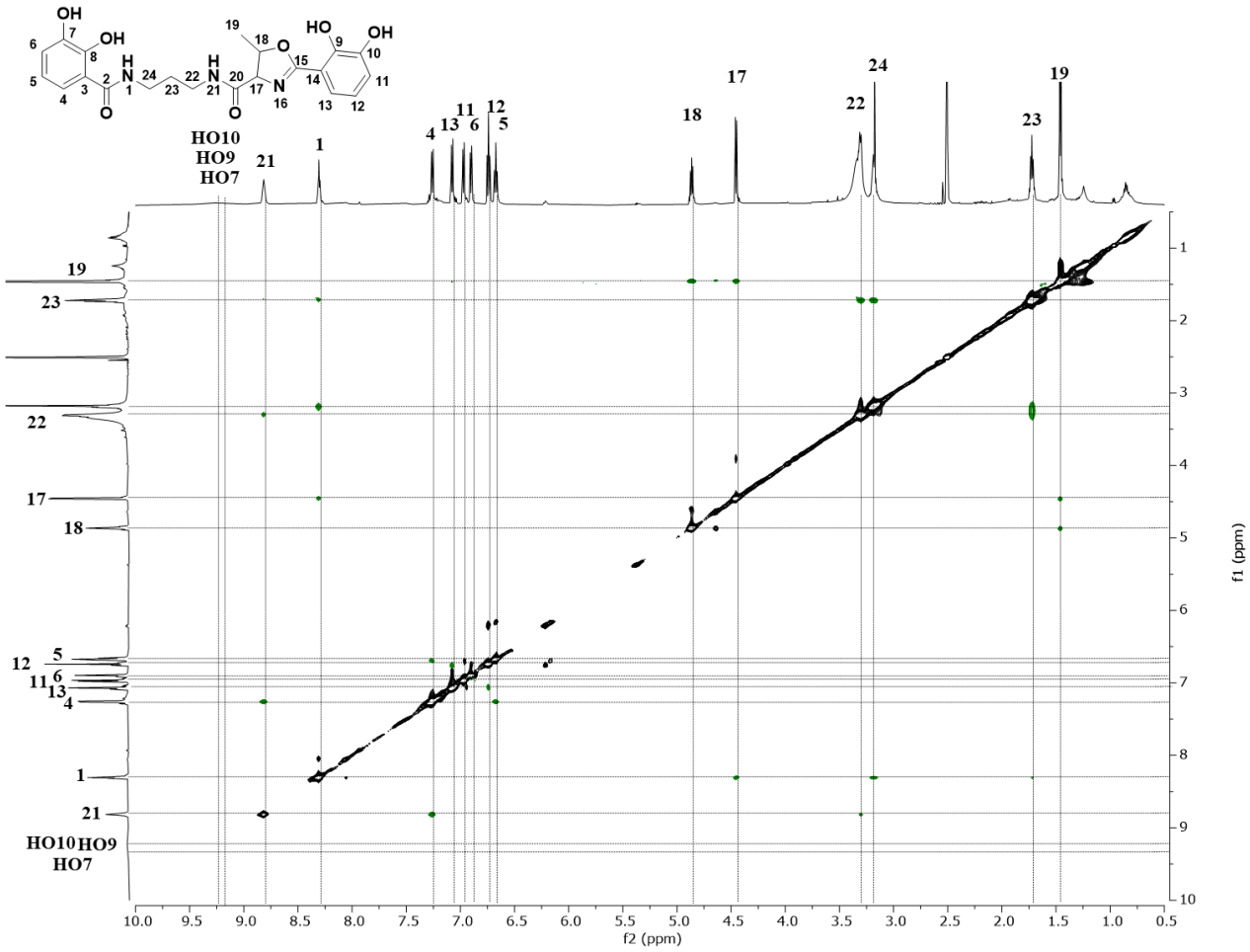

S5. ROESY (600 MHz, DMSO-d_6) spectrum of serratiochelin A (**1**)

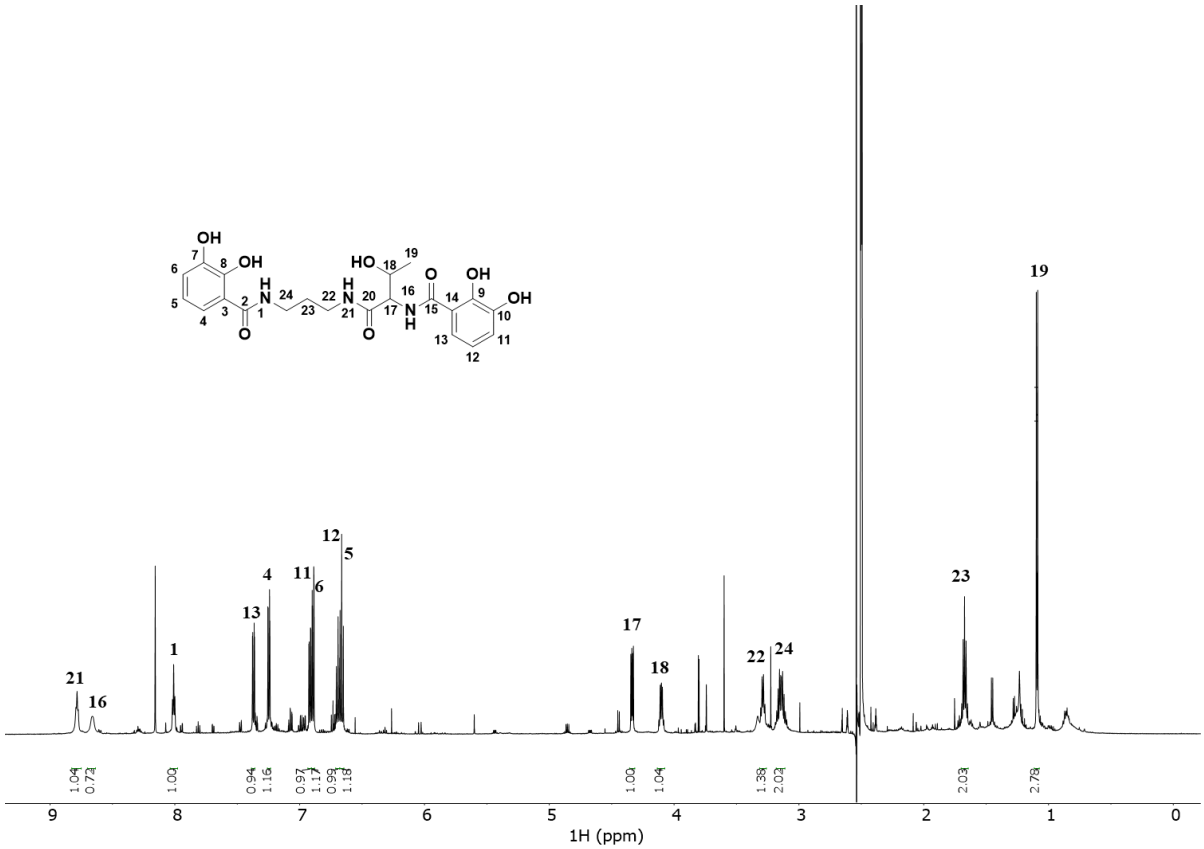

S6. ^{1}H NMR (600 MHz, DMSO-d_6) spectrum of serratiochelin C (**2**)

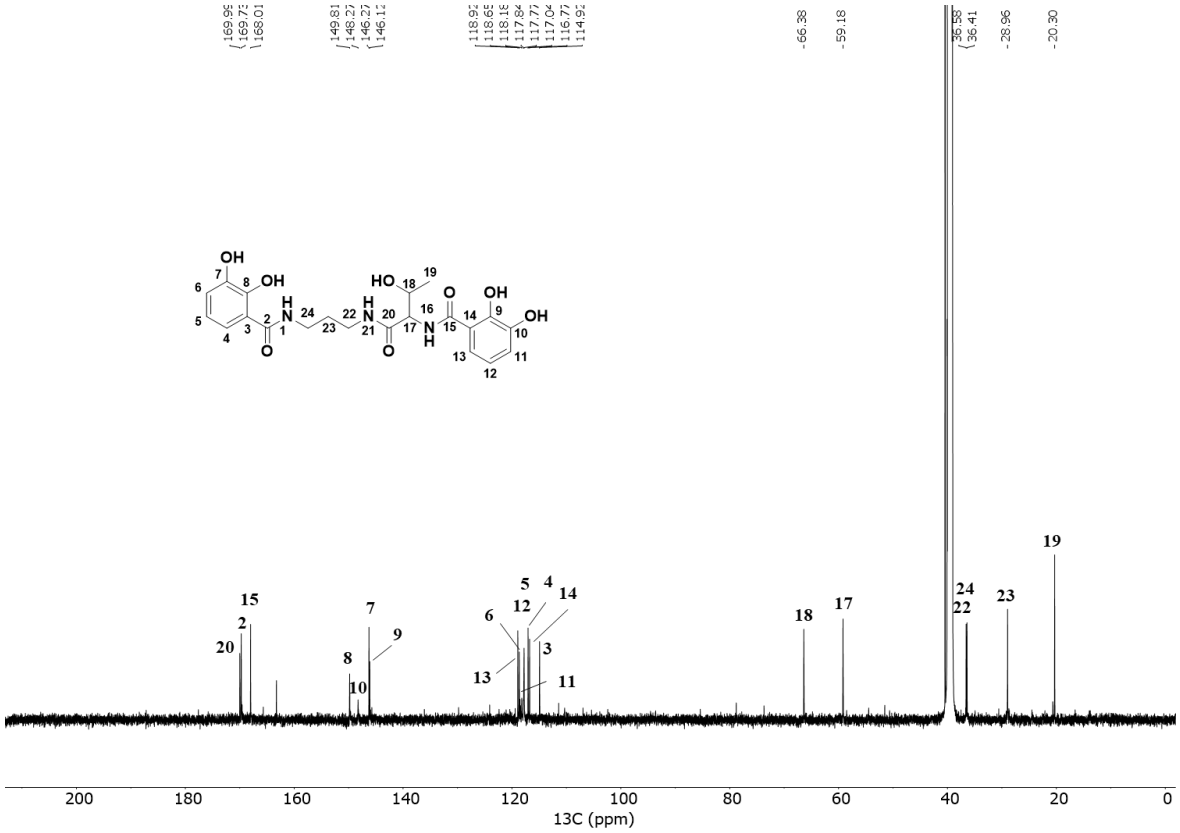

S7. ^{13}C (151 MHz, DMSO-d_6) spectrum of serratiochelin C (**2**)

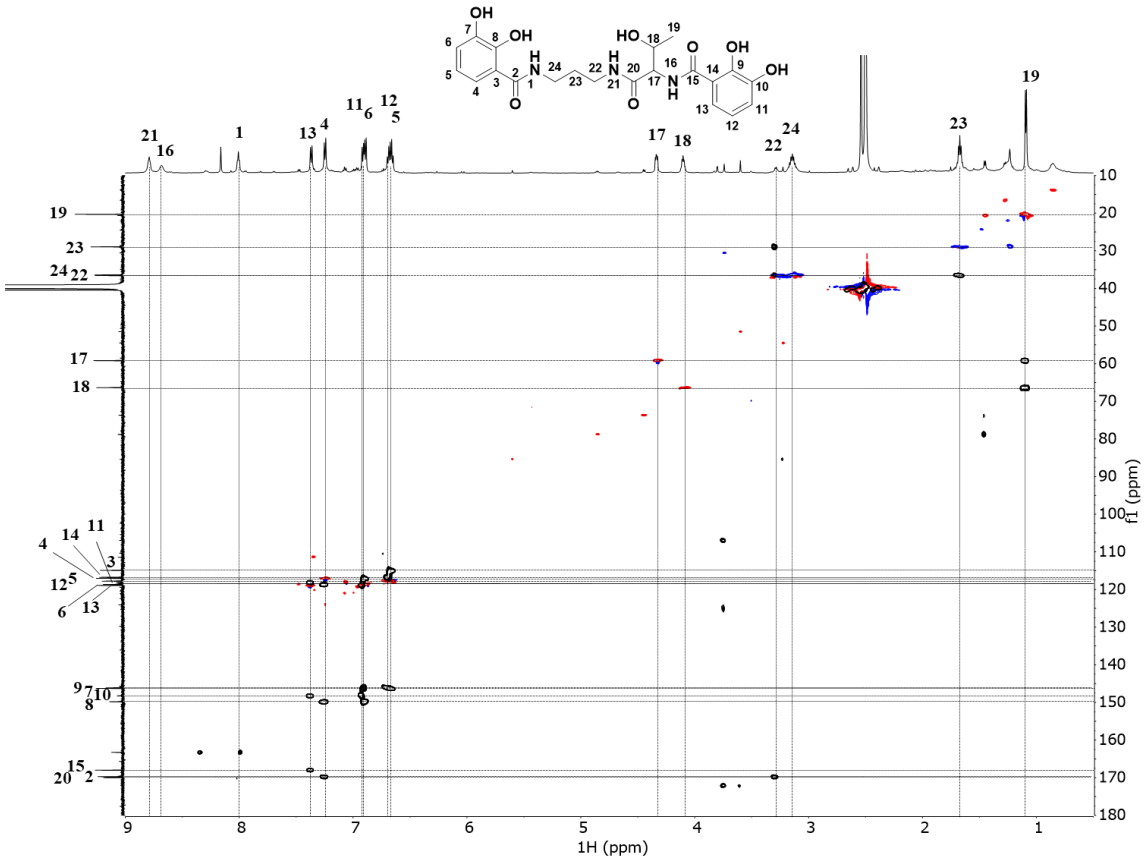

S8. HSQC + HMBC (600 MHz, DMSO-d_6) spectrum of serratiochelin C (**2**)

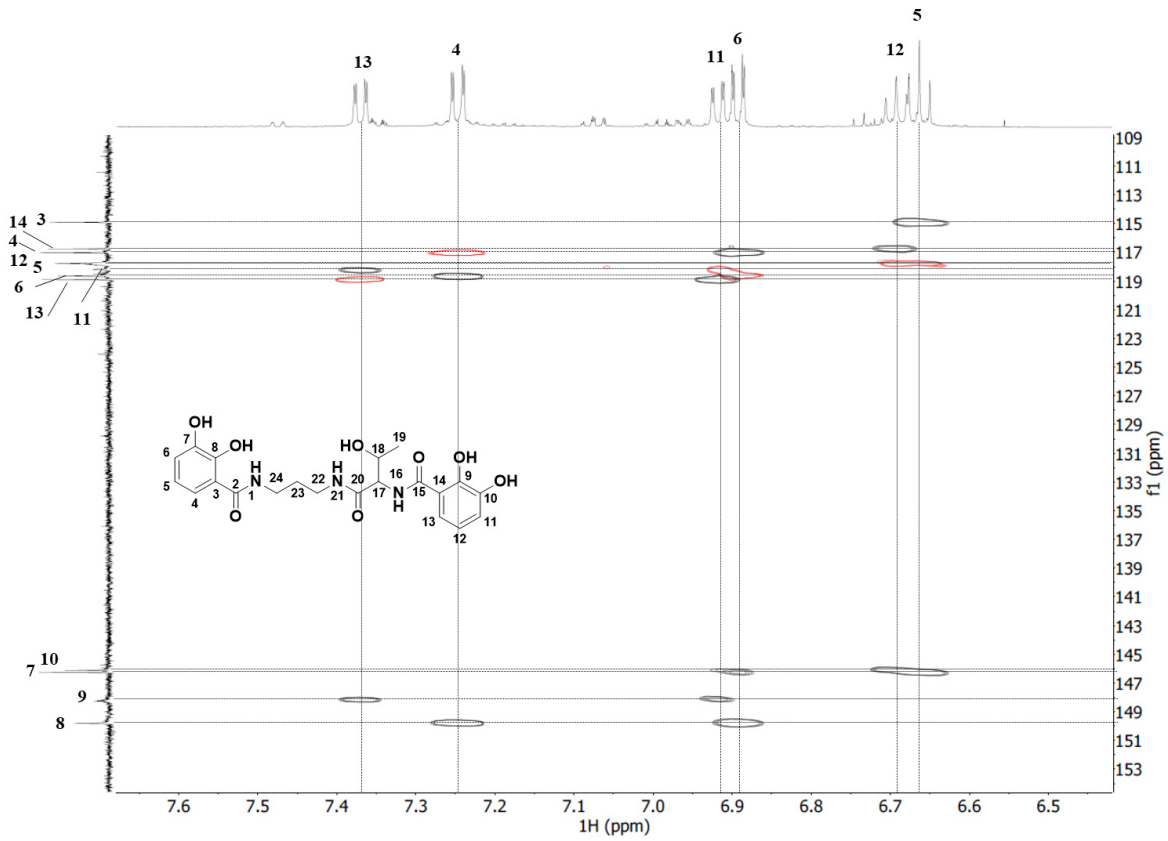

S9. HSQC + HMBC (600 MHz, DMSO-d_6) spectrum of serratiochelin C (**2**), zoomed in crowded area

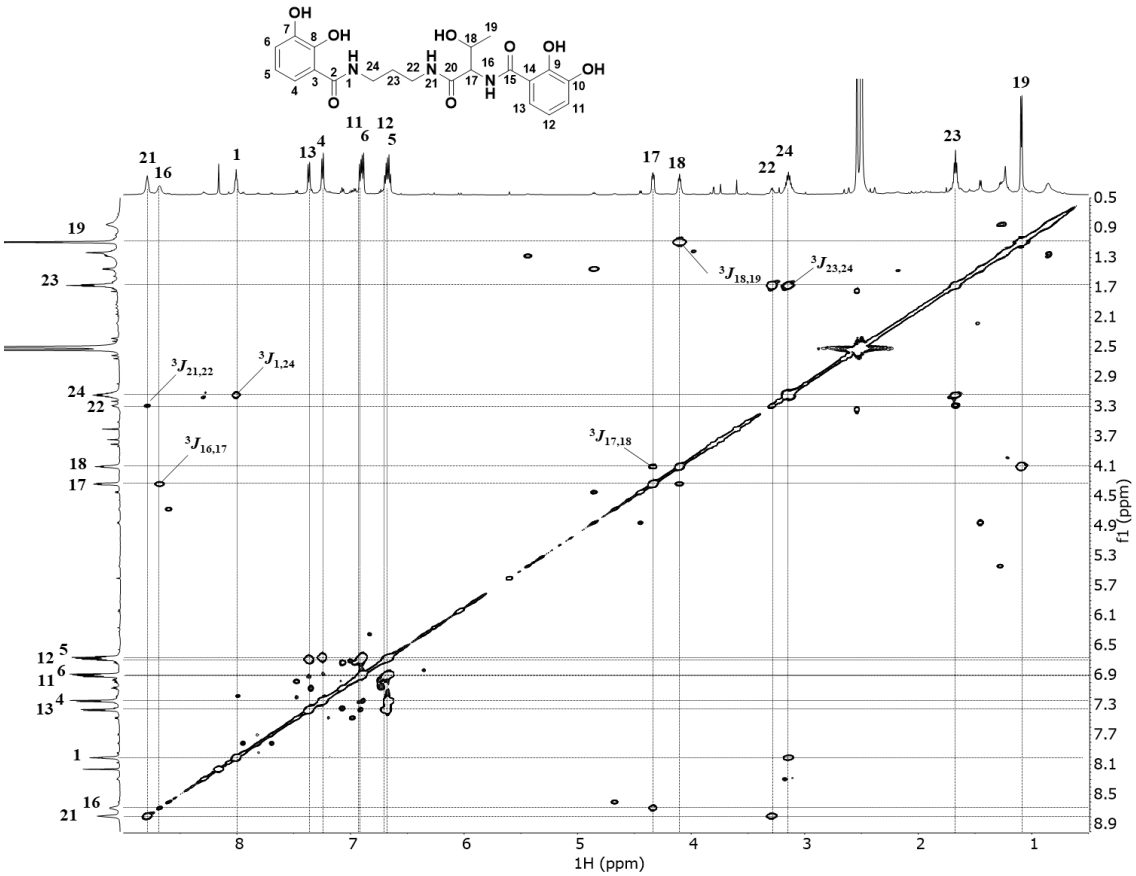

S10. COSY (600 MHz, DMSO-d_6) spectrum of serratiochelin C (**2**)

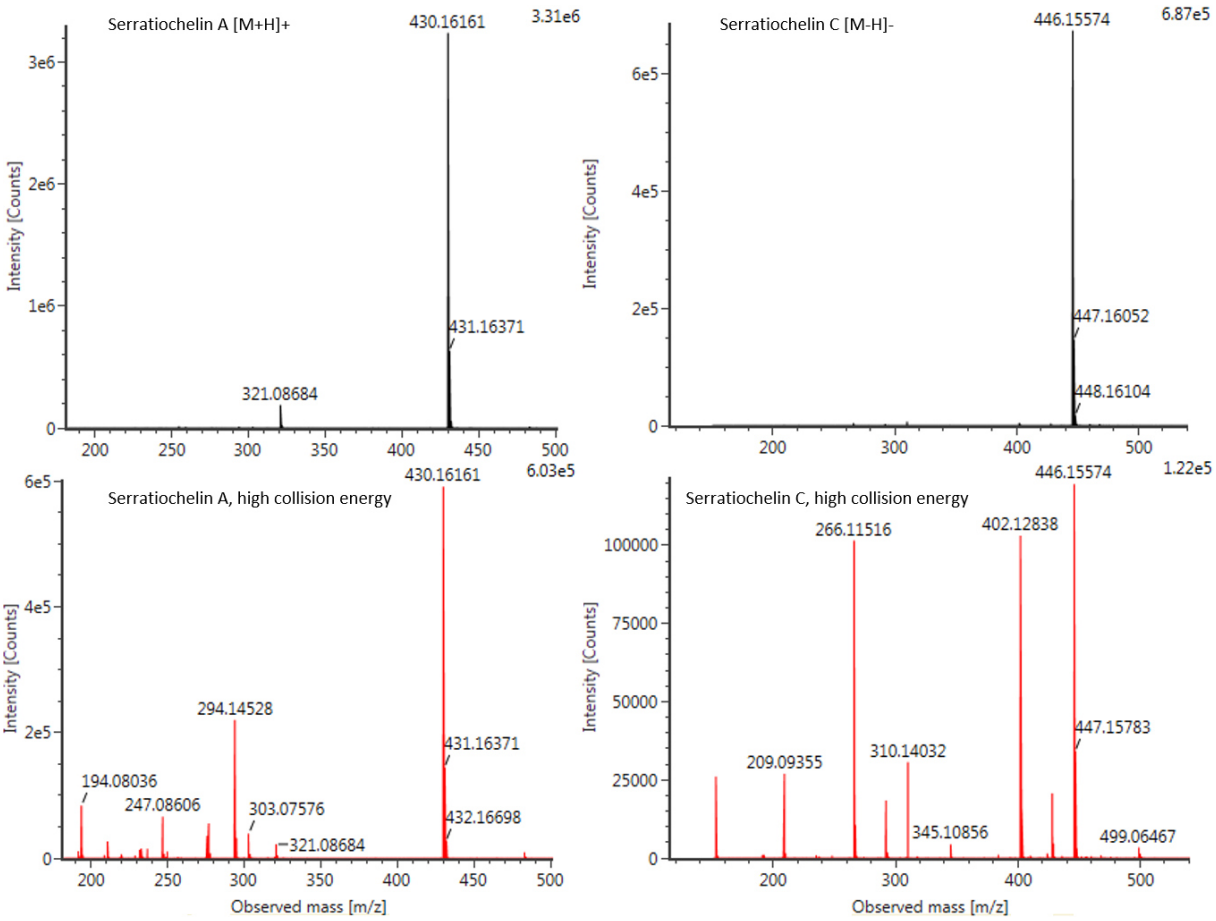

S11. Mass spectra of Serratiochelin A (**1**) (ESI+, left) and Serratiochelin C (**2**) (ESI-, right). The low-collision energy spectra are given in black and the high-collision energy spectra (20-80 eV ramp) in red below.

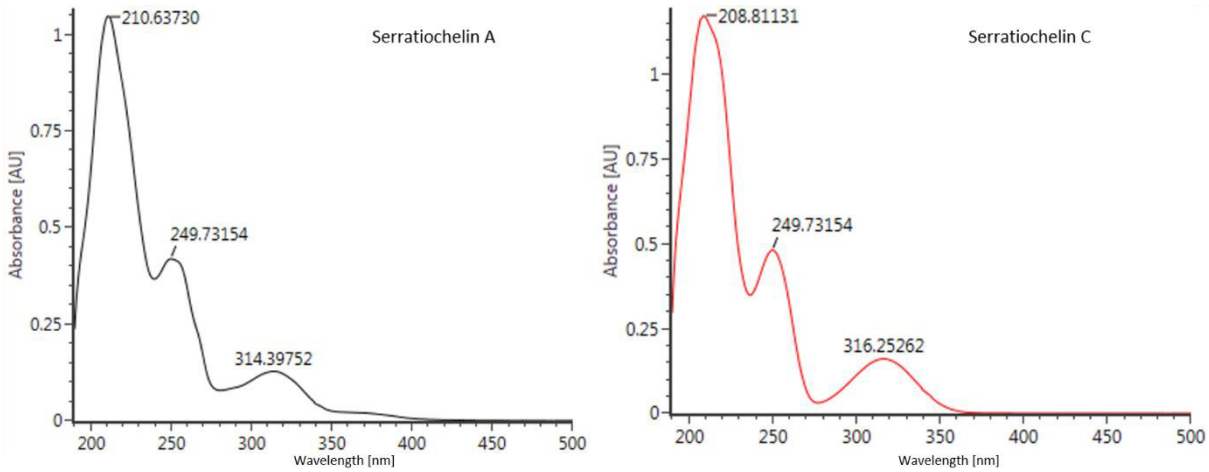

S12. UV/Vis spectra of Serratiochelin A (**1**) and C (**2**) in acetonitrile:water +1% (v/v) formic acid.

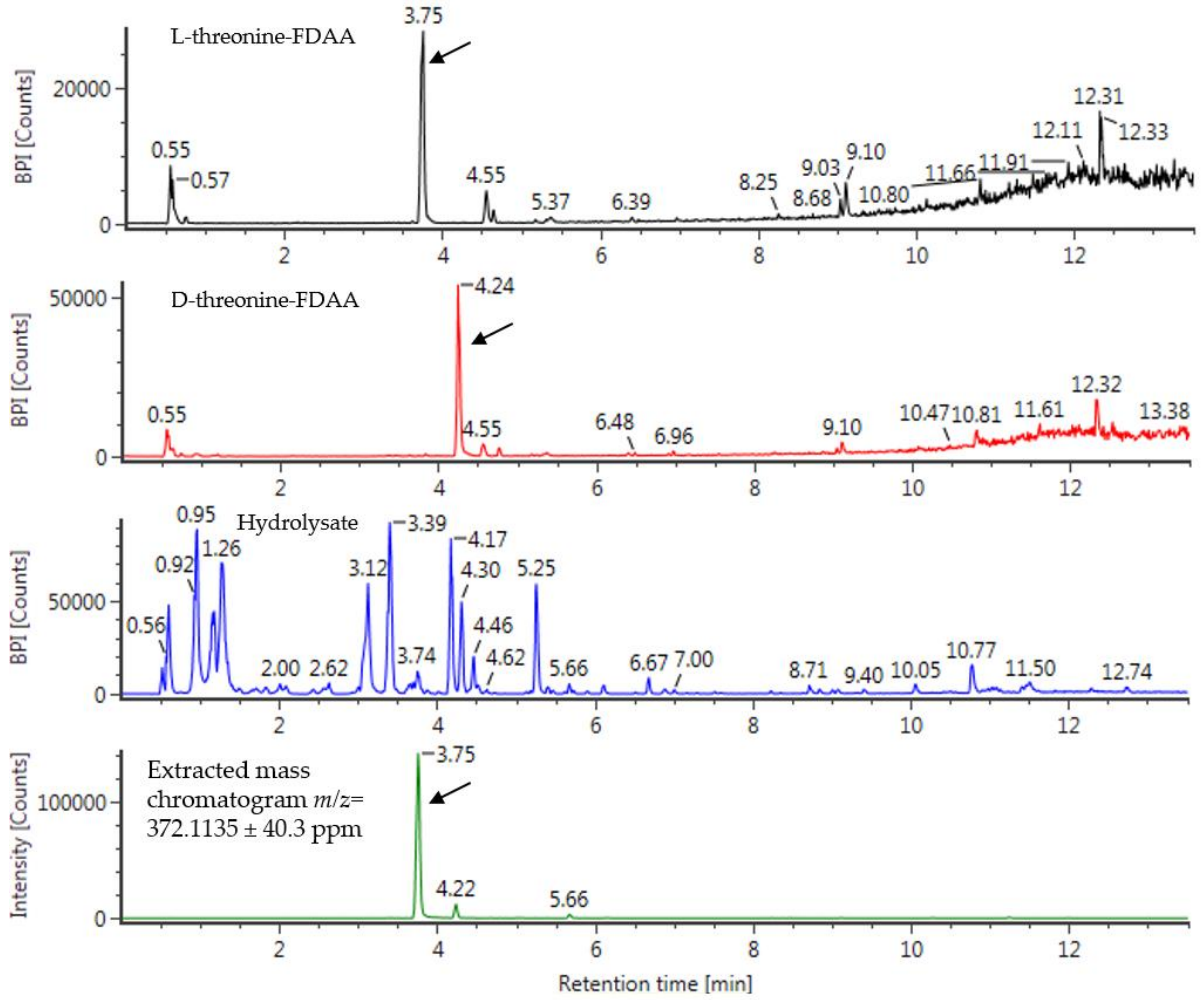

S13. Results of the threonine derivatisation using FDAA. The reactions were analysed using UHPLC-IMS-MS. At the top of the figure in black the chromatogram of L-threonine and below in red D-threonine is given. The chromatogram of the derivatised hydrolysate of serratiochelin A is given in blue (3rd from the top) and at the bottom, the extracted mass-chromatogramm for FDAA-threonine adduct ($C_{13}H_{17}N_5O_8$, calculated monoisotopic mass: 371.1077 u) from the derivatised hydrolysate is given. Comparing the retention times of the L-and D-threonine references we conclude that L-threonine is the present configuration of threonine in serratiochelin A (**1**). The FDAA-threonine peaks are indicated by the black arrows.

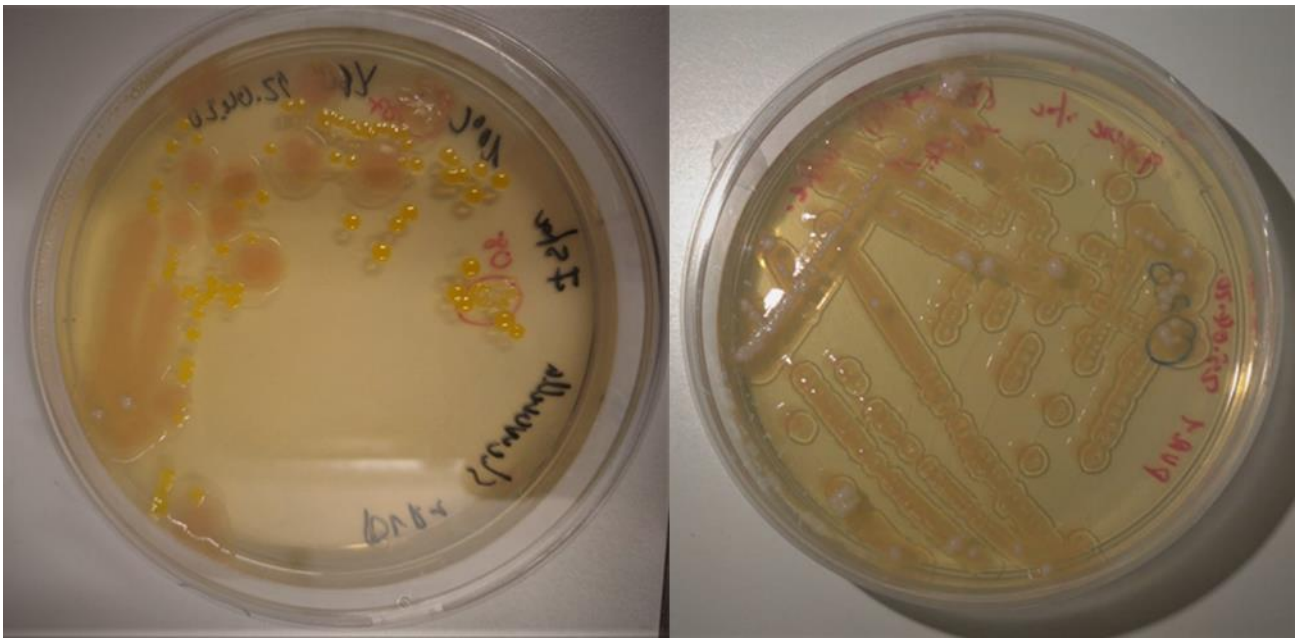

S14. Left: Non-axenic glycerol stock streaked on DVR1 agar displaying three morphologically different bacteria. Through 16S rRNA sequencing the colonies were shown to be *Leifsonia* sp. (yellow colonies), *Shewanella* (pink colonies) and *Serratia* sp. (white colonies). Right: Streak-out of liquid culture (3 days) started by the non-axenic glycerol stock showed *Serratia* sp. (white colonies) growing on top of the *Shewanella* sp. (light pink colonies).

S15. Consensus sequence of *Shewanella* sp.

Multiple sequences of forward and reverse reads were assembled, and the assembly was manually corrected where this was possible. The consensus sequence was used to conduct a Nucleotide BLAST with the nucleotide collection (nr/nt) database, excluding uncultured/environmental sample sequences was conducted giving exclusively hits for *Shewanella* sp. bacteria. The best match (date 20.05.20) was *Shewanella* sp. strain DZ-02-04-aga 16S ribosomal RNA gene, partial sequence (Accession number MK577329), with 100% identity.

>Shewanella_consensus
TGCAGTCGAGCGGTAACACAAGGGAGCTTGCTCCTGAGGTGACGAGCGGCGGACGGGTGAGTAATGCCTAG
GGATCTGCCCAGTCGAGGGGGATAACAGTTGGAAACGACTGCTAATACCGCATACGCCCTACGGGGGAAAGG
AGGGGACCTTCGGGCCTTCCGCGATTGGATGAACCTAGGTGGGATTAGCTAGTTGGTGAGGTAATGGCTCAC
CAAGGCGACGATCCCTAGCTGTTCTGAGAGGATGATCAGCCACACTGGGACTGAGACACGGCCCAGACTCCTA
CGGGAGGCAGCAGTGGGGAATATTGCACAATGGGGGAAACCCTGATGCAGCCATGCCGCGTGTGTGAAGAA
GGCCTTCGGGTTGTAAAGCACTTTCAGTAGGGAGGAAAGGTAGCGTGTTAATAGCACGTTACTGTGACGTTAC
CTACAGAAGAAGGACCGGCTAACTCCGTGCCAGCAGCCGCGGTAATACGGAGGGTCCGAGCGTTAATCGGAA
TTACTGGGCGTAAAGCGTGCGCAGGCGGTTTGTTAAGCCAGATGTGAAATCCCCGGGCTCAACCTGGGAATTG
CATTTGGAACTGGCGAACTAGAGTCTTGTAGAGGGGGGTAGAATTCCAGGTGTAGCGGTGAAATGCGTAGAT
ATCTGGAGGAATACCGGTGGCGAAGGCGGCCCCCTGGACAAAGACTGACGCTCATGCACGAAAGCGTGGGG
AGCAAACAGGATTAGATACCCTGGTAGTCCACGCCGTAAACGATGTCTACTCGGAGTTTGGTGACTTAGTCAC
TGGGCTCCCAAGCTAACGCATTAAGTAGACCGCCTGGGGAGTACGGCCGCAAGGTTAAAACTCAAATGAATTG
ACGGGGGCCCGCACAAGCGGTGGAGCATGTGGTTTAATTCGATGCAACGCGAAGAACCTTACCTACTCTTGAC

ATCCACAGAAGAGACCAGAGATGGACTTGTGCCTTCGGGAACTGTGAGACAGGTGCTGCATGGCTGTCGTCA
GCTCGTGTTGTGAAATGTTGGGTTAAGTCCCGCAACGAGCGCAACCCCTATCCTTATTTGCCAGCACGTAATGG
TGGGAACTCTAGGGAGACTGCCGGTGATAAACCGGAGGAAGGTGGGGACGACGTCAAGTCATCATGGCCCTT
ACGAGTAGGGCTACACACGTGCTACAATGGCGTATACAGAGGGTTGCAAAGCCGCGAGGTGGAGCTAATCTC
ACAAAGTACGTCGTAGTCCGGATCGGAGTCTGCAACTCGACTCCGTGAAGTCGGAATCGCTAGTAATCGTGGA
TCAGAATGCCACGGTGAATACGTTCCCGGGCCTTGTACACACCGCCCGTCACACCATGGGAGTGGGCTGCAAA
AGAAGTGGGTAGTTTAACCTTCGGGAGAACGCTC

S16. Consensus sequence of *Serratia* sp.

Multiple sequences of forward and reverse reads were assembled, and the assembly was manually corrected where this was possible. The consensus sequence was used to conduct a Nucleotide BLAST with the nucleotide collection (nr/nt) database, excluding uncultured/environmental sample sequences was conducted giving exclusively hits for *Serratia* sp. bacteria. The best match (date 20.05.20) was *Serratia plymuthica* PRI-2C chromosome, complete genome (Accession number CP015613), with 100% identity.

>Serratia_consensus
AAGCGCCCTCCCGAAGGTTAAGCTACCTACTTCTTTTGCAACCCACTCCCATGGTGTGACGGGCGGTGTGTACA
AGGCCCGGGAACGTATTCACCGTAGCATTCTGATCTACGATTACTAGCGATTCCGACTTCATGGAGTCGAGTTG
CAGACTCCAATCCGGACTACGACGTACTTTATGAGGTCCGCTTGCTCTCGCGAGTTCGCTTCTCTTTGTATACGC
CATTGTAGCACGTGTGTAGCCCTACTCGTAAGGGCCATGATGACTTGACGTCATCCCCACCTTCCTCCGGTTTAT
CACCGGCAGTCTCCTTTGAGTTCCCGACCGAATCGCTGGCAACAAAGGATAAGGGTTGCGCTCGTTGCGGGAC
TTAACCCAACATTTCACAACACGAGCTGACGACAGCCATGCAGCACCTGTCTCAGAGTTCCCGAAGGCACTAA
GCTATCTCTAGCGAATTCTCTGGATGTCAAGAGTAGGTAAGGTTCTTCGCGTTGCATCGAATTAAACCACATGC
TCCACCGCTTGTGCGGGCCCCCGTCAATTCATTTGAGTTTTAACCTTGCGGCCGTACTCCCCAGGCGGTCGATTT
AACGCGTTAGCTCCGGAAGCCACGCCTCAAGGGCACAACCTCCAAATCGACATCGTTTACAGCGTGGACTACC
AGGGTATCTAATCCTGTTTGCTCCCCACGCTTTCGCACCTGAGCGTCAGTCTTTGTCCAGGGGGCCGCCTTCGC
CACCGGTATTCCTCCAGATCTCTACGCATTTCACCGCTACACCTGGAATTCTACCCCCCTCTACAAGACTCTAGC
TTGCCAGTTTCAAATGCAGTTCCCACGTTAAGCGCGGGGATTTCACATCTGACTTAACAAACCGCCTGCGTGCG
CTTTACGCCCAGTAATTCCGATTAACGCTTGCACCCTCCGTATTACCGCGGCTGCTGGCACGGAGTTAGCCGGT
GCTTCTTCTGCGAGTAACGTCAATGCAATGTGCTATTAACACATTACCCTTCCTCCTCGCTGAAAGTGCTTTACA
ACCCTAAGGCCTTCTTCACACACGCGGCATGGCTGCATCAGGCTTGCGCCCATTGTGCAATATTCCCCACTGCT
GCCTCCCGTAGGAGTCTGGACCGTGTCTCAGTTCCAGTGTGGCTGGTCATCCTCTCAGACCAGCTAGGGATCGT
CGCCTAGGTGAGCCATTACCCCACCTACTAGCTAATCCCATCTGGGCACATCTGATGGCGTGAGGCCCGAAGG
TCCCCCACTTTGGTCCGTAGACGTTATGCGGTATTAGCTACCGTTTCCAGTAGTTATCCCCCTCCATCAGGCAGT
TTCCCAGACATTACTCACCCGTCCGCCGCTCGTCACCCAGAGAGCAAGCTCTCCTGTGCTACCGCTCGACTTGC
AT

S17. Consensus sequence of *Leifsonia* sp.

Multiple sequences of forward and reverse reads were assembled, and the assembly was manually corrected where this was possible. The consensus sequence was used to conduct a Nucleotide BLAST with the nucleotide collection (nr/nt) database, excluding uncultured/environmental sample sequences was conducted giving hits for bacteria of different genera, mainly *Salinibacterium* sp., *Leifsonia* sp., *Agreia* sp., and other un-identified bacteria of marine origin and Actinobacteria, all with % identity above 99%. The best hit (date 20.05.20) was surprisingly found to be *Pseudomonas* sp. AW15 16S ribosomal RNA gene, partial sequence (Accession number FJ362501, 99.93% identity), but the identity

of this sequence is questionable as it has no hits for other *Pseudomonas* sp. through BLAST. The second best hit for our sequence was for *Salinibacterium* sp. strain DZ-02-03-aga 16S ribosomal RNA gene, partial sequence (Accession number MK577334, 99.86% identity).

>Leifsonia_consensus
TGCAGTCGAACGATGAAGCTGGAGCTTGCTCTGGTGGATTAGTGGCGAACGGGTGAGTAACACGTGAGTAAC
CTGCCCTTGACTCTGGAATAAGCGTTGGAAACGACGTCTAATACCGGATACGAGCTTCCGCCGCATGGTGAGG
AGCTGGAAAGAATTTCGGTCAAGGATGGACTCGCGGCCTATCAGGTAGTTGGTGAGGTAATGGCTCACCAAG
CCTACGACGGGTAGCCGGCCTGAGAGGGTGACCGGCCACACTGGAACTGAGACACGGTCCAGACTCCTACGG
GAGGCAGCAGTGGGGAATATTGCACAATGGGCGCAAGCCTGATGCAGCAACGCCGCGTGAGGGACGACGGC
CTTCGGGTTGTAAACCTCTTTTAGTAGGGAAGAAGCGAAAGTGACGGTACCTGCAGAAAAAGCACCGGCTAAC
TACGTGCCAGCAGCCGCGGTAATACGTAGGGTGCAAGCGTTATCCGGAATTATTGGGCGTAAAGAGCTCGTA
GGCGGTTTGTCGCGTCTGCTGTGAAAACTGGGGGCTCAACCCCCAGCCTGCAGTGGGTACGGGCAGACTAGA
GTGCGGTAGGGGAGATTGGAATTCCTGGTGTAGCGGTGGAATGCGCAGATATCAGGAGGAACACCAATGGC
GAAGGCAGATCTCTGGGCCGTTACTGACGCTGAGGAGCGAAAGCATGGGGAGCGAACAGGATTAGATACCCT
GGTAGTCCATGCCGTAAACGTTGGGAACTAGATGTAGGGGCCATTCCACGGTTTCTGTGTCGCAGCTAACGCA
TTAAGTTCCCCGCCTGGGGAGTACGGCCGCAAGGCTAAAACTCAAAGGAATTGACGGGGGCCCGCACAAGCG
GCGGAGCATGCGGATTAATTCGATGCAACGCGAAGAACCTTACCAAGACTTGACATATACGAGAACGGGCTA
GAAATAGTTCACTCTTTGGACACTCGTAAACAGGTGGTGCATGGTTGTCGTCAGCTCGTGTCGTGAGATGTTG
GGTTAAGTCCCGCAACGAGCGCAACCCTCGTTCTTTGTTGCCAGCACGTAATGGTGGGAACTCAAAGGAGACT
GCCGGGGTCAACTCGGAGGAAGGTGGGGATGACGTCAAATCATCATGCCCCTTATGTCTTGGGCTTCACGCAT
GCTACAATGGCCGATACAAAGGGCTGCAATACCGCGAGGTAGAGCGAATCCCAAAAAGTCGGTCTCAGTTCG
GATTGAGGTCTGCAACTCGACCTCATGAAGTCGGAGTCGCTAGTAATCGCAGATCAGCAACGCTGCGGTGAAT
ACGTTCCCGGGCCTTGTACACACCGCCCGTCAAGTCATGAAAGTCGGTAACACCCGAAGCCAGTGGCCTAACC
CGCAAG

Paper III

New suomilides isolated from *Nostoc* sp. KVJ20, bioactivity and biosynthesis

Yannik K.-H. Schneider [1,*], Anton Liaimer [2], Johan Isaksson [3], Kine Ø. Hansen [1], Jeanette Hammer Andersen [1] and Espen H. Hansen [1].

[1)] Marbio, Faculty for Fisheries, Biosciences and Economy, UiT—The Arctic University of Norway, Breivika, N-9037 Tromsø, Norway.

[2)] Department of Arctic and Marine Biology, Faculty for Fisheries, Biosciences and Economy, UiT—The Arctic University of Norway, Breivika, N-9037 Tromsø, Norway.

[3)] Department of Chemistry, Faculty of Natural Sciences, UiT—The Arctic University of Norway, Breivika, N-9037 Tromsø, Norway.

ABSTRACT

Suomilide and the banyasides are highly modified and functionalized non-ribosomal peptides produced by cyanobacteria of the order Nostocales, which have structural similarities to glycosylated aeruginosins, the aeruginosides. Their common structural feature is the complex azabicyclononane core, previously assumed to be derived from the amino acid tyrosine. In these compounds, the azabicyclononane core is functionalized with lipoglycosyl and decorated with sulfate groups, making them chemically complex secondary metabolites. In our study we were able to identify, isolate and determine the structure of two new suomilides, named suomilide B and C (**1** and **2**). In addition, two compounds, suspected of being a new suomilide variant (S-1006, **3**) and the previously reported compound suomilide (**4**), were isolated, but their structures were not characterized. Compounds **1** – **4** were assayed for protease inhibition, anti-proliferative, anti-biofilm and anti-bacterial activities. No bioactivity was found, leaving the question of the biological role of the suomilides open. The sequenced genome of the producer organism *Nostoc* sp. KVJ20 enabled us to propose a biosynthetic gene cluster for suomilides. This was the first genomic investigation of a biosynthetic machinery for this group of structurally distinct cyanobacterial secondary metabolites. Our findings indicated that the azabizyclonoinane-core of the suomilides is derived from prepenate and incorporated by a proline specific NRPS-unit.

INTRODUCTION

Cyanobacteria are well known for being prolific producers of a broad range of bioactive secondary metabolites, some of which are unique to cyanobacteria [1]. Some cyanobacteria have been recognized for the toxins they produce, which are capable of causing severe intoxications in humans and animals [2]. One of the most prominent group of such toxins is the microcystins, a group of phosphatase inhibitors, which are problematic when they enter drinking water supplies during dense cyanobacterial blooms [3]. The diverse and big group of cyanobacterial secondary metabolites are products of a range of biosynthetic machineries such as non-ribosomal peptide synthetases (NRPS) and polyketide synthases (PKS), but there are also peptides that are synthesized ribosomal and modified posttranslationally [4]. For the investigation of the biosynthesis of those metabolites, genome mining tools have been extensively used in the field of cyanobacterial natural products [5]. A very powerful strategy to identify new secondary metabolites and their biosynthetic pathways is the combination of mass spectrometry and genomic studies [6].

In 1997, a new glycoside was isolated from an isolate of the non-toxic cyanobacterium *Nodularia spumigena*. The structure of the compound was elucidated and named suomilide (**4**, Figure 1) [7], but its bioactivity was not investigated. In 2005, two compounds with high similarity to suomilide, banyaside A and B (**5** and **6**, Figure 1), were isolated from a bloom of the cyanobacterium *Nostoc* sp. [8]. When comparing the aglycon of **4** to the aglycon of **5** and **6**, they differ in one amino acid residue; leucine in **5** and **6** and isoleucine in **4**. The conformation of the leucine has been shown to be D in **5** and **6**, while the confirmation was not confirmed for the isoleucine in **4** [7,8]. Compounds **5** and **6** differ between themselves in the modification of the glucose unit, consisting of α-glucose, esterified with hexanoic acid, where **5** is esterified with carbamic acid (Figure 1).

Beside the production of secondary metabolites, cyanobacteria have the capability of atmospheric nitrogen fixation. This feature is utilized by several land plants, ranging from mosses to angiosperms, which developed the ability to attract diazotrophic *Nostoc* as their symbiotic partners [10]. In 2016 Liaimer *et al*. conducted a study where a number of diverse *Nostoc* sp. strains were isolated from the symbiotic organs of the liverwort *Blasia pusilla* found at two different habitats in northern Norway, among which an isolate called *Nostoc* sp. KVJ20 was isolated [11]. Mass spectrometric analysis of extracts from KVJ20 cultures indicated that they contained previously undescribed banyaside and suomilide like (bsl) molecules.

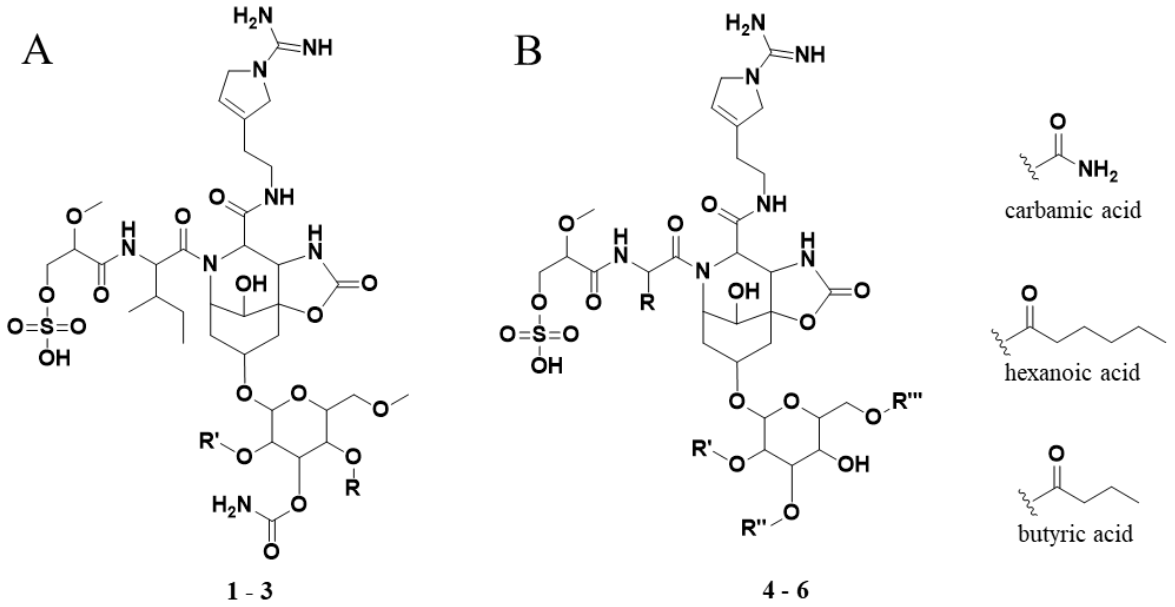

1: R= hexanoic acid, R'= butyric acid
2: R= -H, R'= butyric acid
3: R= hexanoic acid, R'= -H

4: R= isoleucine, R'= hexanoic acid , R''= -H, R'''= hexanoic acid
5: R= leucine, R'= hexanoic acid, R''= carbamic acid, R'''= -H
6: R= leucine, R'= -H, R''= -H. R'''= hexanoic acid

***Figure 1**: A) Structures of suomilide B (**1**), suomilide C (**2**) and S-1006 (**3**). The structures of **1** and **2** were determined using NMR. The structure of **3** is proposed based on HR-MS and NMR analysis. B) The previously isolated molecules suomilide (**4**), banyaside A (**5**) and banyaside B (**6**). All molecules have in common their Abn (azobicyclononane) core and Aeap (1-amino-2-(N-amidino-Δ^3-pyrrolinyl)ethyl), which also can be observed in the aeruginosins, similar to leucine and glycosylation [9]. Suomilide differs from the banyasides by incorporation of isoleucine instead of leucine. The banyasides among themselves differ in the modification of their glycon (α-glucose for **4**, **5** and **6**).*

The crude extracts of KVJ20 showed anti-proliferative activity against a human melanoma cell line (A2058) and a human lung fibroblast cell line (MRC5) [11]. These observations nominated the extract for chemical investigation, which in turn led to the isolation of four bsl compounds. The draft genome of KVJ20 was published in 2019 [12], and enabled us to combine chemical analyses of the culture extracts with genome mining for the possible biosynthetic gene clusters.

In this study, we present the chemical and biological characterization of two novel suomilide-like compounds, suomilide B (**1**) and C (**2**). In addition, the biological characterization of one presumed novel suomilide-like compound, S-1006 (**3**) and S-1047 (**4**), which is presumed to be identical to the previously reported suomilide, is described. The structures of **3** and **4** could not be determined based on our currently available NMR datasets. In addition, we investigated the bsl gene cluster coding for biosynthetic enzymes involved in the suomilide biosynthesis.

RESULTS AND DISCUSSION

Compound Identification and Dereplication

Investigation of a methanol-water extract of KVJ20 cells using UHPLC-IMS-MS led to the identification of four compounds with fragments at *m/z* 610.3206 (in ESI+). This mass is identical to the aglycon of **4**, **5** and **6** since they are structural isomers (Figure 1), after neutral loss of sulphur and its sugar moiety, which indicates that the compounds belong to the bsl family of molecules [8]. The tentative identification of the new compounds structural relationship to the banyasides was supported by comparing their herein obtained MS spectra to the published MS spectrum of synthetic **6** [13]. Signals of a neutral loss of 80 u (in ESI+) indicated that the molecules were carrying a sulfate group (Figure S1). The supernatant of the bacterial cultures were analyzed for the presence of the compounds described above, but none of them were detected, indicating that they were not excreted by the cells to the growth medium. In addition to the above mentioned compounds, dereplication of the cyanobacterial extract gave a hit in the ChemSpider database for elemental composition and one common fragment of the anabeanopeptin-like cyclic peptide schizopeptin *m/z* 792.46506 $[M+H]^+$ (calc. *m/z* 792.46599, for the elemental comp. $C_{42}H_{62}N_7O_8$, one fragment hit at *m/z* 631.380 (Figure S2) [14]. Schizopeptin has not been reported for this strain previously, and its presence is in accordance to the genomic data [12]. As schizopeptin is well described in literature, the peptide was not selected for isolation.

Isolation of **1** - **4**

Isolation of **1** - **4** was done using mass guided preparative HPLC in two campaigns. Each campaign was using the extract of a 5 L cyanobacterial culture (yielding 12.5 g and 16.9 g dry mass of cells, respectively). The compounds where isolated using mass triggered fractionation. For the first isolation step, the compounds were separated using a Sunfire C18 reversed phase column. The collected fractions were reduced to dryness at 40°C *in vacuo*. The fractions were dissolved in DMSO and methanol (**1** dissolved poorly in methanol, but well in DMSO after extensive shaking, **2** - **4** dissolved well in methanol), and separated in a second step using a fluoro-phenyl reversed phase column. The yields were: **1**: 3.7 mg; **2**: 4.1 mg; **3**: 5.9 mg; **4**: 2.6 mg.

Structure Elucidation

Suomilide B (**1**) (Figure 1) was isolated as white crystalline substance. The molecular formula was calculated to be $C_{45}H_{72}N_8O_{20}S$ by HRESIMS, suggesting a presence of 14 degrees of unsaturation. 1D (^{1}H and ^{13}C, Table 1, Figure S4 and S5) and 2D NMR (HSQC, HMBC, COSY, ROESY, Figure S6 – S8) results resembled those reported for **4** and allowed seven substructures of **1** to be assigned. The substructures were isoleucine (Ile), 1-amidino-3-(2-aminoethyl)-3-pyrroline (Aaep), azabicyclononane (Aza), glycolipid with a methylated glucose core decorated with the subunits butyric acid (BA), carbamic acid (CA) and hexanoic acid (HA) (Figure 2, Table 1). An additional substructure, 2-O-methylglyceric acid 3-O-sulfate (MgS), was partially assign and later added a sulfate group at C-1 based on elimination of every other possible binding site for the group (Figure 2).

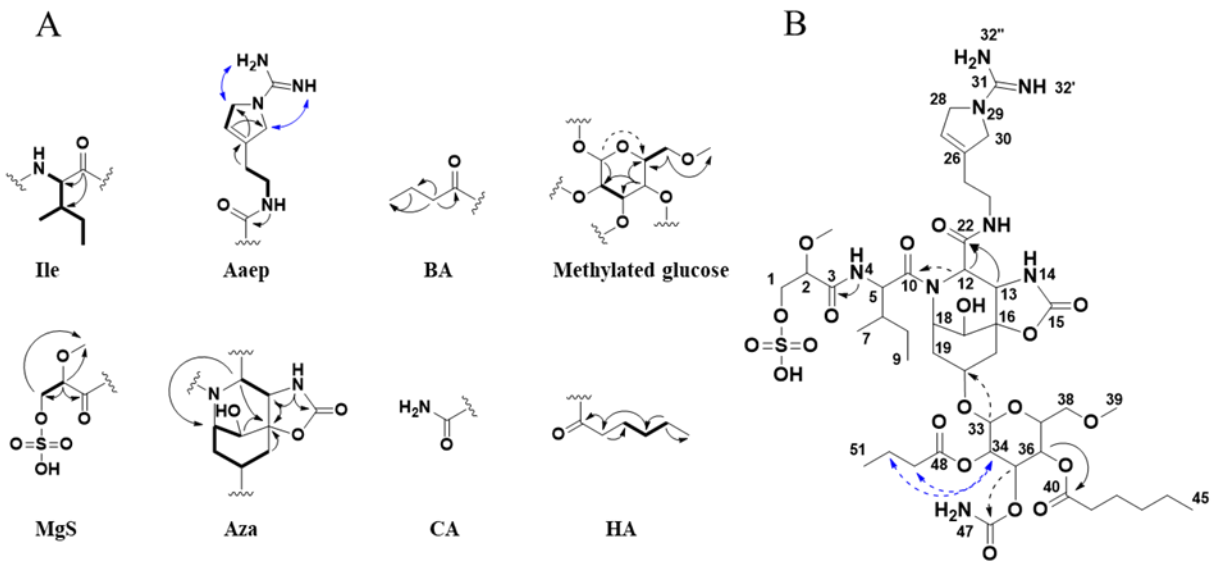

***Figure 2**: A) Selected 2D NMR correlations obtained for substructures of **1**. B) Key 2D NMR correlations used to connect the substructures and elucidate the complete structure of **1**. HMBC (black arrows), COSY (bold), ROESY (blue arrows), Mgs: 2-O-methylglyceric acid 3-O-sulfate, Aaep: 1-amidino-3-(2-aminoethyl)-3-pyrroline, BA: butyric acid, MgS: 2-O-methylglyceric acid 3-O-sulfate, Aza: azabicyclononane, CA: carbamic acid and HA: hexanoic acid. Weak correlations are indicated with dashed arrows.*

The Aza substructure was assigned based on COSY and HMBC correlations, and by comparing our data to previously published data [7]. A COSY spin system was observed from H-17 (δ_H 3.72) to H-21a (δ_H 2.14)/H-21b (δ_H 1.99). The shift value of the tertiary C-17 (δ_C 65.7) placed an –OH group in this position. HMBC correlations furthermore links both H-17 and H-21a to the quaternary C-16 (δ_C 80.5) carbon atom, which was further linked to H-13 (δ_H 4.22) through an HMBC correlation. The downfield shift value of C-16 (δ_C 80.5) suggests that it is linked to

a heteroatom, placing an oxygen in this position. H-13 is linked to H-12 (δ_H 4.52) through a COSY correlation. HMBC correlation was observed between NH-14 (δ_H 7.98) and carbon atoms C-13 (δ_C 58.3) and C-15 (δ_C 156.7). The deschielded shift value of C-15 (δ_C 156.7) is characteristic for a carboxyl carbon, places an oxygen atom at this position, and attaches C-15 to C-16 via an ester linkage. Our 1D NMR data are highly comparable with previously published data for the Aza subunit. When comparing 1D NMR data for protons and carbons 12 to 21 to the same data recorded for suomilide [7], the $\Delta\delta_C$ shift values varies on average 0.11 ppm and $\Delta\delta_H$ shift values varies on average 0.03 ppm (data recorded in d_6-DMSO, Figure S9). This confirmed that **1** had the Aza moiety commonly amongst the bsl family of compounds.

***Table 1**: ^{1}H and ^{13}C NMR Assignments for **1** (^{1}H 600 MHz, ^{13}C 150 MHz, d_6-DMSO).*

	Suomilide B (**1**)			Suomilide B (**1**)	
position	δ_C, type	δ_H (*J* in Hz)	position	δ_C, type	δ_H (*J* in Hz)
1a	66.2, CH_2	3.96 - 3.90, m*	26	135.9, C	
1b		3.76, dt (11.9, 7.7)	27	119.0, CH	5.64, s
2	80.2, CH	3.96 - 3.90, m*	28	55.4, CH	4.17 - 4.11, m*
3	169.8, C		30	54.2, CH	4.17 - 4.11, m*
4		7.94, d (6.9)	31	154.2, C	
5	53.1, CH	4.62, t (6.9)	32'/32"		7.25, s
6	36.5, CH	1.72, m*	33	94.7, CH	4.97, d (3.8)
7	14.5, CH_3	0.92 - 0.83, m*	34	68.0, CH	4.83, dd (11.0, 3.7)
8a	25.4, CH_2	1.29, m*	35	66.6, CH	5.02, dd (11.0, 3.5)
8b		1.19, m	36	68.4, CH	5.34, d (3.3)
9	11.8, CH_3	0.92 - 0.83, m*	37	67.0, CH	4.17 - 4.11, m*
10	171.9, C		38a	70.0, CH_2	3.34, m
12	56.9, CH	4.52, d (2.4)	38b		3.25, dd (10.0, 6.0)
13	58.3, CH	4.22, s	39	58.5, CH_3	3.21, s
14		7.98, s	40	172.0, C	
15	156.7, C		41	33.3, CH_2	2.41 - 2.24, m*
16	80.5, CH		42	24.1, CH_2	1.54, m*
17	65.7, CH	3.72, s*	43	30.6, CH_2	1.28, m*
18	53.4, CH	4.28, s	44	21.8, CH_2	1.28, m*
19a	28.8, CH_2	2.14, d (12.1)	45	13.8, CH_3	0.92 - 0.83, m*
19b		1.72, m*	46	155.4, C	
20	70.0, CH	3.72, m*	47		6.56, s
21a	34.4, CH_2	2.41 - 2.24, m*	48	172.6, C	
21b		1.99, dd (11.1, 5.4)	49	35.3, CH_2	2.41 - 2.24, m*
22	168.8, C		50	18.0, CH_2	1.54, m*
23		7.59, s	51	13.4, CH_3	0.92 - 0.83, m*
24	37.2, CH_2	3.18, m*	2me	57.3, CH_3	3.30, s
25	27.8, CH_2	2.41 - 2.24, m*			

*Peaks are overlapping

The Ile subunit was assigned based on typical proton and carbon chemical shifts and correlations in HMBC and COSY spectra and was found to be attached from C-10 (δ_C 171.9) to position 11 of the Aza subunit through a weak HMBC correlation between H-12 (δ_H 4.52) and C-10 (δ_C 171.9). This places a nitrogen in the 11 position and completes the tricyclic Aza subunit.

The MgS subunit was assigned based on 1D NMR shift values and HMBC and COSY correlations. It was found to be attached to N-4 of the Ile group through an HMBC correlation between NH-4 (δ_H 7.94) and C-3 (δ_C 169.8). A sulfate group at C-1 based on elimination of every other possible binding site for the group.

The glycosyl group of the glycolipid subunit was determined to be methylated glucose based on typical proton and carbon chemical shifts and correlations in HMBC and COSY spectra. The glucose was determined to be methylated through an HMBC correlation between H-38a (δ_H 3.34) and H-38b (δ_H 3.25) and the primary carbon atom C-39 (δ_C 58.5). The glucose subunit was found to be attached through an ether bond to C-20 of the Aza subunit through a weak HMBC correlation between H-33 (δ_H 4.97) and C-20 (δ_C 70.0).

The CA subunit was assigned based on 1D and 2D NMR data and was found to be linked to the glucose subunit through an ester bond determined by a weak HMBC correlation between H-35 (δ_H 5.02) and the quaternary C-46 carbon atom (δ_C 115.4). The HA and BA subunits were identified by correlations in the HMBC and COSY spectra. The HA and BA subunits were linked to the glucose subunit through ester bonds. The HA subunit was placed at C-36-O through an HMBC correlation between H-36 (δ_H 5.34) and C-40 (δ_C 172.9). The BA subunit was found to be linked to C-34 through an ether bond through weak ROESY correlations between H-34 (δ_H 4.83) and the BA protons H-49 (δ_H 2.41 - 2.24) and H-50 (δ_H 1.54). Consequently, the structure of **1** was assigned.

Suomilide C (**2**) (Figure 1) was isolated as white crystalline substance. The molecular formula was calculated to be $C_{39}H_{62}N_8O_{19}S$ by HRESIMS, suggesting a presence of 13 degrees of unsaturation. The mass and elemental composition of **2** indicated that its structure was closely related to that if **1**. By close inspection of 1D (^{1}H, ^{13}C, Table 2, Figure S10 and S11) and 2D (HSQC, HMBC, COSY, TOCSY and ROESY, Figure S12 – S15) NMR data, the structure of **2** was elucidated in a similar manner as described above for **1**. In the ^{13}C spectra, only 22 of the carbon atoms resulted in prominent peaks. The remaining carbon atom shift values were extracted from the HSQC spectra. When comparing the ^{1}H and ^{13}C chemical shift values of **1**

and **2** for the MgS, Ile, Aza, Aaep, CA and BA substructures, the values were found to conform well ($\Delta\delta_C$ average: 0.2 ppm, $\Delta\delta_H$ average: 0.013 ppm). The most noticeable difference between the ^{1}H-NMR datasets of **1** and **2**, was the lack of a proton resonance for H-36 at 5.34 ppm in the ^{1}H spectrum of **2**. Instead, H-36 was found to have a shift value of 3.86 ppm. The shift value of C-36 had also changed from 68.4 ppm in **1** to 66.4 in **2**. The shielding of CH-36 could be explained by elimination of the HA subunit, causing C-36 to be attached to a hydroxyl group rather than an ester, which is the case in **1**. Elimination of HA was in line with the difference in the calculated elemental composition of **1** and **2**. Signals from the HA subunit were however still visible, but were significantly less prominent in the spectra recorded for **2**. This showed that **2** was a variant of **1** lacking the HA substructure, but also indicated that **1** was still present in the sample as a minor component.

***Table 2**: ^{1}H and ^{13}C NMR Assignments for **2** (^{1}H 600 MHz, ^{13}C 150 MHz, d_6-DMSO).*

	Suomilide C (**2**)			Suomilide C (**2**)	
position	δ_C, type	δ_H (*J* in Hz)	position	δ_C, type	δ_H (*J* in Hz)
1a	65.9, CH_2	3.97 - 3.85, m*	23		7.61, s
1b		3.76, dd (11.6, 7.8)	24	36.9, CH_2	3.18, m
2	79.9, CH	3.97 - 3.85, m*	25	27.6, CH_2	2.32 - 2.23, m*
3	169.7, C		26	135.9, C	
4		8.00 - 7.92, m*	27	118.8, CH	5.64, s
5	52.9, CH	4.62, t (7.0)	28	55.4, CH	4.12, m
6	36.3, CH	1.71, m*	30	54.2, CH	4.12, m
7	14.1, CH_3	0.92 - 0.79 (m)*	31	154.0, C	
8a	25.03, CH_2	1.29, m	32'/32"		7.23, s
8b		1.17, m	33	94.6, CH	4.90 - 4.80, m
9	11.5, CH_3	0.92 - 0.79 (m)*	34	68.8, CH	4.90 - 4.80, m
10	171.2, C		35	67.7, CH	4.95, dd (10.7, 3.9)
12	56.6, CH	4.54, m	36	66.4, CH	3.89, m
13	57.9, CH	4.23, m	37	68.7, CH	3.88, m
14		8.00 - 7.92, m*	38a	70.4, CH_2	3.44, m
15	156.7, C		38b		3.38, m
16	80.3, CH		39	58.4, CH_3	3.25, m
17	65.6, CH	3.71, m	46	156.3, C	
18	53.2, CH	4.27, m	47		6.50, s
19a	28.57, CH_2	2.12, d (12.9)	48	172.3, C	
19b		1.71, m*	49	35.2, CH_2	2.32 - 2.23, m*
20	69.1, CH	3.69, m	50	17.8, CH_2	1.53, m
21a	34.4, CH_2	1.96, m	51	14.1, CH3	0.92 - 0.79 (m)*
21b			2me	57.07, CH_3	3.30, s
22	168.7, C				

*Peaks are overlapping

S-1006 (**3**) (proposed structure in Figure 1) was isolated as white crystalline substance. The molecular formula was calculated to be $C_{41}H_{66}N_8O_{19}S$ by HRESIMS, suggesting a presence of 13 degrees of unsaturation. S-1048 (**4**) (believed to be suomilide, Figure 1) was isolated as white crystalline substance. The molecular formula was calculated to be $C_{43}H_{68}N_8O_{20}S$ by HRESIMS, suggesting a presence of 14 degrees of unsaturation. The structures of S-1006 (**3**) and S-1048 (**4**) could be indisputably elucidated using our currently available NMR datasets. However, the datasets show resemblance to those recorded for **1** and **2**, and to previously reported datasets for suomilide. Based on HRMS and NMR data, we therefore presume that the structure of **3** is similar to that of **1** and **2**, lacking the butyric acid substructure which is linked to C-34-O- in **1** and **2**. Furthermore, we speculate that **4** is suomilide as our recorded data are fitting with previously reported HRMS and NMR data for the compound. Further isolation and structure elucidation is in progress.

Biological characterization of **1** - **4**

With the isolated material of **1** – **4** at hand, it was possible to investigate the bioactivity of all four compounds. Since the production of secondary metabolites represents a metabolic and energetic effort, they are likely to give a selective advantage to the producing organism [15] or have a function within the organism. Were therefore tested to see if **1** - **4** had any effect on the survival of bacterial cells, malignant and non-malignant human cells, as well as on bacterial biofilm formation. We also wanted to investigate if the previously observed bioactivity of this strain is related to the isolated suomilides, by assaying the ability of **1** – **4** to act as protease inhibitors. For the bioassays, **1** - **4** were dissolved in DMSO and further diluted in ddH_2O.

Antibacterial and antibiofilm formation activity

There were no significant effects of **1** – **4** when tested at concentrations up to 100 µM against *S. aureus*, *E. coli*, MRSA, *P. aeruginosa*, *E. faecialis* and *S. agalactiae*. There were also no effects on biofilm formation by *S. epidermidis* at concentrations up to 100 µM. Given the results we got from the bacterial bioassays, we conclude that the suomilides do not have an effect on bacterial growth and biofilm formation.

Activity against malignant and non-malignant cell lines

As part of our continuous screening effort to identify bacterial extract with bioactive compounds, the extract of KVJ20 was assayed against three human cell lines. This showed that the extract had anti-proliferative effects on the human non-malignant cell line MRC5 (lung

fibroblast) and the human malignant cell line A2058 (melanoma), but not on the human malignant cell line HT29 (colon carcinoma). Therefore, we further investigated the bioactivity of **1** - **4** against MRC5 and A2058 (Figure 3). Compounds **1** – **4** were furthermore tested for activity against the human malignant cell lines, MOLM13 (acute myeloid leukemia). Compounds **1** - **4** were assayed at concentrations up to 100 µM against all cell lines. While there were no detectable effects on MRC5 and A2058, there was a detectable effect on MOLM13 cells at the highest concentration of 100 µM (Figure 3). The concentration of DMSO at the highest concentration of suomilides was 1.0% (v/v). To investigate the role of DMSO which were as high as 1% at the highest concentration, DMSO controls were included. This might have interfered with the assay results as seen in Figure 4 with larger standard deviations. Apparently, the anti-cancer effect of **2** and **4** have a high standard deviation and varies around the DMSO control. Compounds **1** and **3** have an effect on the proliferation of MOLM13 cells that is higher than the DMSO control. The question remains if the effect is of unspecific nature in combination with DMSO or if a specific effect leads to the observed activity. However, we doom the observed weak effect not to be sufficient for further investigation.

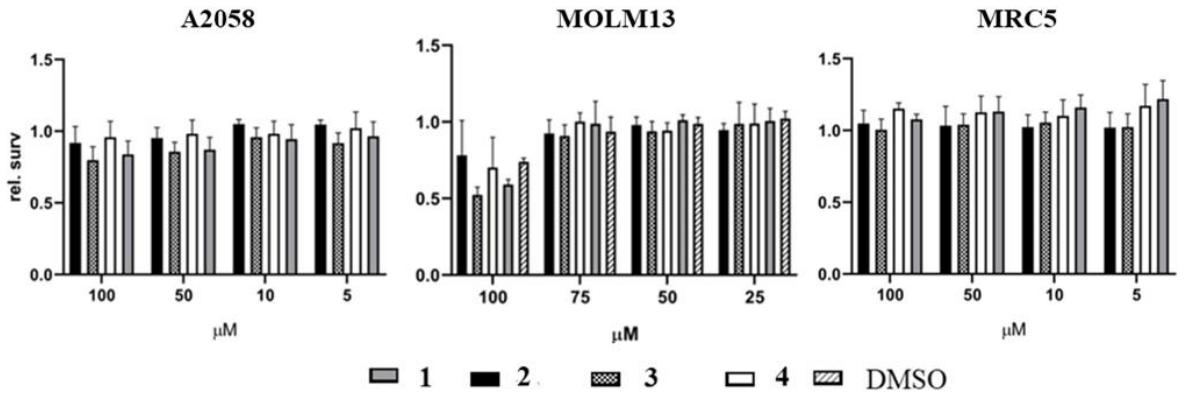

***Figure 3**: Effect of **1** - **4** against the non-malignant human cell line MRC5 (lung fibroblasts) and two human malignant cell lines A2058 (melanoma cell line) and MOLM13 (monocytic leukemia). While A2058 and MRC5 show no sensitivity towards **1** – **4**, MOLM13 were sensitive at 100 µM. The assays were executed in two experiments with three technical replicates each.*

Compounds **5** and **6** were isolated by bioassay guided purification using a serine-protease inhibition assay when discovered in 2005 [8]. The two banyasides were reported to inhibit the catalytic activity of trypsin. Given the high structural similarity between banyasides and suomilides (Figure 1), we tested **1** - **4** in a trypsin inhibition assay, but they showed no activity. As far as we know, the bioactivity of suomilide has not been investigated previously, and the *Nostoc* sp. strain it has been isolated from was reported as non-toxic [7]. This complies with our results, being no activity of **1** - **4** against bacteria or cell lines at high concentrations. Taking

a closer look on the structure of other cyanobacterial protease inhibitors, such as cyanopeptolins, microviridins and others, it appears that they are cyclic peptides in contrast to the rigid modified core of the suomilides and banyasides [16-19]. This leaves the question of the biological function and potential bioactivity of suomilides unanswered. Recently the detection of bsl compounds in a chemotyping study employing mass spectrometry of *Nostoc* like isolates from Hungarian grasslands has been reported [20]. The geographic spread of cyanobacteria capable of producing bsl compounds and glycosylated aeruginosines gives further motivation to investigate those molecules and reveal their biological function.

Biosynthesis of the Suomilides

A previous study predicted 19 gene clusters in KVJ20 containing genes involved in the biosynthesis of nonribosomal peptides, polyketides, and ribosomally synthesized and posttranslationally modified peptides [12]. In addition to well defined anabaenopeptin and nostocyclopeptide gene clusters, we were able to identify genes associated with aeruginosin production and assemble the entire bsl gene cluster. The reassembled bsl cluster can be retrieved under the gene bank accession number: MT269816 (Figure 4). The cluster consists predominantly of genes that are also present in aeruginosin and saxitoxin gene clusters. For aeruginosin, the most similar clusters are aeruginosin 126B (BGC0000297) where 41% of the genes show similarity and aeruginosin 98-A (BGC0000298, 42% of genes show similarity).

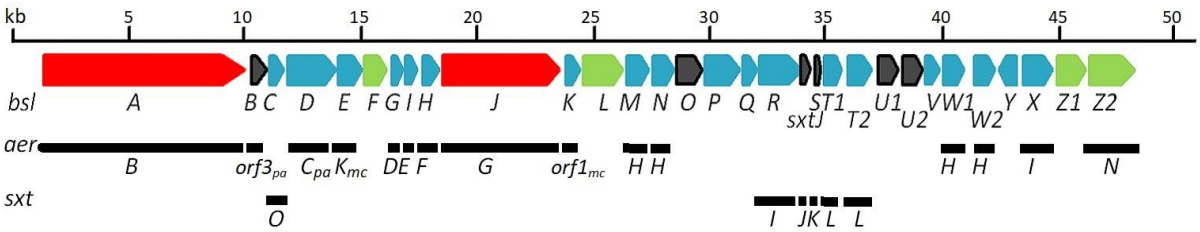

***Figure 4**: bsl-biosynthetic cluster proposed for suomilides: At the top the bsl-gene cluster. Below the indication of which genes are similar to those in the respective gene clusters of aeruginosin (aer) and saxitoxin (sxt). A detailed description is given in Table 3. NRPS genes are given in red, other biosynthetic genes in blue and transporters/transport related genes in green. Open reading frames/hypothetical genes are coloured black.*

For the saxitoxin the clusters BGC0000887, BGC0000188 and BGC0000928 show a similarity of 14%. The genes and the respective cluster they are originating from are given in Table 3 and illustrated in Figure 5. We propose the cluster described in this article (Figure 4 and Table 3) is the biosynthetic cluster producing the suomilides. The proposed functions for the respective genes are given in Table 3.

***Table 3**: Genes of the identified bsl-cluster.*

Gene name	Predicted function / protein family	(Strand) ORF start:stop	BLAST match / % identity	Homology to known genes / compound /organism / notes	Proposed function	Ref.
bslA	D-Ile specific NRPS	(+) 1373:10153	WP_146110921 *Nostoc* sp. *'Peltigera membranacea* cyanobiont' N6 / 88%	*aerB* / aeruginosine / *M. aeruginosa*, *P. agardhii*	Incorporation of D-Ile	[9,22]
bslB	Hypothetical	(+) 10244:11068	WP_162397141 *Nostoc* sp. B(2019) / 92%	*orf3* / aeruginosine / *P. agardhii*	unknown	[9]
bslC	Adenylylsulfate kinase	(+) 11221:11799	WP_169266147 *Brasilonema octagenarum* / 91%	*sxtO* / saxitoxin / *Dolichospermum circinale*	sulfatation	[23]
bslD	Oxidoreductase/ Ferredoxin	(+) 11821:13986	WP_094328884 *Nostoc* sp. '*Peltigera membranacea* cyanobiont' 213 / 87%	*aerC* /aeruginosine / *M. aeruginosa*, *P. agardhii*	electron transfer	[9,22]
bslE	type 2 isopentenyl-diphosphate Delta-isomerase	(+) 13983:15038	WP_096564146 *Scytonema* sp. NIES-4073 / 95%	*aerK* / aeruginosine / *M. aeruginosa*	DMAPP synthesis	[21,22]
bslF	DMT family transporter	(+) 15071:15973	WP_162397144 *Nostoc* sp. B(2019)/ 90%		Transporter	
bslG	Dehydration and decarboxylation of prephenate, BacA	(+) 16026:16634	AVH65362 *Nostoc* sp. *'Peltigera membranacea* cyanobiont' N6 / 93%	*aerD* / aeruginosine / *M. aeruginosa*, *P. agardhii*	Dehydration and decarboxylation of prephenate	[9,21,22]
bslI	cupin domain-containing protein, BacB	(+) 16627:17334	WP_094328882 *Nostoc* sp. '*Peltigera membranacea* cyanobiont' 213	*aerE* / aeruginosine / *M. aeruginosa*, *P. agardhii*	Epoxylation ?	[9,22]
bslH	SDR family oxidoreductase	(+) 17348:18142	WP_162397147 *Nostoc* sp. B(2019)/ 89%	*aerF / aeruginosine / M. aeruginosa*, *P. agardhii*	Oxidation of OH	[9,22]
bslJ	Pro specific NRPS	(+) 18206:23224	WP_104900371 *Nostoc* sp. *'Peltigera membranacea* cyanobiont' N6 / 88%	*aerG / aeruginosine / M. aeruginosa*, *P. agardhii*	Incorporation of Abn	[9,22]
bslK	SDR family oxidoreductase	(+) 23472:24248	WP_094328879 *Nostoc* sp. '*Peltigera membranacea* cyanobiont' 213 / 93%	Orf1 / aeruginosine / *M. aeruginosa*	Oxidation of OH	[22]
bslL	ABC transporter substrate-binding protein	(+) 24281:26077	WP_096564141 *Scytonema* sp. NIES-4073 / 88%		transporter	
bslM	isopenicillin N synthase family oxygenase	(+) 26228:27190	WP_104900374 *Nostoc* sp. *'Peltigera membranacea* cyanobiont' N6 / 92%	*aerH / aeruginosine / M. aeruginosa*, *P. agardhii*	unknown	[9,22]
bslN	isopenicillin N synthase family oxygenase	(+) 27228:28220	WP_162397152 *Nostoc* sp. B(2019)/ 85%	*aerH / aeruginosine / M. aeruginosa*, *P. agardhii*	unknown	[9,22]
bslO	Hypothetical	(+) 28286:29443	AVH65370 *Nostoc* sp. *'Peltigera membranacea* cyanobiont' N6 / 93% OYD97159 *Nostoc* sp. '*Peltigera membranacea* cyanobiont' 213 / 93%		unknown	
bslP	D-alanyl-lipoteichoic acid acyltransferase DltB, MBOAT superfamily	(+) 29495:31012	AVH65371 *Nostoc* sp. *'Peltigera membranacea* cyanobiont' N6 / 93%		acetyltransferase	

			OYD97158 *Nostoc* sp. '*Peltigera membranacea* cyanobiont' 213 / 93%			
bslQ	SAM-dependent methyltransferase	(+) 31040:31762	WP_094328873 *Nostoc* sp. '*Peltigera membranacea* cyanobiont' 213 / 91%		Methyltransferase	
bslR	Carbamoyltransferase	(+) 31810:33648	WP_094328872 *Nostoc* sp. '*Peltigera membranacea* cyanobiont' 213 / 97%	*sxtI* / saxitoxin / *Dolichospermum circinale*	carbamoylation	[23]
sxtJ		(+) 33654:34061	WP_162397157 Nostoc sp. B(2019)/ 88%	*sxtJ* / saxitoxin / *Dolichospermum circinale*	unknown	[23]
bslS	hypothetical	(+) 34061:34225	WP_007355070 *Kamptonema* sp. PCC 6506 / 76%	*sxtK* / saxitoxin / *Dolichospermum circinale*	unknown	[23]
bslT1	SGNH/GDSL hydrolase	(+) 34641:35552	WP_162397158 Nostoc sp. B(2019)/ 83%	*sxtL* / saxitoxin / *Dolichospermum circinale*	hydrolase	[23]
bslT2	SGNH/GDSL hydrolase	(+) 35634:36758	WP_096564131 Scytonema sp. NIES-4073 / 91%	*sxtL* / saxitoxin / *Dolichospermum circinale*	hydrolase	[23]
bslU1	Hypothetical	(+) 36891:37856	WP_096564130 Scytonema sp. NIES-4073 / 87%	Annotated as carbohydrate – binding protein in other annotated genomes	carbohydrate binding protein ?	
bslU2	Hypothetical	(+) 37961:38860	AVH65379 *Nostoc* sp. '*Peltigera membranacea* cyanobiont' N6 / 87% OYD97151 *Nostoc* sp. '*Peltigera membranacea* cyanobiont' 213 / 87%	Annotated as carbohydrate – binding protein in other annotated genomes	carbohydrate binding protein ?	
bslV	radical SAM protein	(+) 38930:39610	WP_171978128 Brasilonema / 95%		methylation or sulphur activation	
bslW1	isopenicillin N synthase family oxygenase	(+) 39713:40720	AVH65381 *Nostoc* sp. '*Peltigera membranacea* cyanobiont' N6 / 93% OYD97149 *Nostoc* sp. '*Peltigera membranacea* cyanobiont' 213 / 93%	*aerH* / *aeruginosine* / *M. aeruginosa*, *P. agardhii*	unknown	[9,22]
bslW2	isopenicillin N synthase family oxygenase	(+) 41045:42028	OYD97148 *Nostoc* sp. '*Peltigera membranacea* cyanobiont' 213 / 93%	*aerH* / *aeruginosine* / *M. aeruginosa*, *P. agardhii*	unknown	[9,22]
bslY	aldo/keto reductase	(-) 42143:42976	AVH65383 *Nostoc* sp. '*Peltigera membranacea* cyanobiont' N6 / 94% OYD97147 *Nostoc* sp. '*Peltigera membranacea* cyanobiont' 213 / 94%		hydration of DB/ reduction of OH	
bslX	glycosyltransferase family 4 protein	(+) 43181:44470	AVH65384 *Nostoc* sp. '*Peltigera membranacea* cyanobiont' N6 / 94%	*aerI* / *aeruginosine* / *P. agardhii*	glycosylation	[9]
bslZ1	MFS transporter	(+) 44638:45984	WP_096570964 *Scytonema* sp. NIES-4073 / 89%		transporter	
bslZ2	ABC transporter, similar to anabaenopeptin transporters	(+) 46051:48060	WP_162397169 Nostoc sp. B(2019)/ 83%	*aerN* / *aeruginosin* / *M. aeruginosa* / *P. agardhii*	transporter	[22]

For the banyasides, the biosynthesis of the Abn moiety was proposed to start from L-tyrosine [8]. The present cluster, however, possesses prephenate decarboxylase (*bslG*). This indicates that the biosynthesis of Abn is starting from prephenate instead of tyrosine. We propose therefore an alternative biosynthesis starting from prephenate, given in Figure 5. The biosynthesis of secondary metabolites from prepenate, employing prepenate decarboxylases, has been observed for bacilysin, salinosporamide A and aeruginoside 126A as well [21]. The gene *bslJ* is coding a NRPS subunit predicted to incorporate isoleucine which is apparently present in the suomilides. However *bslA* is predicted to code for a NRPS incorporating proline, we hypotesize that the NRPS-subunit is binding the azabizyclononane moiety (Figure 5, **VII**) due to its structural similarity to proline. The proposed cluster and its genes can be related to the structural properties of suomilides.

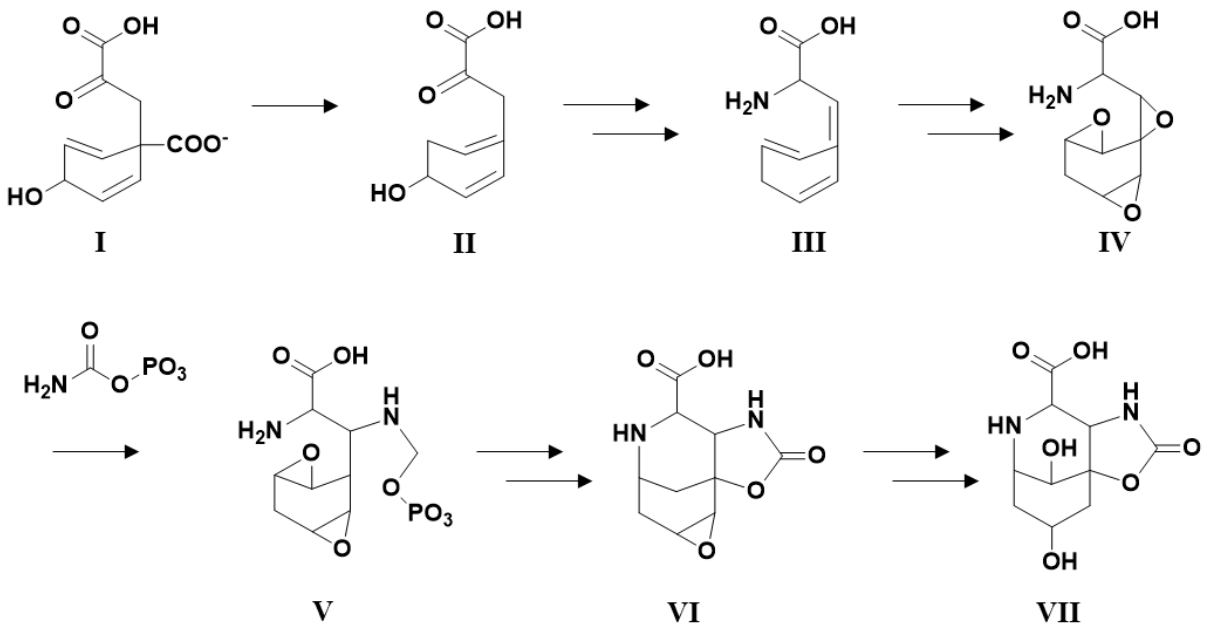

Figure 5*: Proposed biosynthetic pathway for the Abn moiety [8] proposed a biosynthetic pathway starting from tyrosine. Similar to the proposed biosynthesis we proposed biosynthesis starting from prephenate (**I**) instead. The similarity of the azabizyclononane (**VII**) to proline can be imagined, we hypothesize that the peptide bond between **VII** and isoleucine is established via non ribosomal peptide synthesis.*

The suomilides are representing secondary metabolites with significant complexity. Suomilide (putatively the isolated suomilide S-1048(**4**)) was first isolated in 1997 and the new suomilides discovered within this study were tested in a range of bioassays. The question of their biological function is not answered yet but the occurrence of banyaside/suomilide like molecules in

Nostocales and most likely intracellular localization of these gives rise to the assumption that the molecules have an important physiological function yet to be discovered.

CONCLUSIONS

While we were not able to discover the biological role of the suomilides we were able to propose a biosynthetic pathway and assign a biosynthetic cluster which could be valuable for the identification of further suomilides using genomic methods. Further investigation of the suomilides should include assays detecting their effect on animals but also investigations of their effects or function in cyanobacteria seem recommendable since they are not excreted into the media.

EXPERIMENTAL SECTION

UHPLC-HR-MS analysis

UHPLC-HR-MS data for dereplication and structure elucidation was recorded using an Acquity I-class UPLC (Waters, Milford, MA, USA) coupled to a PDA detector and a Vion IMS QToF (Waters). The chromatographic separation was performed using an Acquity C18 UPLC column (1.7 µm, 2.1 mm × 100 mm) (Waters). Mobile phases consisted out of acetonitrile (HiPerSolv, VWR) for mobile phase A and ddH_2O produced by the in-house Milli-Q system as mobile phase B, both containing 1% formic acid (v/v) (33015, Sigma). The gradient was run from 10% to 90% B in 12 min at a flow rate of 0.45 mL/min. Samples were run in ESI+ and ESI- ionization mode. The data was processed and analyzed using UNIFI 1.9.4 (Waters). Calculation of exact ion masses was done by using ChemCalc [24].

Structure Elucidation *via* NMR-Spectroscopy

NMR data of the compounds was recorded on a Bruker Avance III HD spectrometer equipped with an inverse detected TCI probe with cryogenic enhancement on ^{1}H, ^{2}H and ^{13}C. Operating frequencies were 599.90 MHz for ^{1}H and 150.86 MHz for ^{13}C. For taking up the spectra the samples were dissolved in d_6-DMSO and recorded at 298 K. All experiments were recorded using standard pulse sequences for Proton, Presat, Carbon, DQF-COSY, HSQC, HMBC, H2BC, NOESY and ROESY (gradient selected and adiabatic versions, with matched sweeps

where applicable) in Topspin 3.5pl7 and processed in Mnova 12.0.0. The solvent peak of d_6-DMSO was used to reference the spectra.

Origin of Isolate and Genome Sequencing

The isolate originates from 69,64◦ N 18,73◦E, Kvaløya island, Northern Norway and has been termed KVJ20 [11], its draft genome was sequenced and published in 2019 [12].

Cultivation of Cyanobacteria

The subject of investigation, the cyanobacteria *Nostoc* sp. KVJ20 was maintained as described previously [11][25]. The scale up cultures were grown for five weeks in 1 L constantly aerated bottles. The cultures were illuminated with 30 µm/m^2/s using a 36W/77 Osram Fluora light source.

Extraction and Isolation

The cells were harvested by centrifugation, the pellet was freeze dried and sonicated in 100% MeOH, centrifuged again and the methanol supernatant was collected. The pellet was extracted the same way again with 50% MeOH aq. and with 100% ddH_2O, without additional sonification. The extracts were collected and reduced to dryness at 40°C in *vacuo*.

Isolation of the molecules out of the extract was done using a semi preparative HPLC system (Waters) made up by a 600 HPLC pump, a 3100 mass spectrometer, a 2996 photo diode array detector and a 2767 sample manager. For infusion of the eluate and analytes into the mass detector a 515 HPLC pump and a flow splitter were employed. The mobile phases were degassed by an in-line degasser. For controlling the system, the software MassLynx™ 4.1 (Waters) was used. The columns used for isolation were Sunfire RP-18 preparative column (10 µm, 10 mm × 250 mm) and XSelect CSH preparative Fluoro-Phenyl column (5 µm, 10 mm × 250mm), both columns were purchased from Waters. The mobile phases for the gradients were A [ddH2O with 0.1% (v/v) formic acid] and B [acetonitrile with 0.1% (v/v) formic acid], flow rate was set to 6 mL/min. Acetonitrile (Prepsolv®, Merk KGaA, Darmsatdt, Germany) and formic acid (33015, Sigma) were purchased in appropriate quality, ddH2O was produced with the in-house Milli-Q® system. For the MS-detection of the eluting compounds one percent of the flow was split from the fractions in line, blended with 80% Methanol in ddH2O (v/v) acidified with 0.2% Formic acid (Sigma) and directed to the ESI-quadrupole-MS. The fractions

were collected by mass triggered fraction collection and the respective fractions were reduced to dryness under reduced pressure and by vacuum centrifugation, both at 40°C.

*Suomilide B (**1**):* white powder (9.8 mg); UV (ACN:H_2O) λ_{max} 213 nm; ^1H and ^{13}C NMR data in Table 1; HRESIMS *m/z* 1075.4496 $[M - H]^-$ (calcd for $C_{45}H_{71}N_8O_{20}S$, 1075.4510).

*Suomilide C (**2**):* white powder (4.1 mg); UV (ACN:H_2O) λ_{max} 198 nm; ^1H and ^{13}C NMR data in Table 2; HRESIMS *m/z* 977.3781 $[M - H]^-$ (calcd for $C_{39}H_{61}N_8O_{19}S$, 977.3774).

*S-1006 (**3**):* white powder (5.9 mg); UV (ACN:H_2O) λ_{max} 213 nm; HRESIMS *m/z* 1005.4089 $[M - H]^-$ (calcd for $C_{41}H_{65}N_8O_{19}S$, 1005.4087).

*S-1048 (**4**):* white powder (2.6 mg); UV (ACN:H_2O) λ_{max} 217 nm; HRESIMS *m/z* 1047.4171 $[M - H]^-$ (calcd for $C_{43}H_{67}N_8O_{20}S$, 1047.4192).

Investigation of Bioactivity

Protease Inhibition Assay

To test the compounds for their capacity to inhibit proteases, the trypsine digestion of Suc-Ala-Ala-Pro-Phe-pNA in presence of the compounds was measured. Therefore 5 mL of assay solution were prepared out of 500 µL of 1M Tris-HCL (pH 8.0), 500 µL 0.1M $CaCl_2$, 50 µL of 100 mM Suc-Ala-Ala-Pro-Phe-pNA Suc-Ala-Ala-Pro-Phe-pNA (Sigma, S3014) and 3.95 mL of ddH_2O. The reaction was done in microtiter plates ((VWR 734-2073), per well 90 µL of assay solution were mixed with 5 µL of 100 µM suomilides in 10% DMSO (v/v) or PBS buffer as control. The reaction was prepared on ice and 5 µL of Trypsin-solution were added to start the reaction short before starting the photometric measasurement. For quantifying the reaction its product 4-nitroaniline was measured at $\lambda = 410$ nm over 20 min using a Victor™ plate reader (PerkinElmer, Waltham, MA, US) and WorkOut 2.5 (PerkinElmer).

Growth Inhibition Assay

To determine and quantify potential anti-microbial activity, a bacterial growth inhibition assay in liquid media was executed. The samples were tested against *S. aureus* (ATCC 25923), *E. coli* (ATCC 259233), *E. faecialis* (ATCC 29122), *P. aeruginosa* (ATCC 27853), *S. agalactiae* (ATCC 12386) and Methicillin resistant *S. aureus* (MRSA) (ATCC 33591). *S. aureus*, MRSA, *E. coli* and *P. aeruginosa* were grown in Muller Hinton broth (275730, Becton, Dickinson and Company). *E. faecalis* and *S. agalactiae* were cultured in brain hearth infusion broth (53286, Sigma). Fresh bacteria colonies were transferred in the respective medium and incubated at 37 ◦C overnight. The bacterial cultures were diluted to a culture density representing the log phase and 50 µL/well were pipetted into a 96-well microtiter plate (734-2097, Nunclon™, Thermo Scientific, Waltham, MA, USA). The final cell density was 1500–15,000 CFU/well. The compound was diluted in 2% (v/v) DMSO in ddH2O, the final assay concentration was 50% of the prepared sample, since 50 µL of sample in DMSO/water were added to 50 µL bacterial culture. After adding the samples to the plates, they were incubated over night at 37 ◦C and the growth was determined by measuring the optical density at λ = 600 nm (OD600) with a 1420 Multilabel Counter VICTOR3™ (Perkin Elmer, Waltham, MA, USA). A water sample was used as reference control, growth medium without bacteria was used as a negative control and a dilution series of gentamycin (A2712, Merck) from 32 to 0.01 µg/mL was used as positive control and visually inspected for bacterial growth. The positive control was used as system suitability test and the results of the antimicrobial assay were only considered valid when positive control was passed. The final concentration of DMSO in the assays was ≤ 2% (v/v) known to have no effect in the tested bacteria.

Biofilm Inhibition Assay

For testing the inhibition of biofilm formation *Staphylococcus epidermidis* (ATCC 35984) was grown in Tryptic Soy Broth (TSB, 105459, Merck, Kenilworth, NJ, USA) overnight at 37 ◦C. The overnight culture was diluted in fresh medium with 1% glucose (D9434, Sigma-Aldrich) before being transferred to a 96-well microtiter plate; 50 µL/well were incubated overnight with 50 µL of the test compound dissolved in 2 % (v/v) DMSO *aq.* added in duplicates. The bacterial culture was removed from the plate and the plate was washed with tap water. The biofilm was fixed at 65 ◦C for 1 h before 70 µL 0.1% crystal violet (115940, Merck Millipore) was added to the wells for 10 min of incubation. Excess crystal violet solution was then removed and the plate dried for 1 h at 65 ◦C. Seventy microliters of 70% EtOH were then added to each well and the plate incubated on a shaker for 5–10 min. Inhibition of biofilm formation was assessed by

the presence of violet color and was measured at 600 nm absorbance using a 1420 Multilabel Counter VICTOR3 TM. Fifty microliters of a non-biofilm
forming *Staphylococcus haemolyticus* (clinical isolate 8-7A, University hospital, UNN, Tromsø, Norway) mixed in 50 µL autoclaved Milli-Q water was used as a control; 50 µL *S. epidermidis* mixed in 50 µL autoclaved Milli-Q water was used as the control for biofilm formation; and 50 µL TSB with 50 µL autoclaved Milli-Q water was used as a medium blank control.

Cell Proliferation Assay

The inhibitory effect of compounds was tested using an MTS in vitro cell proliferation assay against two cancer cell lines and one physiologic cell line. The cancer cell lines were human melanoma A2058 (ATCC, CLR-1147™) and acute myeloid leukemia MOLM 13 [26], as cell line for the general cytotoxicity assessment, non-malignant MRC5 lung fibroblast cells (ATCC CCL-171™) were employed. The cells were cultured and assayed in Roswell Park Memorial Institute medium (RPMI-16040, FG1383, Merck) containing 10% (v/v) Fetal Bovine serum (FBS, 50115, Biochrom, Cambridge, UK). The cell-concentration was 4000 cells/well for the lung fibroblast cells and 2000 cells/well for the cancer cells. After seeding, the cells were incubated 24 h at 37 ◦C and 5% CO2. The medium was then replaced with fresh RPMI-1640 medium supplemented with 10% (v/v) FBS and gentamycin (10 µg/mL, A2712, Merck). After adding 10 µL of sample diluted in 2% (v/v) DMSO in ddH2O the cells were incubated for 72 h at 37 °C and 5% CO2. For assaying the viability of the cells 10 µL of CellTiter 96®AQueous One Solution Reagent (G3581, Promega, Madison, WI, USA) containing tetrazolium [3-(4,5-dimethylthiazol-2-yl)-5-(3-carboxymethoxyphenyl)-2-(4-sulfophenyl)-2H-tetrazolium, inner salt] and phenazine ethosulfate was added to each well and incubated for one hour. The tests were executed with three technical replicates. The plates were read using a DTX 880 plate reader by measuring the absorbance at λ = 485 nm. The cell viability was calculated using the media control. As a negative control RPMI-1640 with 10% (v/v) FBS was used and 0.5% Triton™ X-100 (Sigma-Aldrich) was used as a positive control. The data was processed and visualized using GraphPad Prism 8.

Genome and Gene-Cluster Analysis

The recently published genome of *Nostoc* KVJ20 [12] was submitted to antiSMASH [27]. Genes predicted to belong to the Aeroginosin biosynthetic gene clusters were found at the edges of several contigs. Therefore we have undertaken analysis of additional data acquired in

connection to the previous genome study and processed in the same way [12]. We were able to find a contig containing the entire operon which was verified again by antiSMASH. The bsl-operon was deposited and can be retrieved under the following accession number: MT269816.

ASSOCIATED CONTENT

Supporting Information. S1: ESI+-IMS-MS spectra of **2**; S2: ESI+-IMS-MS identification of putative schizopeptin 791; S3: Putative identification of schizopeptin 791 *via* its fragments; S4: ^{1}H NMR (600 MHz, DMSO-d_6) spectrum of suomilide B (**1**); S5: ^{13}C (151 MHz, DMSO-d_6) spectrum of suomilide B (**1**); S6: HSQC + HMBC (600 MHz, DMSO-d_6) spectrum of suomilide B (**1**); S7: COSY (600 MHz, DMSO-d_6) spectrum of suomilide B (**1**); S8: ROESY (600 MHz, DMSO-d_6) spectrum of suomilide B (**1**); S9: Comparison of 1D NMR chemical shift values between suomilide B and suomilide; S10: ^{1}H NMR (600 MHz, DMSO-d_6) spectrum of suomilide C (**2**); S11: ^{13}C (151 MHz, DMSO-d_6) spectrum of suomilide C (**2**); S12: HSQC + HMBC (600 MHz, DMSO-d_6) spectrum of suomilide C (**2**); S13 COSY (600 MHz, DMSO-d_6) spectrum of suomilide C (**2**); S14: TOCSY (600 MHz, DMSO-d_6) spectrum of suomilide C (**2**); S15: ROESY (600 MHz, DMSO-d_6) spectrum of suomilide C (**2**).

AUTHOR INFORMATION

*) Author to whom correspondence should be addressed.

Tel: +47 (0) 77649267;

E-mail: yannik.k.schneider@uit.no

ACKNOWLEDGMENTS

We are grateful to Kirsti Helland and Marte Albrigtsen for executing the bioassays with the molecules.

REFERENCES

1. Nunnery, J.K.; Mevers, E.; Gerwick, W.H. Biologically active secondary metabolites from marine cyanobacteria. *Curr. Opin. Biotech.* **2010**, *21*, 787-793, doi:10.1016/j.copbio.2010.09.019.
2. Dittmann, E.; Wiegand, C. Cyanobacterial toxins – occurrence, biosynthesis and impact on human affairs. *Mol. Nutr. & Food Res.* **2006**, *50*, 7-17, doi:10.1002/mnfr.200500162.
3. Namikoshi, M.; Rinehart, K. Bioactive compounds produced by cyanobacteria. *J. Ind. Microbiol.* **1996**, *17*, 373-384, doi:10.1007/bf01574768.
4. Kehr, J.; Picchi, D.G.; Dittmann, E. Natural product biosyntheses in cyanobacteria: A treasure trove of unique enzymes. *Beilstein J. Org. Chem.* **2011**, *7*, 1622-1635, doi:10.3762/bjoc.7.191.
5. Micallef, M.L.; D'Agostino, P.M.; Sharma, D.; Viswanathan, R.; Moffitt, M.C. Genome mining for natural product biosynthetic gene clusters in the Subsection V cyanobacteria. *BMC Genom.* **2015**, *16*, 669, doi:10.1186/s12864-015-1855-z.
6. Kleigrewe, K.; Almaliti, J.; Tian, I.Y.; Kinnel, R.B.; Korobeynikov, A.; Monroe, E.A.; Duggan, B.M.; Di Marzo, V.; Sherman, D.H.; Dorrestein, P.C., *et al*. Combining Mass Spectrometric Metabolic Profiling with Genomic Analysis: A Powerful Approach for Discovering Natural Products from Cyanobacteria. *J. Nat. Prod.* **2015**, *78*, 1671-1682, doi:10.1021/acs.jnatprod.5b00301.
7. Fujii, K.; Sivonen, K.; Adachi, K.; Noguchi, K.; Shimizu, Y.; Sano, H.; Hirayama, K.; Suzuki, M.; Harada, K.-i. Comparative study of toxic and non-toxic cyanobacterial products: A novel glycoside, suomilide, from non-toxic *Nodularia spumigena* HKVV. *Tetrahedron Lett.* **1997**, *38*, 5529-5532, doi:https://doi.org/10.1016/S0040-4039(97)01193-3.
8. Pluotno, A.; Carmeli, S. Banyasin A and banyasides A and B, three novel modified peptides from a water bloom of the cyanobacterium *Nostoc* sp. *Tetrahedron* **2005**, *61*, 575-583, doi:https://doi.org/10.1016/j.tet.2004.11.016.
9. Ishida, K.; Christiansen, G.; Yoshida, W.Y.; Kurmayer, R.; Welker, M.; Valls, N.; Bonjoch, J.; Hertweck, C.; Börner, T.; Hemscheidt, T., *et al*. Biosynthesis and structure of aeruginoside 126A and 126B, cyanobacterial peptide glycosides bearing a 2-carboxy-6-hydroxyoctahydroindole moiety. *Chem. Biol.* **2007**, *14*, 565-576, doi:10.1016/j.chembiol.2007.04.006.
10. Nilsson, M.; Bergman, B.; Rasmussen, U. Cyanobacterial diversity in geographically related and distant host plants of the genus *Gunnera*. *Arch. Microbiol.* **2000**, *173*, 97-102, doi:10.1007/s002039900113.

11. Liaimer, A.; Jensen, J.B.; Dittmann, E. A. Genetic and Chemical Perspective on Symbiotic Recruitment of Cyanobacteria of the Genus *Nostoc* into the Host Plant *Blasia pusilla* L. *Front. Microbiol.* **2016**, *7*, doi:10.3389/fmicb.2016.01693.
12. Halsør, M.-J.H.; Liaimer, A.; Pandur, S.; Ræder, I.L.U.; Smalås, A.O.; Altermark, B. Draft Genome Sequence of the Symbiotically Competent Cyanobacterium *Nostoc* sp. Strain KVJ20. *Microbiol. Resour. Announc.* **2019**, *8*, 1190-1119, doi:10.1128/MRA.01190-19.
13. Schindler, C.S.; Bertschi, L.; Carreira, E.M. Total Synthesis of Nominal Banyaside B: Structural Revision of the Glycosylation Site. *Angew. Chem.* **2010**, *49*, 9229-9232, doi:10.1002/anie.201004047.
14. Reshef, V.; Carmeli, S. Schizopeptin 791, a New Anabeanopeptin-like Cyclic Peptide from the Cyanobacterium *Schizothrix* sp. *J. Nat. Prod.* **2002**, *65*, 1187-1189, doi:10.1021/np020039c.
15. Maplestone, R.A.; Stone, M.J.; Williams, D.H. The evolutionary role of secondary metabolites — a review. *Gene* **1992**, *115*, 151-157, doi:10.1016/0378-1119(92)90553-2.
16. Gallegos, D.A.; Saurí, J.; Cohen, R.D.; Wan, X.; Videau, P.; Vallota-Eastman, A.O.; Shaala, L.A.; Youssef, D.T.A.; Williamson, R.T.; Martin, G.E., *et al*. Jizanpeptins, Cyanobacterial Protease Inhibitors from a *Symploca* sp. Cyanobacterium Collected in the Red Sea. *J. Nat. Prod.* **2018**, *81*, 1417-1425, doi:10.1021/acs.jnatprod.8b00117.
17. Sieber, S.; Grendelmeier, S.M.; Harris, L.A.; Mitchell, D.A.; Gademann, K. Microviridin 1777: A Toxic Chymotrypsin Inhibitor Discovered by a Metabologenomic Approach. *J. Nat. Prod.* **2020**, *83*, 438-446, doi:10.1021/acs.jnatprod.9b00986.
18. Singh, R.K.; Tiwari, S.P.; Rai, A.K.; Mohapatra, T.M. Cyanobacteria: an emerging source for drug discovery. *J. Antibiot. Res.* **2011**, *64*, 401-412, doi:10.1038/ja.2011.21.
19. Mazur-Marzec, H.; Fidor, A.; Cegłowska, M.; Wieczerzak, E.; Kropidłowska, M.; Goua, M.; Macaskill, J.; Edwards, C. Cyanopeptolins with Trypsin and Chymotrypsin Inhibitory Activity from the Cyanobacterium *Nostoc edaphicum* CCNP1411. *Mar. Drugs* **2018**, *16*, 220, doi:10.3390/md16070220.
20. Riba, M.; Kiss-Szikszai, A.; Gonda, S.; Parizsa, P.; Deák, B.; Török, P.; Valkó, O.; Felföldi, T.; Vasas, G. Chemotyping of terrestrial *Nostoc*-like isolates from alkali grassland areas by non-targeted peptide analysis. *Algal Res.* **2020**, *46*, 101798, doi:https://doi.org/10.1016/j.algal.2020.101798.

21. Mahlstedt, S.; Fielding, E.N.; Moore, B.S.; Walsh, C.T. Prephenate decarboxylases: a new prephenate-utilizing enzyme family that performs nonaromatizing decarboxylation en route to diverse secondary metabolites. *Biochem.* **2010**, *49*, 9021-9023, doi:10.1021/bi101457h.
22. Ishida, K.; Welker, M.; Christiansen, G.; Cadel-Six, S.; Bouchier, C.; Dittmann, E.; Hertweck, C.; Tandeau de Marsac, N. Plasticity and evolution of aeruginosin biosynthesis in cyanobacteria. *Appl. Environ. Microbiol.* **2009**, *75*, 2017-2026, doi:10.1128/aem.02258-08.
23. Mihali, T.K.; Kellmann, R.; Neilan, B.A. Characterisation of the paralytic shellfish toxin biosynthesis gene clusters in *Anabaena circinalis* AWQC131C and *Aphanizomenon* sp. NH-5. *BMC Biochem.* **2009**, *10*, 8, doi:10.1186/1471-2091-10-8.
24. Patiny, L.; Borel, A. ChemCalc: A Building Block for Tomorrow's Chemical Infrastructure. *J. Chem. Inf. Model.* **2013**, *53*, 1223-1228, doi:10.1021/ci300563h.
25. Stanier, R.Y.; Kunisawa, R.; Mandel, M.; Cohen-Bazire, G. Purification and properties of unicellular blue-green algae (order Chroococcales). *Bacteriol. Rev.* **1971**, *35*, 171-205.
26. Matsuo, Y.; MacLeod, R.A.F.; Uphoff, C.C.; Drexler, H.G.; Nishizaki, C.; Katayama, Y.; Kimura, G.; Fujii, N.; Omoto, E.; Harada, M., *et al*. Two acute monocytic leukemia (AML-M5a) cell lines (MOLM-13 and MOLM-14) with interclonal phenotypic heterogeneity showing MLL-AF9 fusion resulting from an occult chromosome insertion, ins(11;9)(q23;p22p23). *Leukemia* **1997**, *11*, 1469-1477, doi:10.1038/sj.leu.2400768.
27. Medema, M.H.; Blin, K.; Cimermancic, P.; de Jager, V.; Zakrzewski, P.; Fischbach, M.A.; Weber, T.; Takano, E.; Breitling, R. antiSMASH: rapid identification, annotation and analysis of secondary metabolite biosynthesis gene clusters in bacterial and fungal genome sequences. *Nucleic Acids Res.* **2011**, *39*, 339-346, doi:10.1093/nar/gkr466.

SUPPLEMENTARY MATERIALS

New suomilides isolated from *Nostoc* sp. KVJ20, bioactivity and biosynthesis

Yannik K.-H. Schneider [1], Anton Liaimer [2], Johan Isaksson [3], Kine Ø. Hansen [1], Jeanette Hammer Andersen [1] and Espen H. Hansen [1].

[1)] Marbio, Faculty for Fisheries, Biosciences and Economy, UiT—The Arctic University of Norway, Breivika, N-9037 Tromsø, Norway.

[2)] Department of Arctic and Marine Biology, Faculty for Fisheries, Biosciences and Economy, UiT—The Arctic University of Norway, Breivika, N-9037 Tromsø, Norway.

[3)] Department of Chemistry, Faculty of Natural Sciences, UiT—The Arctic University of Norway, Breivika, N-9037 Tromsø.

Table of contents

Figure S1 ESI+-IMS-MS spectra of suomilide C (2)

Figure S2 ESI+-IMS-MS identification of putative schizopeptin 791

Figure S3 Putative identification of schizopeptin 791 via its fragments

NMR Spectroscopic Data for suomilide B (1)

Figure S4 ^{1}H NMR (600 MHz, DMSO-d_6) spectrum of suomilide B (**1**)

Figure S5 ^{13}C (151 MHz, DMSO-d_6) spectrum of suomilide B (**1**)

Figure S6 HSQC + HMBC (600 MHz, DMSO-d_6) spectrum of suomilide B (**1**)

Figure S7 COSY (600 MHz, DMSO-d_6) spectrum of suomilide B (**1**)

Figure S8 ROESY (600 MHz, DMSO-d_6) spectrum of suomilide B (**1**)

Figure S9 Comparison of 1D NMR chemical shift values between suomilide B and suomilide

NMR Spectroscopic Data for suomilide C (2)

Figure S10 ^{1}H NMR (600 MHz, DMSO-d_6) spectrum of suomilide C (**2**)

Figure S11 ^{13}C (151 MHz, DMSO-d_6) spectrum of suomilide C (**2**)

Figure S12 HSQC + HMBC (600 MHz, DMSO-d_6) spectrum of suomilide C (**2**)

Figure S13 COSY (600 MHz, DMSO-d_6) spectrum of suomilide C (**2**)

Figure S14 TOCSY (600 MHz, DMSO-d_6) spectrum of suomilide C (**2**)

Figure S15 ROESY (600 MHz, DMSO-d_6) spectrum of suomilide C (**2**)

S1. ESI+-IMS-MS spectra of suomilide C (**2**). A: Low-collision energy spectra, the neutral loss of sulfate is indicated by the black arrow. B: High-collision energy spectra (20-60 eV ramp) in red below. The fragment at m/z 601.3206 is the aglycon after loss of the sulfate and sugar-moiety. 899.4340 is the observed loss of sulfate for **2**.

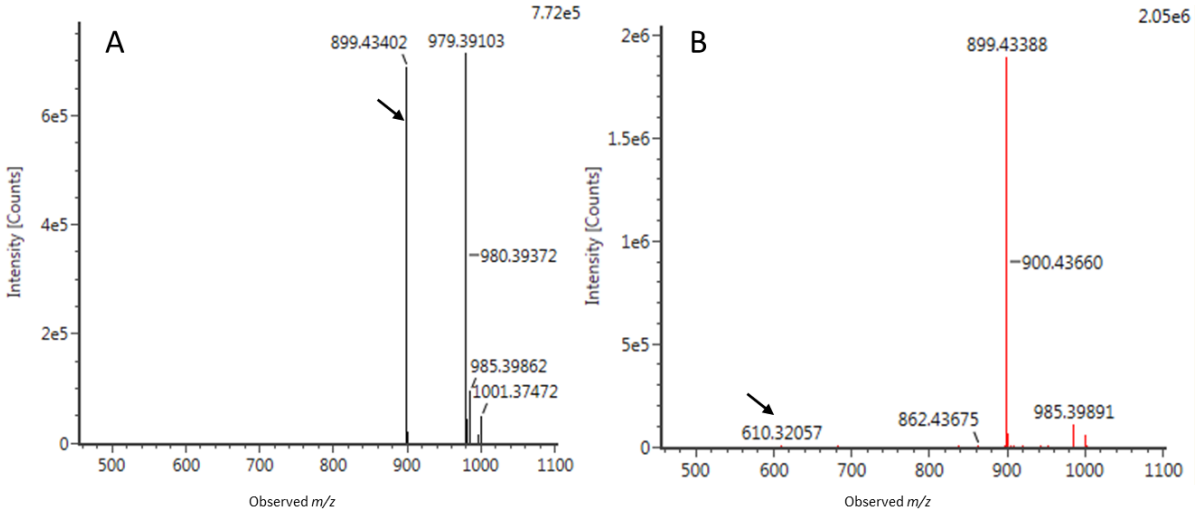

S2. ESI+-IMS-MS identification of putative schizopeptin 791. A: Low collision energy spectra. B: High collision energy spectra (20-60 eV ramp), for assignment of fragments see Figure S3.

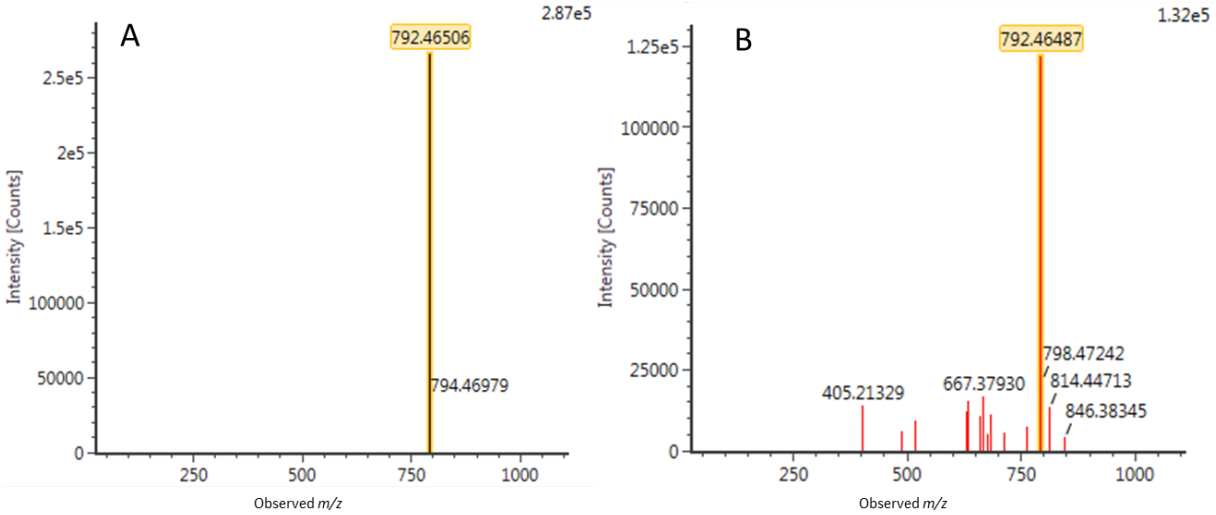

S3. Putative identification of schizopeptin 791 *via* its fragments.

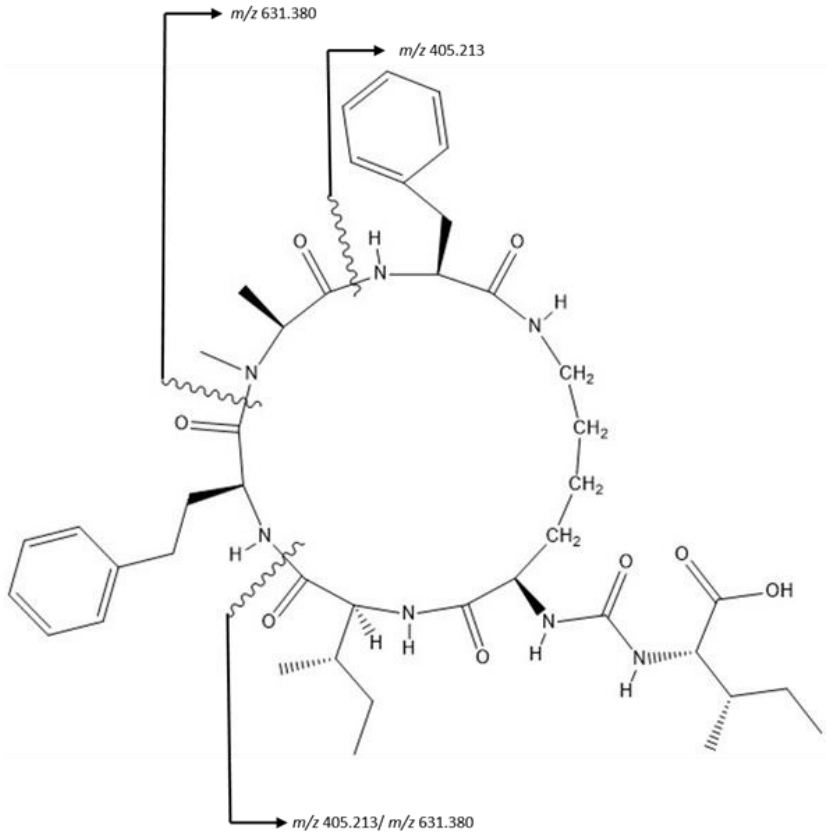

S4. ^{1}H NMR (600 MHz, DMSO-d_6) spectrum of 1075 (**1**)

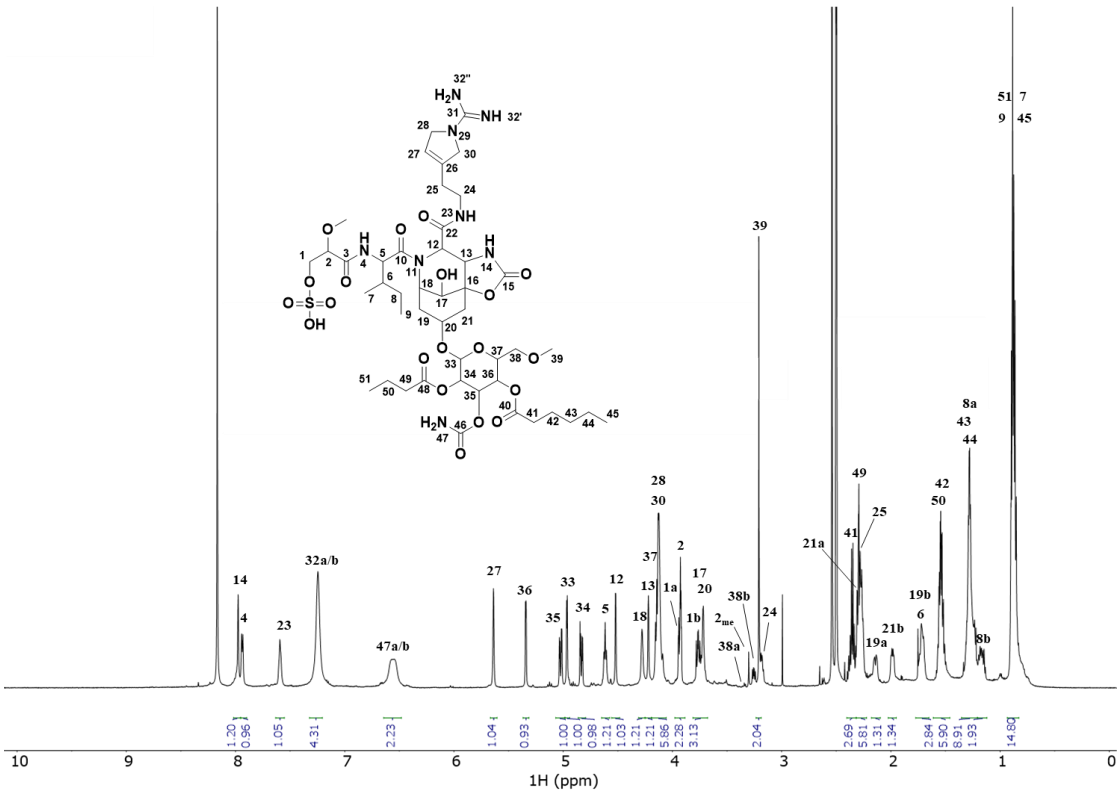

S5. ^{13}C (151 MHz, DMSO-d_6) spectrum of 1075 (**1**)

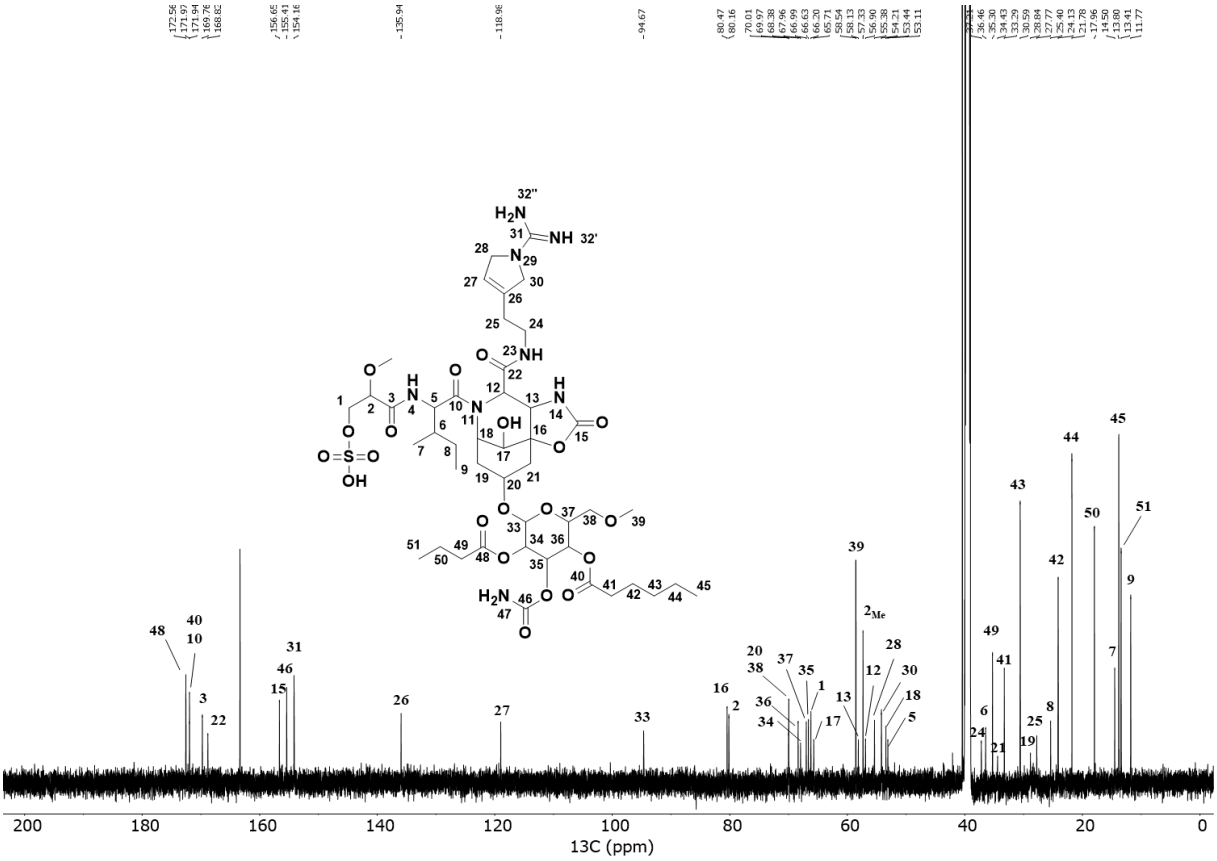

S6. HSQC + HMBC (600 MHz, DMSO-d_6) spectrum of 1075 (**1**)

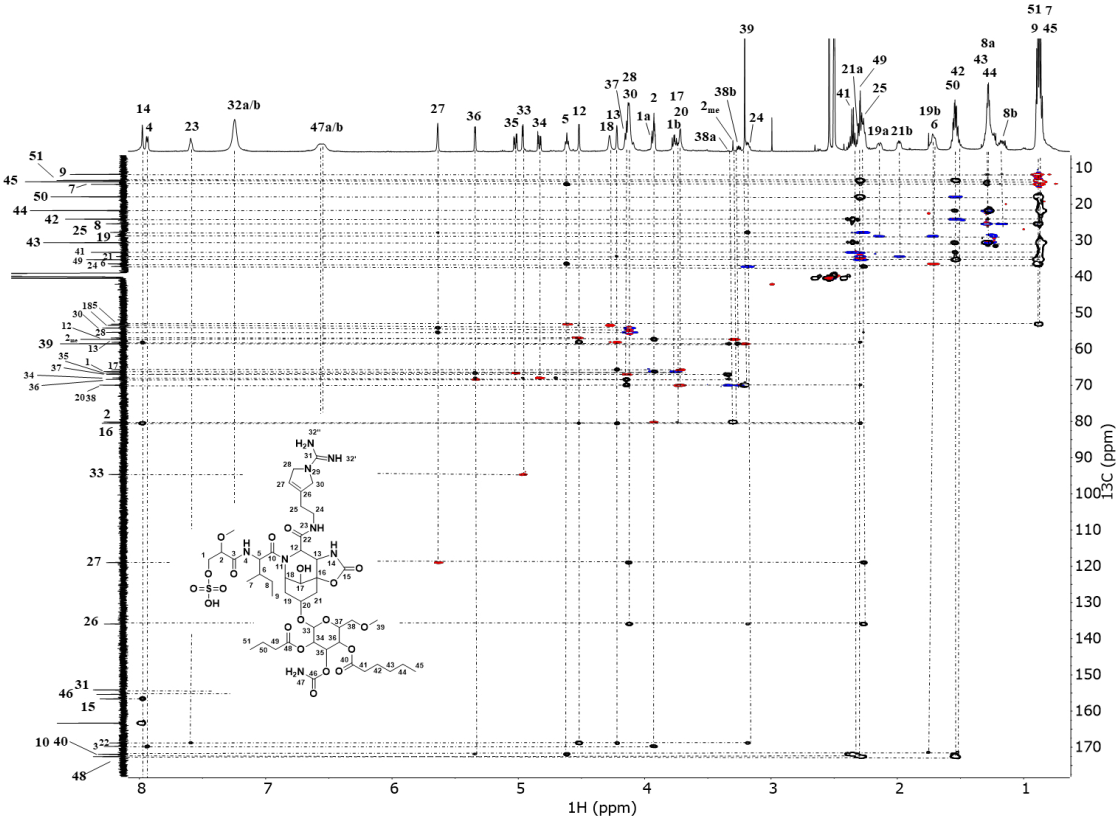

S7. COSY (600 MHz, DMSO-d_6) spectrum of 1075 (**1**)

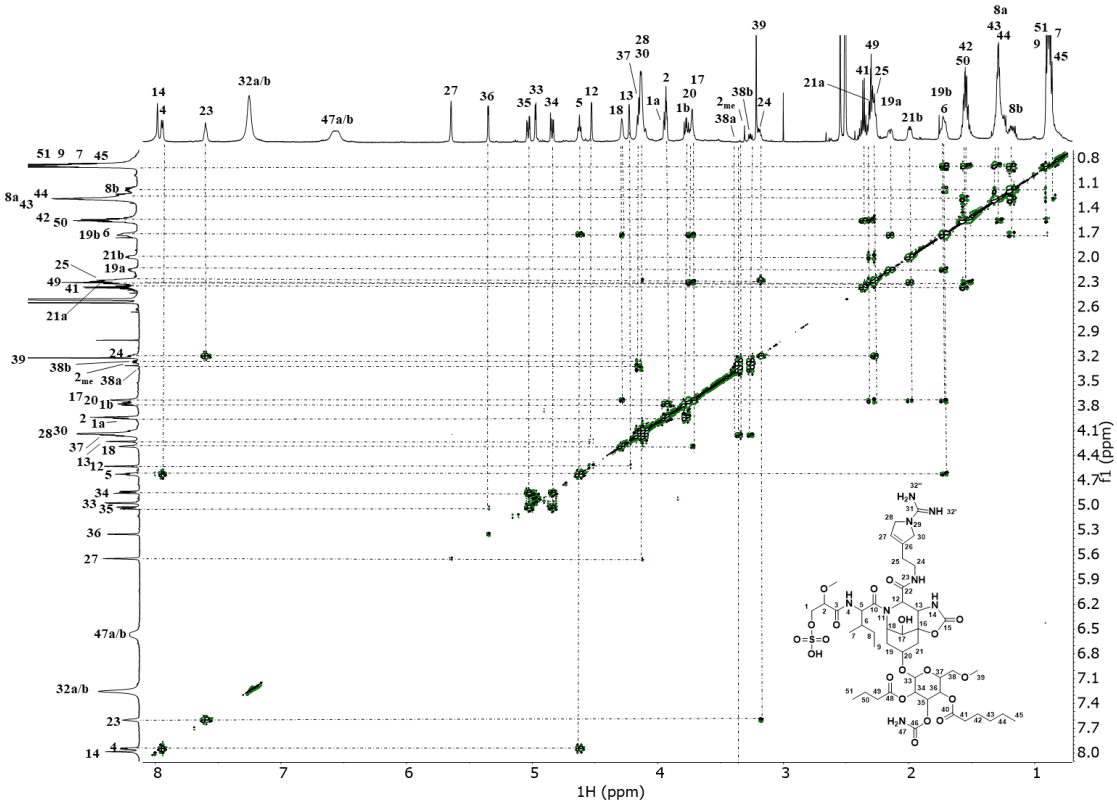

S8. ROESY (600 MHz, DMSO-d_6) spectrum of 1075 (**1**)

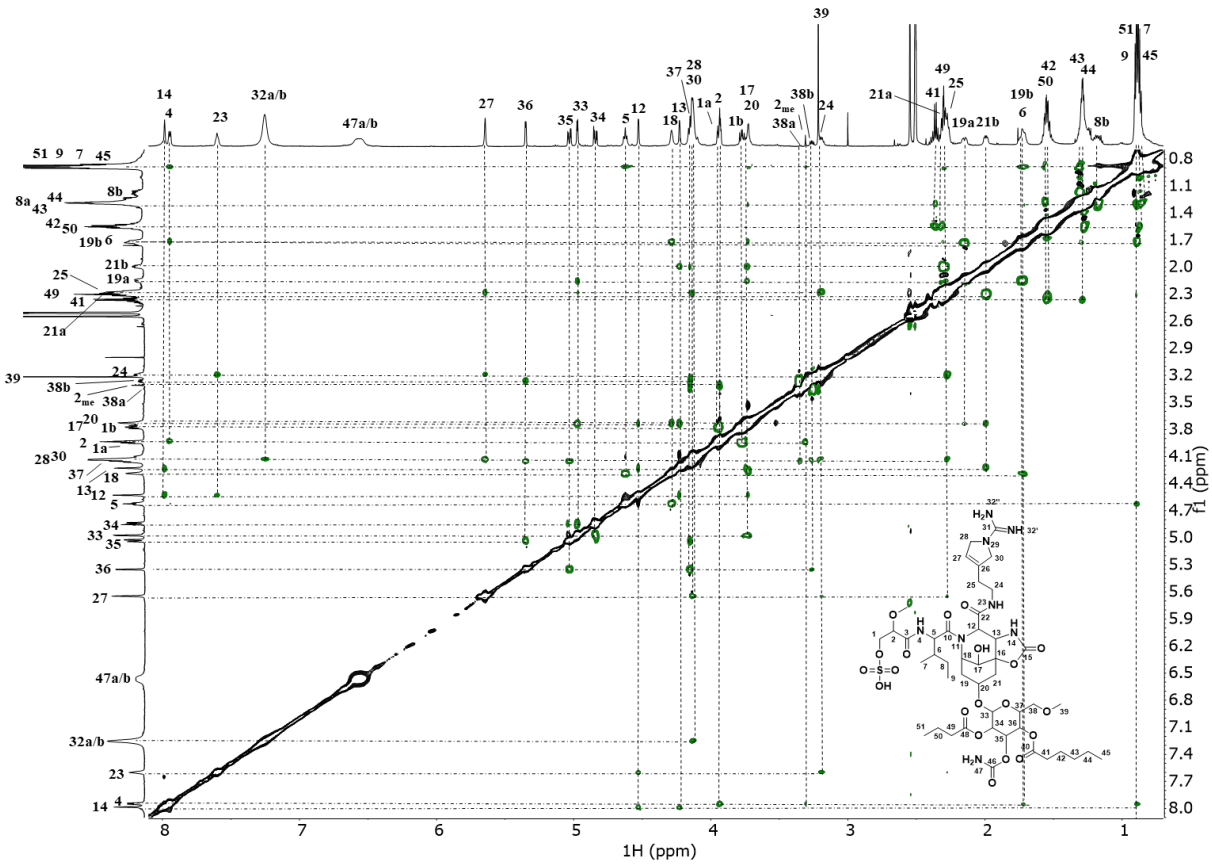

S9. Comparison of 1D NMR chemical shift values between 1075 (**1**) and suomilide

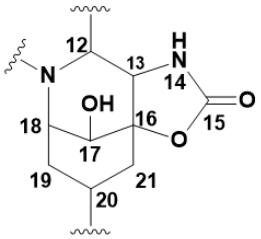

Data recorded for the Aza subunit

	1075 (**1**)		Suomilide			
position	δ_C	δ_H	δ_C	δ_H	$\Delta\delta_C$	$\Delta\delta_H$
12	56,9	4,52	56,6	4,59	0,3	0,07
13	58,3	4,22	58,1	4,27	0,2	0,05
14		7,98		7,95	0	0,03
15	156,7		156,6		0,1	0
16	80,5		80,4		0,1	0
17	65,7	3,72	65,7	3,69	0	0,03
18	53,4	4,28	53,5	4,23	0,1	0,05
19a	28,8	2,14	28,7	2,14	0,1	0
19b		1,72		1,68		0,04
20	70	3,72	69,8	3,62	0,2	0,1
21a	34,4	2,41 - 2,24	34,5	2,27	0,1	n.a.
21b		1,99		1,94		0,005
				Avg:	0,11	0,03

S10. ^{1}H NMR (600 MHz, DMSO-d_6) spectrum of 978 (**2**)

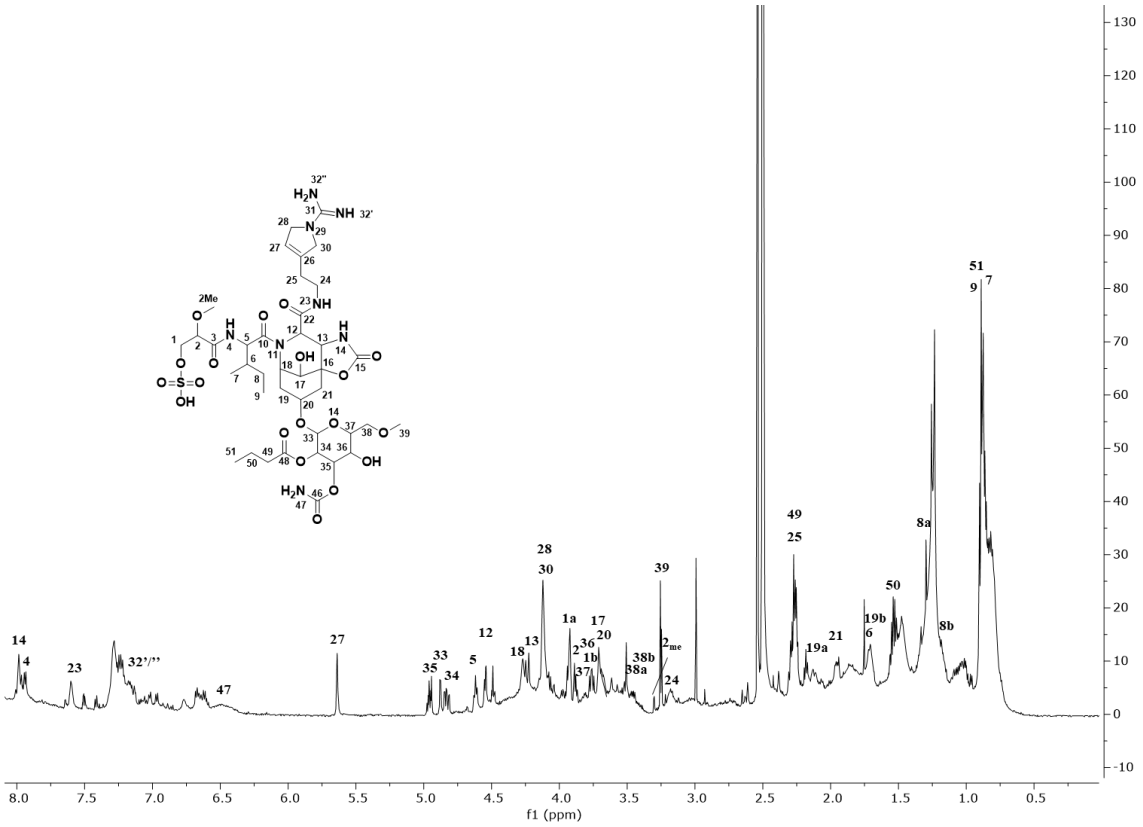

S11. ^{13}C (151 MHz, DMSO-d_6) spectrum of 978 (**2**)

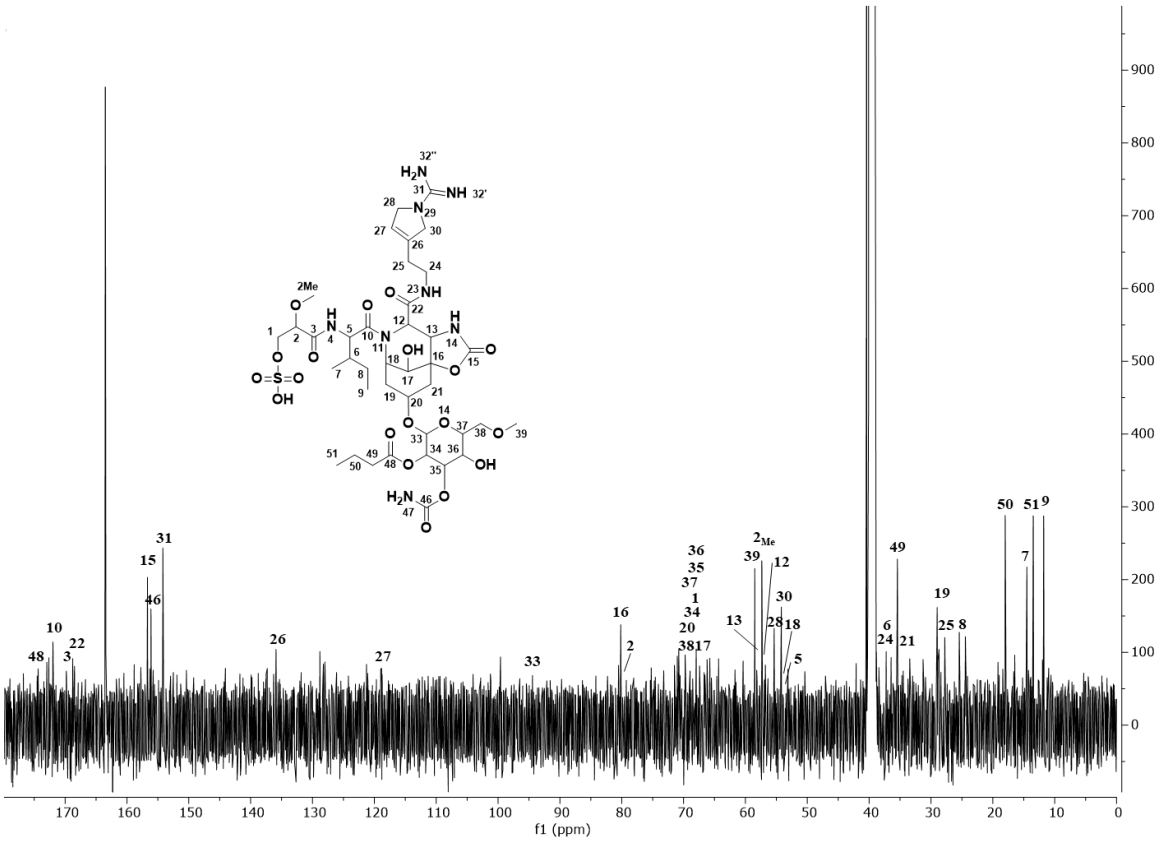

S12. HSQC + HMBC (600 MHz, DMSO-d_6) spectrum of 978 (**2**)

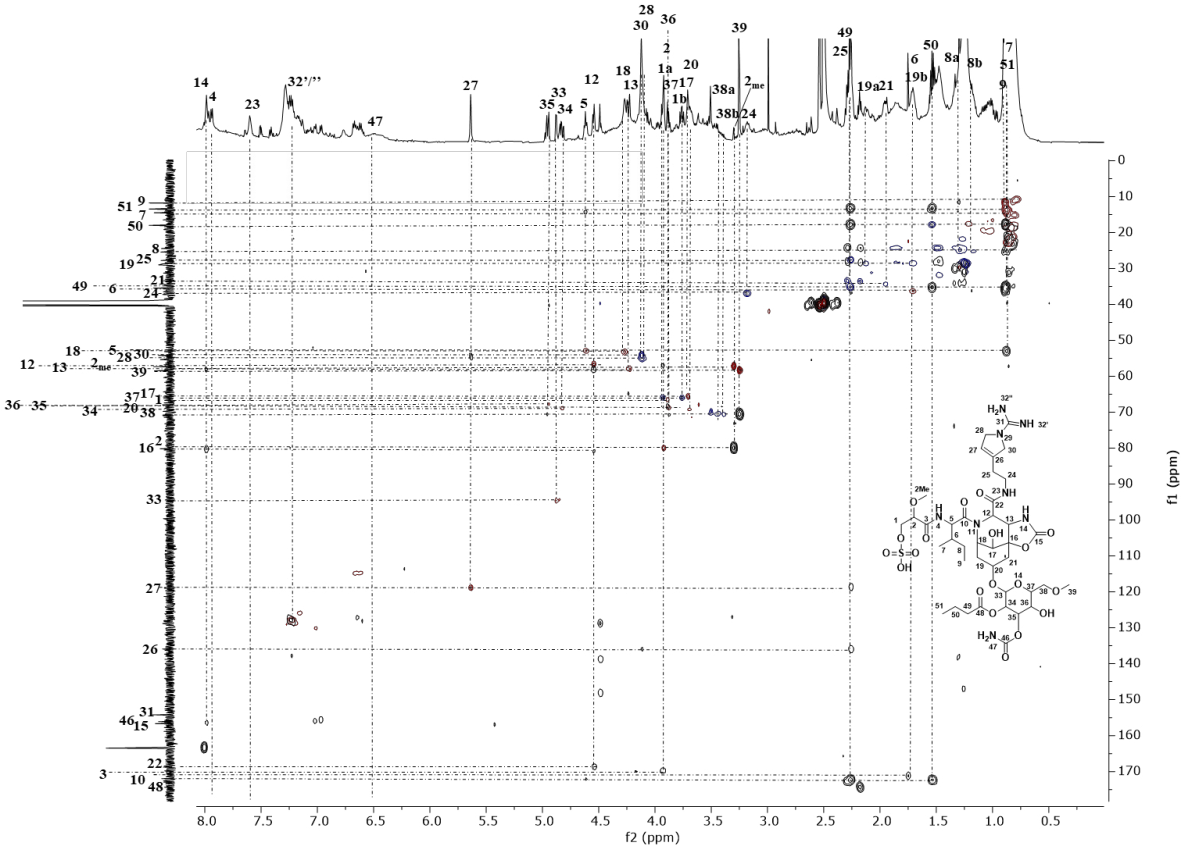

S13. COSY (600 MHz, DMSO-d_6) spectrum of 978 (**2**)

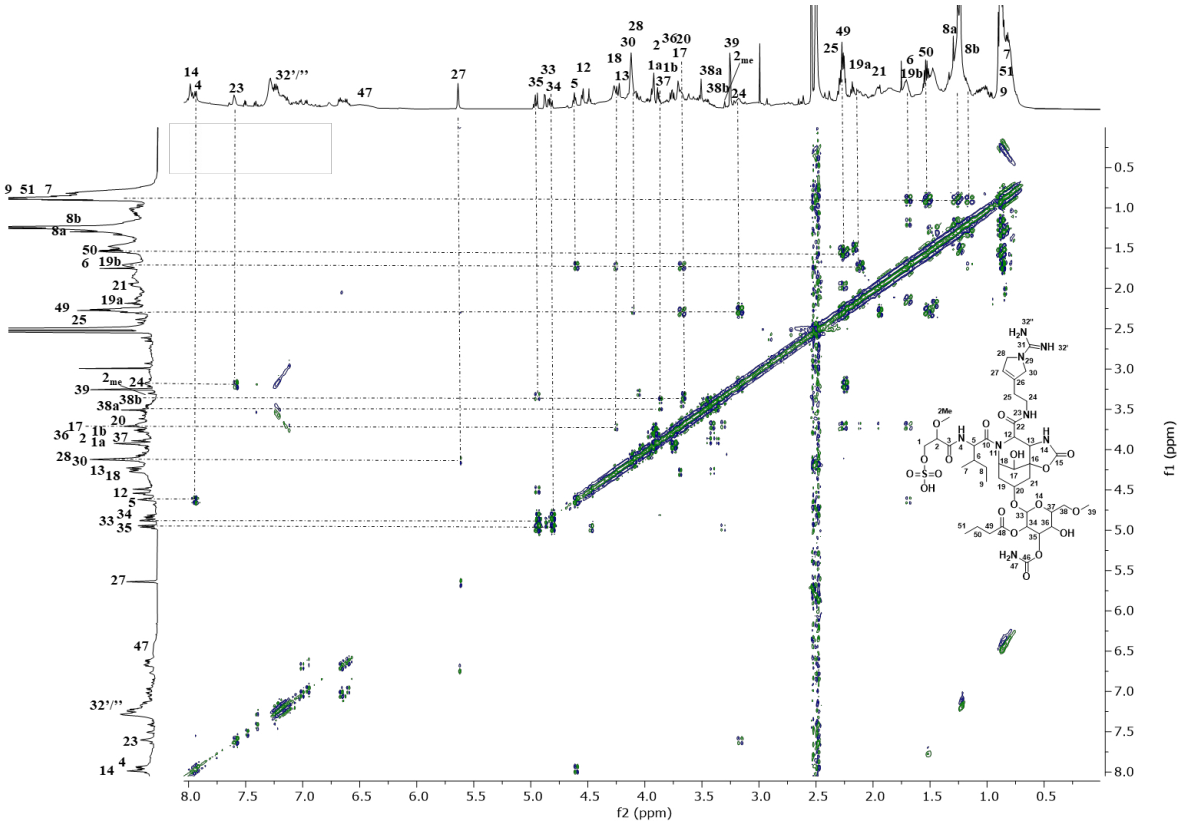

S14. TOCSY (600 MHz, DMSO-d_6) spectrum of 978 (**2**)

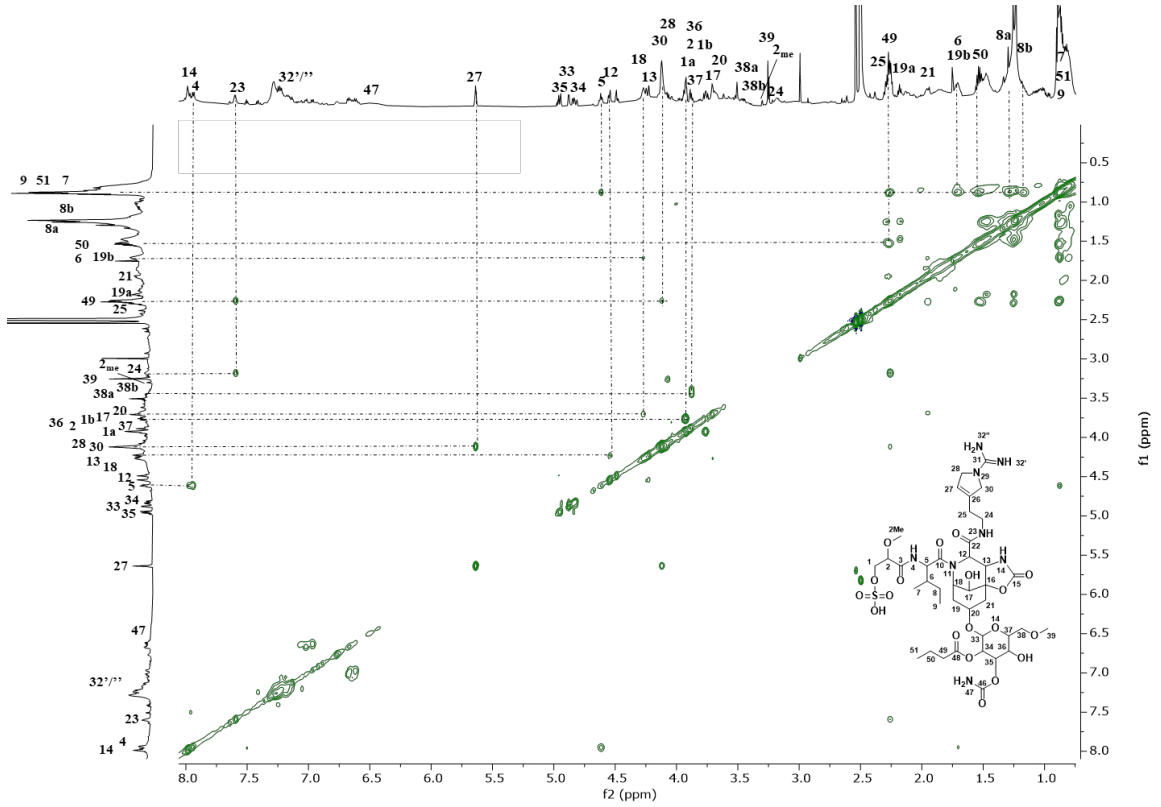
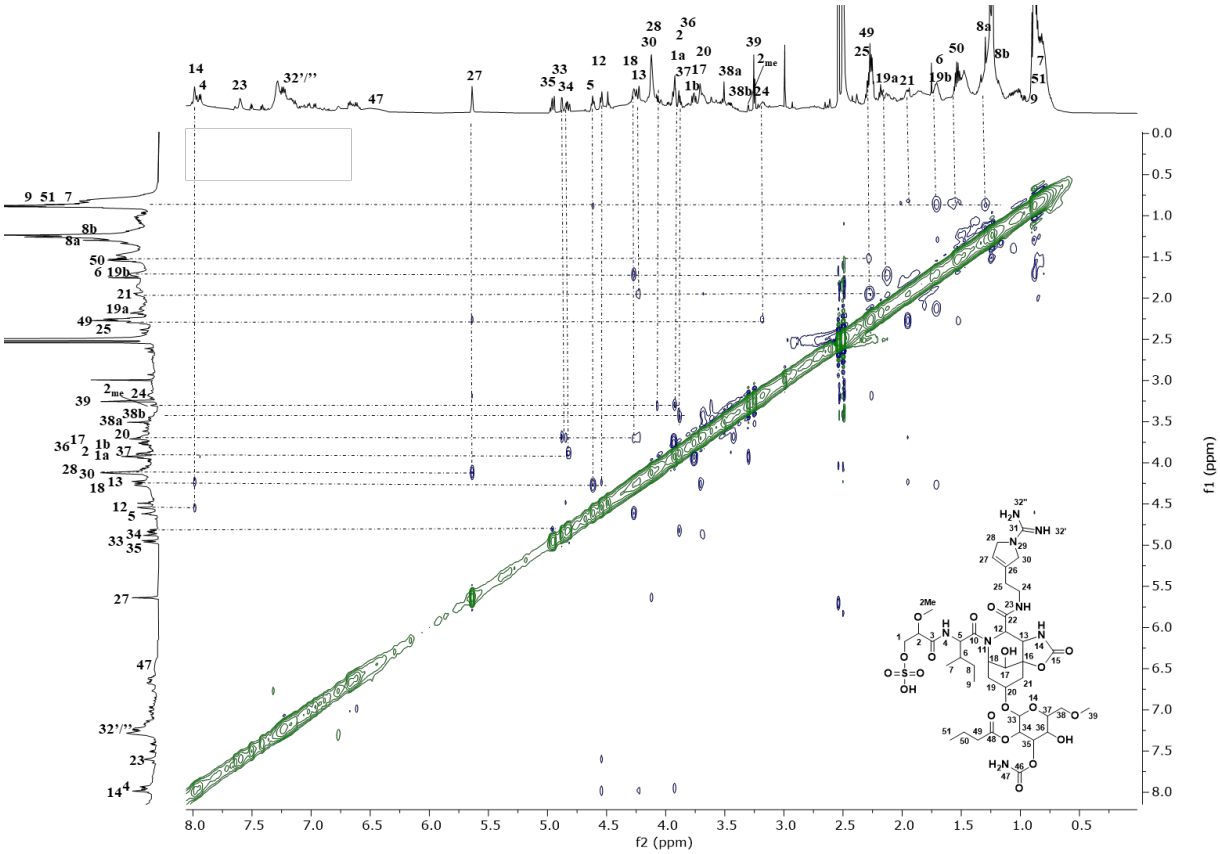
S15. ROESY (600 MHz, DMSO-d_6) spectrum of 978 (**2**)